Synthesis and Characterization of, and Dynamic processes occurring in, Highly Active Pd catalyst for Alkyne & Alkene Hydroesterification

UNIVERSITY OF LIVERPOOL

Thesis submitted in accordance with the requirements of the University of Liverpool for the degree of Master of Philosophy by

Firas T. R. Al-Mosule

September 2013

DECLARATION

I declare that, expect where otherwise stated, the work contained within this thesis is my own research, carried out from September 2009 until September 2012 at the Department of Chemistry, The University of Liverpool.

SIGNED

Firas Al-Mosule

Date: September 2013

Acknowledgements

I would really like to express all my thanks to my supervisors in Liverpool, Dr. Jon Iggo and Dr. Joho Satherley for giving me the opportunity of doing this MPhil research project with them, and for all the great teaching, support and encouragement given during these four years.

This project could not be done without Kate Robertson (Deputy Executive Secretary/Iraq Programme Manager) form CARA (Council for assisting refugee academics) and CARA. Thank you very much for give me the opportunity and fellowship, your help has been invaluable in the development of my knowledge and skills. Big thanks to CARA for the funding.

I would like to thank all the staff in the chemistry department of the University of Liverpool for their help and support, and in particular Tony and George.

Thank you to all the colleagues in the lab, especially Mike for his help with the NMR and HPNMR spectrometers.

Big thanks to all the good friends I made in Liverpool: Ali, Cate, Sara, Mike, Mishari.

I want to give the most felt thanks my family, my father in low Dr. Salah Alnuaimi, for their support and encouragement in the good and bad moment, especially my wife Khalda Alnuaimi for her help and support during my study, we did it, and the MPhil is finally here.

Finally, thank you very much to the most especial person in my family life, Mrs Sana Al-kudairy, you give me and my family the biggest and most useful support.

Abstract

Chapter one reviews the literature surrounding three main areas of interest relevant to the research carried out. These areas include industrial process for the synthesis of methyl methacrylate, the carbonylation of alkynes and alkenes. In addition, review effect of the ligands and counterion on the catalyst system, and dynamic process and NMR of the catalyst.

Chapter two outlines simple, generic procedures to Pd-'chelate-monodentate' complexes and investigates the coordination chemistry and hemilability of such complexes. In addition, an explanation of the organometallic chemistry of the Pd-'chelate-monodentate' complexes and synthesis of these complexes illustrates the possibility of nitrogen playing a role in proton relay. Also, introduces the variable temperature spectra of a $[Pd(\kappa^2\text{-}Ph_2Ppy)(\kappa^1\text{-}Ph_2Ppy)_2][CH_3SO_3]_2$ (**6**), and $[Pd(\kappa^2\text{-}Ph_2Ppy)(\kappa^1\text{-}Ph_2Ppy)Cl][X]$ (**3**[X]), (X = Cl, OTf, BF_4), uses a computer program to simulate gNMR discusses the associative mechanism of exchange in Pd-'chelate-monodentate' complexes. Finally, details the experimental procedures undertaken in the above work.

Chapter three illustrates how can preparation of the new alkanesulfonic acids (R = C_8, C_9, C_{11}, C_{14}, C_{16}, C_{18}) which use instead of methanesulfonic acid in hydroesterification of alkene process. In terms of follow the two strategies, first strategy depends on synthesis of silver alkanesulfonate salts from interaction of sodium alkanesulfonate salts with $AgNO_3$ then reaction with palladium complex. While in the second strategy, free alkanesulfonic acid was prepared *in situ*, via reaction of HBF_4 with a series of sodium alkanesulfonate salts (R = C_8, C_9, C_{11}, C_{14}, C_{16}, C_{18}), then added to palladium complex in a sapphire tube of HPNMR spectroscopy for studies and confirm steps of the catalytic cycle.

Chapter four draws on the conclusions derived from the above work and relates it to work previously carried out in the field.

Table of contents

Chapter One:

Chapter Four:

Chapter One

Introduction

1. Introduction

1.1. MMA production processes[1]

Methyl methacrylate (MMA) is an important monomer. There has been a great increase in the production of MMA in the world in the last 15 years, which has now reached 2.2 million tonnes per year, due to increasing demand for its polymerization and copolymerization products, for example, from production of Perspex (polymethyl methacrylate, PMMA), MMA 's main application. Methacrylic polymer, which has the characteristics of high transparency and weather resistance, is used in many fields, for example, signboards, building materials, vehicles and lighting equipment. MMA is also used to produce resins, plastic coatings, adhesives, lubricating agents, printing / dyeing assistants and insulation filling materials, impregnates for electric motor coils, and glazing agents for paper.

Several routes to MMA are currently operated commercially and environmentally friendly such as (i) ACH route with integral H_2SO_4 recovery, (ii) BASF route from ethylene via propionaldehyde, (iii) Lucite (formerly INEOS) methyl propionate/HCHO, (iv) Shell/INEOS route via propyne carbonylation, most of which the largest in terms of total production is ICI's less environmentally friendly ACH process and the most recent is, Lucite International's ALPHA process

1.1.1. The acetone-cyanohydrin (ACH) process

The ACH process for production of MMA was developed by ICI and commercialized in 1937, based on the process for the industrial production of methacrylic ester developed by Rohm & Hass Co, in 1933. The acetone-cyanohydrin ACH process was the sole industrial process until 1982, and is still the most used process for the production of (MMA) today.

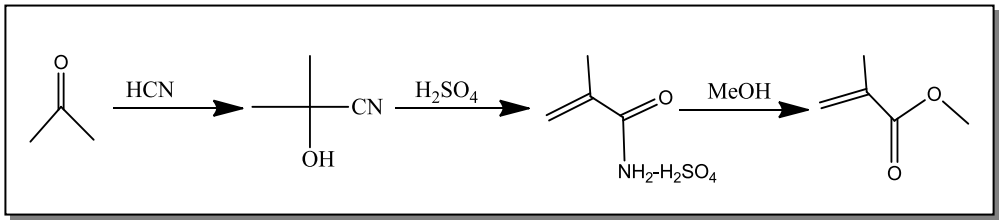

Scheme 1.1. ACH process for the production of MMA.

The ACH process (Scheme 1.1) starts with a base catalysed reaction between acetone and hydrogen cyanide HCN producing the intermediate acetone cyanohydrin ACH, the intermediate cyanohydrin is converted with sulfuric acid to a sulfate ester of the methacrylamide, methanolysis of which gives ammonium bisulfate and MMA. There are problems and environmental issues with the ACH process, viz dealing with the large quantities of ammonium bisulphate by-product and of a shortfall in the supply of toxic hydrogen cyanide HCN. Moreover, it requires high capital and energy costs for the intensive acid recovery and regeneration.

Mitsubishi Gas Chemicals improved the ACH process (Scheme 1.2) in 1997 to address these problems. In this process, first, acetone cyanohydrin is hydrated to α-hydroxy isobutylamide with the manganese oxide catalyst in the absence of sulphuric acid, and then esterified by methylformate to give methyl α-hydroxy isobutyrate and formamide, which is subsequently dehydrated to give HCN, which is recycled in the (ACH) preparation process. Finally, methyl α-hydroxy isobutyrate is converted to (MMA) in a dehydration reaction.

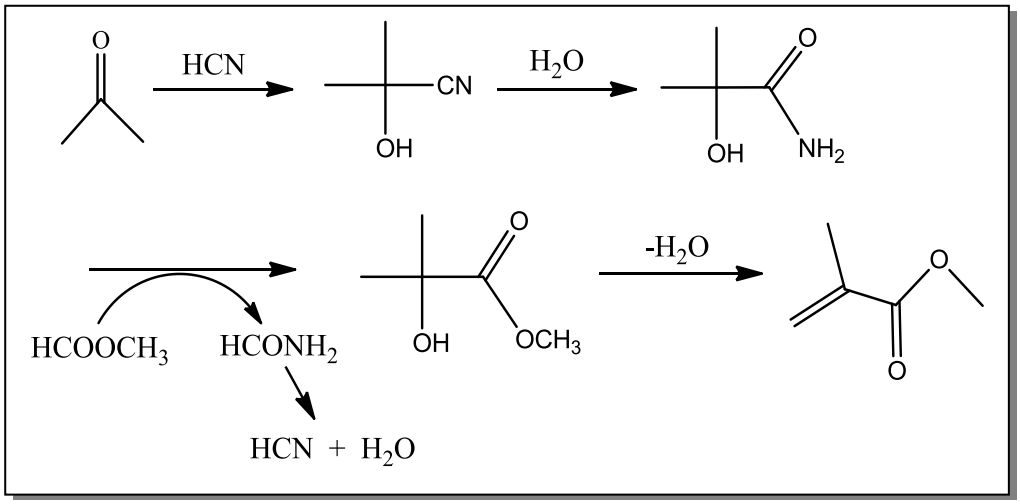

Scheme 1.2. Improved ACH process for the production of MMA.

The advantage of this process is the elimination of sulphuric acid and methanol, and the reduced amount of HCN used. However, the disadvantage of the new (ACH) process is the number of reaction steps involved.

Mitsubishi Gas Chemical has recently suggested (scheme 1.3) a new modification[2] of its process which involves the use of methanol instead of methylformate for the reaction with α-hydroxy isobutylamide to produce methyl α-hydroxy isobutylate and ammonia. The ammonia produced is recycled to HCN via treatment with methanol and O_2.

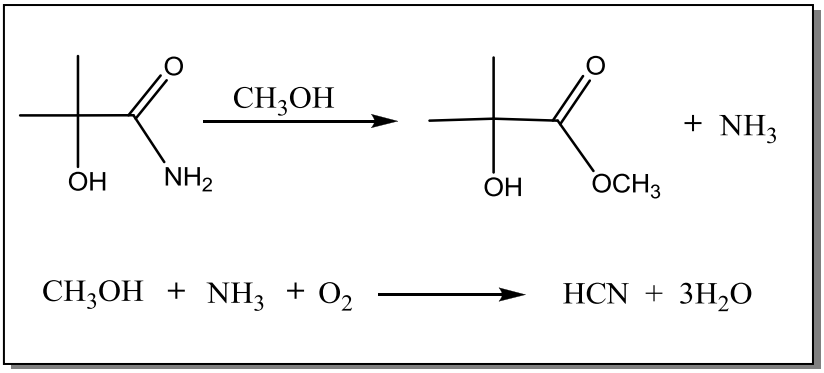

Scheme 1.3. New route for producing methyl α-hydroxy isobutyrate.

1.1.2. BASF's hydroformylation of ethene

In 1989, BASF developed and commercialized a route[1] from ethene with a 40,000 t per year of MMA production plant. This process (Scheme 1.4) involves homogenous rhodium-catalysed hydroformylation of ethene yielding propanal.

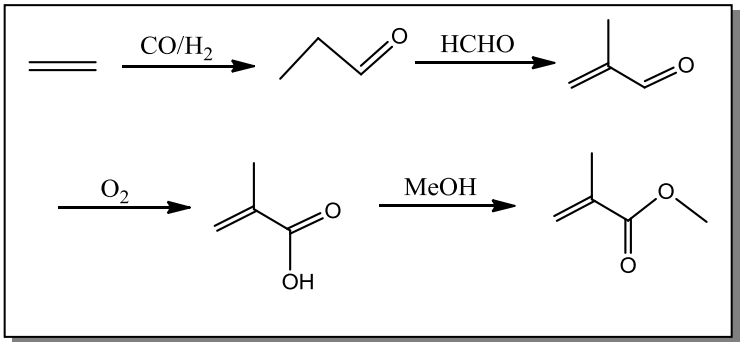

Scheme 1.4. BASF's hydroformylation of ethene to MMA.

In this path, ethene is converted to methacrolein then methacrylic acid as in (Scheme 1.4). The main drawback of this process is the moderate yield (< 85 % moles based on propanal).

Several routes via methyl propionate (MeP) or propionic acid routes have been proposed by many companies over the years. For example, Reppe's metal carbonyl catalysed hydrocarbonylation reaction of ethene can be used to produce methyl propionate. MMA is then produced by condensation reaction with formaldehyde, illustrated in (Scheme 1.5).

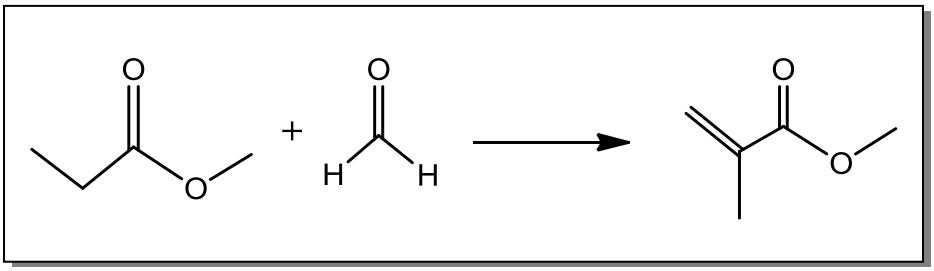

Scheme 1.5. Methyl propionate with formaldehyde to produce MMA.

Lucite's Alpha process

Lucite International has recently commercialized an MeP route to MMA which can cut the cost of making methyl methacrylate by 40 %. The two-stage (ALPHA) process does not use acetone or HCN as raw materials, but is based on ethene, carbon monoxide and methanol. The ALPHA process depends on combined carbonylation and esterification of ethene to methyl propanoate with > 99.9% selectivity, which is then reacted with formaldehyde under almost anhydrous condition to form methyl methacrylate. An industrial plant has been built in Singapore (2008) with a production of 120000 tons per year at start up. This is the only process existing at present to compete with the ACH process in economic and productivity terms.

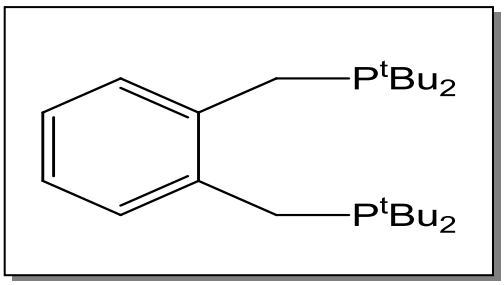

Figure 1.1. ALPHA (d^{t}bpx) ligand.

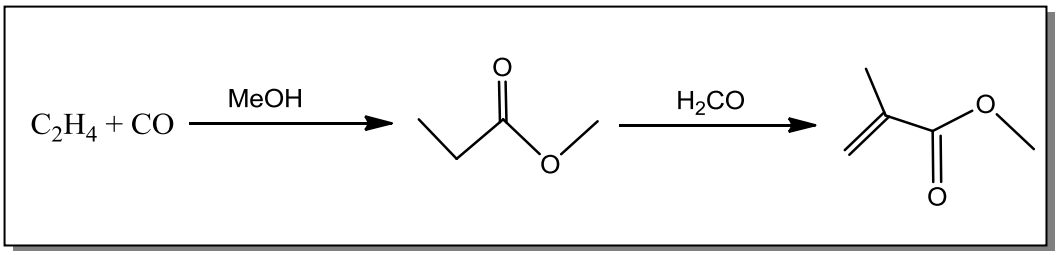

Scheme 1.6. Lucite's ALPHA process for the production of MMA.

This process (Scheme 1.6) uses sterically bulky diphosphine ligands, the catalyst being formed *in situ via* the reaction of [Pd(d^{t}bpx)(dba)] (d^{t}bpx =1,2((CH$_3$C)$_2$PCH$_2$)$_2$ C$_6$H$_4$) called (ALPHA) (Figure 1.1) compound (dba = trans,trans-(PhCH=CH)$_2$CO) with CH$_3$SO$_3$H in MeOH.[3]

1.2. Palladium catalysed carbonylation of alkynes

The transition metal catalysed carbonylation of alkynes has been known since the revolutionary work of Reppe.[4] The commercial production of acrylic acid and its esters via the carbonylation of acetylene uses Reppe's nickel carbonyl catalyst. MMA can therefore, at least in principle, be manufactured by the carbonylation of propyne using similar nickel or palladium catalysts to those first reported by Reppe.[5,6] Over many years, efforts have been made to obtain MMA from propyne in the same way as acrylic acid, but the yield of MMA is very low when using the same catalyst under like conditions. The procedure was also tried using a known palladium catalyst suitable for Reppe type carbonylation, but it did not work sufficiently.[7]

In the mid-1980's Drent and co-workers at Shell developed a novel one-step attractive process starting from propyne for producing (MMA). Drent found that a palladium catalyst source in the form of palladium acetate, in conjunction with an organo phosphine and protonic acid gave a good yield.[8] However, this process was not commercially introduced due a lack of acceptable catalyst activity and selectivity.

Drent made a great effort to find a new class of highly efficient homogeneous palladium catalysts for the carbonylation of alkynes.[9,10,11] The general reaction, which uses alkyne as a substrate and a nucleophilic co-reagent (water, aliphatic alcohols, carboxylic acids and amines), as shown in (Scheme 1.7).

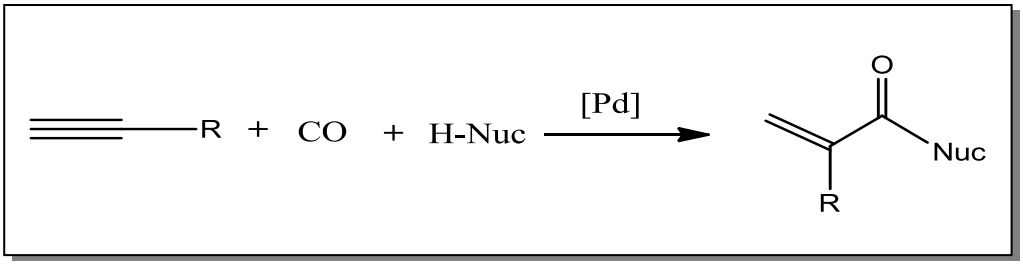

Scheme 1.7. Palladium catalysed alkoxycarbonylation of alkynes.

The activity and selectivity were observed to increase remarkably upon replacing PPh_3 with 2-pyridyldiphenyl phosphine Ph_2Ppy, under mild conditions (45 ^oC instead of 115 ^oC).[4]

1.2.1. Carbonylation of propyne

When propyne is used as substrate and methanol the nucleophilic co-reagent, the product is MMA, with the potential of reaching selectivity of up to 99.9% and yields up to 100,000 mol of MMA for 1 mol Pd per hour.[4,12,13] The process is called hydroesterification when the nucleophile used is an aliphatic alcohol (primary, secondary and tertiary), see Scheme 1.8.

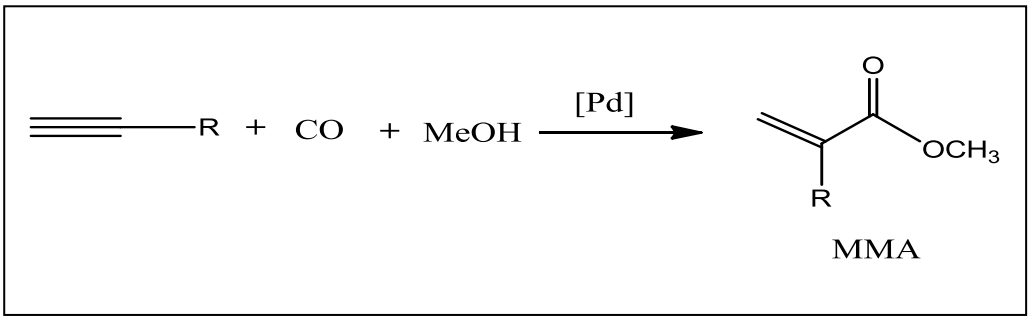

Scheme 1.8. Palladium catalysed hydroesterification of propyne.

Propyne is obtained as a by-product from an ethylene plant. This process, therefore, has many advantages if it is placed close to a big ethylene production plant. Although this route appears attractive, being a single step process and the extremely high catalyst performance, it is not without its difficulties. These include the availability/cost of propyne and the exothermic nature of the reaction which is compounded by the extremely active catalysts which makes the reaction hard to control on an industrial scale. ICI bought the patents for this technology from Shell in ca. 1996; it is sometimes referred to as the Lucite BETA process.

1.2.2. Effect of ligand structure

The ligand can not only stabilize Pd hydroesterification catalyst, but also fundamentally change the selectivity and activity. As clearly mentioned above, when replacing PPh_3 with 2-pyridyldiphenyl phosphine (Ph_2Ppy), the activity and selectivity of palladium catalysed propyne carbonylation is significantly enhanced.

2-pyridyldiphenyl phosphine (Ph_2Ppy) is an unsymmetrical bidentate ligand with a nitrogen donor atom and a phosphorus atom that can connect two identical or different metal centers, see (Figure 1.2).[14]

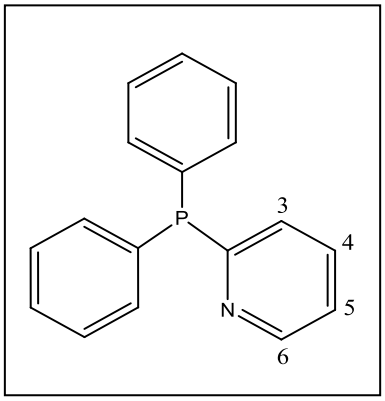

Figure 1.2. 2-pyridyldiphonylphosphine ligand.

Consequently, a study was undertaken to further investigate the effect of the presence and position of pyridyl group in the ligand in the hydroesterification of propyne (Table 1.1).[4, 12, 13]

Table 1.1. Effect of position of pyridyl in the hydroesterification[a] of propyne

Ligand	$Pd(OAc)_2$ (mmol)	T (^oC)	Average Rate (mol of propyne/mol of Pd h)	MMA sel. (%)
PPh_3	0.100	115	Approximately 10	89.0
4-$PyPPh_2$	0.100	90	Approximately 10	90.0
3-$PyPPh_2$	0.100	70	1000	99.2
2-$PyPPh_2$	0.100	45	40 000	98.9
2-$PyPPh_2$	0.012	115	5 000 000[b]	N/A

[a] Conditions: 30 ml of propyne, 50 ml of methanol, 60 bar CO, 3.0 mmol of ligand, 0.2 mmol of CH_3SO_3H; 2-Py = 2-pyridyl. [b] Note: Calculated by the author from the original data obtained at 45 ^oC by using an estimated 20 Kcal/mol activation energy.

Apparently, the pyridyl nitrogen is most effective in the 2-position giving optimal interaction with the metal center.[15]

1.2.3. Mechanistic studies

Both Drent[4] and Scrivanti[16], Dervisi and Tooze[17-19] proposed mechanisms, based on the large differences observed in catalyst characteristics when changing the ligand from PPh_3 to Ph_2Ppy. The proposal is that the active site of the palladium (II) catalyst contains two Ph_2Ppy ligands (Figure 1.3). One of the ligands is coordinated to the palladium (II) cationic centre through both phosphorus and nitrogen creating a four-membered ring structure, whilst the other Ph_2Ppy is monodentate coordinated through phosphorus only, henceforth called Pd-'chelate-monodentate' complex.

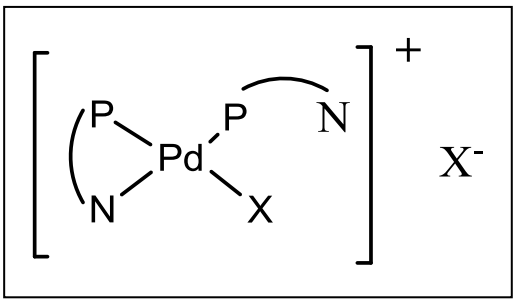

Figure 1.3. Active species as proposed by Drent[4].

It is suggested that in addition to stabilising the soluble palladium(II) catalyst complexes and adjustment of the electrophilicity of the palladium(II) centre, the Ph_2Ppy ligand plays a crucial role in both the selectivity and rate determining step.[4] This enormous kinetic effect has been attributed to the nitrogen base that is closely associated with the metal, which in turn enables the ligand to assist the chemical transformation. This shows the ligand assisted nature of the catalytic process.

Also, Drent[4] and Scrivanti[16] both report that an excess of strong acid that has weakly coordinating anions (such as, methanesulfonic acid) is required to protonate the nitrogen of a pendant pyridylphosphine ligand to achieve high activities in the hydroesterification of alkyne catalyst by Pd/PPh_2py. Drent[4] suggests that the protonated from of the pendant pyridyl nitrogen ligand ($P\text{-}NH^+$) satisfies a key role in the termination step by acting as a "proton messenger" in the methoxycarbonylation of alkynes (Scheme 1.9).

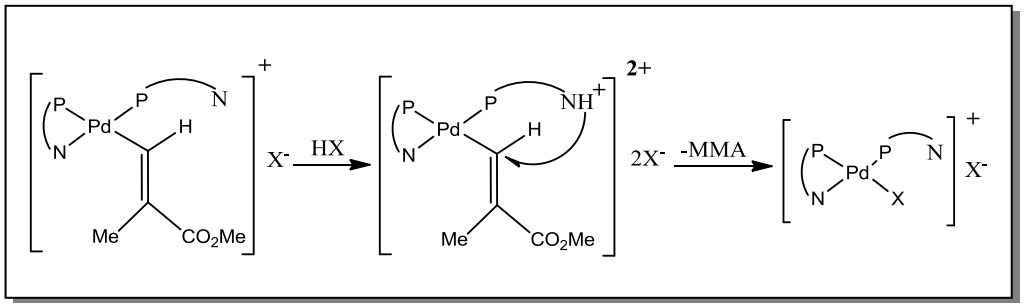

Scheme 1.9. Mechanistic of as proposed by Drent.

Scrivanti[16] suggest that a proton transfer from the pendant pyridyl nitrogen ligand (P-NH^+) is the initiation step of the methoxycarbonylation of alkynes (Scheme 1.10).

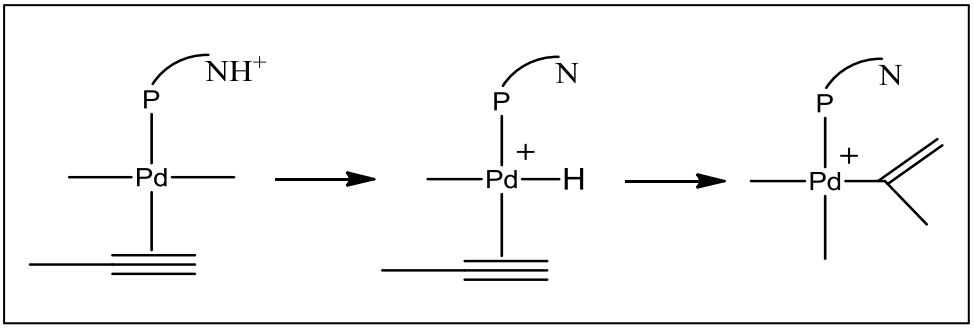

Scheme 1.10. Mechanistic of as proposed by Scrivanti.

1.3. Palladium catalysed carbonylation of alkenes

Interest in palladium catalyzed olefin carbonylation was re-awakened by the discovery of a class of highly efficient cationic palladium catalysts for CO/ethene carbonylation. Pd-catalysed carbonylation of olefins can be tuned to produce selectively esters by alkoxycarbonylation, or aldehydes (alcohols)[15], or ketones depending on the polarity of the solvent.

The methoxycarbonylation of ethylene in methanol is a homogeneous palladium catalyzed reaction for the production of methyl propanoate (MeP) (Scheme 1.11).

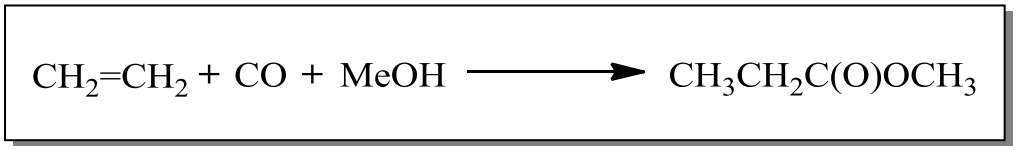

Scheme 1.11. Methoxycarbonylation of ethylene to MeP

In 1992, Drent found that the palladium complex L_2PdX_2 (L= 1,3-bis(di-*tert*-butylphosphine)propane (d^tbpp) a bulky bidentate ligand, X= $CH_3SO_3^-$) selectively catalysed the production of (MeP) when applied in ethene methoxycarbonylation.[20]

In 1996, Tooze reported that the (d^tbpx) ligand combined with $[Pd_2(dba)_3]$, gave an exceptionally active and selective system for the methoxycarbonylation of ethene to (MeP). This work represented a landmark achievement in terms of the stability, activity and reaction rate of (MeP) catalysts compared to those on PPh_3[21] and (d^tbpp)[20].

1.3.1. Mechanism of Methoxycarbonylation

Two mechanisms can be proposed for the methoxycarbonylation of alkenes (Scheme 1.12).

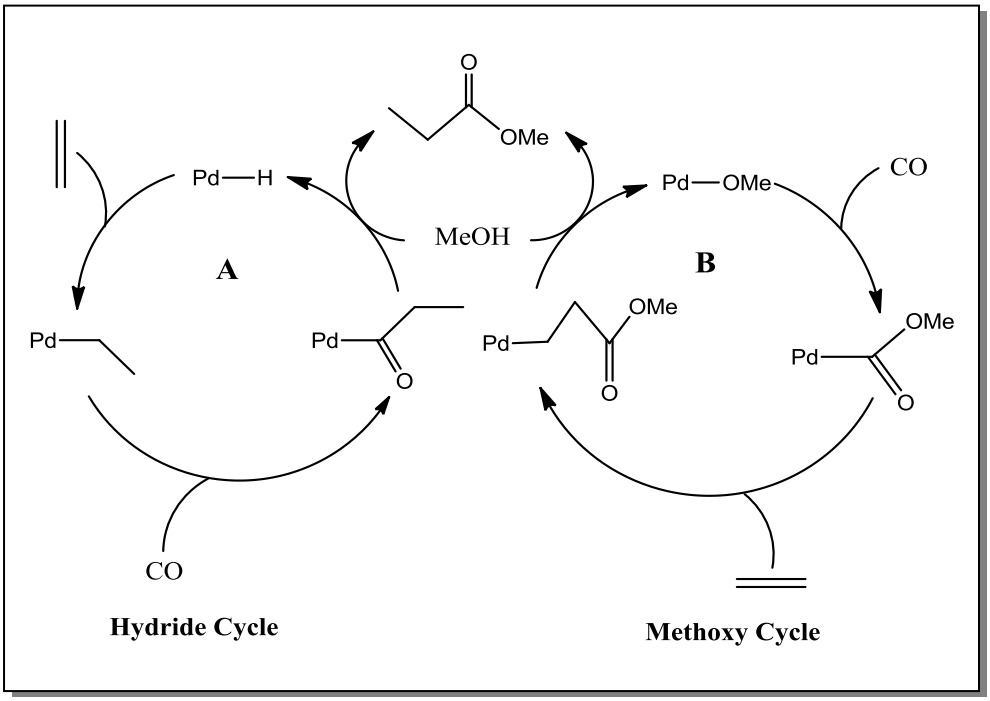

Scheme 1.12. The two mechanisms for the methoxycarbonylation of alkene.[3]

The hydride mechanism (**A**) starts with the formation of a palladium hydride complex formed by protonation of the palladium centre, ethene reacts immediately with the hydride complex, followed by insertion into the Pd-H bond, sequential coordination and insertion of CO leads to an acyl complex.

Inter- or intra-molecular nucleophilic attack of methanol on the acyl carbonyl leads to the formation of methyl propanoate and reformation of the palladium hydride species, completing the catalytic cycle.[22,23,24]

The methoxy mechanism (**B**) involves initial formation of a methoxcarbonyl complex.[25] Then, the migratory insertion of CO into a Pd-OMe bond is followed by coordination and insertion of ethene followed by methanolysis to give the product and regenerate the catalyst. [25]

The catalytically active species is thought to be a d^8 square-planar cationic complex $L_2Pd(H \text{ or } OCH_3)S$, where L_2 is the cis-coordination bidentate diphosphine ligand and S is solvent. The fourth co-ordination site at palladium is filled by an anion, a solvent molecule or mono-dentate ligand. The competition among all these species is very important for the catalysis and explains the sensitivity of the system to the choice of solvent and counterion.[26] *Cis*-chelation by the neutral diphosphine ligand is considered essential for placing the palladium-hydride or palladium-carbon bond in the catalytic intermediates *cis* to the fourth coordination site that is available to substrate molecules. This is an ideal situation for migratory insertion of the substrate molecules to generate intermediate Pd-alkyl and Pd-acyl species.[27] These steps will now be discussed in detail.

Initiation

There are two important initiation mechanisms that must occur, first formation of a Pd-OMe complex to initiate the methoxycarbonylation,[25] and second formation of a palladium hydride complex to initiate the hydride mechanism.[22]

A carbomethoxy-palladium complex can be generated from a palladium (II) salt, an alcohol, and carbon monoxide (by migratory insertion of CO into a Pd–OMe bond or by nucleophilic attack of methanol on coordinated CO) (Scheme 1.13).[25, 28]

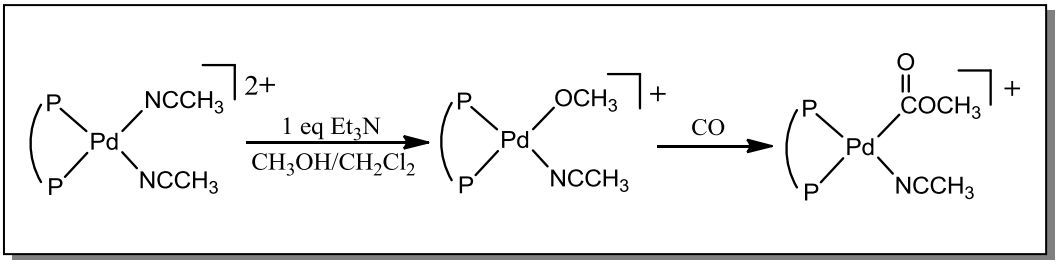

Scheme 1.13. Palladium carbomethoxy formation.

A more general route to carbomethoxy-palladium complexes involves the oxidative addition reaction of halides, such as benzyl chloride, to zerovalent palladium complexes followed by nucleophilic attack on a coordinated carbon monoxide molecule.[29] This latter method, although it cannot be relevant to the catalytic reaction, can provide access to putative catalytic intermediates.

Palladium hydrides can be generated both from zerovalent palladium complexes (oxidative addition) and from divalent palladium complexes (treatment with hydridic reagents).

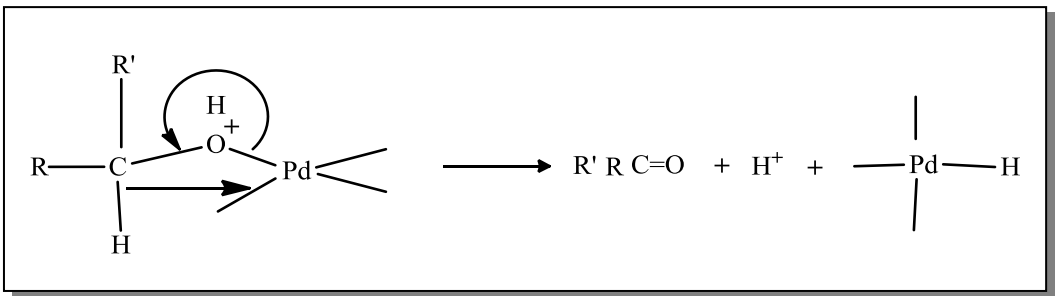

Scheme 1.14. Formation of a Pd-H initiator from a Pd (II) complex.

Formation of Pd-hydrides from the reaction of Pd (II) complexes and MeOH has been widely claimed as one of the possible routes to hydride species during the catalytic alkoxycarbonylation of ethene.[24] For example, the hydride initiator complex for the Lucite ALPHA process $[Pd(d^tbpx)H(MeOH)]^+$ can be obtained from the Pd(II) complex $Pd(d^tbpx)(\eta^1\text{-}TfO)_2$ in the absence of acid probably via β-hydride elimination from a molecule of alcohol co-ordinated to the metal, (scheme 1.14). Other methods include β-elimination reactions, ligand exchange, and heterolytic addition of H_2 to Pd (II) complexes.

C-C bond formation

C-C bond formation can be either by insertion of carbon monoxide into a Pd-alkyl bond (hydride cycle) and migratory insertion of ethene into the resulting Pd-acyl bond (scheme1.15) or olefin into a performed Pd-carbomethoxy bond (methoxy cycle scheme 1.16).[28]

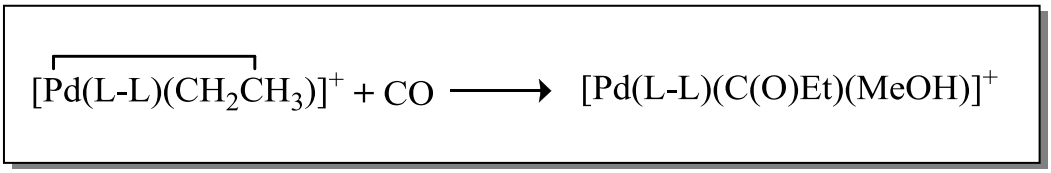

Scheme 1.15. Insertion of CO into a Pd-alkyl bond

The formation of $[Pd(L\text{-}L)(C(O)Et)(MeOH)]^+$ involves facile equilibria. The insertion of an olefin into a metal-carbon bond of a Pd- carbomethoxy intermediate was prospered to be the slowest (rate-determining) and irreversible step although subsequently Liu has shown this to be a facile reaction.[30, 31]

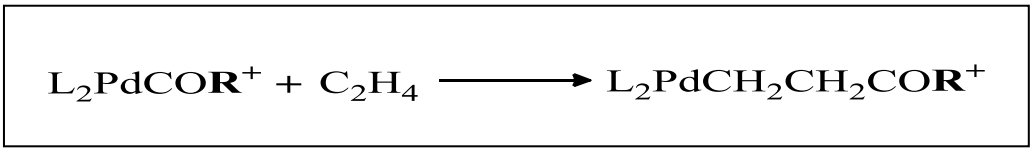

Scheme 1.16. Insertion of ethene into a Pd-carbon bond. The group **R** represents MeO

The reason for the perfect alternation is probably the stronger co-ordination of CO to Pd(II) compared with ethene. Once a palladium-alkyl is formed, the stronger CO co-ordination ensures that the next monomer to insert will usually be a CO molecule.[32] Naturally, CO co-ordinates more strongly to a palladium-acyl but since CO insertion is thermodynamically unfavourable,[33] the system will now wait for an ethene molecule to displace CO, to coordinate and insert. This competition between ethene and CO also explains the necessity of using a high C_2H_4/CO ratio, in order to have high rates of product formation.

Termination

The termination step is very important and can be crucial in achieving the desired ester product. There are three possible termination modes (A) *β*-hydride elimination yielding an unsaturated end group and is only relevant in co-polymerization catalysis (scheme 1.17) this mechanism has only been observed in non-alcoholic solvent,[34,35] (B) involves nucleophilic attack of methanol on an acyl intermediate, leading to an ester end group and Pd-H species (Scheme 1.18). Finally, (C) involves protonation of the metal center in a complex containing an alkyl intermediate followed by reductive elimination to form a keto end group and to initiate the carbomethoxy cycle (scheme1.19). Mechanism (A) and (B) are ending with new catalyst containing a metal hydride, whilst mechanism (C) is ending with a metal methoxy. Which of these possible pathways is dominant, depends on the nature the solvent, the anion (X^-), the ligand (L_2), and the presence of additional substrates such as (H_2).[36]

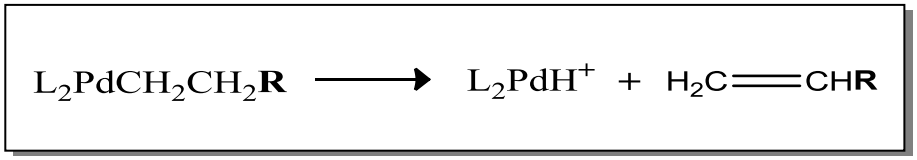

Scheme 1.17. (A) *β*-elimination from the growing polymer chain giving a vinyl end group.

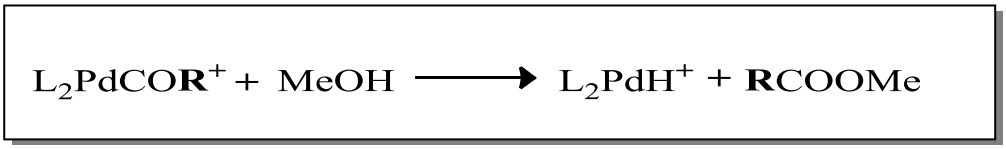

Scheme 1.18. (B) Methanolysis of an acyl gives an ester end group.

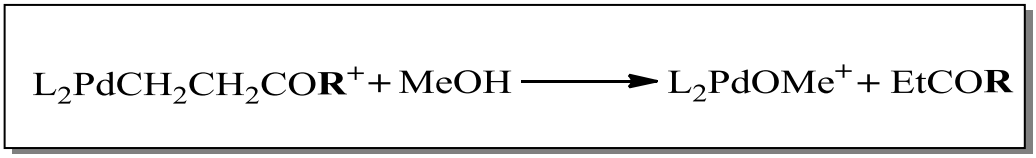

Scheme 1.19. (C) Protonolysis of an alkyl gives a keto end group.

The termination mechanism (B) is (alkoxycarbonylation) which relates to my project. This step includes alcoholysis of the first Pd-acyl in protic solvents and presumably requires a fairly electron poor metal center which leads to nucleophilic attack of methanol to give product (methylpropionate (MeP)) and new catalyst is containing a metal hydride.[3, 37] Curiously, electron rich metal centers tend to follow the hydride route, that means diphosphine ligand becomes unidentate at the first catalytic cycle, it is partly because of the tension between the high electron density on the metal complex afforded by the bidentate (ALPHA) ligand. Cole-Hamilton[29] proposed that one arm of the phosphine ligand decoordinates from the metal centre to give a three coordinate intermediate, with the acyl group *trans* with dissociating P; acyl groups have a very high *trans* influence and hence also a high *trans* effect in dissociative processes , the metal then becomes much lower in electron density leading to (i) coordinate of methanol to the vacant site much faster which than attacks the acyl carbon directly or (ii) protonates the free phosphine centre to generate a methoxy ligand on Pd. Elimination of ester and reforming of the hydride results. Steric crowding around the metal will be reduced and the ligand will return to the bidentate coordination to reinitiate the first stage or transfer of the proton from phosphorus to metal center and recoordination of the phosphine completes the methanolysis process.[23,37, 38]

Van Leeuwen[39] and Liu[40] report that the coordination of CH_3OH to the Pd centre is an essential prerequisite to methanolysis of the Pd-acyl bond, and that *cis*-coordination of alcohol and acetyl are needed to form an ester (methyl propanoate) by *intra*-molecular nucleophilic attack on the acyl carbon. In addition, the bulk of the bidentate ligand (d^tbpx) inhibits ethene coordination which becomes unfavourable; only CO or CH_3OH can coordinate cis to the acyl group. In its turn, elimination is also accelerated by an increasing steric bulk, and therefore, the fastest catalysts for making MeP use the bulkiest ligands like (d^tbpx).

1.4 Chemoselectivity

Organometallic catalysts consist of a central metal surrounded by organic or inorganic ligand. The properties of the catalyst are determined by both the metal and the ligands, this means that the selectivity and activity of an organometallic catalyst can be relatively easily adjusted by varying the ligand environment.

For example, variation of the ligand and anionic components can be used to control chemoselectivity in hydrocarbonylation of olefins by cationic palladium catalysts of the type under consideration in this thesis.

Ligands containing phosphorus as the donor element have found widespread application not only in organometallic chemistry but also in homogeneous catalysis in industrial applications. Phosphorus ligands like (ALPHA) have both (σ-basicity) electron donor and (π-acidity) electron acceptor electronic effects toward the metal, thus increasing the stability of complexes. In addition, the steric and bite angle effects of diphosphine can result in steric interactions that can change the energies of the transition states and catalyst resting states, therefore changing the activity or selectivity of the catalytic system.[27]

Increasing ligand basicity should lead to a decreasing electrophilicity of a metal center like palladium (II). Likewise, weaker acids (anion) are generally associated with increasing coordination strength of the anion to the palladium center.[41] Furthermore, the anion should be easily displaced from the coordination sites around the metal centre (e.g. palladium) by incoming reactants, strongly coordinating anions like halide may thus lead to inactive catalysts (poison). As a result, basic ligand and strong acids with non-coordinating anions are favoured in hydroesterification.

1.4.1. The Effect of Counterion on the Activity and Stereoselectivity of Palladium (II)

All reported homogeneous Pd based alkene hydroesterification of catalysts systems have an acid residue counterion either from the Pd^{2+} or from the acid

promoter; the nature of the counterion can considerably affect both the activity and selectivity. For example, Drent found that the rate of conversion of ethene to methyl propanoate is significantly influenced by the anion.[15] Also, in the hydroesterification of propyne to methyl methacrylate (MMA),[12,13] the large activity and relatively small selectivity differences of these reactions are dependent on the acid (Table 1.2)[15]

Table 1.2. Effect of acid type in the hydroesterification[a] of propyne

Acid type	Acid Intake (mmole)	Temperature (^oC)	Average Rate (mol (mol Pd)$^{-1}$ h^{-1}	Selectivity (% MMA)
CH_3SO_2OH	2.0	45	40,000	98.9
p-CH_3PhSO_2OH	2.0	45	20,000	99.1
$PhPO(OH)_2$	2.0	50	4,000	98.9
CH_3COOH	10.0	50	100	99.0
HCl	2.0	50	ca. 10	98.0

[a] Conditions: 30ml propyne, 50ml MeOH, 60bar CO, 0.025 mmol $Pd(OAc)_2$, 1.0mmol Ph_2Ppy

Extensive studies have shown that the counterion effect in terms of the catalytic performance, reaction rate and yield, in many cases is achieved through the competition between it and the substrate for coordination to the metal ion. When less strongly coordinating anions are used, better results are obtained.[42,43] Alternatively, the anion might affect the catalyst reaction through ion pairing in which no direct, covalent bond is formed between the anion and the cationic metal complex. NMR studies of ion-pairing in transition metal chemistry have appeared in the literature since the mid 1980s. In these studies Nuclear Overhauser Effect (NOE) NMR spectroscopy is used to detect inter-ionic dipolar interactions[44] between the atoms of the cations and those of the anions (counterion) in solution, which provides beneficial information about the interplay between inter-ionic weak interactions and the reactivity of complexes. In addition, semi-quantitative or quantitative NOE experiments allow inference of the relative anion-cation positions and orientations, when both moieties are unsymmetrical.[45]

PGSE (pulsed field gradient spin-echo) NMR experiments provide an estimate of the average magnitude of the ionic species present and, thus, the aggregation tendency.

Together the NOE and PGSE results provides a reasonable picture of how cations and anions interact in solution, the positive charge distribution together with ability of the anion to approach the positively charged positions (steric effects due to molecular shape), represent the determining factors in the extent of ion pairing. This helps to rationalize observed experimental anion effects in the case of transition-metal complexes when used in homogenous catalysis. In spite of the small size of such anions as (hydride or chloride ligand) compared with cation size that means the anion will not approach formally negatively charged donors.[46,47,48] For example, in the methoxycarbonylation of ethene using the Lucite catalyst, Pregosin *et al*[49] suggested that the stability of Pd(II)-hydride complex [Pd(dtbpx)H(MeOH)][OTf] (the active catalyst) might be dependent on coordination of the an ion pairing with the $CF_3SO_3^-$ anion H-bonding to the complexed solvent molecule. To test this idea, diffusion data for Pd(II)-hydride in methanol were collected at 240 K using ^{31}P (instead of ^{1}H) as a diffusion probe for the cation and ^{19}F for the anion. The results showed that the anion and cation diffuse independently i.e. there is no strong hydrogen bond between cation and anion in Pd(II)-hydride.

1.5. Characterisation of the catalyst

Both NMR and IR spectroscopy play a very important role in the study of the variation of the ligand environment surrounding a metal centre of a catalytic complex in a controlled way.

NMR spectroscopy is one of the most convenient techniques available for the characterisation of organometallic complexes, catalyst precursors and intermediates – via multinuclear characterization of species through analysis of chemical shifts and coupling patterns – and of chemical dynamics (degenerate exchange, reaction kinetics, diffusion).[50]

However, the inherent low sensitivity of NMR requires relatively high concentrations of samples to be used, often much greater than catalytic concentrations, and some species observed may not be involved in the catalytic process. However, the NMR signal normally reflects quantitatively the species present; therefore we can determine the concentrations of intermediates along with total mass balance and also concentration of starting materials and products without the need for prior knowledge of IR extinction coefficients – which is usually not available.

IR spectroscopy has several advantages over NMR: IR has high sensitivity; no need for high field superconducting magnets, low noise rf electronics are not required, an IR-cell can be used as an online detector connected to a reaction vessel. However, in addition to the problems of gas dissolution IR has the disadvantages that the structural information that can be obtained is much less than that for NMR.

An additional challenge is that many homogenous catalytic systems operate under gas pressure (10 to > 100 bar).

Many designs of high pressure NMR experimental systems for in situ studies of reacting systems in which gas is consumed have been developed, however, only a few laboratories in the world have these systems.[51, 52]

NMR spectroscopy is a resonance spectroscopy where transitions between quantized energy levels are excited and the frequency dependence of the absorption (or emission) of energy is monitored to produced a spectrum. The energy levels involved in NMR spectroscopy arise from the interaction of the nuclear spin with the spectrometer magnetic field, with the magnetic fields set up by other nuclear spins and with the magnetic fields set up by the electrons in the sample. The number of energy levels and transitions depend on the number of chemically distinct sites present and on the interactions between spins (spin-spin coupling). This means the NMR signal generally contains connectivity information carried by easily readable (through-bond) coupling patterns and constants, whilst energy level separation is determined by the environment and gives rise to the chemical shift.

The NMR phenomenon is based on the fact that nuclei of atoms have magnetic properties that can be utilized to yield chemical information. Quantum mechanically subatomic particles (protons, neutrons and electrons) have spin.

1.6. Dynamic processes and NMR

Dynamic NMR is one of the branches of NMR spectroscopy. NMR techniques can be used to determine e.g. whether molecular structure is rigid can rotation about the bonds in a molecule, or a change in conformation, occur? can ligands can migrate between different sites in a molecule.

Intramolecular processes that can be studied by NMR and are called *fluxional* processes. Intermolecular processes such as the exchange of bound and free ligands can also be studied by NMR and are called *exchange* processes.

These changes in the NMR spectrum are due to exchange between sites with different chemical shift and /or different coupling constant. The most important kind of information obtained in this way concerns the rate constants for the processes studies; the rate associated with the dynamics of discrete equilibria occurring in catalytic cycles (such as a reversible transformation taking place within the coordination sphere of a transition metal complex, or ligand dissociation) can be determined. Evidence for this type of degenerate exchange is usually observed in the form of temperature dependent changes in the NMR lineshape analysis which is one of several strategies available to determine the thermodynamic and kinetic parameters of a dynamic process. Use of an extended temperature range in conventional lineshape analysis improves the quality of the estimated activation parameters. The effect of exchange on coupling differs between a fluxional process and an intermolecular exchange process. In a fluxional process the ligand/migrating group is bonded at all times to the molecule and hence couplings are retained, an averaging of the coupling constant is seen in an intramolecular process.

In an intermolecular process, the bond between the exchanging group and the rest of the molecule breaks, and coupling is lost.

In NMR we can distinguish two limiting exchange regimes: (A) slow exchange that is much slower than the difference in resonance frequencies, a separate resonance at the characteristic resonance position is observed. (B) Fast exchange that is much faster than the difference in resonance frequencies, a single line is observed at the weighted average resonance position. Between the fast and slow motion regimes is the coalescence point where the separate resonance of the exchanging sites have just merged into a single peak. All these regimes depend on the temperature, we can change the rate of a dynamic process by altering the temperature; at low temperature the process will be slow like (A), whilst at high temperature the process will be fast like (B) and at intermediate temperature the lines first broaden then coalesce (Figure 1.4). in the fast exchange regime the line width becomes narrower as the rate of exchange increases.[53,54]

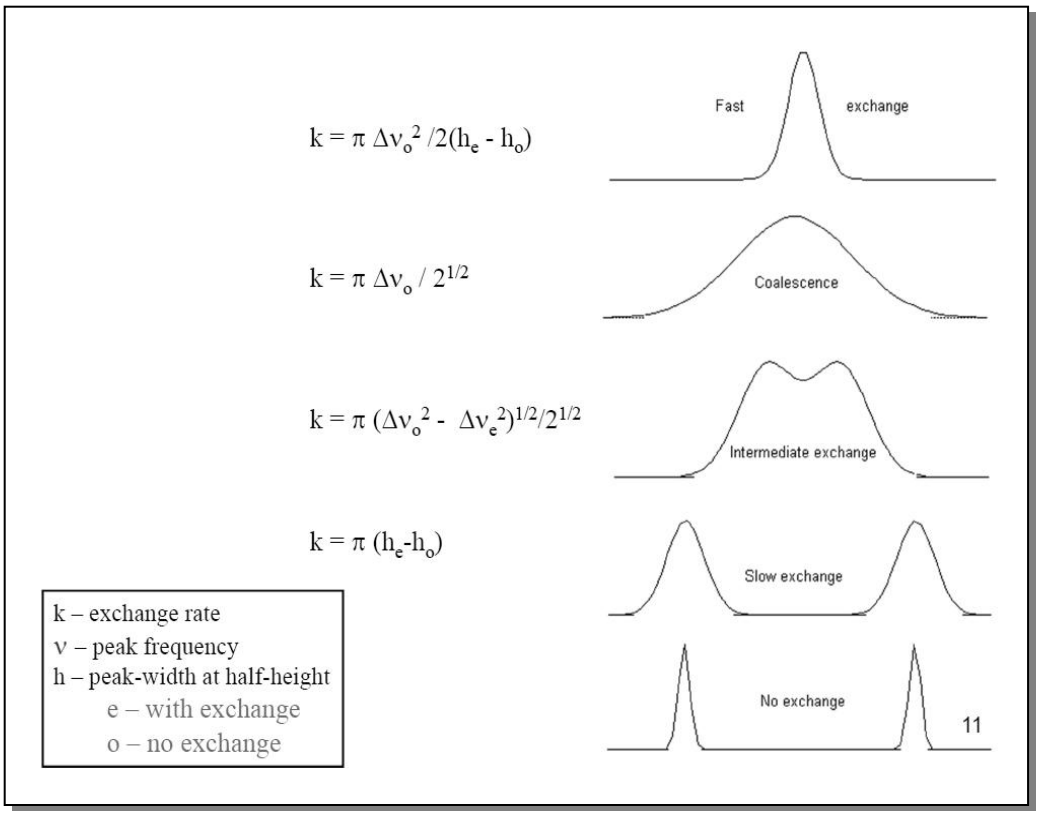

Figure 1.4. Effect of temperature on the resonances and the Exchange Rate

In calculating the average resonance position we must remember to take account of the number of each type of site participating in the exchange/fluxional process.

1.7. Aims of the thesis

1.7.1. Phosphino-Pyridine (PN) ligand

One aspect of this reaction (hydroesterification of alkyne) is the role(s) played by the pyridylphosphine ligand employed. This is now generally accepted to act as a proton transfer agent but may also act as a hemilabile ligand, protecting the catalytic site from decomposition. The nature of this hemilabilty is the focus of the chapter two.

1.7.2. Effect of alkane sulfonate

Methanesulfonic acid is used in the Lucite Alpha process to generate the hydride species in dry methanol via β-hydride elimination. However, the methanesulfonate anion stays in the reactor during the Lucite Alpha process, and forms estersulfonate as a result of reaction with MeOH solvent. This cannot easily be removed from the product steam, because, it has a boiling point very similar to the product (methyl propanoate). We were, therefore, interested in looking at the performance of other alkanesulfonic acids in the system and to study the synthesis of the catalyst precursors and the mechanistic work of alkene hydroesterification. This work is described in chapter three.

1.8. References

1. K. Nagai, *Appl Catal a-Gen*, 2001, **221**, 367-377.
2. k. Kida, *(Mitsubishi Gas Chemical Co. Ltd)*, 1999, **EP 941, 984**
3. W. Clegg, G. R. Eastham, M. R. J. Elsegood, R. P. Tooze, X. L. Wang and K. Whiston, *Chem Commun*, 1999, 1877-1878.
4. E. Drent, P. Arnoldy and P. H. M. Budzelaar, *J Organomet Chem*, 1993, **455**, 247-253.
5. J. happel, J. H. Blanck and Y. Sakakibara, *(standard Oil Co.), US*, 1970, **3,496**, 221.
6. J. Happel, S. Umemura, Y. Sakakibara, H. Blanck and S. Kunichika, *Ind. Eng. Chem., Process Desibn Develop.*, 1975, **14**, 44.
7. Noborn Kawata, Kosaka Honna and Hirozo Sugahara, *(Idemitsu Kasdan Co.), 1977, US 4055721*.
8. E. Drent, *(Shell)*, 1986, **EP 0186228**.
9. E. Drent, *(Shell)*, 1990, **EP 0386833**.
10. E. Drent, *(Shell)*, 1992, **EP 0495547**.
11. E. Drent and E. Kragtwijk, *(Shell)*, 1992, **EP 0495548**.
12. E. Drent, P. Arnoldy and P. H. M. Budzelaar, *J Organomet Chem*, 1994, **475**, 57-63.
13. J. Keijsper, P. Arnoldy, M. J. Doyle and E. Drent, *Recl Trav Chim Pay B*, 1996, **115**, 248-255.
14. J. P. Farr, M. M. Olmstead, F. E. Wood and A. L. Balch, *J Am Chem Soc*, 1983, **105**, 792-798.
15. G. Kiss, *Chem Rev*, 2001, **101**, 3435-3456.
16. A. Scrivanti, V. Beghetto, E. Campagna, M. Zanato and U. Matteoli, *Organometallics*, 1998, **17**, 630-635.
17. A. Dervisi, P. G. Edwards, P. D. Newman and R. P. Tooze, *J Chem Soc Dalton*, 2000, 523-528.
18. A. Dervisi, P. G. Edwards, P. D. Newman, R. P. Tooze, S. J. Coles and M. B. Hursthouse, *J Chem Soc Dalton*, 1999, 1113-1120.

19. A. Dervisi, P. G. Edwards, P. D. Newman, R. P. Tooze, S. J. Coles and M. B. Hursthouse, *J Chem Soc Dalton*, 1998, 3771-3776.
20. E. Drent and E. Kragtwijk, *Eur. Pat. Appl, ,* 1992 **EP 0495548**.
21. W. G. Reman, G. B. Deboer, S. A. J. Van Langen and A. Nahuijsen, *Eur. Pat. ,* 1989, **EP 0411721**.
22. W. Clegg, G. R. Eastham, M. R. J. Elsegood, B. T. Heaton, J. A. Iggo, R. P. Tooze, R. Whyman and S. Zacchini, *J Chem Soc Dalton*, 2002, 3300-3308.
23. W. Clegg, G. R. Eastham, M. R. J. Elsegood, B. T. Heaton, J. A. Iggo, R. P. Tooze, R. Whyman and S. Zacchini, *Organometallics*, 2002, **21**, 1832-1840.
24. B. A. Markies, D. Kruis, M. H. P. Rietveld, K. A. N. Verkerk, J. Boersma, H. Kooijman, M. T. Lakin, A. L. Spek and G. Vankoten, *J Am Chem Soc*, 1995, **117**, 5263-5274.
25. J. K. Liu, B. T. Heaton, J. A. Iggo and R. Whyman, *Angew Chem Int Edit*, 2004, **43**, 90-94.
26. I. del Rio, C. Claver and P. W. N. M. van Leeuwen, *Eur J Inorg Chem*, 2001, 2719-2738.
27. E. Drent, J. A. M. Vanbroekhoven and M. J. Doyle, *J Organomet Chem*, 1991, **417**, 235-251.
28. Z. Z. Jiang and A. Sen, *J Am Chem Soc*, 1995, **117**, 4455-4467.
29. R. I. Pugh and E. Drent, *Catalytic Synthesis of Alkene-Carbon Monoxide Copolymers and Cooligomers, Vol. 27 (ed,: A. Sen), Kluwer, Dordrecht*, 2003.
30. T. W. Lai and A. Sen, *Organometallics*, 1984, **3**, 866-870.
31. E. Drent, J. A. M. v. Broekhoven and P. H. M. Budzelaar, *Applied Homogeneous Catalysis with Organometallics compounds*,, ed. B. Cornils and W. A. Herrmann, VCH, 1996.
32. F. C. Rix and M. Brookhart, *J Am Chem Soc*, 1995, **117**, 1137-1138.
33. A. Sen, J. T. Chen, W. M. Vetter and R. R. Whittle, *J Am Chem Soc*, 1987, **109**, 148-156.

34. W. Keim, H. Mass and S. Mecking, *Z Naturforsch B*, 1995, **50**, 430-438.
35. E. Drent, J. A. M. vanBroekhoven and P. H. M. Budzelaar, *Recl Trav Chim Pay B*, 1996, **115**, 263-270.
36. E. Drent and P. H. M. Budzelaar, *Chem Rev*, 1996, **96**, 663-681.
37. G. R. Eastham, R. P. Tooze, M. Kilner, D. F. Foster and D. J. Cole-Hamilton, *J Chem Soc Dalton*, 2002, 1613-1617.
38. T. G. Appleton, H. C. Clark and L. E. Manzer, *Coordin Chem Rev*, 1973, **10**, 335-422.
39. P. W. N. M. van Leeuwen, M. A. Zuideveld, B. H. G. Swennenhuis, Z. Freixa, P. C. J. Kamer, K. Goubitz, J. Fraanje, M. Lutz and A. L. Spek, *J Am Chem Soc*, 2003, **125**, 5523-5539.
40. J. K. Liu, B. T. Heaton, J. A. Iggo and R. Whyman, *Chem Commun*, 2004, 1326-1327.
41. Y. Koide, S. G. Bott and A. R. Barron, *Organometallics*, 1996, **15**, 2213-2226.
42. C. A. Reed, *Accounts Chem Res*, 1998, **31**, 133-139.
43. S. H. Strauss, *Chem Rev*, 1993, **93**, 927-942.
44. H. P. Mo and T. C. Pochapsky, *Prog Nucl Mag Res Sp*, 1997, **30**, 1-38.
45. A. Macchioni, *Eur J Inorg Chem*, 2003, 195-205.
46. M. Alajarin, A. Pastor, R. A. Orenes, E. Martinez-Viviente and P. S. Pregosin, *Chem-Eur J*, 2006, **12**, 877-886.
47. S. P. Smidt, N. Zimmermann, M. Studer and A. Pfaltz, *Chem-Eur J*, 2004, **10**, 4685-4693.
48. E. Martinez-Viviente and P. S. Pregosin, *Helv Chim Acta*, 2003, **86**, 2364-2378.
49. P. S. Pregosin, E. Martinez-Viviente and P. G. A. Kumar, *Dalton T*, 2003, 4007-4014.
50. D. C. Roe, P. M. Kating, P. J. Krusic and B. E. Smart, *Top Catal*, 1998, **5**, 133-147.
51. J. A. Iggo, D. Shirley and N. C. Tong, *New J Chem*, 1998, **22**, 1043-1045.

52. S. C. van der Slot, P. C. J. Kamer, P. W. N. M. van Leeuwen, J. A. Iggo and B. T. Heaton, *Organometallics*, 2001, **20**, 430-441.

53. F. A. Cotton and G. Wilkinson, *Advenced Inorganic Chemistry*, Wiley, Chichester, 1988.

54. J.A. Iggo, *NMR Spectroscopy in Inorganic Chemistry*, (Oxford university Press Inc., New York), United state, 1999.

Chapter Two

Coordination chemistry and dynamic processes of Pd(II) chelate complexes of 2-pyridyldiphenylphosphine in hydroesterification of alkyne

This work has appeared in DALTON TRANSACTIONS Volume: **39** Issue: **34** Pages: **7921-7935** DOI: **10.1039/b918162h** Published: 26th **July 2010.**
Title: **The synthesis of, and characterization of the dynamic processes occurring in Pd(II) chelate complexes of 2-pyridyldiphenylphosphine**.
Author(s): Jianke Liu, Chacko Jacob, Kelly J. Sheridan, Firas Al-mosule, Brian T. Heaton, Jonathan A. Iggo, Mark Matthews, Jeremie Pelletier, Robin Whyman, Jamie F. Bickley and Alexander Steiner.

Chapter Two

Coordination chemistry and dynamic processes of Pd(II) chelate complexes of 2-pyridyldiphenylphosphine in hydroesterification of alkyne

Part 1: Coordination chemistry of Pd(II) chelate complexes of 2- pyridyldiphenylphosphine

2.1. Introduction

In recent years, the coordination chemistry of chelated ligands containing mixed functionalities on transition metal centres has been an extremely active area of research.[1-7] In particular, a distinctive class of these ligands, which contain both substitutionally inert and substitutionally labile groups, has received considerable attention. These ligands, termed hemilabile ligands, have weakly chelating groups that are capable of temporarily coordinating to a transition metal centre in the absence of substrate. However, in the presence of substrate, the labile portion of the ligand can be displaced by in coming molecules to form a metal-substrate complex. In addition, the substitutionally inert portion of these ligands keeps them attached in close proximity to transition metal centres. Consequently, recoordination of the weakly chelating portion of the ligand can be achieved after a bound substrate molecule has been transformed into a more weakly bonding group or depleted from the reaction mixture such that the metal-substrate complex is no longer favoured. The bifunctional character of hemilabile ligands has been shown to be useful in a wide range of applications including homogeneous transition metal catalysis.

Jeffrey and Rauchfuss[8] in 1979 first introduced the concept of "*hemilabile* ligand" to describe a ligand which has a combination of hard and soft donor atoms e.g. phosphine-amine and phosphine-ether ligands that 'would bind well enough to permit isolation but would readily dissociate the hard end component, and therefore generating a vacant site for substrate binding', although there are a few earlier examples of ligands that contain mixed-bonding characteristics.[5, 9-12]

Since then, a wide range of hemilabile ligands of differing reactivities have been synthesised and complexed to various metal centres. There are some basic characteristics which are present in all hemilabile ligands, illustrated in (Scheme 2.1).[6, 13] Firstly, at least two donor atoms with different types of bonding groups (X & Y) are present in the ligand. Secondly, one group (X) bonds strongly to a metal centre while the other group (Y) is weakly bonding and can be easily displaced by incoming ligands or solvent (Z), that yet remains available for recoordination to the metal centre. Consequently, this displacement reaction can be a reversible process.

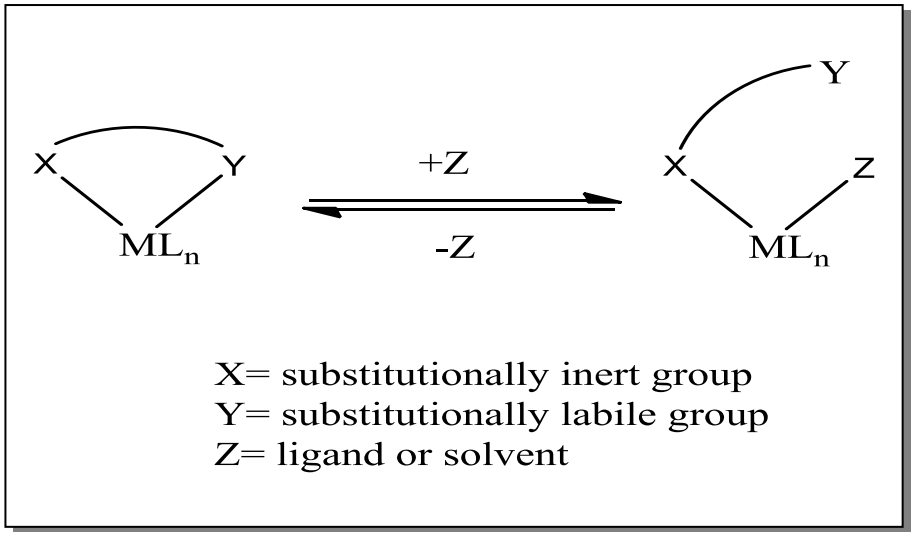

Scheme 2.1. Labile properties of hemilabile ligands.

A thermodynamically stable metal complex will have the substitutionally inert ligand group (X) binding to soft metals if (X) is a soft base, such as the case with phosphine base hemilabile ligands, or to hard metals if (X) is a hard base such as oxygen or nitrogen. In addition, the effect of changing the oxidation state of the metal in a complex must be taken into account when considering the binding properties of the labile donor atom (Y) in hemilabile ligands.

There is a variety of ways in which a hemilabile ligand can behave depending on: the nature of the ligand itself; the number of hemilabile donors coordinated to the metal and the metal complex to which it is coordinated. For example, if two or more hemilabile ligands are coordinated to a metal centre, a fluxional

process can occur that involves the dissociation and recoordination of the weakly bonding moieties via an intramolecular exchange process such as in the ether-phosphine Ru(II) complex shown in Scheme 2.2.[14] and the dichlorobis(*o*-(diphenylphosphino)anisole) ruthenium(II) complex in the original paper of Rauchfuss and Jeffrey, Scheme 2.3.[8]

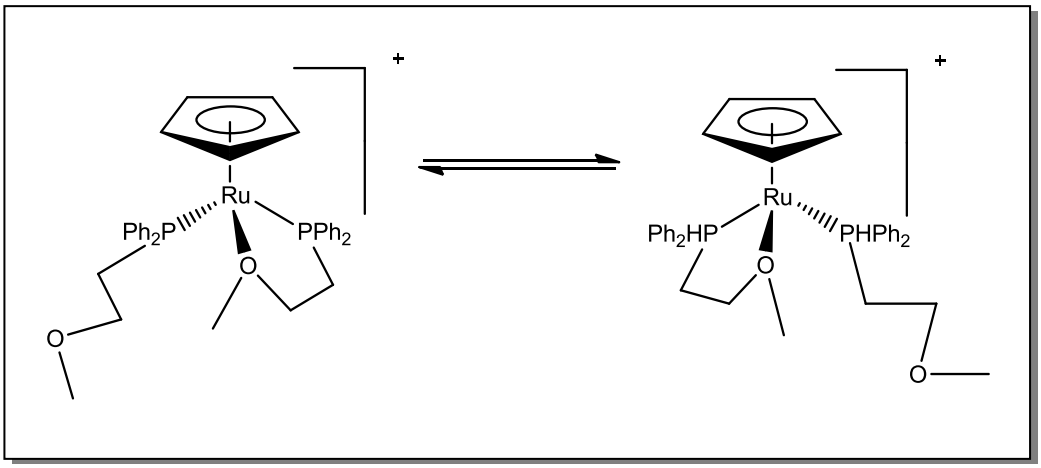

Scheme 2.2. Fluxional process of ether-phosphine ligand.

Reaction of the ruthenium (II) complex $[RuCl_2(\widehat{PO})_2]$ with CO at room temperature, initially gives a fluxional monomeric complex $[RuCl_2(P\sim O)(\widehat{PO})$ CO]. The fluxional process involves interchange of chelated and monodentate P,O ligands. Displacement of chelating P,O ligand by further CO results in the conversion of $[RuCl_2(P\sim O)(\widehat{PO})CO]$ to trans-$[RuCl_2(P\sim O)_2$ $(CO)_2]$, in which both P,O ligands are monodentate (Scheme 2.3).

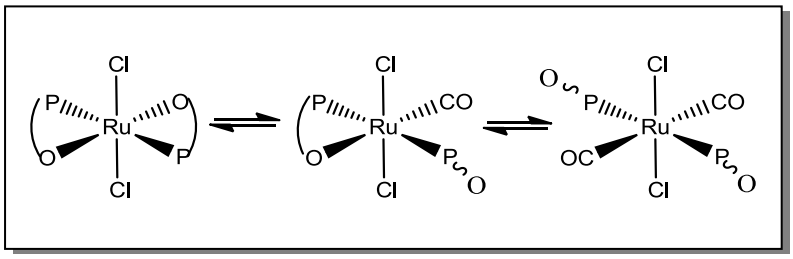

Scheme 2.3. Hemilabile of P, O ligand as observed by Jeffrey and Rauchfuss.

Ligand exchange reactions can also be observed in complexes containing hemilabile ligands, such as, equilibria between the weakly bonding group of a

hemilabile ligand and a coordinating counterion. For example, Chadwell *et al*[15] reported an exchange between a polydentate ether-phosphine ligand and two triflate counterions of an Fe(II) complex (Scheme 2.4).

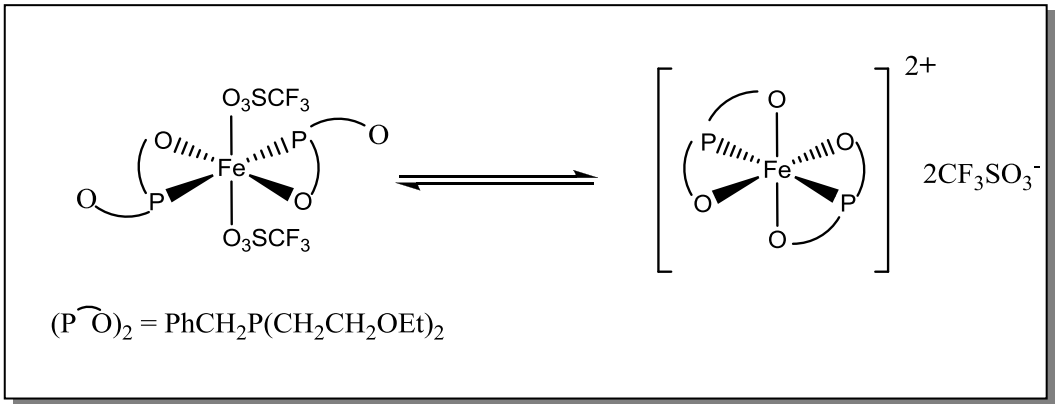

Scheme 2.4. Hemilability of ether-phosphine ligand

The complexation of substrates by organotransition metal compounds represents an important step in the course of catalytically operating process. Complexes which contain labile molecules have the ability to be transformed into reactive intermediates with an empty coordination site.[16]

2.1.1. Electronic properties of phosphine ligand

The tight moiety of hemilabile ligands is often a phosphine. Phosphines, and in particular tertiary phosphines, are one of the most versatile ligands that can bind to late transition metals, due to the formation of stable metal-phosphorus bonds.[17, 18]

Tertiary phosphines PR_3 (R=*alkyl, aryl*), are important because they constitute a series of ligands in which the electronic and steric properties can be altered in a predictable way over a very wide range by changing R.[19, 20] These ideas have found wide application not only in organometallic and inorganic chemistry but also in industrial applications of homogeneous catalysis. *Alkyl phosphines* are strong bases, and, as expected, are good σ-donors. Conversely, organo*phosphites* are strong π-acceptors and form stable complexes with electron rich transition

metals. However, they are also good σ-donors forming stable complexes with high-valent metals.

The σ-basicity and π-acidity of phosphorus ligands has been studied by looking at the stretching frequencies of the co-ordinated CO ligands in complexes. For example, Strohmeier[21] and Horrocks[22] compared phosphorus ligand properties by measuring the CO stretching vibrations in $((CH_3)_6C_6)Cr(CO)_2L$ (L = phosphorus ligand). Tolman formulated the ideas of electronic parameter and ligand cone angle to explain the electronic and steric effects of phosphorus ligands in the nickel/phosphite catalysed hydrocyanation of butadiene to adiponitrile[23] and Tucci has illustrated how changing the R group of the phosphine ligand can significantly alter the reaction result in cobalt hydroformylation (table 2.1).[24, 25]

Table 2.1. Hydroformylation of Hex-1-ene using $Co_2(CO)_3$/2L as catalyst precursor, (T = 160°C;$p \approx 71$ atm $H_2/CO = 1.2/1$[24])

L	*p*Ka	Electronic parameter* (ν cm^{-1})	Cone angle* (θ °)	k_r† x 10^3 (min^{-1})	Linear product (% total)	Aldehyde to alcohol ratio†
PPr^i_3	9.4	2059.2	160	2.8	85.0	---
PEt_3	8.7	2061.7	132	2.7	89.6	0.9
PPr^n_3	8.6	2060.9‡	132	3.1	89.6	1.0
PBu^n_3	8.4	2060.3	132	3.3	89.6	1.1
PEt_2Ph	6.3	2063.7	136	5.5	84.6	2.2
$PEtPh_2$	4.9	2066.7	140	8.8	71.7	4.3
PPh_3	2.7	2068.9	145	14.1	62.4	11.7

* Calculated from data in[23]

† calculated from data in [24]

‡ estimated

2.2. 2-pyridyl diphenylphosphine (Ph_2Ppy)

Heterodifunctional ligands containing both "soft" phosphorus and "hard" nitrogen donor are extremely useful in both coordination chemistry and homogenous catalysis due to the presence of two different donor atoms (P, N): the nitrogen atom has stronger σ-donor and weaker π-acceptor properties than the phosphorus atom. The π-acceptor phosphorus atom can stabilize the metal in

a low oxidation state, whereas the σ-donor of nitrogen has the ability to stabilize a higher oxidation state and makes the metal more susceptible to an oxidative addition reaction.[2, 3] Selective binding to metal ions of different types (hard and soft), may result in hemilabile behaviour via reversible dissociation of the weaker metal-ligand bond, thus generating a vacant site for substrate binding. This also can help to stabilize an intermediate oxidation state or geometries during a catalytic cycle.

Ph_2Ppy is an unsymmetrical potentially hemilabile bidentate ligand with a nitrogen donor atom. Palladium complexes of which afford extraordinary activity and high selectivity towards the formation of MMA in the methoxy-carbonylation of propyne.

The explanation for the enhanced catalytic activity of (Ph_2Ppy) vs (PPh_3) complexes is still not totally understood, and hence a general consensus regarding the catalytic reaction mechanism has, as yet, not been reached. Drent[26, 27] has proposed intermediates in which both phosphorus bound monodentate and chelating pyridylphosphines (henceforward called "chelate-monodentate" complexes) are present (Figure 2.1), and the ligand acts as a proton relay, to obtain high catalytic performance, while, Dervisi[28-31] suggested that the pyridylphosphine ligands are monodentate only and are not actively involved in the catalysis when the concentration of Ph_2Ppy is high in the reaction system. But, when the concentration of Ph_2Ppy is low, the pyridylphosphine ligands are coordinated as chelate, and it will be active in the catalysis reaction.

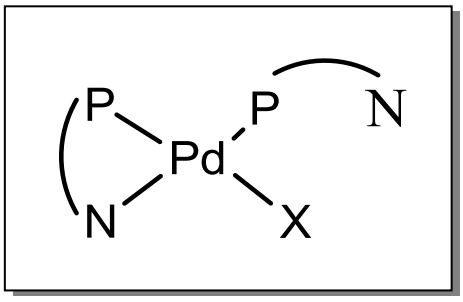

Figure 2.1. Structure of active catalytic species. N-P represents Ph_2Ppy ligand, X represents acidic anion.

One of the difficulties in establishing the mechanism of this catalysis is that the coordination chemistry of 2-pyridyldiphenylphosphine, Ph_2Ppy with palladium (II) has, surprisingly, been little explored.

The focus of this work was not ligand electronic and steric effects but the hemilability of 2-pyridyldiphenylphosphine (Ph_2Ppy), which, as shown above, has a dramatic effect on catalyst activity in palladium catalysed alkoxycarbonylation of alkynes.

Understanding the nature of the coordination mode of the ligand in the catalytic complex involved is fundamental to the understanding of the overall reaction mechanism.[31-35]

Balch and co-workers initiated work on the chemistry of (Ph_2Ppy) in the early 1980s, studying the synthesis, structure and reactivity of Ph_2Ppy-containing complexes.

A small number of chelating 4-membered ring complexes containing (Ph_2Ppy) of metals other than Pd(II) has been reported. The X-ray crystal structures of these complexes, reveal a highly compressed P-M-N angle, which is nearly 70^o, the other three angles consequently open up so that e.g. the P-M-L (L *trans* to N) is over 100^o and the other two angles are near the ideal 90^o.[32, 36-38] Within the chelate ring, there is also significant angular compression. Both the C-N-M and the N-C-P angles are reduced from the ideal value of 120^o and the C-P-M angle is reduced below the expected value of 109.5^o. In addition, the chelate P-C distance is longer than the non-chelate P-C distances. The ring strain in these chelated complexes render them unstable, thus the nitrogen donor is readily displaced from a low valent metal giving phosphorus bound monodentate complexes.[3]

This strained hemilabile coordination mode may play a key role in catalysis. Furthermore, the substitutionally inert portion can be used to change the selectivity of the transition-metal centre and the presence of the labile donor group may allow this part of the ligand to play a dual role.[39, 40]

Protonation of the pendant pyridyl nitrogen is proposed to be an important step in catalytic hydroesterification of alkyne using Pd/pyridylphosphine catalysts.[31, 41-43] The likelihood of pyridinium species being important in the catalytic

cycle is due to the presence of a strong acid with weakly coordinating conjugate base which was a necessary co-catalyst in this transformation (Scheme 2.5).[40]

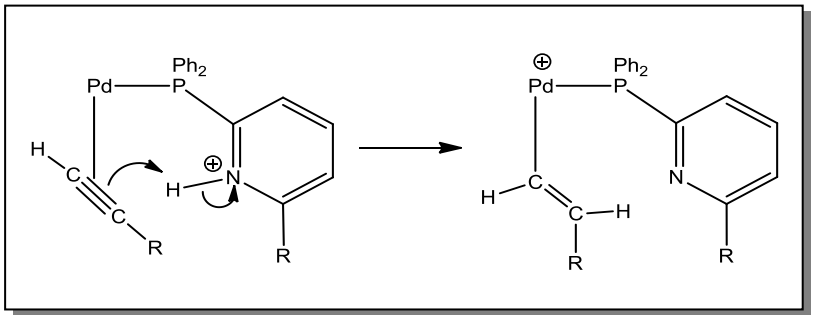

Scheme 2.5. One proposed role for bifunctional pyridylphosphine.

2.3. Synthesis of Pd(II) complexes with both chelating and monodentate (Ph_2Ppy) ligands

2.3.1. Formation of "Pd(κ^1-Ph_2Ppy)$_2$" precursors

Sheridan[44] has previously reported that the direct addition of (Ph_2Ppy) to [$Pd(PhCN)_2Cl_2$] in dichloromethane solution, with varying (metal: ligand) ratios of 4:1 to 1:2, gives mixtures of complexes. For example, the ^{31}P NMR spectrum (Figure 2.2) of the solution of a 1:1 mixture of (Ph_2Ppy) and [$Pd(PhCN)_2Cl_2$] , shows three sharp singlets.

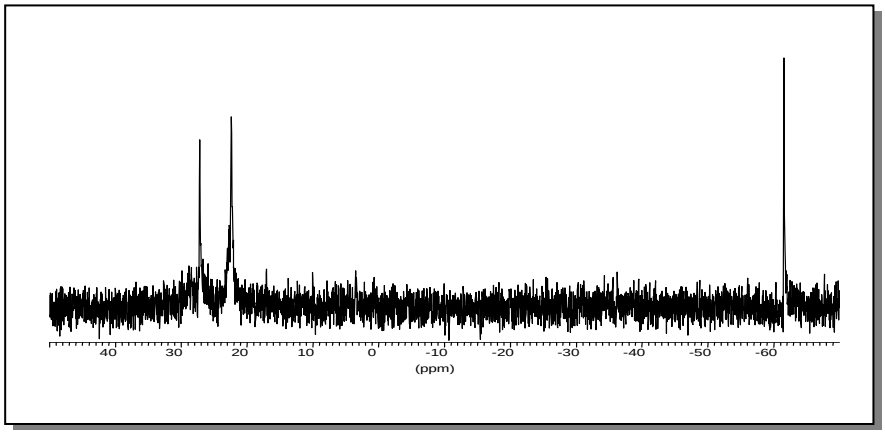

Figure 2.2. The $^{31}P\{^1H\}$ NMR spectrum recorded at 293 K of isolated product from the reaction of [$Pd(PhCN)_2Cl_2$] with 1 equivalent of Ph_2Ppy in CH_2Cl_2.

The two high frequency resonances, δ(P) 29.0 and 22.8 ppm, indicate (Ph_2Ppy) ligands bound through phosphorus only (*cf.* that of the free ligand δ(P) -4.5 ppm).[2] The chemical shift of the third resonance is at extremely low frequency, δ(P) -61.6 ppm and is characteristic of a strained, four-membered chelate ring.[45] Normally coordination of a phosphine ligand produces a shift of the ^{31}P resonance to high frequency relative to the free ligand, however, in the case of a four-membered chelate rings, there are large shielding effects which result in the ^{31}P resonance of the coordinated phosphorus atom occurring at low frequency relative to the free ligand,

The absence of coupling indicated only one type of phosphorus is present in each of the complexes and the three complexes were tentatively formulated as [Pd(κ^2-Ph_2Ppy)Cl_2], **1**, *cis*-[Pd(κ^1-Ph_2Ppy)$_2Cl_2$], **2a** (δ(P) 29.0 (s) ppm), and *trans*-[Pd(κ^1-Ph_2Ppy)$_2Cl_2$], **2b** (δ(P) 22.8 (s) ppm).[46-49]

2.3.2. Solvent assisted synthesis of "chelate-monodentate" complexes

Balch *et al*[50] have previously reported the existence of an equilibrium between phosphorus-bound monodentate *cis*[Pt(Ph_2Ppy)$_2X_2$] (X= I, Cl) and "chelate-monodentate" [Pt(κ^2-Ph_2Ppy)$_2$(κ^1-Ph_2Ppy)X][X] (X= I, Cl) complexes in chloroform solution. The position of the equilibrium shifts in favour of the cationic "chelate-monodentate" complex at low temperature, due, Balch suggested to the entropic contribution of two monodentate (Ph_2Ppy) ligands vs one monodentate (Ph_2Ppy) ligands becoming less significant at low temperature, consequently, ionization of halide from the platinum centre in [Pt(Ph_2Ppy)$_2X_2$] (assisted by intramolecular attack of a pyridyl nitrogen) in chloroform solution is feasible. This may reflect the greater propensity of square-planar platinum complexes to react by a dissociative pathway.[51] By contrast, Sheridan[44] found no evidence for the formation of a "chelate-monodentate" structure from the palladium complexes **2a/b** in dichloromethane at low temperatures. However, addition of a few drops of MeOH to a dichloromethane suspension of **2a/b** was found

to result in complete dissolution of the solid and $^{31}P\{^{1}H\}$ NMR spectroscopy revealed the formation of the cationic Pd(II)- "chelate-monodentate" complex [Pd(κ^2-Ph_2Ppy)(κ^1-Ph_2Ppy)Cl][Cl], **3**[Cl] (Scheme 2.6).

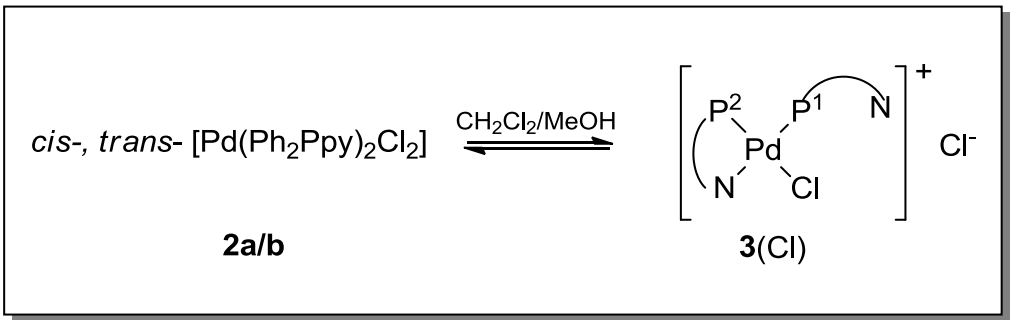

Scheme 2.6. Synthesis route to the ionic Pd(II) "chelate-monodentate"

The $^{31}P\{^{1}H\}$NMR spectrum of **3**(Cl) shows two broad sets of resonances at 293 K. Whereas, at 233 K the $^{31}P\{^{1}H\}$NMR spectrum (Figure 2.3) becomes two sharp doublets at δ(P) 44.4 (d) and -44.0 (d) ppm indicating a fluxional process is occurring, $^{2}J(P^{1}\text{-}P^{2})$ = 33.0 Hz indicating the presence of two mutually *cis*, inequivalent phosphorus atoms.

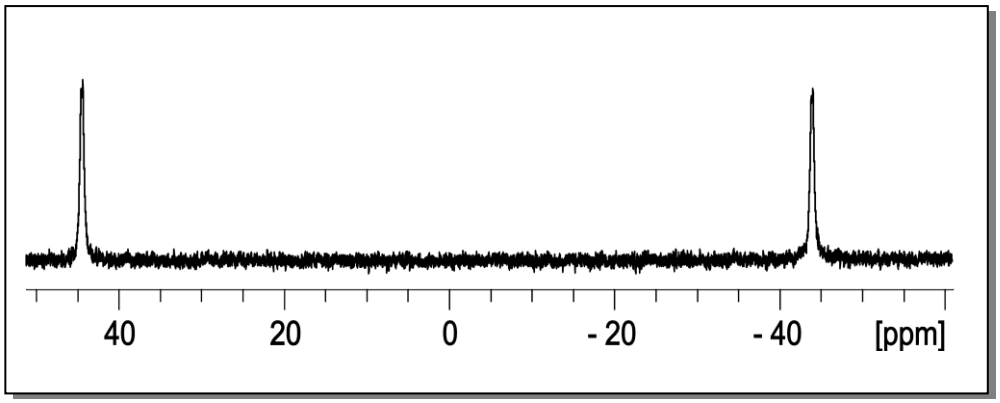

Figure 2.3. $^{31}P\{^{1}H\}$NMR spectrum, at 233 K, of [Pd(κ^2-Ph_2Ppy)(κ^1-Ph_2Ppy)Cl][Cl], **3**[Cl] in CH_2Cl_2/MeOH

The resonance at low field (high frequency) (δ(P) 44.4 ppm) is consequently assigned to the phosphorus of a monodentate pyridylphosphine ligand *trans* to the chelating nitrogen of the pyridine ring, P^1 in (Scheme 2.6). While, the

resonance at high field (very low frequency) (δ(P) -44.0 ppm) can be assigned to the phosphorus of a chelating Ph_2Ppy ligand[45] with P *trans* to Cl, P^2 (Scheme 2.6). We therefore decided to investigate further the possibility of using solvation of the anion for removing halide and substituting with other ligands.

Results and discussion

2.4. Preparation of "chelate-monodentate" complexes by removal of halide

The presence of a tightly bound halide ligand in the fourth coordination site at Pd(II) has been observed to suppress strongly the activity of the Pd centre in organometallic catalytic reactions. For example, Liu *et al*[52-54] recently have shown that the presence of a strongly coordinating ligand such as chloride at the metal centre can have a profound effect on the individual reaction steps in the carbonylation of alkene catalysed by Pd(II) diphosphine cations, by completely inhibiting the reaction by preventing coordination of other molecules such as carbon monoxide, ethene and methanol. Therefore, the preference is to use less tightly bound ligands for example (OTf^-, CH_3CN^-, $MeSO_3^-$, $CF_3CO_2^-$) (OTf = $CF_3SO_3^-$) over ligands such as chloride. Sheridan[44] showed that addition of the more polar solvent MeOH to CH_2Cl_2 solutions of **2a/b** aids the removal of bound chloride as a counterion resulting in the formation of the Pd(II)- "chelate-monodentate" complex, **3**[Cl]. However, the dynamic exchange process observed in **3**[Cl] indicates that Cl^- might re-enter the coordination sphere displacing the chelating nitrogen. Therefore, we tried to remove the coordinated chloride from **3**[X] and replace it with labile anions. The dynamic process in **3**[Cl] has also been further investigated.

Other counterions of salt **3** can be prepared by the addition of one to four equivalents of TIX (X = BF_4, OTf, $MeSO_3$) to a dichloromethane solution of **2** or to a dichloromethane-methanol solution of **3**[Cl], to give [Pd(κ^2-Ph_2Ppy)(κ^1-Ph_2Ppy)Cl][X], **3**[X], (X = BF_4, OTf, $MeSO_3$). The salts TIX (X = BF_4, OTf (CF_3SO_3), $MeSO_3$) we prepared by treating thallium carbonate with acid (HBF_4,

CF_3SO_3H, $MeSO_3H$). Tl^+ was used instead of Ag^+ due to thallium being superior to silver in at least two respects: (i) Tl^+ is less oxidizing than Ag^+; (ii) Tl^+ lacks the affinity of Ag^+ for neutral C, N, and P-donor bases, which prevents the decomposition of labile complexes via abstraction of ligands weakly coordinated to metallic centers. But, we should keep in mind that thallium compounds are very toxic and may cause alopecia.

The $^{31}P\{^1H\}$NMR spectra of **3**[X] in CH_2Cl_2 at 233 K reveals two sharp doublet at δ(P) 44.7 and –43.8 (+/–0.1) ppm with $^2J(P^1\text{-}P^2)$ = 38.2 Hz with only small counterion dependent shifts of the resonances, Table 2.2 (Figure 2.4), indicative of a "chelate-monodentate" structure being formed.

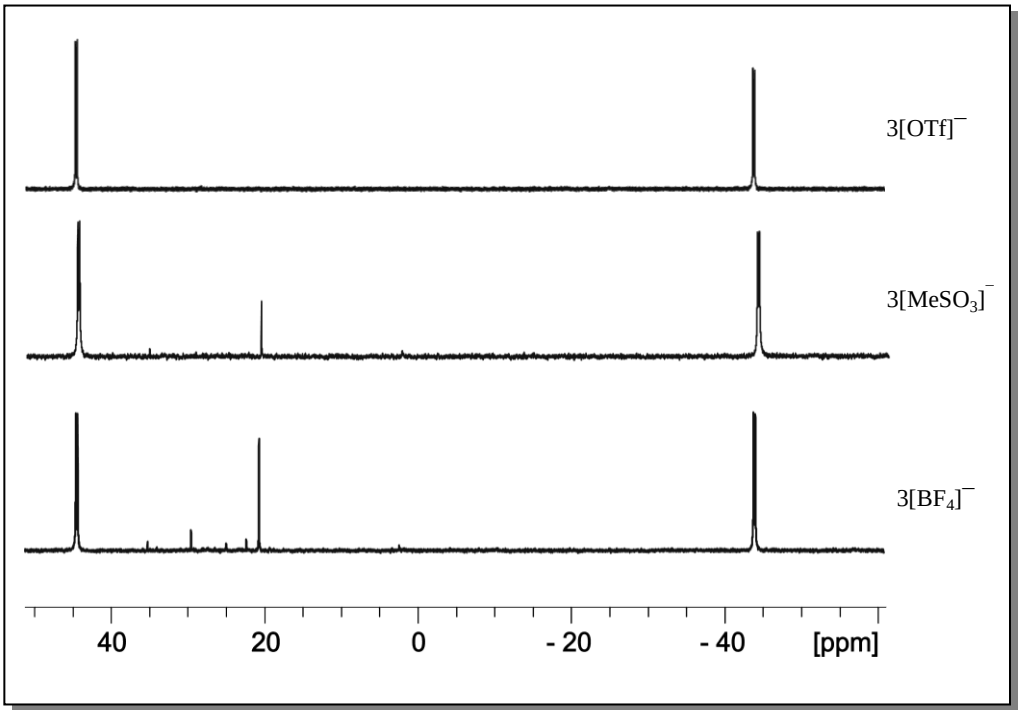

Figure 2.4. $^{31}P\{^1H\}$ NMR spectrum of **3**[X], (X = Cl, BF_4, OTf, $MeSO_3$) in CH_2Cl_2 /MeOH recorded at (top) 233 K.

Although, the position of the resonance and coupling constant is essentially the same in all four salts **3**[X] as is expected when only the counter ion is changed,[36, 37] the variable temperature behaviour exhibited in the $^{31}P\{^1H\}$ NMR spectra reveals a profound change in the rate of the exchange process which

enables the mechanism of the exchange reaction to be elucidated, see section 2.6.

2.5. Preparation of "chelate-monodentate" complexes from Pd(II) precursors

Although the procedure above allowed removal of one halide ion, the second remains coordinated to Pd.

It has been shown that halide salts interfere with palladium chemistry. Although we are able to exchange the counterion in salts such as **3**[Cl], we cannot be certain that the resulting solution does not contain traces of chloride and the coordinated chloride remains in the cation. Therefore, we investigated $Pd(OAc)_2$ as a precursor to "chelate-monodentate" complexes.

2.5.1. The role of the acid

As previously mentioned in chapter one, Drent[26] and Scrivanti[55] observed that in order to achieve high activities for the carbonylation of alkynes, an excess of strong acid over the stoichiometric amount was required to remove acetate as acetic acid from the palladium coordination sphere. In addition, once an excess of acid is present, studies show that the reaction order with respect to acid concentration is close to zero. It is thought that the acid may not, therefore, be directly involved in the termination step, but rather is required to protonate the nitrogen of the pyridyl phosphine ligand; the idea of a proton messenger has been put forward by both Drent[26] and Scrivanti[55].

Before attempting the synthesis of Pd complexes, we first investigated the protonation of Ph_2Ppy

2.5.2. Protonation of Ph_2Ppy

For comparative purposes, the ^1H and $^{31}P\{^1H\}$NMR spectra of the free Ph_2Ppy in CH_2Cl_2 were recorded prior to reaction with acid and after addition of one equivalent of HBF_4 to the solution. The ^1H NMR spectra at 298 K show that the

resonances of all the hydrogen atoms of the pyridyl moiety (δ(H-3Py) = 7.13 (d) ppm, δ(H-4Py) = 7.6 (t) ppm, δ(H-5Py) = 7.20 (t) ppm, δ(H-6Py) = 8.70 (d) ppm) move to the lower fields (δ(H-3Py) = 7.72 (d) ppm, δ(H-4Py) = 8.39 (t) ppm, δ(H-5Py) = 7.94 (t) ppm, δ(H-6Py) = 8.85(d) ppm) after addition of acid with the N-H of the pyridinium salt being a very broad featureless singlet at δ(H-1Py) = 11 ppm (Figure 2.5).[39]

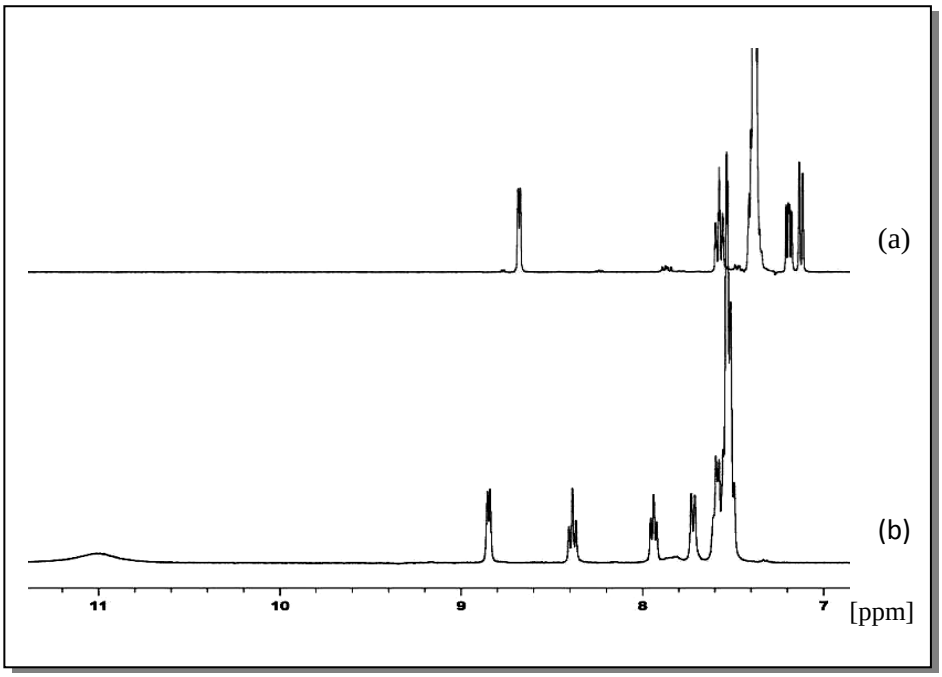

Figure 2.5. The ^{1}H NMR spectra of free Ph_2Ppy (a) without acid (b) with 1 eq HBF_4, in CH_2Cl_2 recorded at 298 K.

This observation is consistent with protonation at nitrogen and not phosphorus to give Ph_2PpyH^+ (Scheme 2.7).

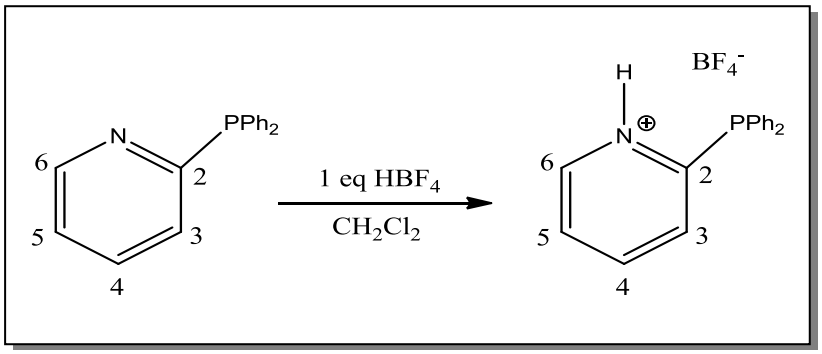

Scheme 2.7. Protonation of Ph_2Ppy.

The $^{31}P\{^{1}H\}$NMR spectrum shows a sharp singlet at δ(P) = - 7.8 ppm which has shifted upfield relative to the free ligand δ(P) = - 4.47 ppm. Although the phosphorus moves upfield upon addition of acid no P-H coupling is observed, indicating protonation has not occurred on the phosphorus atom. We, therefore, decided to further investigate the role of the acid by use of different types and equivalents of acids.

2.5.3. Protonation of palladium complexes of Ph_2Ppy

Addition of two equivalents of HX, (X = OTf, $MeSO_3$, CF_3CO_2) to a dichloromethane solution of $Pd(OAc)_2$ and two equivalents of Ph_2Ppy results in the formation of $[Pd(\kappa^2\text{-}Ph_2Ppy)(\kappa^1\text{-}Ph_2Ppy)(X)][X]$ (**4**[X]). The $^{31}P\{^{1}H\}$ NMR spectrum of **4**[X], recorded at 193 K in CH_2Cl_2 is consistent with the presence of a "chelate-monodentate" structure for the cation showing high field resonances δ(P) -39.3 (± 0.1) ppm, due to the phosphorus of the chelating Ph_2Ppy and a monodentate pyridylphosphine ligand resonating at low field δ(P) 40.8 ppm, (Figure 2.6). If excess acid is used in the synthesis, a different complex $[Pd(\kappa^2\text{-}Ph_2Ppy)(\kappa^1\text{-}Ph_2PpyH)(X)][X]_2$ (**4'** $[X]_2$), which is formed from (**4** [X]), is obtained.

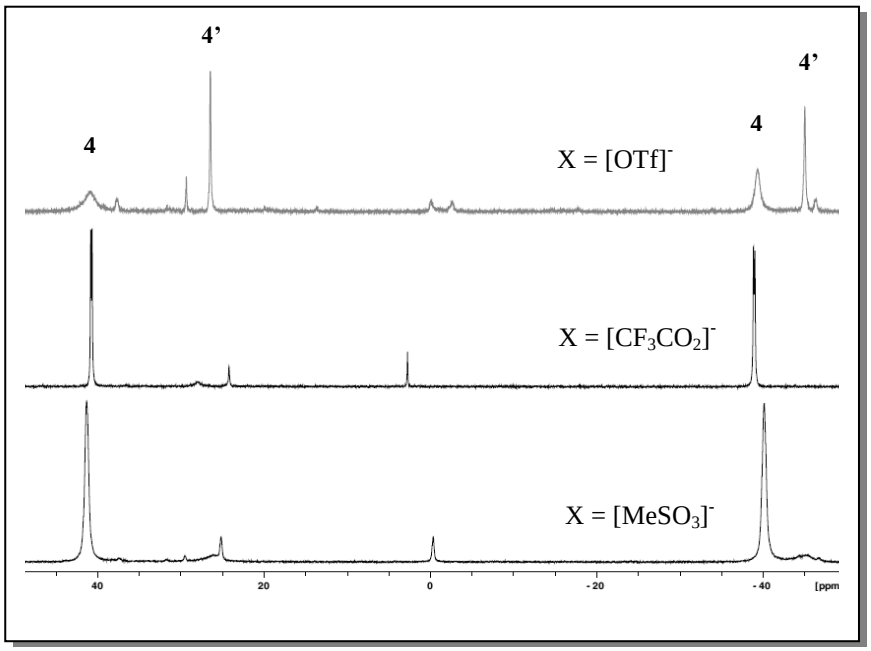

Figure 2.6. The $^{31}P\{^{1}H\}$ NMR spectrum of **4**[X], and the protonated analogues **4'**$[X]_2$, (X = OTf, CF_3CO_2, $MeSO_3$) in CH_2Cl_2 recorded at 193 K.

One anion of [X] is coordinated to the palladium centre and one anion [X] is present as a counterion.

4[X] and **4'**$[X]_2$ cations can coexist. Thus the complex **4'** $[MeSO_3]_2$ is obtained by addition of 3 equivalents of $MeSO_3H$ to a dichloromethane solution of $[Pd(OAc)_2]$ with 2 equivalents of Ph_2Ppy, but using ca. 2 equivalents of $MeSO_3H$ the $^{31}P\{^1H\}$ NMR spectrum reveals the presence of two complexes, in the ratio 8.5:1.5, the major complex showing resonances at δ(P) = 41.2, and -40.0 ppm, $^2J(P^1\text{-}P^2)$ = 29.8 Hz, for **4,** and the minor complex a pair of broad resonances at δ(P) = 26.0 and -45.8 ppm, for **4'** (Figure 2.6).

The ^1H NMR spectrum of **4'** $[MeSO_3]_2$ at 193 K shows a broad resonance at ca δ(H) = 17.1 ppm that integrates 1:1 against each H^6 proton of the pyridyl rings and is assigned to protonation at nitrogen (Figure 2.7).[46]

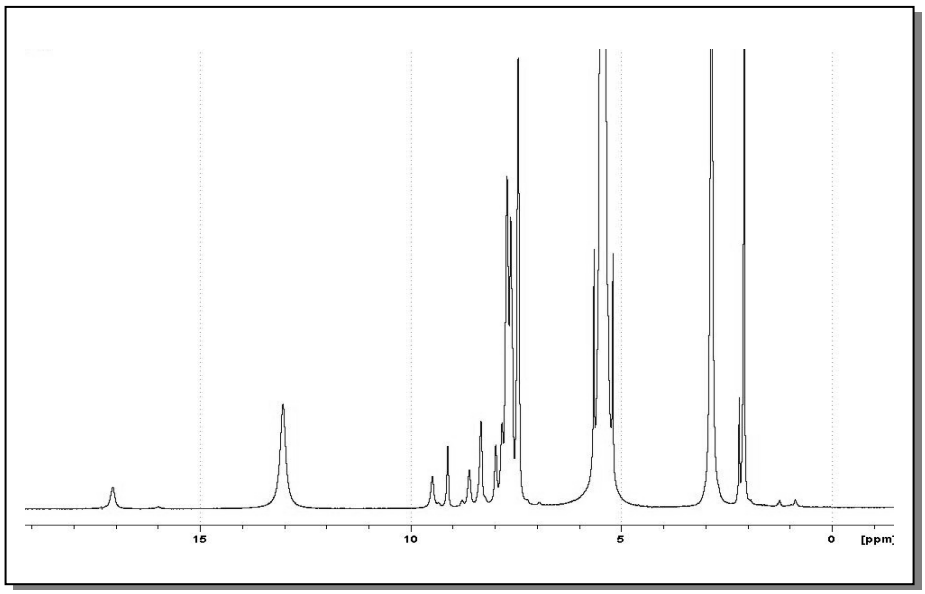

Figure 2.7. The ^1H NMR spectra of **4'** $[MeSO_3]_2$ in CH_2Cl_2 recorded at 193 K.

All of the proton resonances of the pyridyl moiety are shifted downfield in the same way, consistent with protonation of the nitrogen, for example the H^6 proton shifts from (H) = 9.17 to 9.48 ppm (Figure 2.8, 2.9).

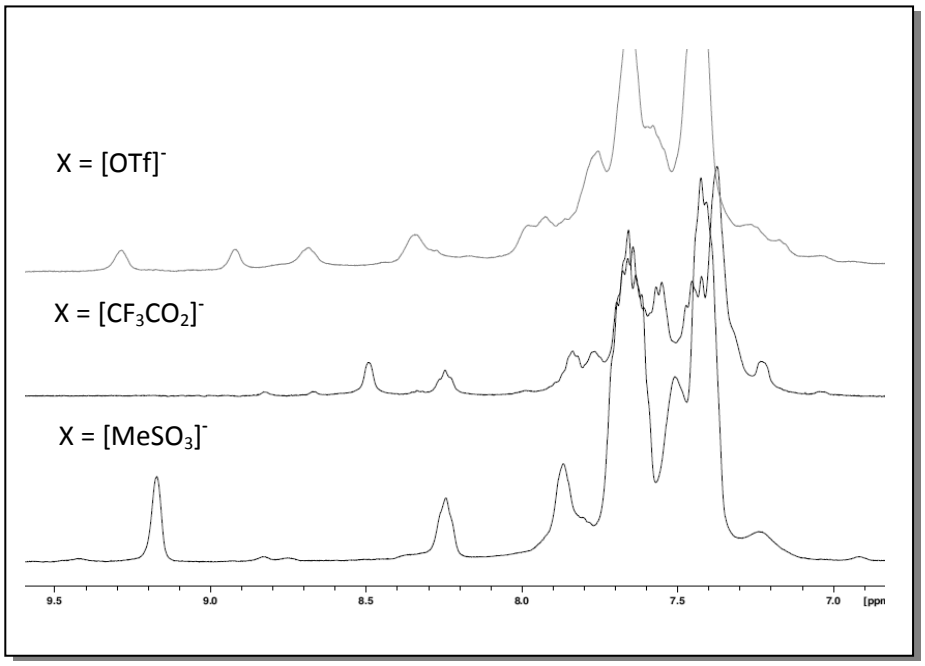

Figure.2.8. ^{1}H NMR spectra of **4**[X], (X = OTf, CF_3CO_2, $MeSO_3$) in CH_2Cl_2 recorded at 193 K.

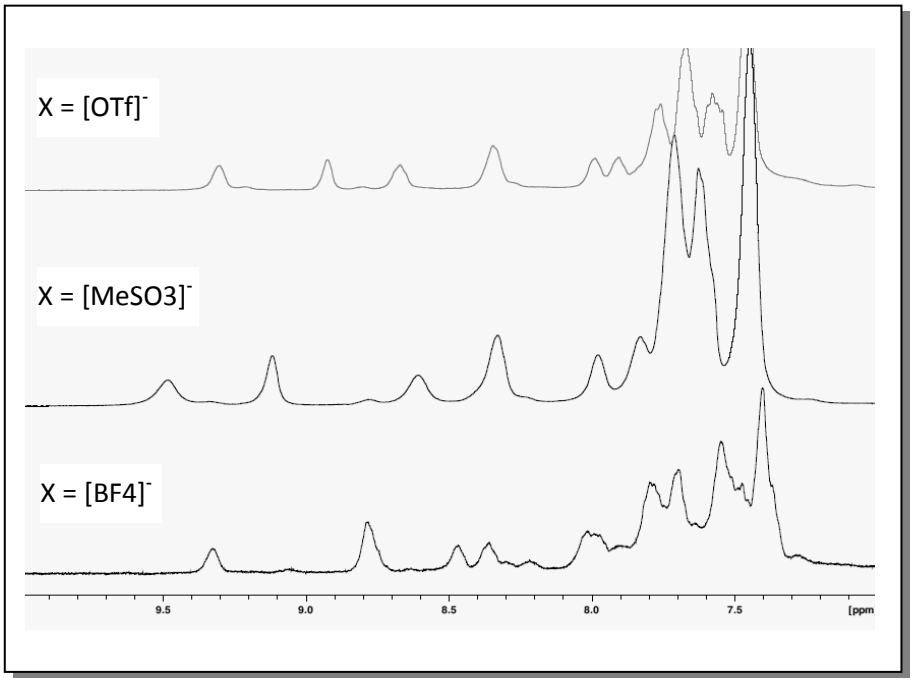

Figure.2.9. ^{1}H NMR spectra of **4'** $[X]_2$, (X = OTf, $MeSO_3$, BF_4) in CH_2Cl_2 recorded at 193 K.

Addition of further equivalents of HX, (X = OTf, $MeSO_3$, BF_4) results in the complete formation $[Pd(\kappa^2\text{-}Ph_2Ppy)(\kappa^1\text{-}Ph_2PpyH)(X)][X]_2$ (**4'** $[X]_2$). The $^{31}P\{^1H\}$ NMR spectra of **4'** $[X]_2$, recorded at 193 K in CH_2Cl_2 show slight variation with X (Figure 2.10).

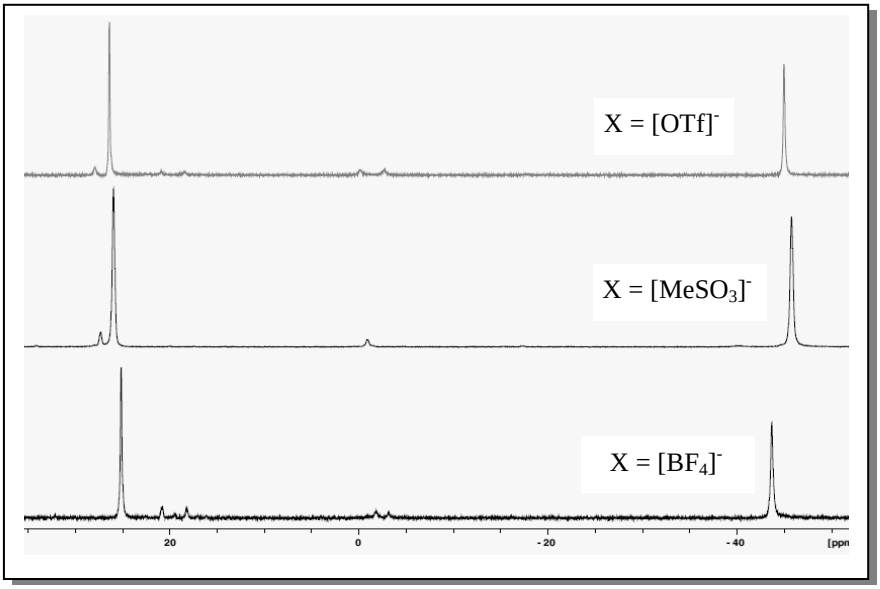

Figure 2.10. The $^{31}P\{^1H\}$ NMR spectrum of **4'** $[X]_2$, (X = OTf, $MeSO_3$, BF_4) in CH_2Cl_2 recorded at 193 K.

We have only been able to obtain impure oils or solids of **4**[X] and **4'**$[X]_2$ and the ^1H and ^{19}F NMR spectra of **4**[X] and **4'**$[X]_2$ are uninformative regarding the ligand in the fourth coordination site at Pd due to exchange of coordinated X and the counterion, (X = OTf, $MeSO_3$). However, the ^1H and ^{19}F NMR spectra of compounds containing the more coordinating trifluoroacetate anion are informative.

A complex analyzing for "$Pd(Ph_2Ppy)_2(CF_3CO_2)_2$" can be precipitated as a solid from solutions of Pd-acetate- Ph_2Ppy + CF_3CO_2H using Et_2O. The $^{31}P\{^1H\}$ NMR spectrum at 193 K (Figure 2.11a) of the redissolved solid in CH_2Cl_2 reveals the presence of two complexes, in the ratio 7:1, the major complex showing a broad singlet at δ(P) = 27.6 br ppm, indicating a bis-monodentate complex analogous to **2**, $[Pd(\kappa^1\text{-}Ph_2Ppy)_2(CF_3CO_2)_2]$ (**2**$[CF_3CO_2]$), whilst, the minor complex shows a pair of broad resonances at 40.8 and – 38.6 ppm,

indicative of a chelate-monodentate complex **4**[CF_3CO_2], addition of MeOH results in dramatic change in the amount of the two complexes (Figure 2.11b) indicating the eqn shown in (Scheme 2.8).

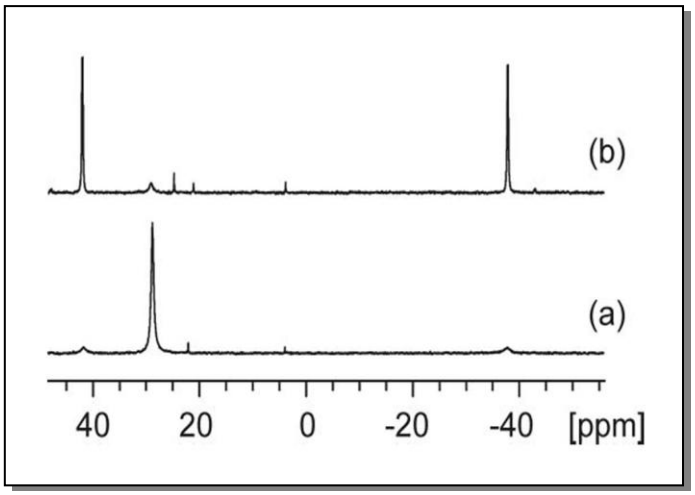

Figure.2.11. The $^{31}P\{^1H\}$ NMR spectra of "$Pd(Ph_2Ppy)_2(CF_3CO_2)_2$" at 193 K in (a) CH_2Cl_2 and (b) after addition of MeOH.

$$[Pd(\kappa^1\text{-}Ph_2Ppy)_2(CF_3CO_2)_2] \underset{}{\overset{+MeOH}{\rightleftharpoons}} [Pd(\kappa^1\text{-}Ph_2Ppy)(\kappa^2\text{-}Ph_2Ppy)(CF_3CO_2)][(CF_3CO_2)]$$

Scheme 2.8. Redistribution of [$Pd(\kappa^1$-$Ph_2Ppy)_2(CF_3CO_2)_2$] on addition of MeOH.

The ^{19}F NMR spectrum (Figure 2.12c) shows a sharp singlet at δ(F) = -75.9 and a broad asymmetrical resonance at δ(F) = -74.0 (*cf* [Et_3NH][CF_3CO_2] δ(F) = -76.1) (Figure 2.12d). The shift of the upfield resonance is consistent with the presence of a CF_3COO^- counterion, while the downfield shift of the former resonance is consistent with coordination to Pd, consistent with the presence of both[**2**$(CF_3CO_2)_2$] and **4**[CF_3CO_2] in the solution, (scheme 2.8), (*cf* Pd(acetate)$_2$ + CF_3CO_2H δ(F) = -74.6).

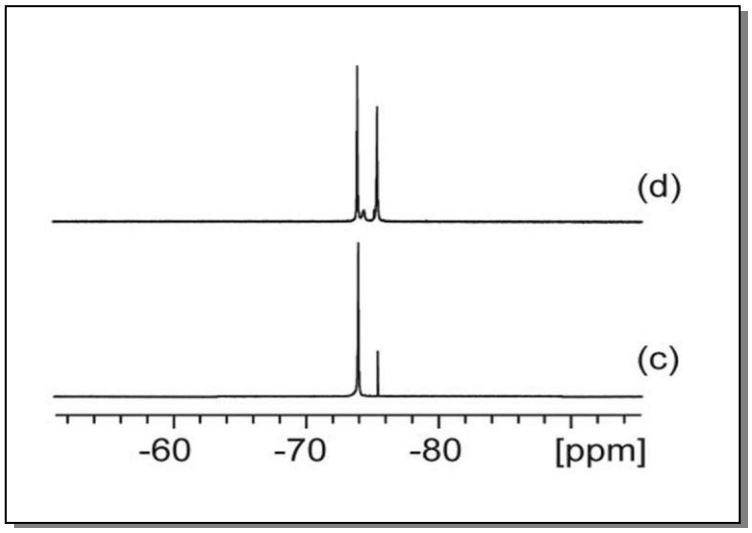

Figure.2.12. The ^{19}F NMR spectra of "$Pd(Ph_2Ppy)_2(CF_3CO_2)_2$" at 193 K in (c) CH_2Cl_2 and (d) after addition of MeOH.

Deconvolution of the ^{19}F NMR spectrum above affords a ratio of major complex (**2**): counterion of 7.5:1 consistent with the $^{31}P\{^1H\}$ NMR spectroscopic data. On addition of methanol to solvate any liberated $CF_3CO_2^-$ ions released into solution, changes are observed in the ^{19}F, $^{31}P\{^1H\}$, and the pyridyl region of the ^1H NMR spectra (Figures 2.12, 2.11, 2.9, 2.8) consistent with a change in the predominant coordination mode of the Ph_2Ppy ligands from *bis*-monodentate to chelate-monodentate. The ratio of [**2**(CF_3CO_2)] to **4**$[CF_3CO_2]$ determined by integration of the $^{31}P\{^1H\}$ NMR spectrum and by deconvolution of the ^{19}F NMR spectrum is 1:7 and 1:10 respectively, values in good agreement with (Scheme 2.8). These data are strongly indicative that the formulations of [**2**(CF_3CO_2)] and **4**$[CF_3CO_2]$, and of **4** more generally as $[Pd(\kappa^2\text{-}Ph_2Ppy)(\kappa^1\text{-}Ph_2Ppy)(X)][X]$ are correct. The formulation of **4'** as the protonated form of **4** is established by the ^1H and $^{31}P\{^1H\}$ NMR spectra discussed before.

For X = BF_4 a different complex is obtained on addition of two equivalents of HBF_4, the complex shows a single broad peak at $\delta(P)$ = - 42.9 ppm (Table 2.2) in the $^{31}P\{^1H\}$ NMR spectrum consistent with a chelating structure. This

complex is converted into **4'** $[BF_4]_2$ by addition of extra equivalents of HBF_4 and is tentatively assigned a bis chelating structure $[Pd(\kappa^2\text{-}Ph_2Ppy)_2]$ $[BF_4]_2$ **5**. Formation of **5** is attributed to the very low coordinating ability of the $[BF_4]^-$ anion, compare with **1** of $[Pd(\kappa^2\text{-}Ph_2Ppy)Cl_2]$ salt at δ(P) = - 61 ppm.

We mentioned before that **4'** $[MeSO_3]_2$ is obtained in CH_2Cl_2 solution. However, in MeOH, a different complex is formed. Thus, the addition of a few drops of CH_3SO_3H to the reaction mixture of $Pd(OAc)_2$ with 3.1 equivalents Ph_2Ppy results in an immediate colour change from yellow to red solution. The major species present in this solution is the previously unreported complex $[Pd(\kappa^2\text{-}Ph_2Ppy)(\kappa^1\text{-}Ph_2Ppy)_2][MeSO_3]_2$, (**6**), which is unstable in solution giving unidentified products on standing for a few days at RT. The $^{31}P\{^1H\}$ NMR spectrum of **6** at 183 K shows the presence of one chelating and two monodentate Ph_2Ppy ligands (Figure 2.13).

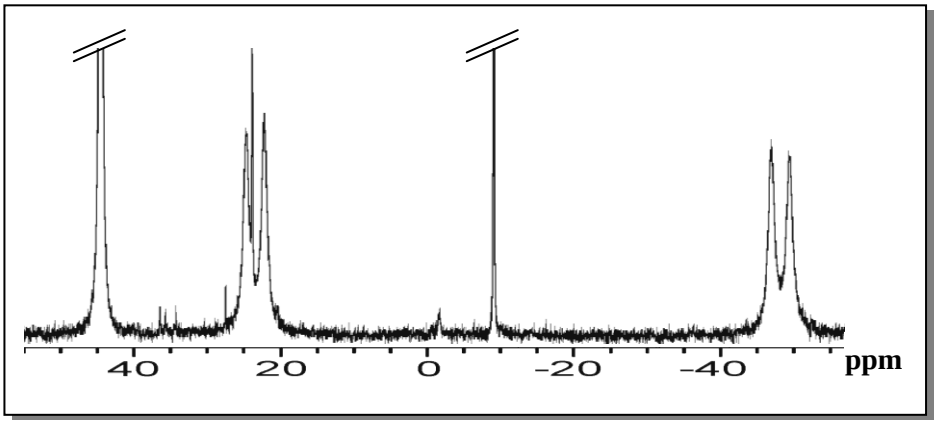

Figure 2.13 $^{31}P\{^1H\}$ NMR spectrum of **6** in MeOH at 183 K

The resonances at δ(P) 44.7 ppm (singlet), 23.6 (doublet) and -47.7 (doublet) ppm, $^2J(P^2\text{-}P^3)$ = 388 Hz, are consistent with the presence of two monodentate and one chelating Ph_2Ppy ligand respectively in the complex. It is not clear from the chemical shifts of the monodentate ligands, δ(P) 44.7 and 23.6 ppm if these ligands are protonated at the pyridyl nitrogen. The low frequency shift of the latter is consistent with such protonation but may also reflect the differing *trans* ligands. In the presence of excess acid, the excess of free PPh_2py ligand is protonated at the pyridyl nitrogen, resulting in a *ca.*

1.4 ppm low frequency shift of the ^{31}P NMR resonance to δ(P) -8.76 ppm. 2-pyridyldiphenylphosphine Ph_2Ppy is potentially a hemilabile ligand. Thus, for example, the complexes **3**, and **6** are dynamic in solution, as shown by variable temperature $^{31}P\{^1H\}$ spectroscopy of these complexes. Therefore, we began our investigations of these dynamic processes with these complexes.

Part 2: Dynamic processes of Pd(II) chelate complexes of 2-pyridyldiphenylphosphine

2.6. Dynamic process in square planar complexes

No molecule is strictly rigid; all molecules constantly execute a set of vibrations such that each atom oscillates with amplitudes of a few tenths of an angstrom about their average position. Moreover, there are molecules that are able to undergo rapid deformational rearrangements of much greater amplitude, so much so that atoms are able to change place with each other.[56] For example, rotation can occur about the bonds in a molecule, rings can spin or change conformation and ligands can migrate between different sites in a molecule. Such molecules are deemed to be stereochemically non-rigid. There are three recognised re-arrangements:

1. Isomerisation is an intramolecular rearrangement which changes the chemical equivalence in the resultant compound (Scheme 2.9).

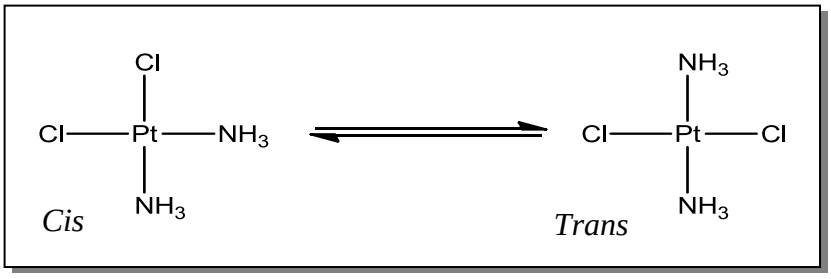

Scheme 2.9. *Cis-trans* isomerisation on square planar platinum

2. An intramolecular process which involves two or more chemically equivalent configurations (Scheme 2.10), this is called a fluxional process.

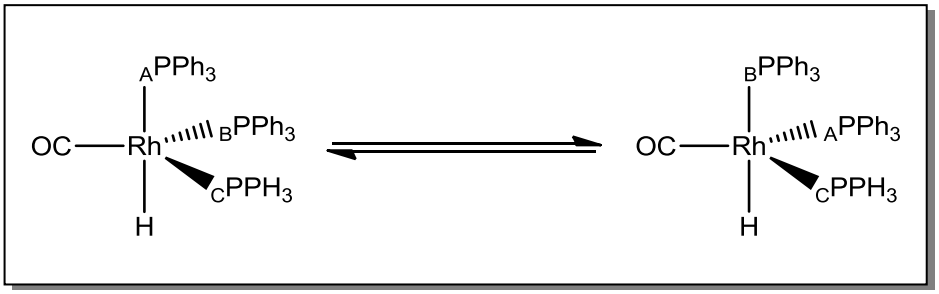

Scheme 2.10. Ligand migration, a fluxional process

3. An intermolecular process which involves two or more chemically equivalent configurations via the exchange of bound and free ligands (Scheme 2.11), this is called an exchange process.

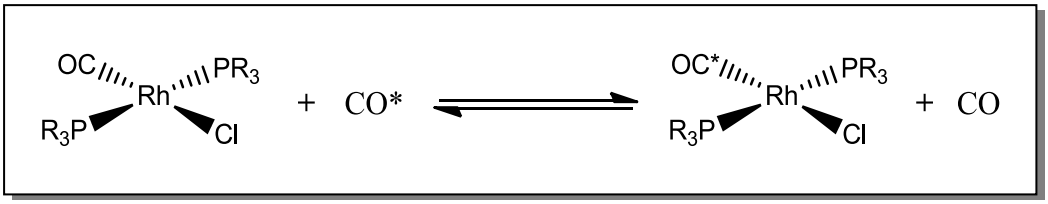

Scheme 2.11. Exchange process involving exchange of free and coordinated ligands

The intimate mechanism of substitution reactions in square-planar transition metal complexes has been studied for many years,[57-59] for example, water exchange reactions at *trans*-$[Pt(NH_3)_2T(H_2O)]^{2+}$ complexes (T = H_2O, NH_3, OH^-, F^-, Cl^-, Br^-, H_2S, CH_3S^-, SCN^-, CN^-, PH_3, CO, CH_3^-, H^-, C_2H_4). All reactions were found to have a TBP (trigonal-bipyramid) transition state. As the reaction proceeds, the entering ligand pushes the leaving ligand away from the square plane and weakens the metal-leaving ligand bond. At the same time, the entering ligand was found to shift away from the *trans*-directing ligand, reducing the electron repulsion between the entering ligand and the lone pairs on the central atom. The stability of the transition state structure is determined by both the σ-donation ability and π-back-bonding ability of the ligands.[59]

So far we have looked at how NMR spectroscopy can be used to determine a rigid molecular structure, but as mentioned in chapter one, NMR can be used to study intramolecular (fluxional) and intermolecular (exchange) processes.

When studying dynamic systems both the timescale of the method itself and also the frequency separation of resonances must be taken into account. In terms of NMR spectroscopy, the rate of exchange, *k*, of a given process is described as being slow or fast on the NMR timescale, that is slow or fast when compared to the difference in resonance frequencies, δv, of the exchanging nuclei. Altering the temperature of the system affects the exchange rate and these timescale. At low temperatures the rate of the process will be lessened, and it is now likely that the process is operating in the slow exchange regime in which the resonances in exchange are broadened but remain separate. The degree of broadening, Δv, depends on how much time the nuclei spend in each site, τ, and can be defined as, (Equation. 1).

$$\Delta v = \frac{k}{\pi} = \frac{1}{\pi\tau} \qquad (1)$$

Conversely, increasing the temperature will speed up any slow exchange processes which are occurring, moving them into the fast exchange regime. Fast exchange is the opposite extreme, when only a single line is observed at the mean resonance frequency. In this limit, the linewidth can be defined as, (Equation. 2).

$$\Delta v = \frac{\pi(\delta v)^2}{2k} = \frac{1}{2}(\delta v)^2\tau \qquad (2)$$

In contrast to slow exchange, the single resonance observed in fast exchange becomes narrower as the rate increases, due to the more effective averaging of the separate environments. In between these two extremes lies the coalescence

point, where the separate resonances of the exchanging sites have just merged into a single peak.

Consequently, we can follow the course of a dynamic process by studying it over a wide temperature range.

Exchange is characteristic of certain classes of organometallic compounds, such as complexes containing hemilabile ligands, which, in solution, undergo intramolecular exchange processes, e.g. Scheme 2.12 shows the dynamic behaviour of a bidentate phosphine-amine complex in which bound and unbound amino groups exchange at room temperature in CD_2Cl_2.[60]

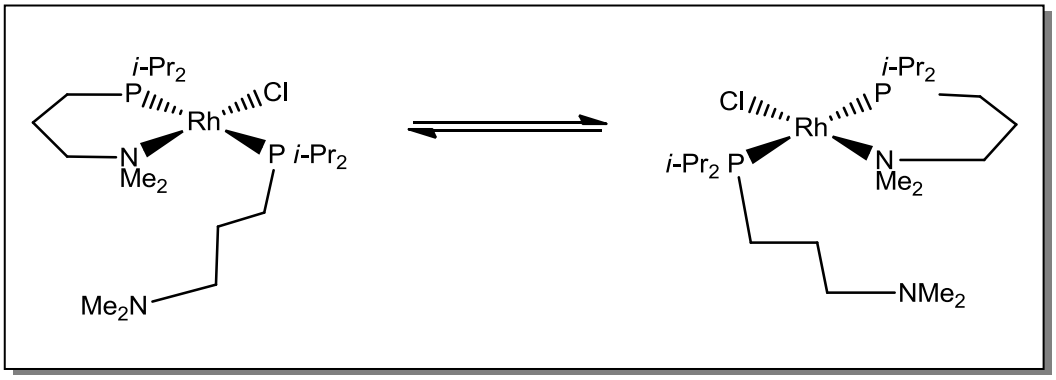

Scheme 2.12. Exchange process of phosphine-amine ligand.

The existence of an intermediate which can be detected (by spectroscopy, kinetic or product distribution studies) distinguishes these mechanisms from those where none can be seen. The latter are termed (***I***) (for **i**nterchange) mechanisms. The former are termed **D** (**d**issociative) if the leaving ligand is lost in the intermediate (*c.f.* S_N1 mechanism in organic chemistry), or **A** (**a**ssociative) if the entering ligand is coordinated in the intermediate. An ***I*** process is synchronous and as such has no intermediate, only a transition state. The transition state will determine both the rate and the stereochemistry of the reaction. Pure I reactions, however, will rarely occur and most likely there will be a preference for I_a (associative-interchange) or I_d (dissociative-interchange) respectively, in which the entering and leaving groups are either firmly I_a or weakly I_d embedded in the coordination sphere.

To distinguishing between mechanisms I_a and A, I_d and D in processes operating at square-planar 16-electron complexes is very difficult. From theory it might appear that square planar substitution would involve an associative mechanism. For both steric and electronic reasons exchange reactions would appear to proceed most readily by an expansion of coordination number to include the entering ligand. The metal is exposed for attack from two positions above and below the molecular plane. In addition, these low-spin d^8 systems have a vacant d_z^2 orbital of low energy which can help accommodate the pair of electrons donated by the entering ligand. Experience in palladium chemistry also tells us that T-shaped intermediate TS are unlikely to be abundant under catalytic conditions when high levels of coordinating molecules (L or S) are present.[51]

2.7. Derivation of thermodynamic parameters

The entropy of activation in the absence of complicating factors such as changes in solvation is determined largely by the loss of translational and rotational freedom as several particles come together in the activated complex. Important changes in vibrational freedom my also occur if the activated complex is more or less tightly bound than the reactants.[61]

The entropy of activation is defined by (Equation. 3):

$$\Delta v = k = \frac{k_B T}{h} e^{-\frac{\Delta H^{\ddagger}}{RT}} e^{\frac{\Delta S^{\ddagger}}{R}} \qquad (3)$$

Where *E*a is the Arrhenius activation energy and $\Delta H^{\ddagger}$, the enthalpy of activation in solution is given by (Equation. 4):

$$Ea = \Delta H^{\ddagger} + RT \qquad (4)$$

To derive the thermodynamic parameters necessary to determine whether the exchange process occurring in **6** are associative or dissociative an exchange-

calculation will be performed using the NMR simulator software package, gNMR. To obtain the rate constant **k** from which $\Delta S^{\ddagger}$ and $\Delta H^{\ddagger}$ can be obtained via an Eyring plot.

Results and discussion

2.8. Dynamic process in chelate-monodentate Pd(II) complexes of Ph_2Ppy

2-pyridyldiphenylphosphine Ph_2Ppy is potentially a hemilabile ligand. Thus, the complexes **3**(Cl), and **6** are dynamic in solution, as shown by variable temperature $^{31}P\{^{1}H\}$ NMR spectrum.

For understanding NMR spectra and the influence of Ph_2Ppy in the palladium catalysed hydroesterification of alkynes, we should know how these mechanism exchanges occur in solution.

There are two mechanisms that may be considered for any ligand exchange or any single step in a series of exchange processes. First, there is the dissociative (D) mechanism in which a ligand dissociates from the metal centre and the vacancy in the coordination sphere is taken by the exchanging ligand. The intermediate has a lower coordination number than both the reactant and the product (Scheme 2.13).

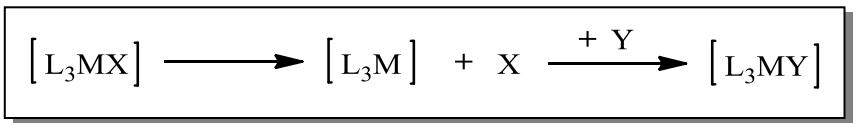

Scheme 2.13. Ligand exchange in square planar d^8 via a dissociative mechanism.

For example, dissociation of the chelating nitrogen ligand (P^1N) in **6**, followed by coordination of the nitrogen of a monodentate Ph_2Ppy ligand (P^2N or P^3N) (Scheme 2.14), constitutes a dissociative mechanism.

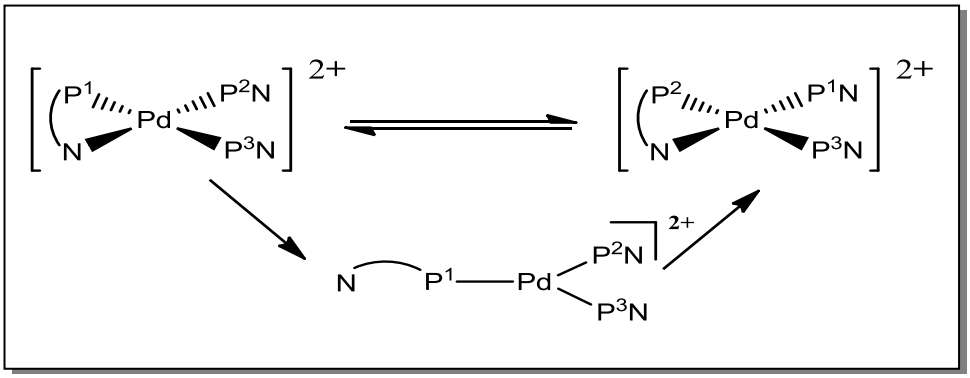

Scheme 2.14. Dissociative mechanism in **6.**

The other mechanism is associative (A), in this case the new ligand, Y directly attacks the original complex to form a five-coordinate intermediate in the rate determining step (Scheme 2.15). In contrast to a dissociative mechanism, in an associative mechanism the intermediate will have a higher coordination number than both the reactant and the product.

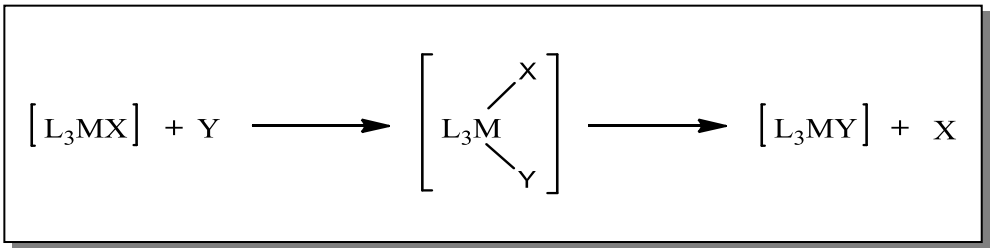

Scheme 2.15. Ligand exchange in square planar d^8 via an associative mechanism.

An associative mechanism in **6** could occur via either an intermolecular or intramolecular process. An intramolecular process may be the coordination of P^2N or P^3N followed by the dissociation of the nitrogen of P^1N (Scheme 2.16).

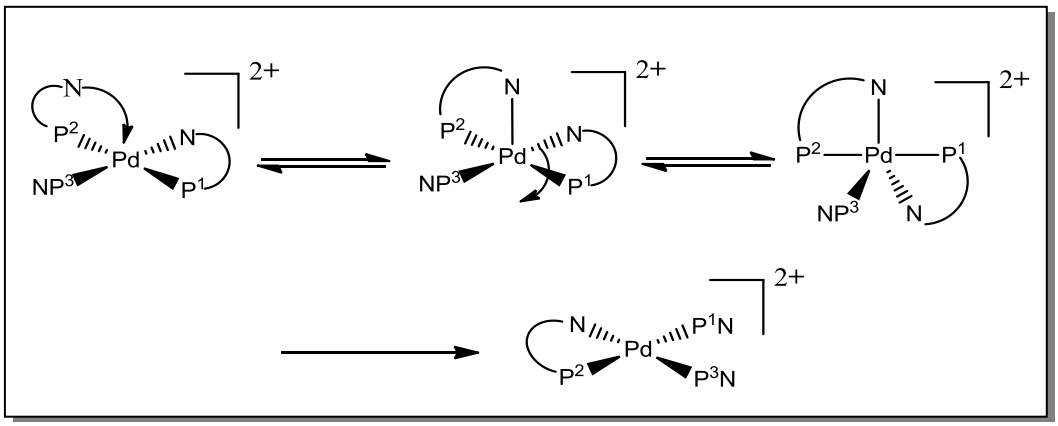

Scheme 2.16. Intramolecular associative mechanism in **6.**

Alternatively, coordination of an external ligand, such as a solvent or traces of excess Ph_2Ppy in solution, to the palladium centre, with subsequent dissociation of the coordinated nitrogen of P^1N constitutes an intermolecular associative mechanism, shown in Scheme 2.17.

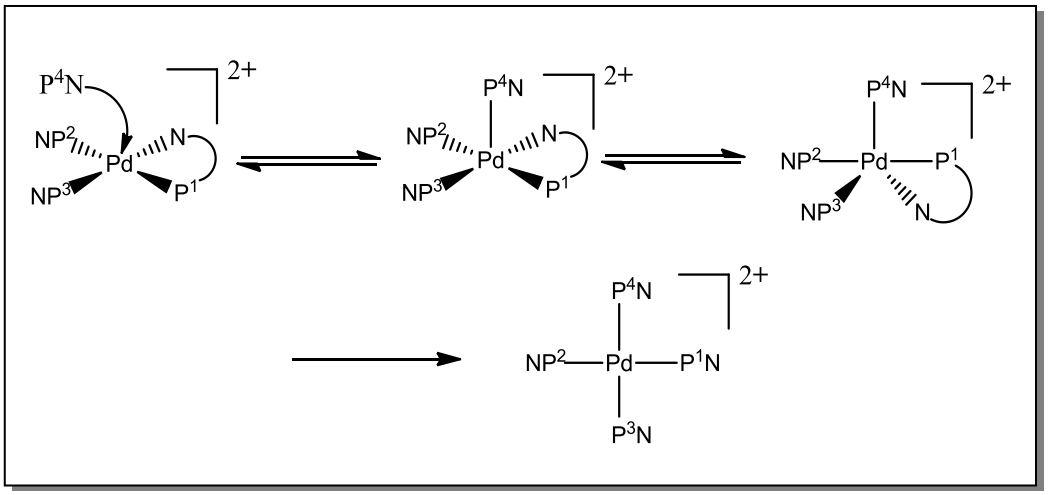

Scheme 2.17. Possible intermolecular associative mechanism in **6.**

Both dissociative and associative mechanisms have two transition states, one for each stage of the substitution, although the relative barrier heights on either side of the intermediate are different. For a dissociative mechanism, the formation of the intermediate has the larger barrier height, whereas for an associative mechanism, the barrier to the decomposition of the intermediate is the larger of the two.

The determination of thermodynamic parameters (particularly activation parameters) can be used to support the nature of a reaction, whether it proceeds via a dissociative or an associative pathway. However, caution must be shown when interpreting the derived thermodynamic data as evidence for the existence of 3-coodinate intermediate. Ligand associative substitution by the solvent or an intramolecular process can easily be mistaken for a dissociative process. Typically, rate –retarding effects by added ligands are often taken as evidence of a dissociative pre-equilibrium, although more often they seem to be associated with an associative-interchange (I_a) mechanism,[61] which is the usual path for ligand substitution in Pd(II) complexes. Solvation effects, ion pairing, salt effects and agostic interactions may also interfere with kinetic results.

Thermodynamic data for entropy $\Delta S^{\ddagger}$ and enthalpy $\Delta H^{\ddagger}$ can provide very useful information about the mechanism of exchange. The enthalpy and entropy change as the reactants go from the ground to the activated state, (as does the volume difference between the ground and activated state). $\Delta S^{\ddagger}$ and $\Delta H^{\ddagger}$ can be derived by measuring the rate of reaction, k, as a function of temperature *T*. The most useful of these two parameters is probably $\Delta S^{\ddagger}$, since this can be related to whether a mechanism is dissociative or associative. If there is an increase in disorder as the reactants reach the transition state, this implies that bond–breaking is the important step (I_d or D), hence $\Delta S^{\ddagger}$ will be positive. If a reaction proceeds by an associative mechanism (I_a or A), $\Delta S^{\ddagger}$ will be negative, as entropy is lost as the new bond forms on going to the transition state or intermediate.

However, in solution, where charged particles are involved, solvation effects often dominate the entropy of activation. If ions come together in the transition state with a neutralization of charge, then solvent molecules are released and the entropy $\Delta S^{\ddagger}$ of activation becomes more positive, which would otherwise point towards a dissociative process in the absence of solvation effects. Conversely, if ions are formed from neutral molecules, solvent molecules are strongly orientated or frozen around the ions and this entropy is lost, $\Delta S^{\ddagger}$ becomes more negative, the effect being greater the large the change in solvation which would otherwise point towards an associative process. If for example the process was an associative one, then the negative contributions of the associative mechanism would have to compensate for any solvation effects in order for the data to be correctly interpreted.[62] For instance, in DMSO exchange of $[PtPh_2(Me_2SO)_2]$, which was determined to be dissociative ($\Delta V^{\ddagger} = +4.9 \pm 0.5$ cm^3 mol^{-1}), shows a negative $\Delta S^{\ddagger} = -16 \pm 2$ cal K^{-1} mol^{-1}.[63]

Although, there is evidence for dissociative processes in Pt(II) complexes,[64] dissociative ligand substitution at Pd(II) is extremely uncommon,[51, 62, 65] the reason being that in the presence of an incoming ligand or solvent, the alternative associative substitution is much faster.

Rare examples of dissociative mechanisms at Pd have been reported by Espinet[51, 62, 65] who used NMR spectroscopy to study the dynamic behaviour of the complexes $[Pd(C_6F_5)X(SPPy_nPh\text{-}N,S)]$ (Py = pyridin-2-yl; X = Br, n =1, 3; n

= 2, X = Cl, Br, I). A dynamic process was determined to occur through rotation of the C_6F_5 group around the Pd-C bond in $CDC1_3$ solution. The rotation occurs via simple halide dissociation and a contact ion pair in a cage of solvent. The enthalpy values observed for the slow rotation in $CDC1_3$ must correspond closely to the dissociation of halide. Eyring plots were used to determine the thermodynamic parameters of activation which revealed activation entropies for these dissociative processes in $CDCl_3$ are negative.

Complex $[Pd(\kappa^2\text{-}Ph_2Ppy)(\kappa^1\text{-}Ph_2Ppy)_2][MeSO_3]_2$, (**6**), might seem an unlikely prospect for a dissociative process, it is dicationic and does not contain any organic ligands that might increase the electron density at palladium and hence enhance a dissociative pathway. However, the presence of the highly strained $Pd(\kappa^2\text{-}Ph_2Ppy)$ four-membered ring might be expected to destabilize the ground state, favouring dissociation of the chelating nitrogen.

The behaviour of the resonances of the phosphorus atoms of both the chelating and monodentate ligands of **3 + 4'** observed in $^{31}P\{^1H\}$NMR spectrum of appears similar – a broadening on increasing the temperature. Whereas, the fluxionality observed for **6** is more complex, as shown (Figure 2.14), and the NMR spectra contain more information. So, we began our investigations of dynamic processes in Pd complexes of Ph_2Ppy with **6**.

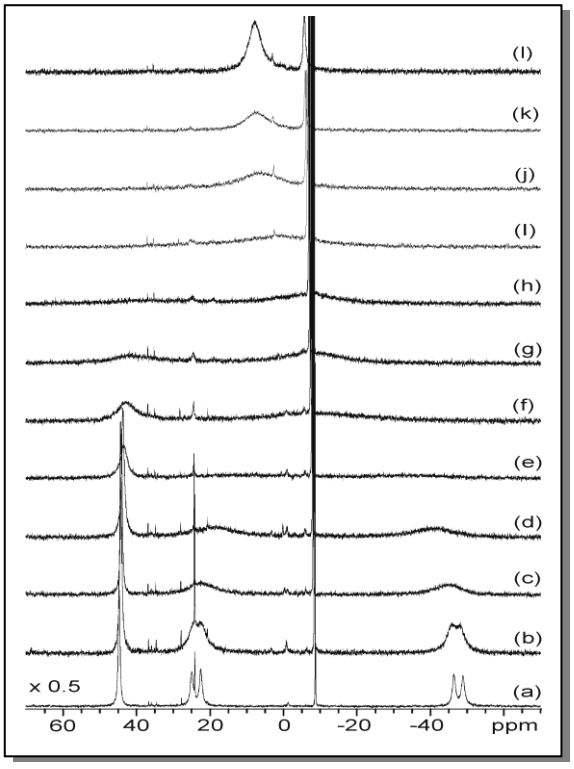

Figure 2.14. $^{31}P\{^1H\}$ NMR spectrum of **6** in MeOH (a) 183 K, (b) 193 K, (c) 203 K, (d) 213 K, (e) 223 K, (f) 233 K, (g) 243 K, (h) 253 K, (i) 263 K, (j) 273 K, (k) 283 K, (l) 293 K. The resonance at *ca.* $\delta(P)$ = -8.7 ppm is due to free $[PPh_2pyH]$ $[MeSO_3]$.

2.8.1. Dynamic process in [Pd(κ^2-Ph_2Ppy)(κ^1-Ph_2Ppy)$_2$][$MeSO_3$]$_2$ (6)

Two coalescence temperatures can be clearly seen in the variable temperature $^{31}P\{^1H\}$ NMR spectra of [Pd(κ^2-Ph_2Ppy)(κ^1-Ph_2Ppy)$_2$][$MeSO_3$]$_2$, in MeOH (Figure 2.14), in the presence of a slight excess of Ph_2Ppy (Table 2.3, sample 3), indicate that two stereospecific fluxional processes are occurring in solution., the first, occurs between 213 K and 233 K (Figure 2.14, d-f), the second between 253 K and 263 K (Figure 2.14, h-i). Impurities can be seen in many of the spectra ESI†(Supplementary Figure.1).

The fluxionality observed for **6** is complex, the NMR spectra of **6** (Figure 2.14) reveal that two stereospecific fluxional processes are occurring. The low-temperature fluxional process equivalences P^2N and P^3N the trans disposed chelating and monodentate Ph_2Ppy ligands (Scheme 2.18).

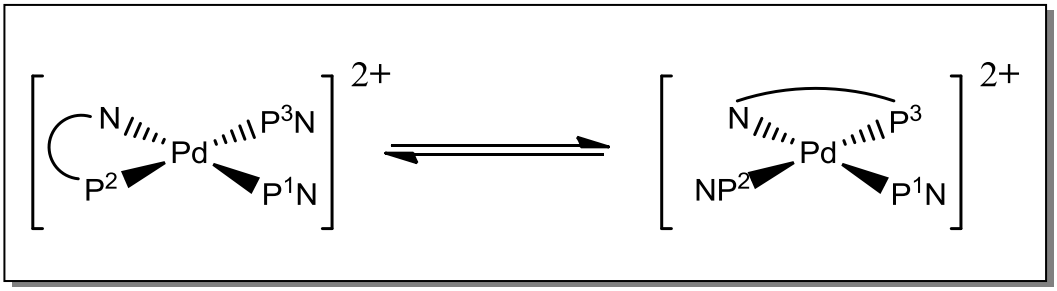

Scheme 2.18 The low-temperature fluxional process occurring in **6.**

Warming to RT, results in a dramatic change, the $^{31}P\{^1H\}$ NMR spectrum of **6**, showing only one major resonance (Scheme 2.19), mean that fluxional process (es) equivalencing of P^1N with P^2N and P^3N is occurring at RT.

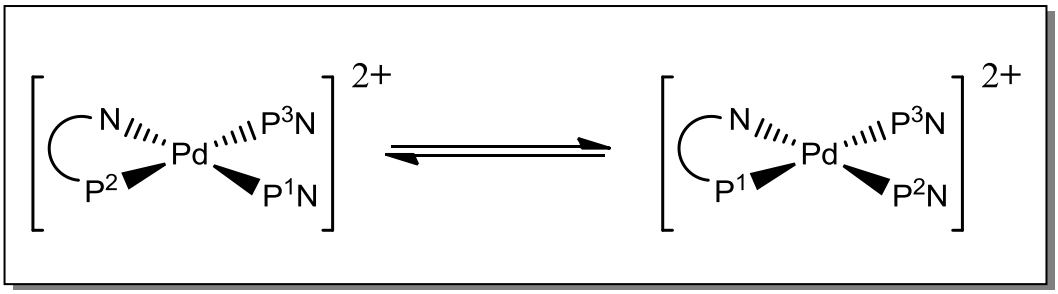

Scheme 2.19 The room-temperature fluxional process occurring in **6.**

Due to its instability, solutions of **6** were prepared "*in situ*" with nominal Pd:P ratios of 1:3 and 1:3.4 and nominal Pd:$MeSO_3H$ ratios of 1:2, 10, 15 or 25. This allowed the effects of excess ligand and excess acid on the fluxional processes to be investigated. Also, we prepared **6** *in situ* in CD_2Cl_2 as a non-coordinating solvent, and in mixed solvent MeOH-CD_2Cl_2. The VT $^{31}P\{^1H\}$ NMR spectra have been simulated using gNMR5.1 and the activation parameters obtained (Table 2.3) which also gives the reaction rate constants at 213 and 243 K for the low and high temperature processes respectively. The spectra, spectral simulations, Eyring and Arrhenius plots are given in the Experimental Section, (Supplementary Figures 1-18).

Table 2.3. Activation parameters ($\Delta S^{\ddagger}$/J mol^{-1}K^{-1}, $\Delta H_1^{\ddagger}$/kJ mol^{-1}, E_{act}/kJ mol^{-1}) for the dynamic processes in **6**[a].

sample	solvent	Pd:P	Pd: $MeSO_3H$	k_1^{213} [b] /10^4 s^{-1}	k_2^{243} [b] /10^4 s^{-1}	$\Delta S_1^{\ddagger}$ [c]	$\Delta S_2^{\ddagger}$ [c]	$\Delta H_1^{\ddagger}$ [d]	$\Delta H_2^{\ddagger}$ [d]	E_{act}^1 [d]	E_{act}^2 [d]
1	MeOH	3.1	10	1.52	1.91	-15	-11	31	37	33	39
2	MeOH	3.1	10	1.23	1.37	-12	-12	32	37	34	39
3	MeOH	3.4	10	1.36	1.29	-10	-8	33	38	35	40
4	MeOH	3.4	25	1.07[e]	1.90	-25	-33	29	39	31	41
5	MeOH	3.2	15	1.43	1.43	-25	-33	29	32	31	34
6	MeOH	2.9	25	1.11	1.16	-17	-25	31	34	34	31
7	MeOH/CD_2Cl_2 2:9	3.1	25	8.92	1.69	-41	-32	22	32	25	34
8	MeOH/CD_2Cl_2 4:3	3.1	5	4.11	2.13	-20	-25	24	31	28	33
9	CD_2Cl_2	2.9	2	1.15[e]	1.92[f]	-4	-21	33	35	35	37

[a] Prepared *in situ*. [b] Error ~ +/- 10%. [c] Error ~ +/- 5 J mol^{-1} K^{-1}. [d] Error ~ +/- 5%. [e] T = 208 K. [f] T = 238 K.

From (Table 2.3) we note that the rate constants of the low– and high-temperature processes differ by an order of magnitude, confirming that two independent processes occur. Activation entropies are negative, consistent with an associative process. However, changes of solvents might also

contribute to change of the activation entropy, so caution must be exercised when interpreting the data.[51, 61, 62] However, such effects are likely to be minimized in **6** since the potential dissociating ligand, the pyridyl group, is not charged. Changes in solvation are therefore expected to make only a small contribution to the activation process/parameters unless protonation-deprotonation of the pyridyl nitrogen contributes significantly.

However, the rate of the low energy process is strongly influenced by solvent, being faster in MeOH:CD_2Cl_2 mixtures than in pure MeOH. Inspection of Table 5 reveals that this rate acceleration is due to a lower enthalpy of activation, being *ca.* 23 kJ mol^{-1} and 33 kJ mol^{-1} respectively. (The entropy of activation is more negative in the mixed solvent). The rate of the dynamic process is marginally influenced by the presence of excess acid, seen by comparing samples 3 and 4 or excess ligand, as seen when comparing samples 1 – 3 in (Table 2.3).

The resonance of $[PPh_2pyH]^+$ at *ca.* δ(P) = -8.7 ppm, remains sharp until after the onset of both fluxional processes (Figure 2.14) and Supplementary Figure. 11, even when present at low concentration Supplementary Figure. 5, 9, 13 and 15, indicating that free $[PPh_2pyH]^+$ is not involved in these dynamic processes. However, in a saturation transfer experiment a small amount of transfer to free $[PPh_2pyH]^+$ was observed, indicating that exchange with free ligand occurs, albeit slowly compared to the intramolecular exchange processes. This is consistent with intermolecular exchange being slow.

Two associative pathways can account for the occurrence of two stereoselective exchanges with different rates in $[Pd(\kappa^2\text{-}Ph_2Ppy)(\kappa^1\text{-}Ph_2Ppy)_2][MeSO_3]_2$ (Scheme 2.20 and 2.21).

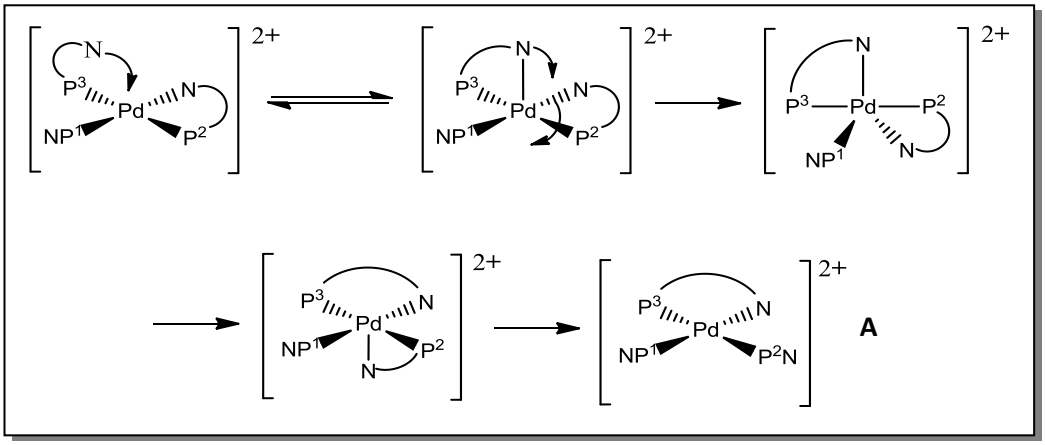

Scheme 2.20 Intramolecular low temperature associative mechanism in **6** following that of Hall[57].

It is not necessary that the higher energy process simultaneously equivalences all three Ph_2Ppy ligands, only that it equivalences P^1N with one of P^2N or P^3N since the lower energy process already equivalence P^2N and P^3N. It is reasonable to assume that the highly strained Pd(κ^2-Ph_2Ppy) four membered ring will prefer to adopt an axial-equatorial, rather than an equatorial-equatorial, conformation, then only two trigonal bipyramidal intermediate are accessible, since the law of microscopic reversibility requires that the intermediate be symmetrical (**A** and **B** in Schemes 2.20 and 2.21).

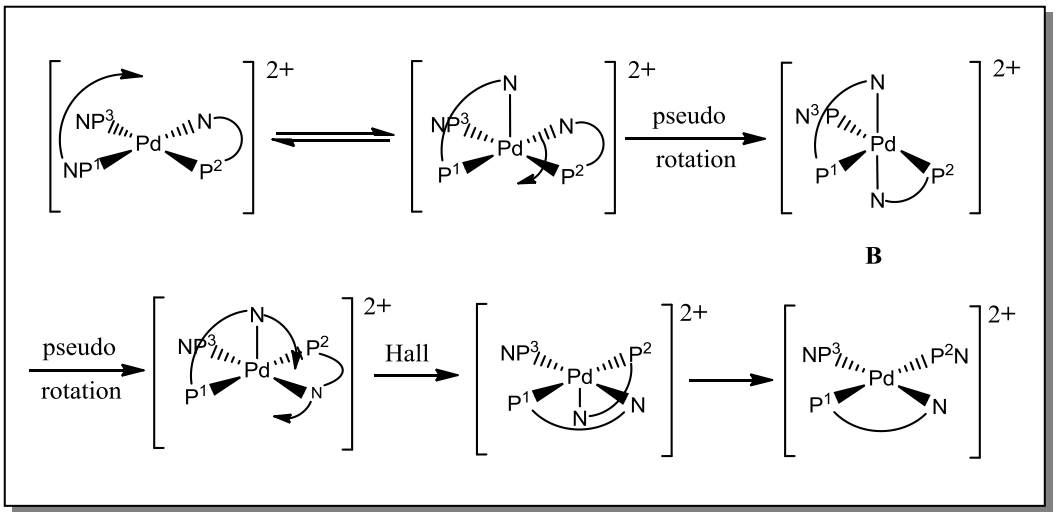

Scheme 2.21. Intramolecular high-temperature associative mechanism in **6** involving pseudo rotation and following Hall[57].

Structures **A** and **B** have different pathways of formation, **A** is directly accessible from the square-planar structure formed on chelation of the nitrogen of P^3N, while, **B** is not directly accessible following the least energetic pathway proposed by Hall[57].

In (Scheme 2.20) the nitrogen of P^3N moves into square plane of the complex and displaces the pyridyl nitrogen of P^2N, without movement of the phosphorus atoms in **6**, stereospecific equivalence of P^2N and P^3N can be obtained by following the least energetic pathway of Hall[57, 59, 66] while P^1N remains distinct. The rate of this process is affected by solvent, and this might be explained by competition between the incoming pyridyl nitrogen and methanol solvent for the apical coordination site.[62]

Intermediate **B** is not directly accessible but might be accessed *via* a series of being pseudo rotations and will presumably, therefore, be subject to a greater activation barrier. The solvent effect on the rate of this process is small compared with **A** intermediate process, consistent with a mechanism in which the rate determining step occurs later in the reaction coordinate.

Alternative, high energy processes that would equivalence all three PPh_2Ppy ligands, are exchange with free phosphine displacing the chelating pyridyl nitrogen (Scheme 2.22), or a square-planar to tetrahedral reorganization of the metal centre.

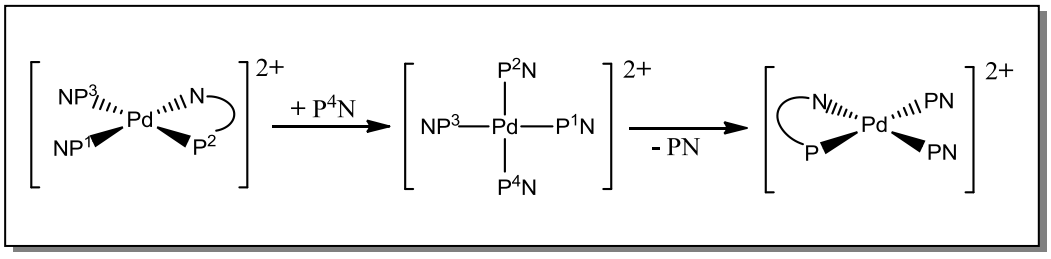

Scheme 2.22. Exchange of free phosphine on **6**

The rate of the exchange processes is essentially unaffected by the presence of 0.1 – 1 equivalents of free PPh_2Ppy in the solution and, minimal broadening of the resonance due to PPh_2Ppy in the $^{31}P\{^1H\}$ NMR spectrum is observed. Although detectable, exchange of free and coordinated phosphine in equimolar

solutions of **6** and excess PPh_2Ppy in much slower than both the high and low temperature processes (Figure 2.14). We therefore discount this possibility, and favour the intramolecular association shown in (Scheme 2.21).

On the other hand, a dissociative process may occur in **6** due to the highly strained Pd(κ^2-Ph_2Ppy) ring. This process gives a T-shaped "three-coordinate" solvated intermediate. Equivalencing of the *trans* disposed ligands P^2N and P^3N, is then readily envisioned. However, Y-shaped structures, which have previously been proposed as high energy transition states, are necessary to interconvert these ligands with P^1N.[67]

Although, Stambuli *et al*,[68] have recently reported the vacant fourth coordination site of T-shaped Pd(II) complexes stabilized by an agnostic interaction when incorporating extremely bulky phosphine ligands, a dissociative pathway is not consistent with the negative entropy of activation and low activation barriers observed.

2.8.2 Dynamic process in [Pd(κ^2-Ph_2Ppy)(κ^1-Ph_2Ppy)Cl][X], (3[X])

Chloride assisted interconversion of chelating and monodentate Ph_2Ppy is observed, on comparing the $^{31}P\{^1H\}$ NMR spectrum of **3**[Cl] with **3**[BF_4] and **3**[OTf] in the temperate range 193 K and 293 K. The $^{31}P\{^1H\}$ NMR spectrum of **3**[BF_4] remains sharp throughout this temperature range whereas the resonances for **3**[Cl] show significant broadening at room temperature with the spectra of **3**[OTf] showing intermediate behaviour, indicating that the dynamic process is faster in **3**[Cl] (Supplementary Figure. 19-22). The position of the resonances of **3**[Cl] and separation is essentially invariant on raising the temperature to 293 K, as shown in Figure 2.15, indicating that the chelating structure persists at high temperature and that exchange between the chelating and monodentate Ph_2Ppy ligand or between "chelate-monodentate" and bis-monodentate complexes is slow on the timescale of the NMR chemical shifts at 293 K or that the concentration of the bis monodentate complex in equilibrium with the chelate-monodentate is, at all times, very low.

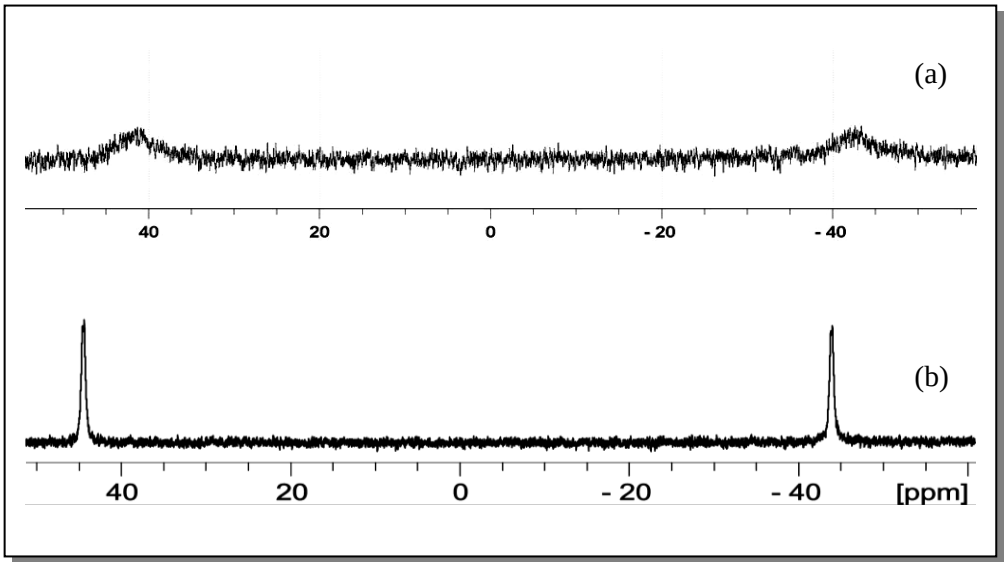

Figure 2.15. The $^{31}P\{^{1}H\}$ NMR spectrum of [Pd(κ^2-Ph_2Ppy)(κ^1-Ph_2Ppy)Cl][Cl], **3**[Cl] in CH_2Cl_2/MeOH (a) at 293 K, (b) at 233 K.

The chemical shifts and coupling constant in the $^{31}P\{^{1}H\}$ NMR spectrum of **3**[Cl], **3**[OTf] and **3**[BF_4] are essentially the same (Figure 2.3 and 2.4), as is expected since only the counterion has changed,[36, 37] indicating that the onset of the fluxional process is strongly influenced by the counterion. It is hard to write down a process exchanging chelating and monodentate Ph_2Ppy involving only intramolecular attack that accounts for the observed difference in rate for **3**[Cl] and **3**[BF_4]. Exchange in **3**[OTf] is an order of magnitude *slower* than in **3**[Cl] and increasing MeOH content in the solvent mixture significantly depresses the rate. Coordination of an external ligand, such as solvent or traces of excess Ph_2Ppy in solution, to the palladium centre, with subsequent dissociation of the coordinated nitrogen of PN constitutes an intermolecular associative process since competition between the incoming ligand and solvent for the fifth metal coordination site can occur.[69] The observed decrease in rate with increasing methanol content of the solvent mixture, which might weaken the Pd-Cl bond through increased solvation of bound chloride, is also in consistent with a D process.

Hall[57] studied the mechanism of substitution reactions of square planar transition metal complexes and reported calculations which showed that at the early stage

of an associative substitution reaction, the entering ligand (E) attacks at the vacant axial position to a form a square pyramidal structure and at the same time pushes the leaving ligand (L) away from a square plane (Scheme 2.23).

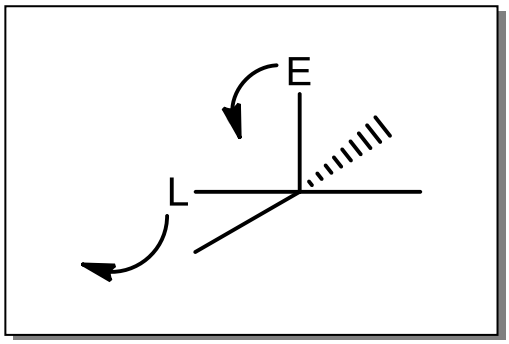

Scheme 2.23. Mechanism of ligand substitution in square planar complexes as calculated by Hall.[57]

When the entering and leaving groups are equivalent, the principle of microscopic reversibility demands that the entering and leaving groups occupy equivalent positions in the transition state as long as there is no intermediate. Scheme 2.24 shows the two possible outcomes of intramolecular attack of nitrogen.

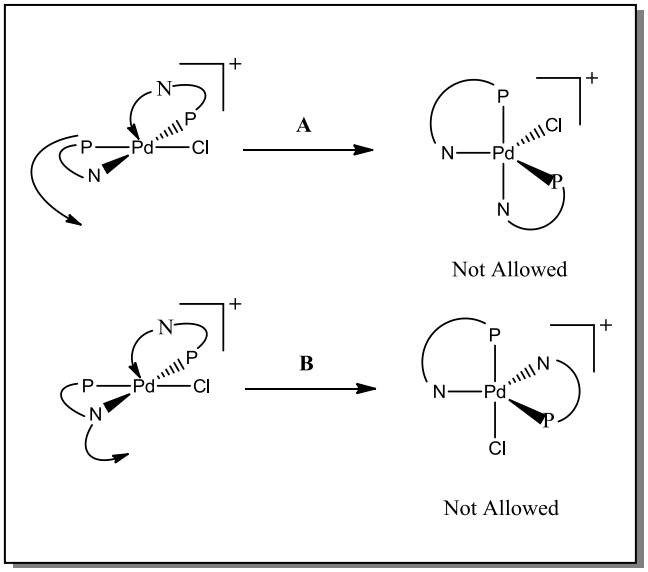

Scheme 2.24. Substitution of Ph_2Ppy in 3[Cl] following the reaction coordination calculated by Hall.[57]

Neither pathway A nor B is allowed by microscopic reversibility; in addition the isomer in pathway B is not expected due to the bite angle of the ligand being smaller than the 120^{o} required when occupying the equatorial sites.

Neither of these pathways are thus able to interconvert P^1N and P^2N and thus account for the dynamic exchange process seen in the variable temperature $^{31}P\{^1H\}$ NMR spectra of **3**[Cl].

If dissociation of Cl^- from Pd is rate determining, then the influence of the counterion on the rate is difficult to explain: BF_4^- and OTf^- are known to have much lower coordination ability than Cl^-. We suggest instead that re-coordination of the halide to palladium (Scheme 2.25) to give a bis-monodentate intermediate, must occur albeit slowly on the NMR timescale. This is consistent with the influence of counterion and the rate of suppression by MeOH.

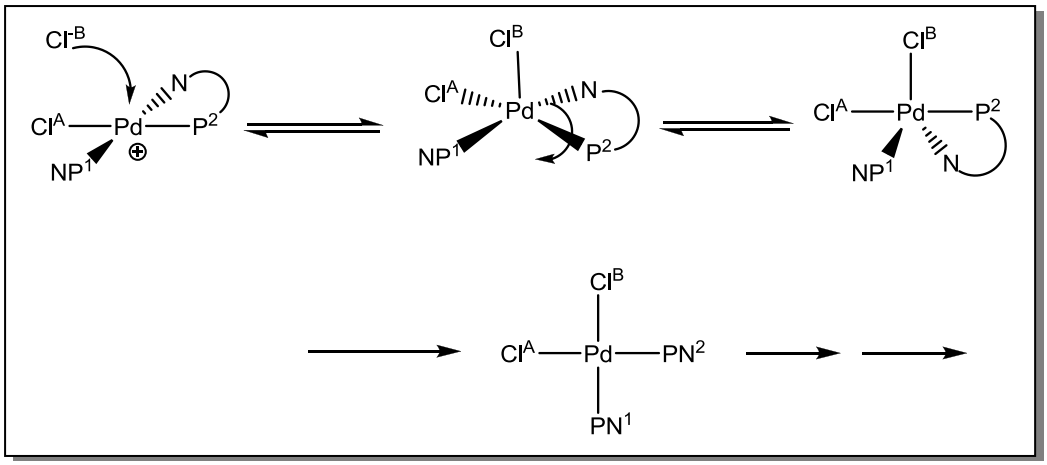

Scheme 2.25. Mechanism of exchange in **3**[Cl] via recoordination of halide.

Scheme 2.25 above can explain the equivalencing of the Ph_2Ppy ligands in **3**[Cl] but cannot for **3[**OTf], since the ligands remain distinct in the transition state, one being *trans* to ligated (Cl), the other *trans* to ligated (OTf).

Cis-trans isomerisation at Pd in the transition state/intermediate is required to obtain equivalencing of the PN ligands (Scheme 2.26).

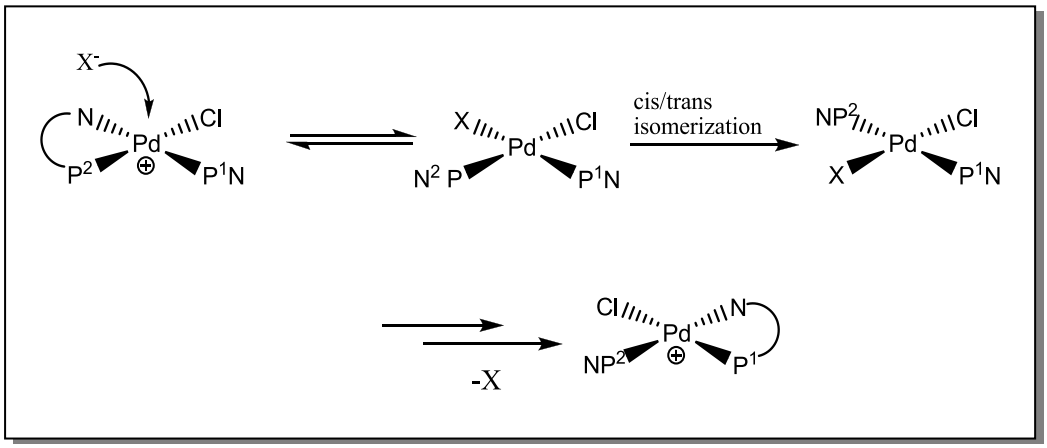

Scheme 2.26. Proposed fluxional pathway in **3**[OTf].

Alternatively, X could substitute Cl → $Pd(PN)_2X_2$ followed by isomerisation then Cl re-enter coordination sphere of Pd displacing X.

2.9. Conclusions

Prior to the work presented above there was a limited amount of work on the chemistry of palladium(II) complexes of 2-pyridyldiphenylphosphine (Ph_2Ppy). Previous work had found that the monodentate coordination mode of Ph_2Ppy to Pd through phosphorus is preferred. In contrast to these earlier reports, the present work has shown that chelating P,N palladium(II) complexes of Ph_2Ppy can be readily prepared, if an appropriate choice of solvent is made.

The preference of Ph_2Ppy to coordinate to palladium via phosphorus only, when in the presence of strongly coordinating anionic ligands like Cl^- to give the bis-monodentate complex $[Pd(\kappa^1\text{-}Ph_2Ppy)_2Cl_2]$, can be overcome by the use of solvent systems such as MeOH or CH_2Cl_2-MeOH, in which MeOH presumably solvates the halide ligand allowing the formation of fluxional "chelate-monodentate" complexes such as $[Pd(\kappa^2\text{-}Ph_2Ppy)_2(\kappa^1\text{-}Ph_2Ppy)Cl][Cl]$.

Protonation of the pyridyl nitrogen of monodentate coordinated Ph_2Ppy in these Pd(II) complexes by the strong acid in dichloromethane is feasible, such as proposed in alkyne methoxycarbonylation catalyst processes by Drent,[26, 27] Tooze,[30] Scrivanti,[39, 55] Elsevier,[70] and Tang[31], but in methanol, we have shown that such protonation does not preclude the formation of chelating coordinated $\kappa^2\text{-}Ph_2Ppy$ complexes.

Generally, the rate determining step of a ligand substitution on Pd(II) metal centre is accepted to be the formation of a five-coordinate intermediate in an associative mechanism, also a few rare examples of dissociative mechanisms do exist.[62, 65]

Variable temperature $^{31}P\{^1H\}$ NMR spectroscopy revealed two stereospecific exchanges occur in **6** as a dynamic process, one at lower temperature, which equivalences the *trans* disposed ligands P^2N and P^3N, the other at higher temperature, which equivalences all three PN ligands (Schemes 2.21 and 2.22). Both mechanisms were found to have negative entropy of activation indicating that they follow an intramolecular associative exchange pathway. Also, the dynamic exchange process in **3** is probably associative, however, it involves re-coordination of the counterion displacing the chelating nitrogen. That means

using Ph_2Ppy as a ligand of the palladium catalysed alkoxycarbonylation of propyne has no influence over ligand substitution reaction, which remains associative in nature.

Table 2.2 $^{31}P\{^{1}H\}$ NMR data for Pd(II)-Ph2Ppy compounds at 193k in dichloromethane unless otherwise stated

	Compound	$\delta(P^1)$/ ppm	$\delta(P^2)$/ ppm	$\delta(P^3)$/ ppm	$^2J(P^1\text{-}P^2)$/ Hz	$^2J(P^2\text{-}P^3)$/ Hz
1	$[Pd(\kappa^2\text{-}Ph_2Ppy)Cl_2]$	---	-61.6 s	---	---	---
2a	*cis*-$[Pd(Ph_2Ppy)_2Cl_2]$[a]	29.0 s	---	---	---	---
2b	*trans*-$[Pd(Ph_2Ppy)_2Cl_2]$[a]	22.8 s	---	---	---	---
2$[CF_3CO_2]$	$[Pd(\kappa^1\text{-}Ph_2Ppy)_2(CF_3CO_2)_2]$	27.6 br	---	---	---	---
3[Cl]	$[Pd(\kappa^2\text{-}Ph_2Ppy)(\kappa^1\text{-}Ph_2Ppy)Cl][Cl]$[b, c]	44.4 d	-44.0 d	---	33.0	---
3$[BF_4]$	$[Pd(\kappa^2\text{-}Ph_2Ppy)(\kappa^1\text{-}Ph_2Ppy)Cl][\ BF_4]$[b, c]	44.8 d	-43.8 d	---	38.2	---
3[OTf]	$[Pd(\kappa^2\text{-}Ph_2Ppy)(\kappa^1\text{-}Ph_2Ppy)Cl][\ OTf]$[b, c]	44.6 d	-43.9 d	---	38.1	---
3$[MeSO_3]$	$[Pd(\kappa^2\text{-}Ph_2Ppy)(\kappa^1\text{-}Ph_2Ppy)Cl][\ MeSO_3]$	44.7 d	-43.8 d	---	38.2	---
4[OTf]	$[Pd(\kappa^2\text{-}Ph_2Ppy)(\kappa^1\text{-}Ph_2Ppy)(OTf)][\ OTf]$	40.8 d	-39.3d	---	Unresolved	---
4$[MeSO_3]$	$[Pd(\kappa^2\text{-}Ph_2Ppy)(\kappa^1\text{-}Ph_2Ppy)(MeSO_3)][MeSO_3]$	41.2 d	-40.0 d	---	29.8	---
4$[CF_3CO_2]$	$[Pd(\kappa^2\text{-}Ph_2Ppy)(\kappa^1\text{-}Ph_2Ppy)(CF_3CO_2)][CF_3CO_2]$	40.8 d	-38.6 d	---	24.4	---
4'[OTf]	$[Pd(\kappa^2\text{-}Ph_2Ppy)(\kappa^1\text{-}Ph_2PpyH)(OTf)][OTf]_2$	26.4	-45.0	---	---	---
4'$[MeSO_3]$	$[Pd(\kappa^2\text{-}Ph_2Ppy)(\kappa^1\text{-}Ph_2PpyH)(MeSO_3)][MeSO_3]_2$	26.0 br	-45.8 br	---	Unresolved	---
4'$[BF_4]$	$[Pd(\kappa^2\text{-}Ph_2Ppy)(\kappa^1\text{-}Ph_2PpyH)(BF_4][\ BF_4]_2$	25.2	-43.7	---	---	---
5	$[Pd(\kappa^2\text{-}Ph_2Ppy)_2][BF_4]_2$	---	-42.9 br	---	---	---
6	$[Pd(\kappa^2\text{-}Ph_2Ppy)(\kappa^1\text{-}Ph_2Ppy)_2][MeSO_3]_2$	44.7 s br	-47.7 d br	23.6 d br	Unresolved	388

[a] At 293 K. [b] In dichloromethane-MeOH solution.[c] At 233K.

2.10 Experimental

2.10.1 General methods and procedures

All manipulations involving solutions or solids were performed under an atmosphere of nitrogen using standard Schlenk techniques. All solvents were dried and distilled under nitrogen following standard literature methods; i.e. CH_2Cl_2 over CaH_2, MeOH over $Mg(OMe)_2$, MeCN over CaH_2, Et_2OH over Mg. Deuterated solvents were degassed by 3 freeze – pump – thaw cycles under vacuum in a liquid nitrogen bath, then nitrogen saturated and stored over activated 4 Å molecular sieves under nitrogen for at least 24 hours prior to use. All reactions were carried out in a 10 mm NMR tube. Some compounds were obtained as impure oils and have been characterized in solution only by NMR spectroscopy. No yield or elemental analysis is reported for these compounds. All experiments have been carried out following standard safety procedures.

All $^{31}P\{^1H\}$, ^1H NMR measurements were performed on Bruker DPX400 and Avance2-400 instruments using commercial probes. Chemical shift were referenced to TMS following IUPAC guidelines. Spectra of samples dissolved in non-deuterated solvents were referenced using an external CD_2Cl_2 solvent lock. Chemical shift errors are as follows; $^{31}P \pm 0.1$ ppm, $^{13}C \pm 0.5$ ppm, $^1H \pm 0.1$ ppm. Coupling constant errors are as follows; $^{31}P \pm 1.0$ Hz, $^{13}C \pm 0.5$ Hz, $^1H \pm 0.1$ Hz. In reporting NMR data the letters s, d, t etc in multiplicities have their normal meaning (singlet, doublet, triplet, etc). Mass spectrometric analyses were run on a Micromass LCT instrument using a 'Time of Flight' mass analyser. The samples were run in ES+ (positive electrospray) ionisation mode. Microanalyses were performed at the University of Liverpool using a Leeman CE440 CHN analyser. All chemical reagents were purchased from Aldrich Chemical Co., except $[Pd(Ph_2CN)_2Cl_2]$[71] which were prepared by published methods.

2.10.2. Experiments

A - [Pd(κ^2-Ph$_2$Ppy)Cl$_2$] (1). Ph2Ppy (0.037 g, 0.14 mmol) was added to a solution of [Pd(PhCN)$_2$Cl$_2$] (0.054 g, 0.14 mmol) in dichloromethane (10 mL) and the mixture stirred for 30 minutes. The resultant yellow solution was reduced to half volume *in vacuo* and diethyl ether was added to precipitate the product as an impure yellow solid. The yellow solid was filtered through a sinter, washed with diethyl ether (3 x 20 mL) and dried *in vacuo*. The product comprises a mixture of 1 with 2a/b from which pure 1 could not be isolated. Yield: 0.054 g. $^{31}P\{^1H\}$ NMR in CH_2Cl_2: δ(P) -61.6(s, **1**); 29.0 (s, **2a**); 22.8(s, **2b**).

B - [Pd(κ^2-Ph$_2$Ppy)(κ^1-Ph$_2$Ppy)Cl]Cl (3(Cl)). A few drops of MeOH were added to a suspension of **2a/b** (0.025 g, 0.036 mmol) in dichloromethane (2 mL) and the mixture shaken for a few minutes until a clear yellow solution was obtained. Solvent was removed *in vacuo* to give a yellow powder. Yield: 0.0238 g, 95%. Anal. Calc for $C_{34}H_{28}N_2P_2Cl_2Pd$: C, 58.02; H, 4.01; N, 3.98; Cl, 10.07. Found: C, 57.59; H, 3.98; N, 3.69; Cl, 10.33%. MS (ES^+, *m/z*): 667, [M^+]. NMR in CH_2Cl_2/MeOH at 233 K: δ(H) 8.77 (br, 1H, Ph$_2$Ppy, H^6-py), 8.12 (br, 1H, *J*(HH) ~ 7 Hz, Ph$_2$Ppy, H^4-py), 7.9 – 7.3 (24H, Ph$_2$Ppy); δ(P) 44.4 (d, $^2J(P^1\text{-}P^2)$ = 33.0 Hz, (κ^1-Ph$_2$Ppy), -44.0 (d, κ^2-Ph$_2$Ppy).

C – TIX (X = BF$_4$, MeSO$_3$). Solution of Diethylether (20 ml) has tetrafloroboric acid, dietherether (2.8 ml , 2 mmol) was add as dropwise to a solution has of TI_2CO_3 (0.024 g, 0.5 mmol) in (24 ml) diethylether with magnetic stirrer. This gave a white precipitate of $TIBF_4$. The solid was collected by filtration. The solid of TIX (X = BF_4, $MeSO_3$) was washed with Et_2O to remove acid, collected by filteration and dried *in vacuo.*

TIOTf. was prepared *via* add trifluoromethanesulfonic acid (0.88 ml, 1 mmol) as dropwise to a solution of TI_2CO_3 (0.024 g, 0.5 mmol) in (24 ml) diethylether with magnetic stirrer, this interaction was made with water bath.

This gave a white precipitate. The solid was collected by filtration. The solid of TIOTf was washed with Et_2O to remove acid, collected by filteration and dried *in vacuo.*

D - [Pd(κ^2-Ph_2Ppy)(κ^1-Ph_2Ppy)Cl][BF_4] (3[BF_4]). Dichloromethane (2 mL) was added to a solid mixture of Tl[BF_4] (0.029 g, 0.1 mmol) and **2a/b** (0.070 g, 0.1 mmol). The resulting soution was stirred for 1 hour. The resultant solution was then filtered from the precipitate of TlCl into 25 mL of Et_2O. The resulting precipitate was washed three times with Et_2O by decantation, collected by filtration and dried *in vacuo*. Anal. Calc for $C_{34}H_{28}N_2P_2ClBF_4Pd$: C, 54.07; H, 3.74; N, 3.71. Found: C, 53.88; H, 3.63; N, 3.66%. MS (ES^+, *m/z*): 667, [M^+]. NMR in CH_2Cl_2 /MeOH at 233 K: δ(H) 8.77 (br, 1H, Ph_2Ppy, H^6-py), 8.12 (t, 1H, *J*(HH) ~ 7 Hz, Ph_2Ppy, H^4-py), 7.9 – 7.3 (24H, Ph_2Ppy); δ(P) 44.8(d, κ^1-Ph_2Ppy), -43.8(d, $^2J(P^1\text{-}P^2)$ = 38.2 Hz; κ^2-Ph_2Ppy); δ (F) -152.5.

E - [Pd(κ^2-Ph_2Ppy)(κ^1-Ph_2Ppy)Cl][$MeSO_3$] (3[$MeSO_3$]). Dichloromethane (2 mL) was added to a solid mixture of Tl[$MeSO_3$] (0.035 g, 0.1 mmol) and **2a/b** (0.070 g, 0.1 mmol). The resulting soution was stirred for 1 hour. The resultant solution was then filtered from the precipitate of TlCl into 25 mL of Et_2O. The resulting precipitate was washed three times with Et_2O by decantation, collected by filtration and dried *in vacuo*. NMR in CH_2Cl_2 /MeOH at 233 K: δ(H) 8.77 (br, 1H, Ph_2Ppy, H^6-py), 8.12 (t,br, 1H, *J*(HH) ~ 7 Hz, Ph_2Ppy, H^4-py), 7.9 – 7.3 (24H, Ph_2Ppy); δ(P) 44.7 (d, $^2J(P^1\text{-}P^2)$ = 38.2 Hz. κ^1-Ph_2Ppy), -43.8 (d, κ^2-Ph_2Ppy). $\delta(^{19}F)$ -153.03 ppm. MS (ES^+, *m/z*): 667, [M^+].

F - [Pd(κ^2-Ph_2Ppy)(κ^1-Ph_2Ppy)Cl][OTf] (3[OTf]). Dichloromethane (2 mL) was added to a solid mixture of Tl[OTf] (0.035 g, 0.1 mmol) and **2a/b** (0.070 g, 0.1 mmol). The resulting soution was stirred for 1 hour. The resultant solution was then filtered from the precipitate of TlCl into 25 mL of Et_2O. The resulting precipitate was washed three times with Et_2O by decantation,

collected by filtration and dried *in vacuo*. Anal. Calc for $C_{35}H_{28}ClF_3N_2O_3P_2PdS.0.5CD_2Cl_2$: C, 49.52; H, 3.51; N, 3.25. Found: C, 49.32; H/D, 3.40; N, 3.25%. NMR in CH_2Cl_2/MeOH at 233 K: δ(H) 8.77 (br, 1H, Ph_2Ppy, H^6-py), 8.12 (t, 1H, J(HH) ~ 7 Hz, Ph_2Ppy, H^4-py), 7.9 – 7.3 (24H, Ph_2Ppy); δ(P) 44.6 (d, $^2J(P^1\text{-}P^2)$ = 38.1 Hz, κ^1-Ph_2Ppy), -43.9 (d, κ^2-Ph_2Ppy). MS (ES^+, *m/z*): 667, [M^+].

G - <u>Pd(κ^2-Ph_2Ppy)(κ^1-Ph_2Ppy)X][X] (4[X]). (X = $MeSO_3$, OTf, CF_3CO_2). $MeSO_3H$ (13 μL, 0.20 mmol) was added to a solution of Pd(acetate)$_2$ (0.022 g, 0.1 mmol) and Ph_2Ppy (0.053 g, 0.2 mmol) in dichloromethane (2 mL) to give a yellow/orange solution. into 25 mL of Et_2O. The resulting precipitate was washed three times with Et_2O by decantation, collected by filtration and dried *in vacuo*. The (OTf, CF_3CO_2) complexes were prepared analogously.

4[$MeSO_3$]: NMR in CH_2Cl_2 at 193 k: δ(H) 9.17 (br, 1H, Ph_2Ppy, H^6-py), 8.25 (t, br, 1H, J(HH) ~ 7 Hz, Ph_2Ppy, H^4-py), 7.98-7.11 (24H, Ph_2Ppy); δ(P) 41.2 (d, $^2J(P^1\text{-}P^2)$ = 29.8 Hz, κ^1-Ph_2Ppy), -40.0 (d, κ^2-Ph_2Ppy). **8**[X] (X = OTf, CF_3CO_2) were prepared similarly.

4[OTf]: Calc. for $C_{36}H_{28}F_6N_2O_6P_2PdS_2$: C, 46.44; H, 3.03; N, 3.01. Found: C, 46.84; H/D, 3.40; N, 3.17 %. NMR in CH_2Cl_2 at 193 K: δ(H) 8.7 (br, 1H, Ph_2Ppy, H^6-py), 8.35 (br, 1H, J(HH) ~ 7 Hz, Ph_2Ppy, H^4-py), 8.07 – 7.13 (24H, Ph_2Ppy); $^{31}P\{^1H\}$ δ(P) 40.8 (d, br, κ^1-Ph_2Ppy), -39.3 (d, br, κ^2-Ph_2Ppy).

5[CF_3CO_2] NMR in CH_2Cl_2 at 193 K: δ(H) 8.5 (br, 1H, Ph_2Ppy, H^6-py), 8.25 (t,br, 1H, J(HH) ~ 7 Hz, Ph_2Ppy, H^4-py), 7.9 – 7.2 (24H, Ph_2Ppy); δ(P) 40.7 (d), -38.9 (d), $^2J(P^1\text{-}P^2)$ = 24.4 Hz, κ^1-Ph_2Ppy), -38.6 (d, κ^2-Ph_2Ppy).

H - <u>[Pd(κ^2-Ph_2Ppy)(κ^1-Ph_2PpyH)X][X]$_2$ (4'[X]). Addition of one equivalent of XH (0.1 mmol) which (X = OTf, $MeSO_3$, BF_4) with stirring to a solution **(4(X))** in a dichloromethane (2 ml) solution perpared as described above. The resulting solution was stirred for 1 h, then filtered by 10 mL of Et_2O. The resulting precipitate was washed three times with Et_2O by decantation, collected by filtration and dried *in vacuo*.

4'[OTf] NMR in CH_2Cl_2 at 193 K: δ(H) 9.31 (br, 1H, Ph_2Ppy, H^6-py), 8.93 (br, 1H, Ph_2Ppy, H^4-py), 8.67 (t, br, 1H, J(HH) ~ 7 Hz, Ph_2Ppy, H^5-py), 8.35 (br, 1H, Ph_2Ppy, H^4-py), 8.05 – 7.2 (22H, Ph_2Ppy); δ(P) 26.4 (d, br, $^2J(P^1\text{-}P^2)$ = 8 Hz, κ^1-Ph_2Ppy), -45.0 (d, br, κ^1-Ph_2Ppy).

4'[$MeSO_3$] NMR in CH_2Cl_2 at 193 K: δ(H) 9.48 (br, 1H, Ph_2Ppy, H^6-py), 9.11 (br, 1H, Ph_2Ppy, H^4-py), 8.61 (br, 1H, J(HH) ~ 7 Hz, Ph_2Ppy, H^5-py), 8.35 (br, 2H, Ph_2Ppy, H^4-py), 8.06 – 7.3 (22H, Ph_2Ppy); δ(P) 26.0 (br, κ^1-Ph_2Ppy), -45.8 (br, κ^2-Ph_2Ppy).

4'[BF_4] NMR in CH_2Cl_2 at 193 K: δ(H) 9.33 (br, 1H, Ph_2Ppy, H^6-py), 8.79 (br, 2H, Ph_2Ppy, H^4-py), 8.5 (br, 1H, J(HH) ~ 7 Hz, Ph_2Ppy, H^5-py), 8.36 (br, 1H, Ph_2Ppy, H^4-py), 8.09 – 7.2 (22H, Ph_2Ppy); δ(P) 25.2 (κ^1-Ph_2Ppy), -43.7 (κ^2-Ph_2Ppy).

I – <u>[Pd(κ^2-Ph_2Ppy)$_2$][BF_4]$_2$ (5).</u> $HBF_4.Et_2O$ (27 μL, 0.20 mmol) was added to a solution of Pd(acetate)$_2$ (0.022 g, 0.1 mmol) and Ph_2Ppy (0.053 g, 0.2 mmol) in dichloromethane (2 mL) to give an immediate yellow/orange prescipitate. The precipitate was collected by filtration, washed three times with Et_2O and dried *in vacuo*. The precipitate analysed as **9**.$2CH_3CO_2H.H_2O$. Resonances attribuable to acetic acid and water integrating 1:2:1 (**9**:AcOH:H_2O) were observed in the ^{1}H NMR spectrum.

Anal. Calc for $C_{38}H_{38}B_2F_8N_2O_5P_2Pd$: C, 48.31; H, 4.05; N, 2.97 Found: C, 47.39; H, 3.95; N, 3.4%. NMR in $CDCl_3$ at 293 K: δ(H) 9-6.7 (PPh_2py, 26H), 2.51 (CH_3CO_2H + H_2O, 4H), 2.18 (CH_3CO_2H, 6H) ; In CH_2Cl_2 at 193 K: δ(P) -42.9 (br, κ^2-Ph_2Ppy).

J - <u>[Pd(κ^2-Ph_2Ppy)(κ^1-Ph_2Ppy)$_2$][$MeSO_3$]$_2$ (6). Methanol (2 mL) was added to a solid mixture of [Pd(OAc)$_2$] (0.116 g, 0.52 mmol) and Ph_2Ppy (0.409 g, 1.55 mmol). The resultant yellow solution turned red on addition of $MeSO_3H$ (67 μL, 1.04 mmol). A red oil was obtained upon removal of the solvent *in vacuo*. NMR in MeOH at 293 K: δ(H) 8.26 (br, 3H, Ph_2Ppy, H^6-py), 7.99 (t, br, 3H, J(HH) ~ 5.4 Hz, Ph_2Ppy, H-py), 7.7 – 7.3 (33H, Ph_2Ppy). NMR in

MeOH at 183 K: δ(H) 9 – 7 (33H, Ph_2Ppy); δ(P) 44.7 (s, br, κ^1-Ph_2Ppy), 23.6 (d, br, ^2J(*tans*-P^2-P^3) = 388 Hz, κ^1-Ph_2Ppy) -47.7(d, br, κ^2-Ph_2Ppy).

K - <u>Variable temperature NMR spectroscopic measurements for 3.</u> Typically, a 0.0178 mmol solution of **3**(Cl) in dichloromethane was used. For **3**[OTf], one equivalent of Ag[OTf] was added to the solution, and the supernatant liquid decanted from the AgCl precipitate before transferring the solution to an NMR tube. The variable temperature $^{31}P\{^1H\}$ NMR spectra were recorded, and simulated using gNMR5.1.

L - <u>Determination of activation parameters for 6.</u> Typically, $MeSO_3H$ (130 mg, 1.37 mmol) was added to a suspension of (0.015 g, 0.064 mmol) palladium acetate in methanol (0.75 mL) to give a red solution. This solution was transferred to an NMR tube and the variable temperature $^{31}P\{^1H\}$ NMR spectra recorded, simulated using gNMR5.1 and $\Delta S^{\ddagger}$, $\Delta H^{\ddagger}$, and E_{act} were obtained from Eyring and Arrhenius plots respectively.

2.10.3. gNMR simulations

Simulation of variable temperature $^{31}P\{^1H\}$ NMR spectra was performed using gNMR5.1. Coupling constants and limiting chemical shifts were determined from a low temperature, "static" spectrum. Coupling constants were treated as constant in the simulations, however, pronounced temperature effects on the chemical shift were noted. Chemical shifts were therefore corrected iteratively in the simulations, using as a criterion the assumption that chemical shift varies linearly with temperature. Linewidths used in the simulations were estimated from the line widths of resonances not involved in a dynamic process over the temperature range studied, and were treated as constant.

In Addition, the intermediate situations happen between the low-temperature (or "slow-exchange") limit and the high temperature limit is particularly interesting. As the temperature is raised, the initially sharp lines broaden and coalesce until,

in the fast-exchange limit, a sharp spectrum is obtained again, it is possible to determine a rate constant from the line broadening by fitting. The temperature dependence of the rate constant can then be used to extract activation energies and entropies.

Supplementary Figure 1. Experimental and simulated variable temperature $^{31}P\{^{1}H\}$ NMR spectra of **6** in MeOH Pd:PPh_2py:CH_3SO_3H = 1:3.4:10. (sample 3). The sharp resonance at ca -8 ppm is due to $[PPh_2pyH]^+(MeSO_3)$. (sample 3).

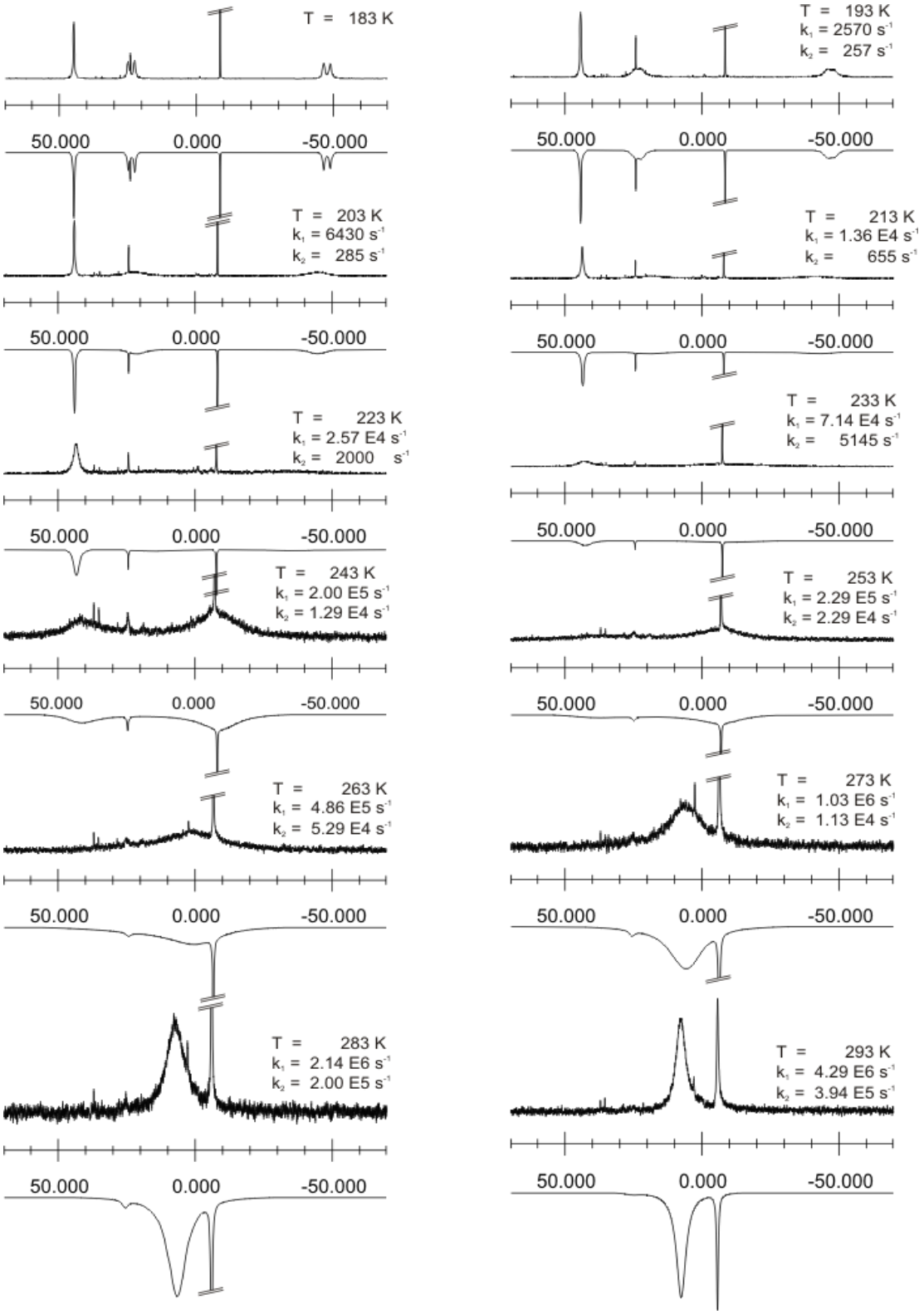

Supplementary Figure 2. Eyring and Arrhenius plots for **6** in MeOH Pd:PPh_2py:CH_3SO_3H = 1:3.4:10. (sample 3).

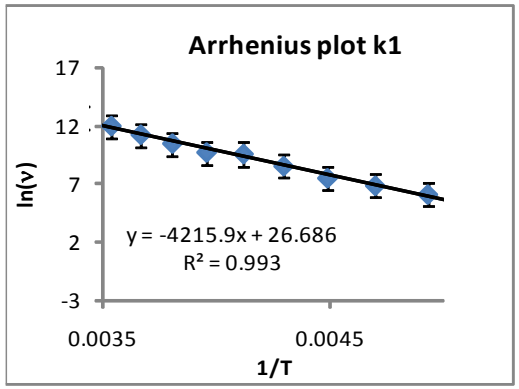

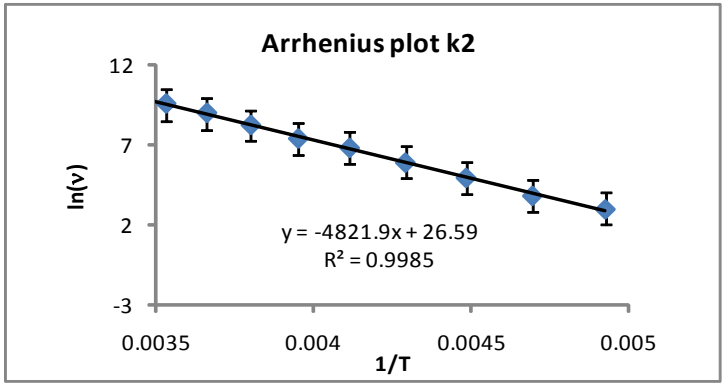

h	6.63E-34	J s^{-1}
kB	1.38E-23	J K^{-1}
R	8.314	J mol^{-1} K^{-1}

Eyring	**k1**	**k2**	
intercept	22.6	22.75	
gradEy	-3911	-4579	
ΔH	33	38	kJ mol^{-1}
ΔS	-10	-8	J K^{-1} mol^{-1}
Arrhenius			
Eact	35	40	kJ mol^{-1}
gradAhr	-4216	-4822	

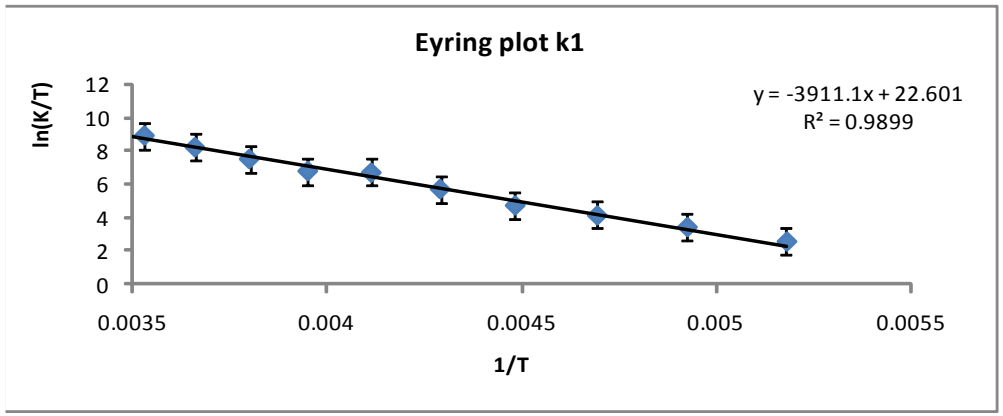

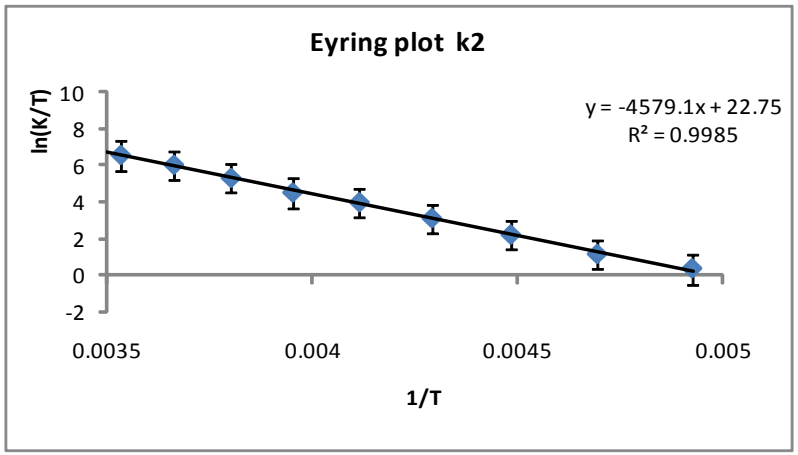

Supplementary Figure 3. Experimental and simulated variable temperature $^{31}P\{^{1}H\}$ NMR spectra of **6** in MeOH Pd:PPh_2py:CH_3SO_3H = 1:3.4:25. The resonance at ca -8 ppm is due to $[PPh_2pyH]^+(MeSO_3)$. (sample 4).

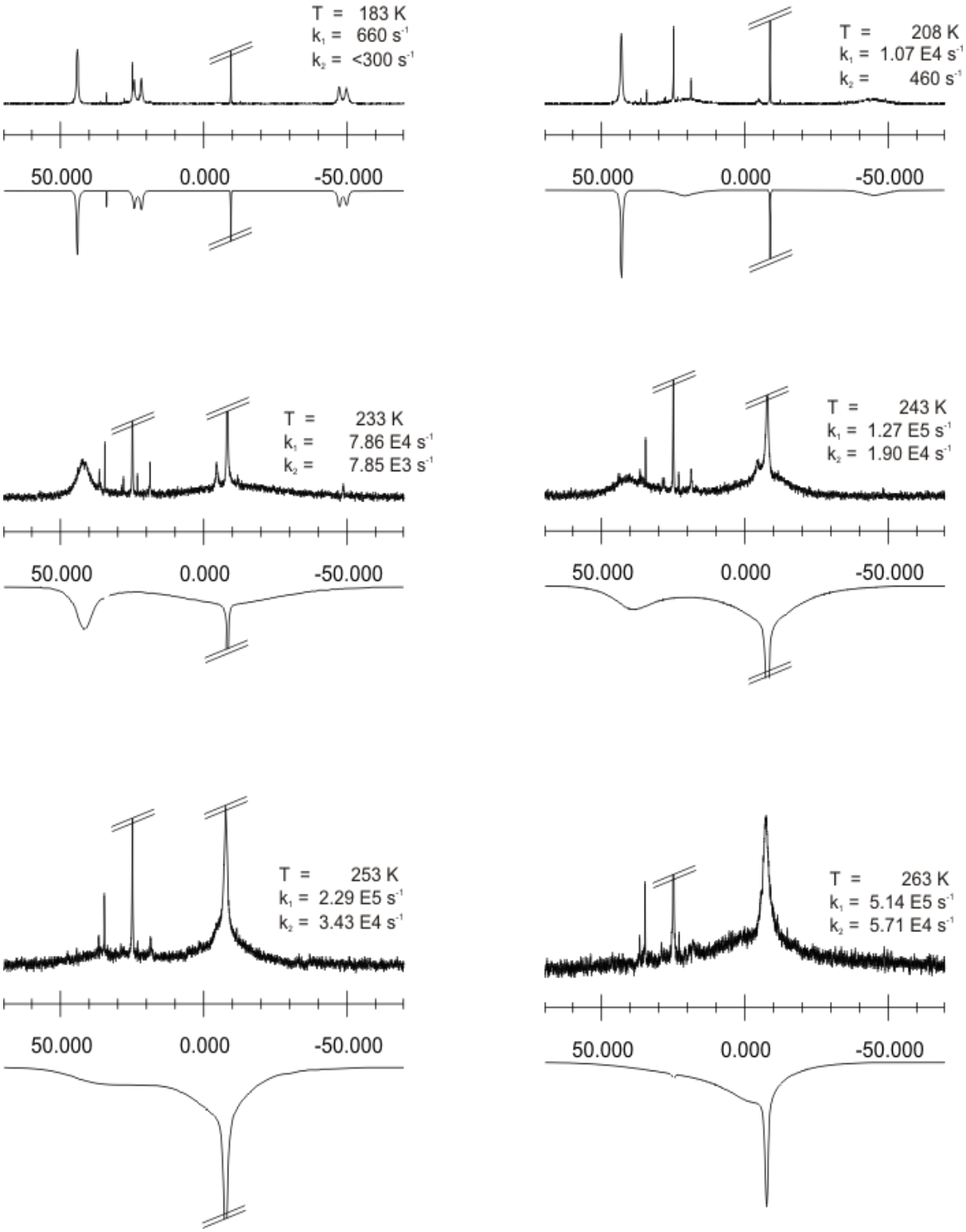

Supplementary Figure 4. Eyring and Arrhenius plots for **6** in MeOH Pd:PPh_2py:CH_3SO_3H = 1:3.4:25. (sample 4).

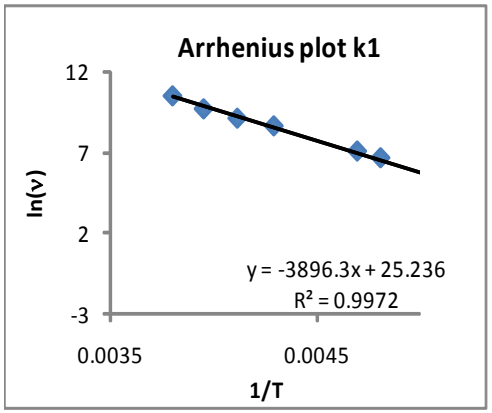

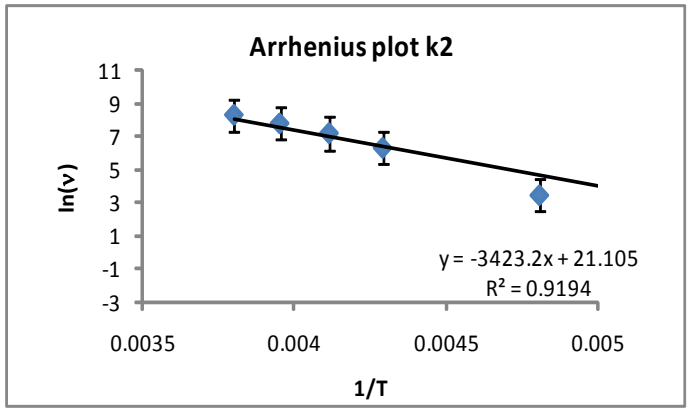

h	6.63E-34	J s^{-1}
kB	1.38E-23	J K^{-1}
R	8.314	J mol^{-1} K^{-1}

Eyring	**k1**	**k2**	
intercept	20.756	19.798	
gradEy	-3515	-4654	
ΔH	29	39	kJ mol^{-1}
ΔS	-25	-33	J K^{-1} mol^{-1}
Arrhenius			
Eact	31	41	kJ mol^{-1}
gradAhr	-3747	-4886	

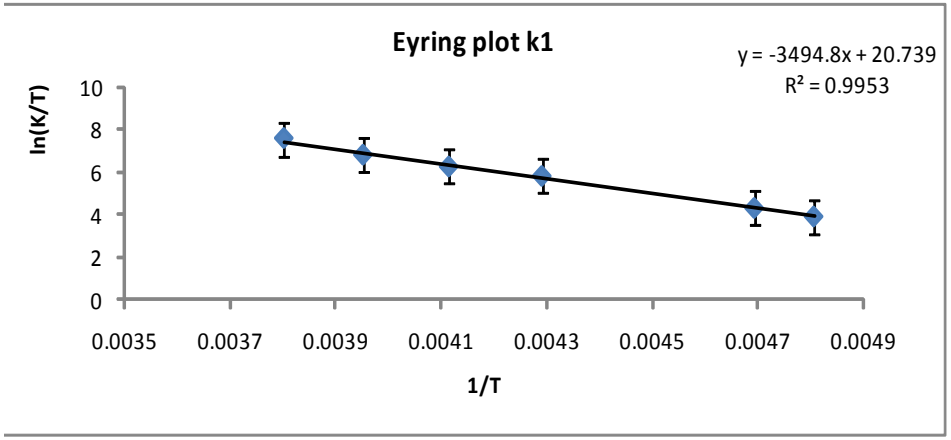

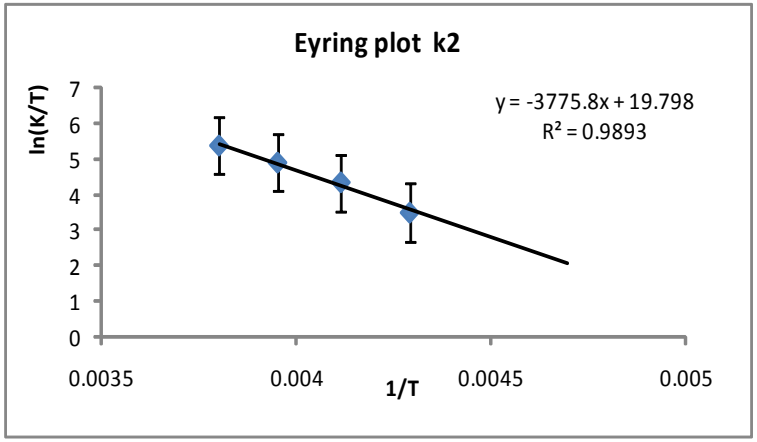

Supplementary Figure 5. Experimental and simulated variable temperature $^{31}P\{^{1}H\}$ NMR spectra of **6** in MeOH Pd:PPh_2py:CH_3SO_3H = 1:3.2:15. (sample 5).

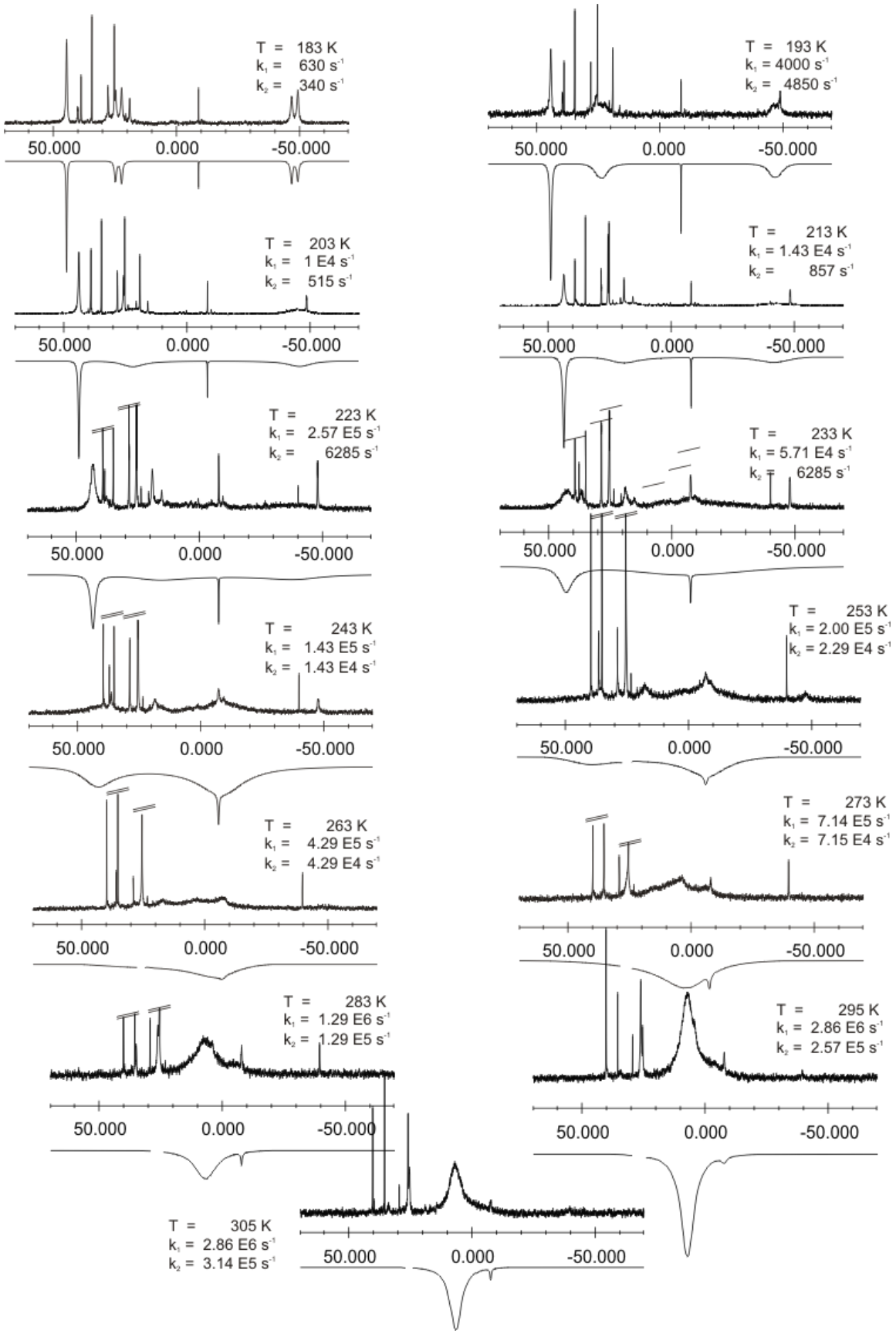

Supplementary Figure 6. Eyring and Arrhenius plots for Eyring and Arrhenius plots for **6** in MeOH Pd:PPh_2py:CH_3SO_3H = 1:3.2:15. (sample 5).

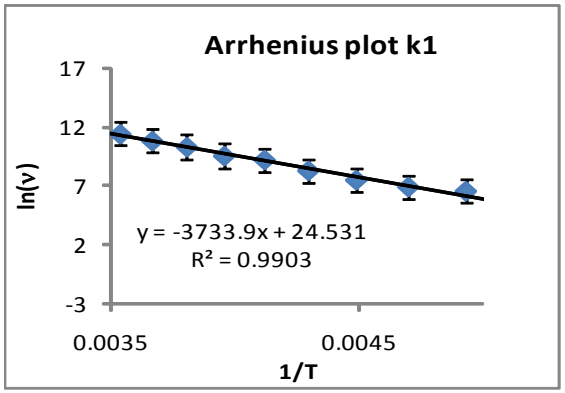

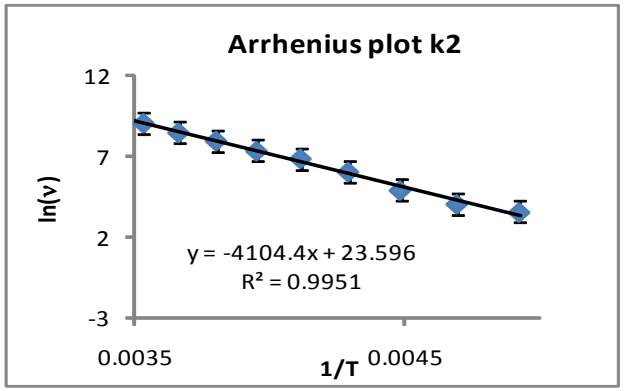

h	6.63E-34	J s^{-1}
kB	1.38E-23	J K^{-1}
R	8.314	J mol^{-1} K^{-1}

Eyring	**k1**	**k2**	
intercept	20.72	19.74	
gradEy	-3500	-3857	
ΔH	29	32	kJ mol^{-1}
ΔS	-25	-33	J K^{-1} mol^{-1}
Arrhenius			
Eact	31	34	kJ mol^{-1}
gradAhr	-3734	-4104	

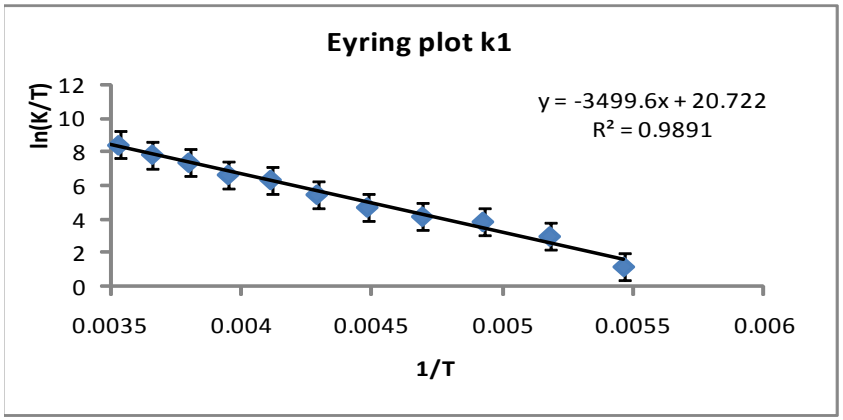

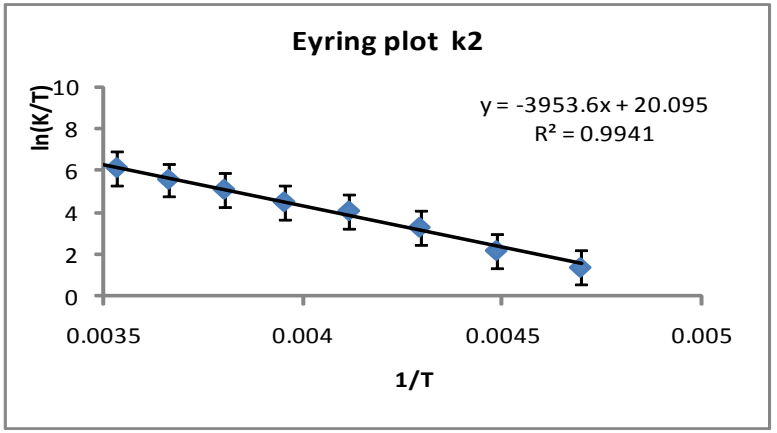

Supplementary Figure 7. Experimental and simulated variable temperature $^{31}P\{^{1}H\}$ NMR spectra of **6** in MeOH Pd:PPh_2py:CH_3SO_3H = 1:2.9:25. (sample 6).

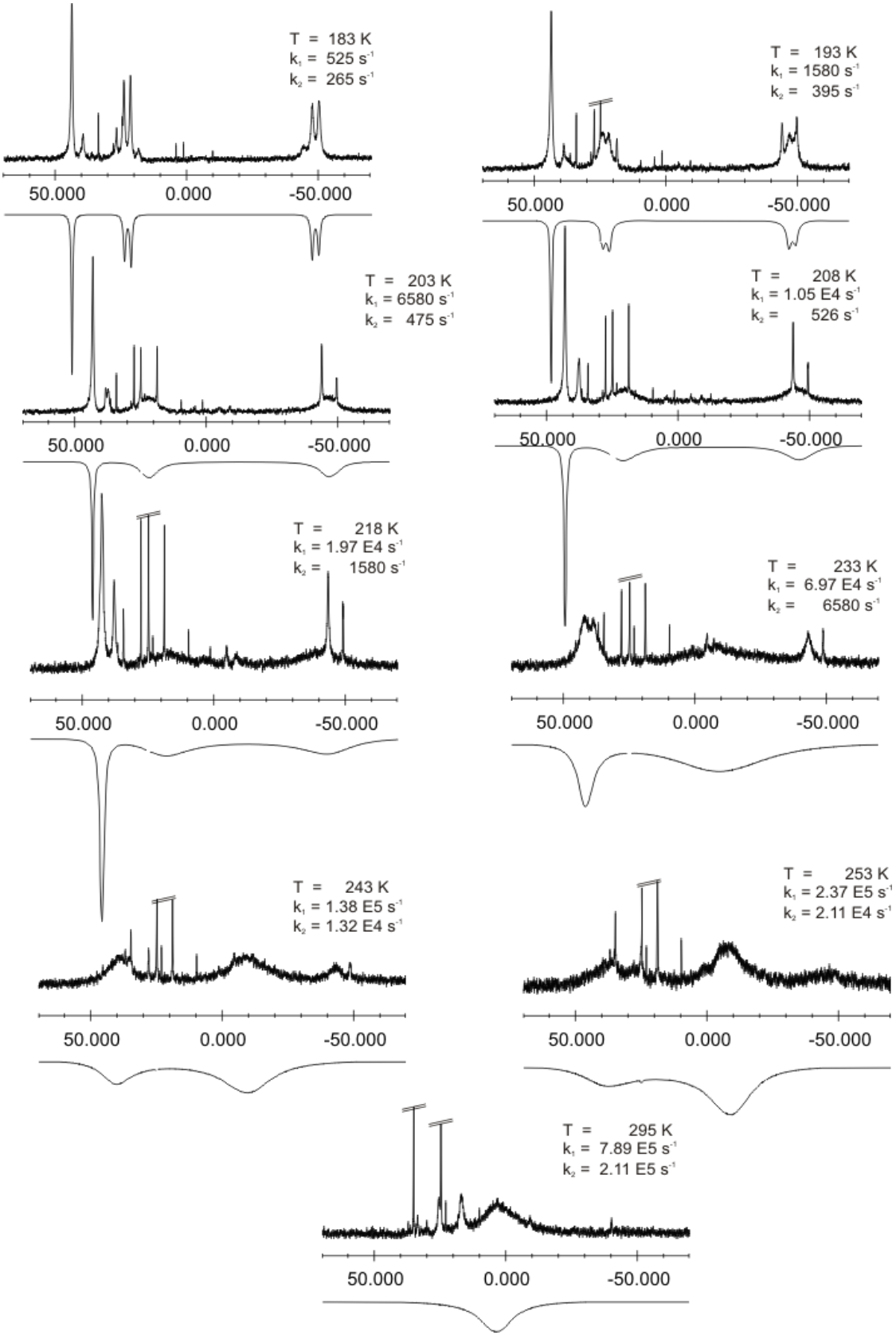

Supplementary Figure 8. Eyring and Arrhenius plots for **6** in MeOH Pd:PPh_2py:CH_3SO_3H = 1:2.9:25. (sample 6).

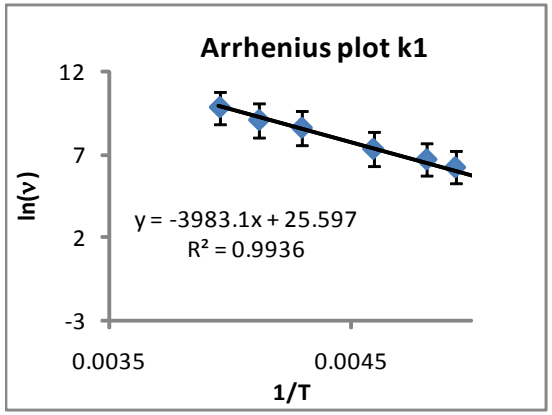

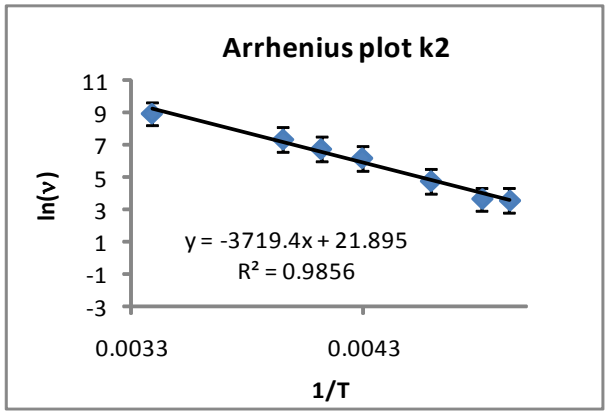

h	6.63E-34	J s^{-1}
kB	1.38E-23	J K^{-1}
R	8.314	J mol^{-1} K^{-1}

Eyring	**k1**	**k2**	
intercept	21.7	20.75	
gradEy	-3736	-4101	
ΔH	31	34	kJ mol^{-1}
ΔS	-17	-25	J K^{-1} mol^{-1}
Arrhenius			
Eact	34	31	kJ mol^{-1}
gradAhr	-4046	-3719	

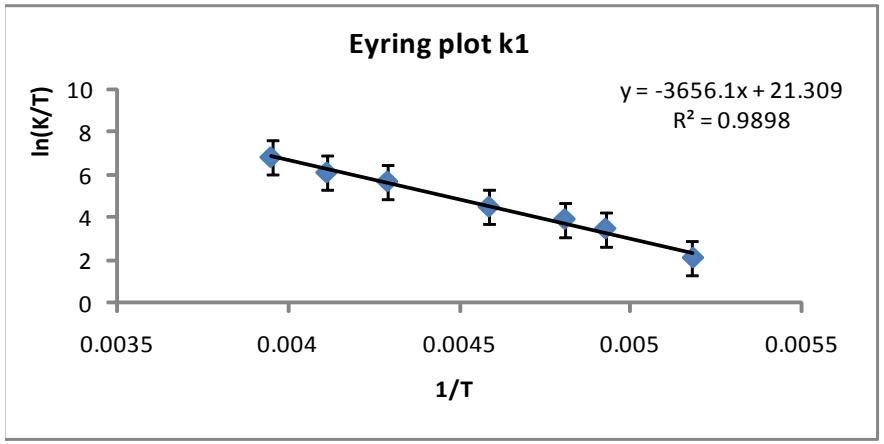

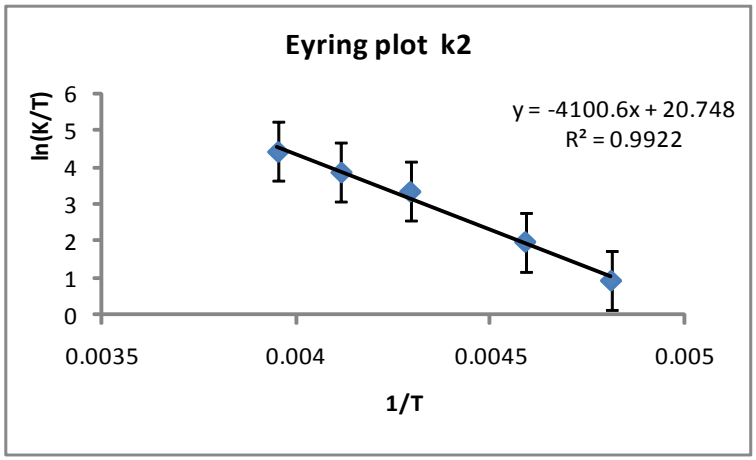

Supplementary Figure 9. Experimental and simulated variable temperature $^{31}P\{^{1}H\}$ NMR spectra of **6** MeOH:CD_2Cl_2 4:3; Pd:PPh_2py:CH_3SO_3H = 1:3.1:5. (sample 8).

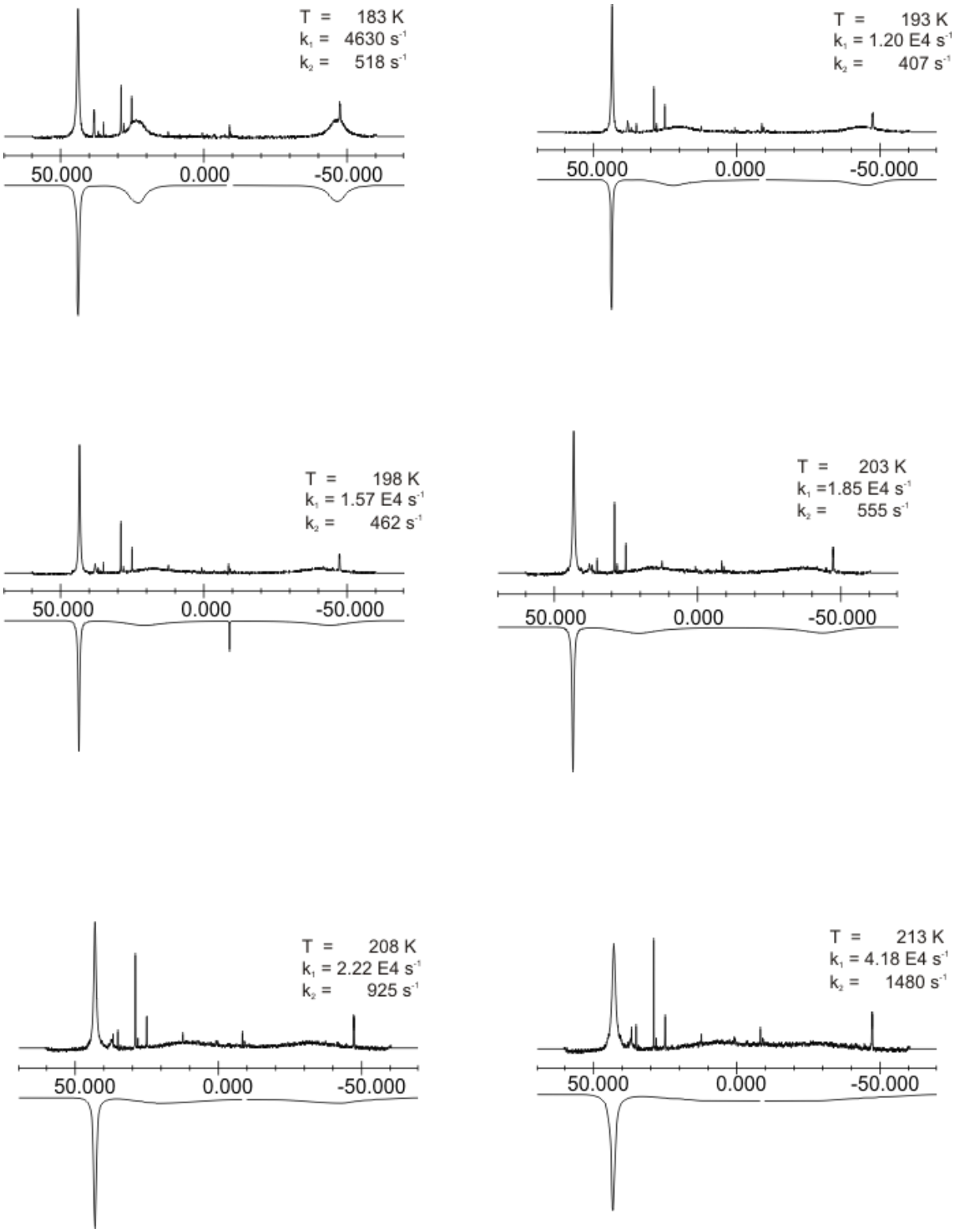

Supplementary Fig 9 continued

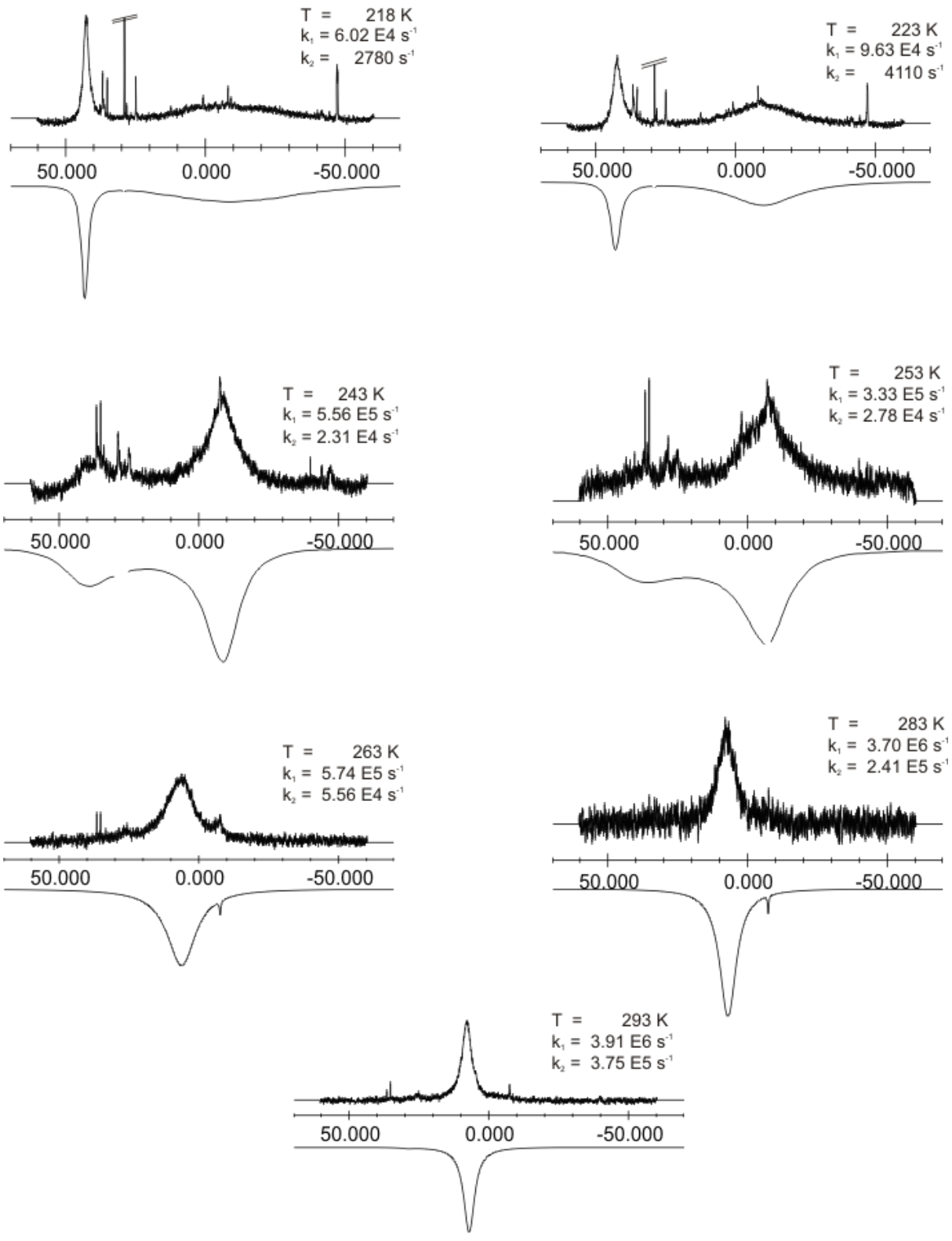

Supplementary Figure 10. Eyring and Arrhenius plots for **6** MeOH:CD_2Cl_2 4:3; Pd:PPh_2py:CH_3SO_3H = 1:3.1:5. (sample 8).

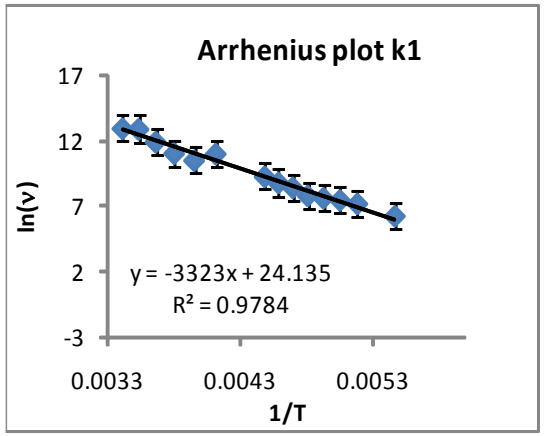

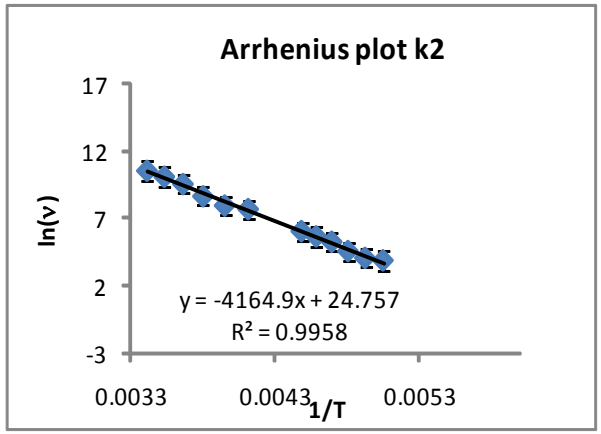

h	6.63E-34	J s^{-1}
kB	1.38E-23	J K^{-1}
R	8.314	J mol^{-1} K^{-1}

Eyring	**k1**	**k2**	
intercept	21.38	20.71	
gradEy	-2905	-3684	
ΔH	24	31	kJ mol^{-1}
ΔS	-20	-25	J K^{-1} mol^{-1}
Arrhenius			
Eact	28	33	kJ mol^{-1}
gradAhr	-3323	-3978	

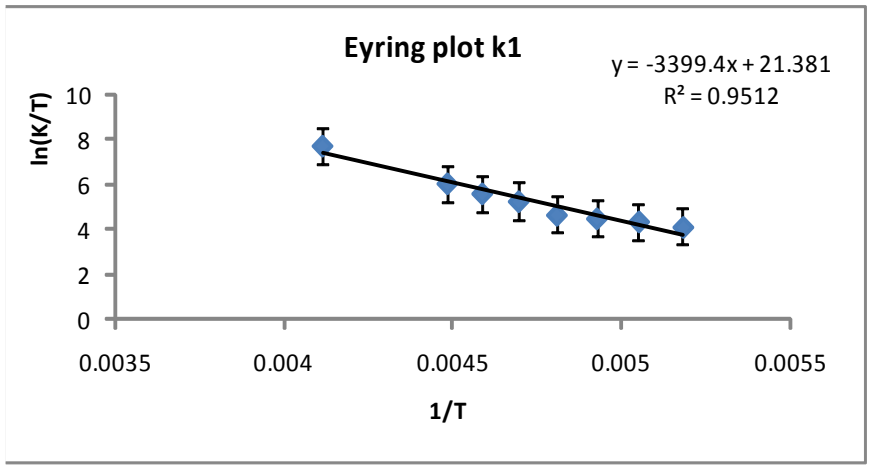

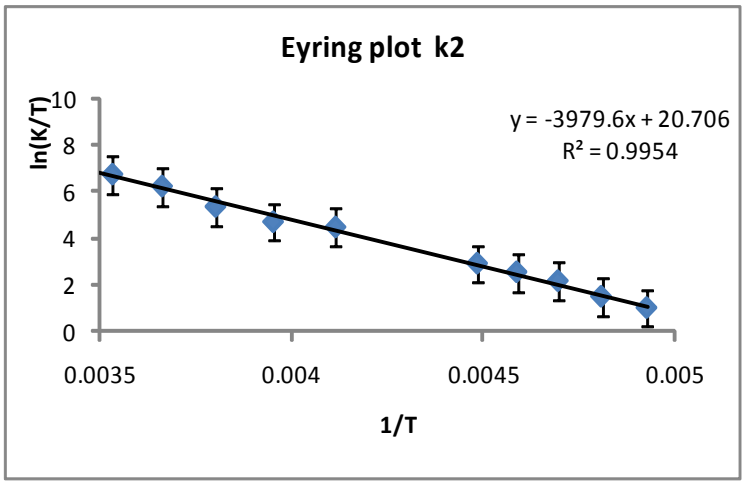

Supplementary Figure 11. Experimental and simulated variable temperature $^{31}P\{^{1}H\}$ NMR spectra of **6** in MeOH. Pd:PPh_2py:CH_3SO_3H = 1:3.1:10. (sample 1).

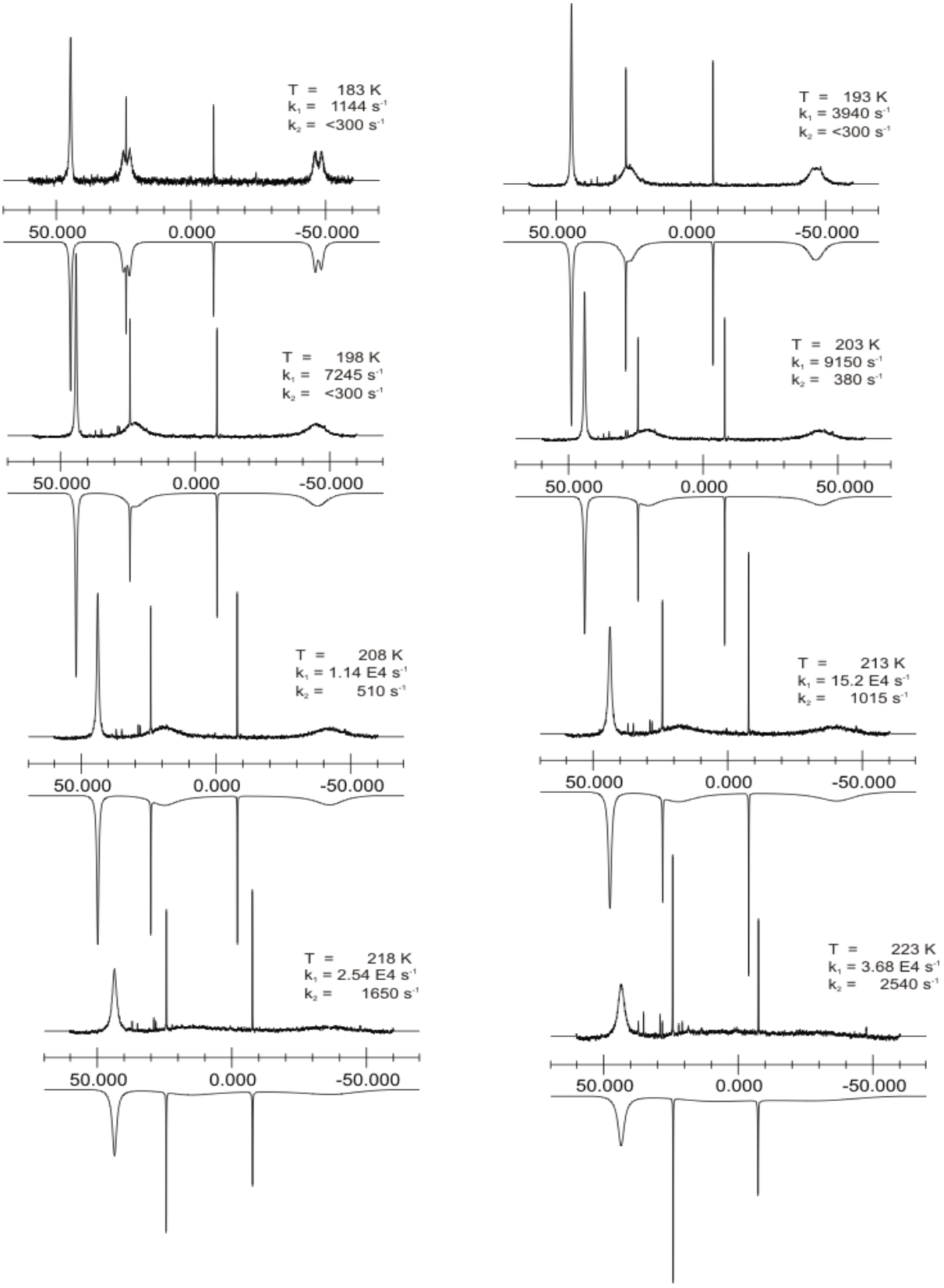

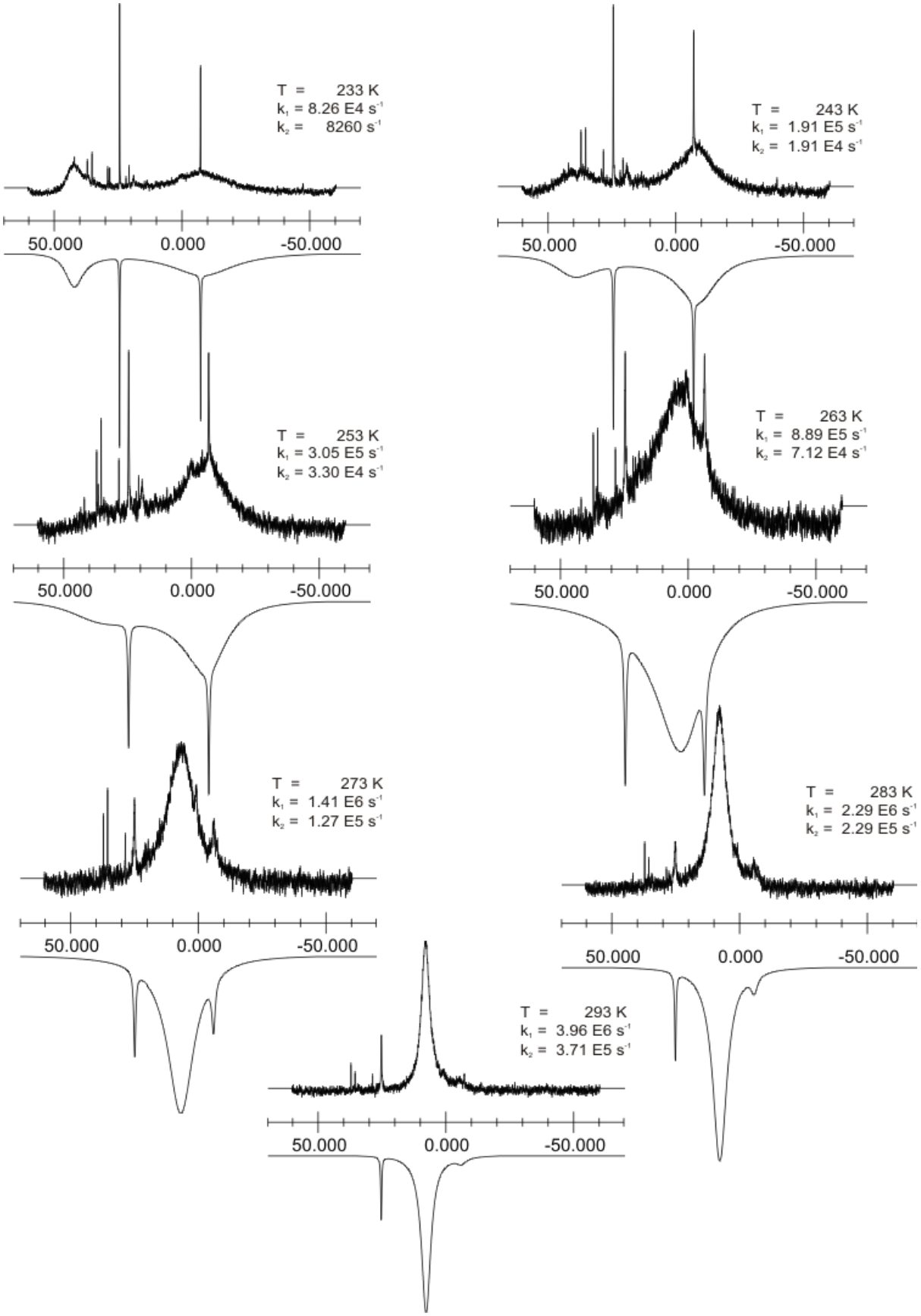

Supplementary Fig 11 continued

Supplementary Figure 12. Eyring and Arrhenius plots for **6** in MeOH. Pd:PPh_2py:CH_3SO_3H = 1:3.1:10. (sample 1).

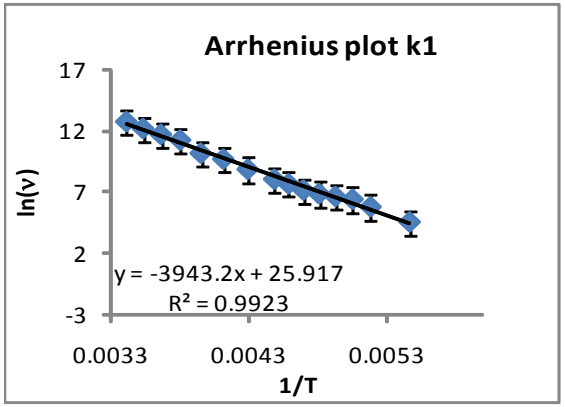

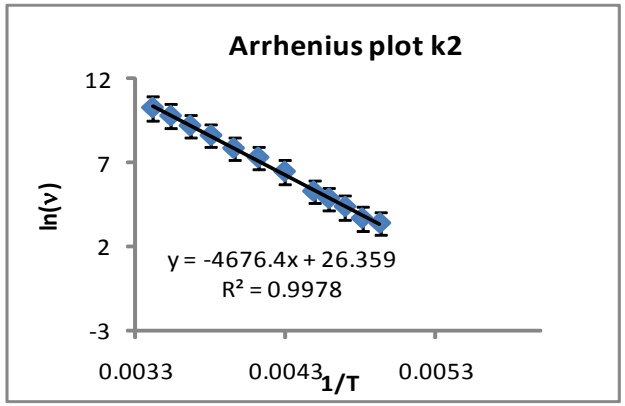

h	6.63E-34	J s^{-1}
kB	1.38E-23	J K^{-1}
R	8.314	J mol^{-1} K^{-1}

Eyring	**k1**	**k2**	
intercept	22.01	22.41	
gradEy	-3713	-4435	
ΔH	31	37	kJ mol^{-1}
ΔS	-15	-11	J K^{-1} mol^{-1}
Arrhenius			
Eact	33	39	kJ mol^{-1}
gradAhr	-3943	-4676	

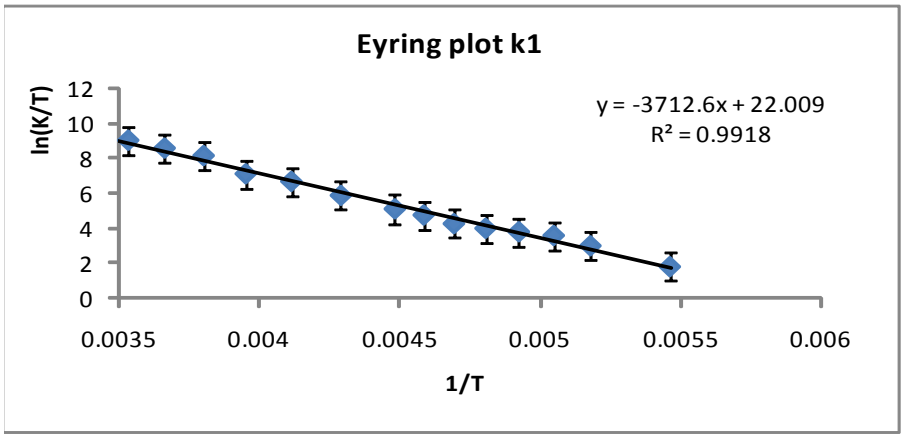

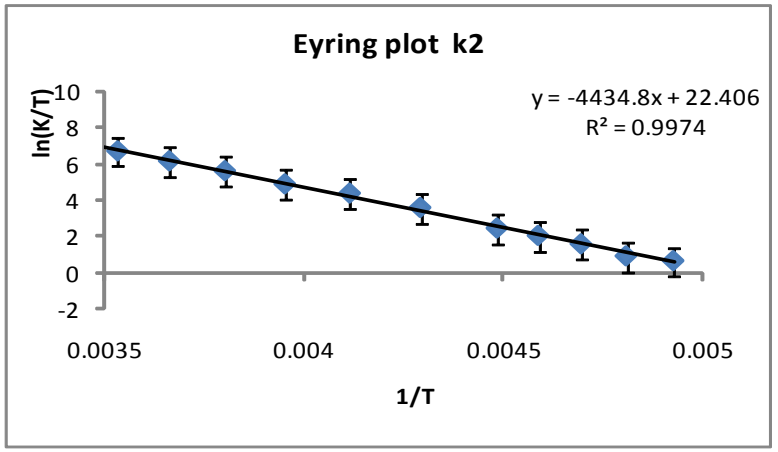

Supplementary Figure 13. Experimental and simulated variable temperature $^{31}P\{^{1}H\}$ NMR spectra of **6** in MeOH Pd:PPh_2py:CH_3SO_3H = 1:3.1:10. (sample2).

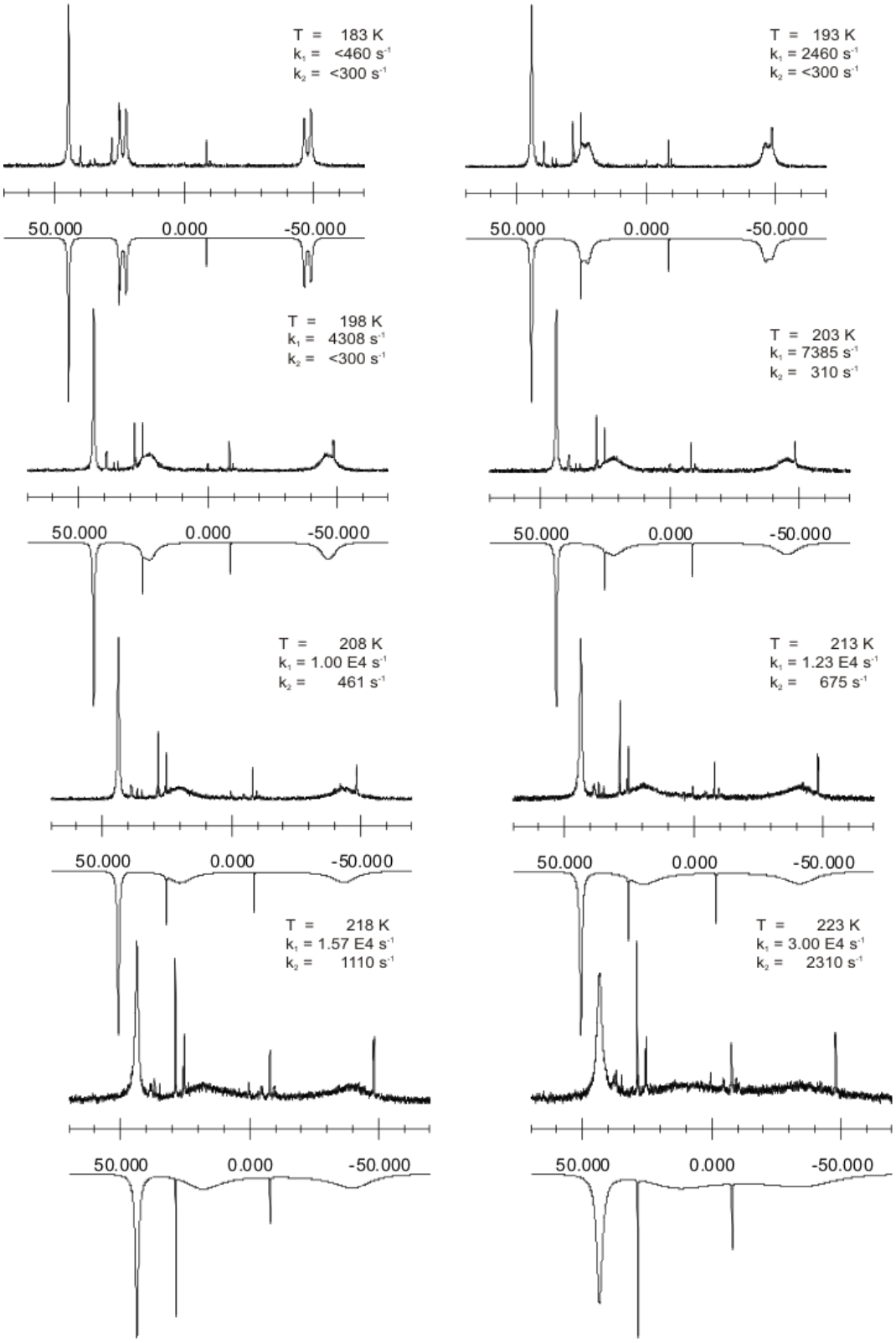

Supplementary Fig 13 continued

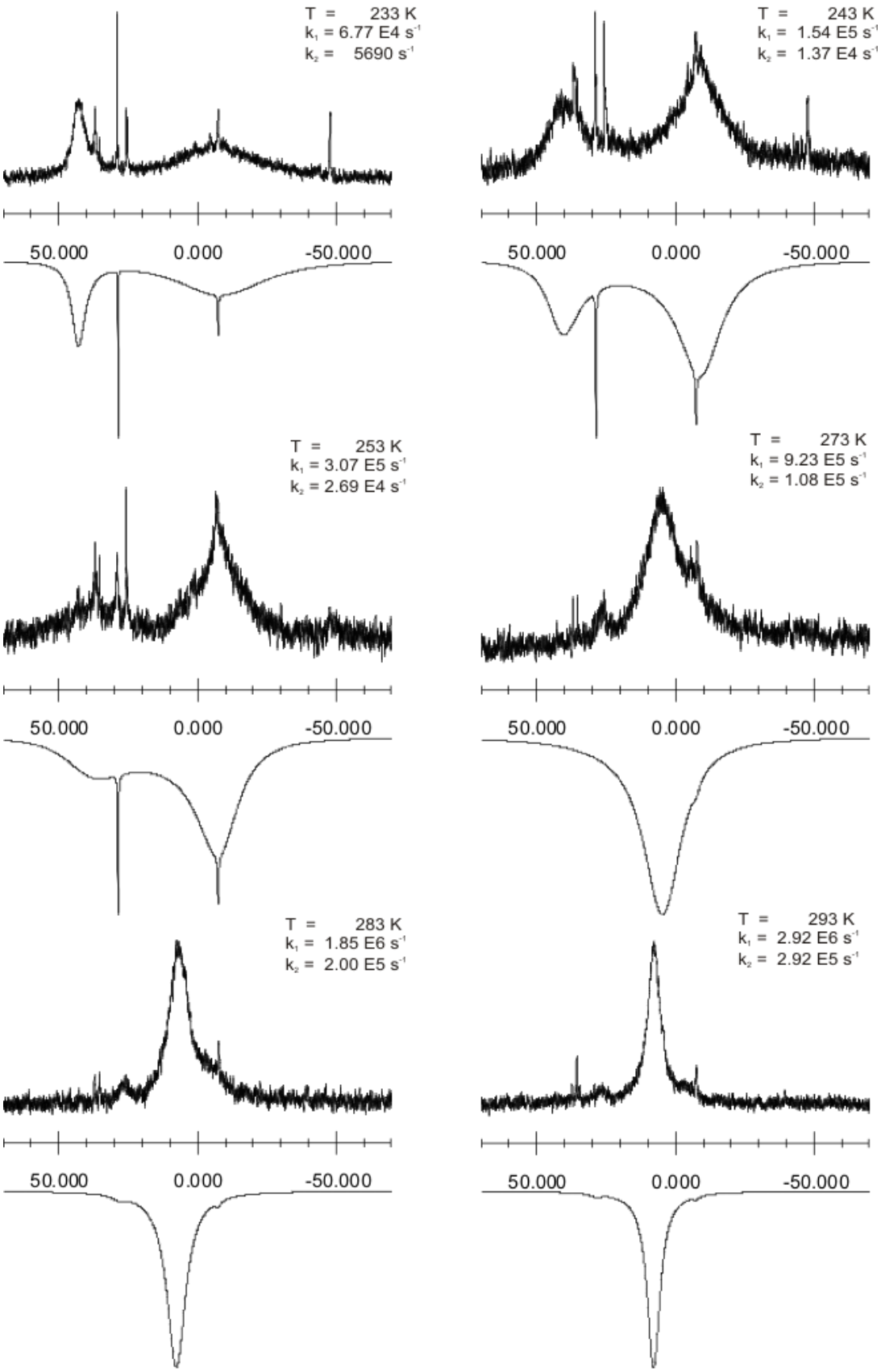

Supplementary Figure 14. Eyring and Arrhenius plots for **6** in MeOH Pd:PPh_2py:CH_3SO_3H = 1:3.1:10. (sample 2).

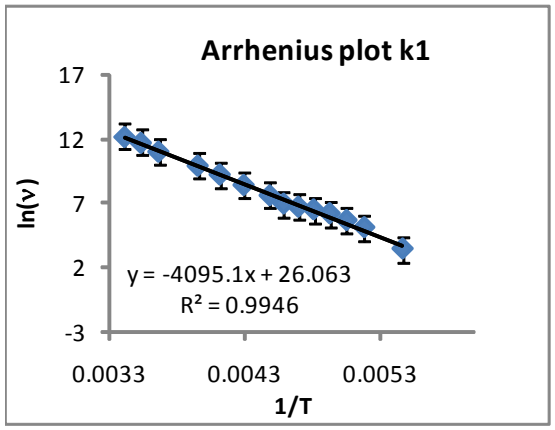

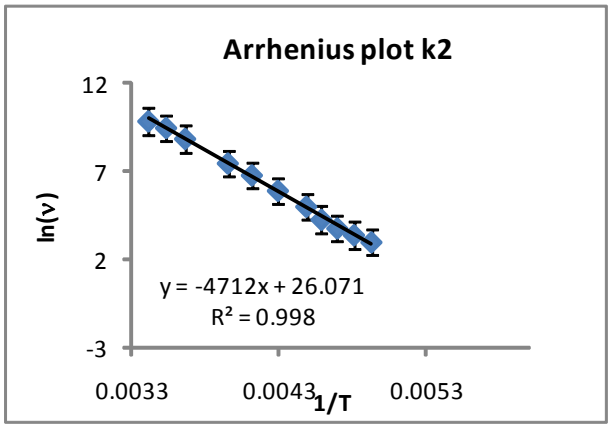

h	6.63E-34	J s^{-1}
kB	1.38E-23	J K^{-1}
R	8.314	J mol^{-1} K^{-1}

Eyring	**k1**	**k2**	
intercept	22.277	22.301	
gradEy	-3850	-4470	
ΔH	32	37	kJ mol^{-1}
ΔS	-12	-12	J K^{-1} mol^{-1}
Arrhenius			
Eact	34	39	kJ mol^{-1}
gradAhr	-4095	-4712	

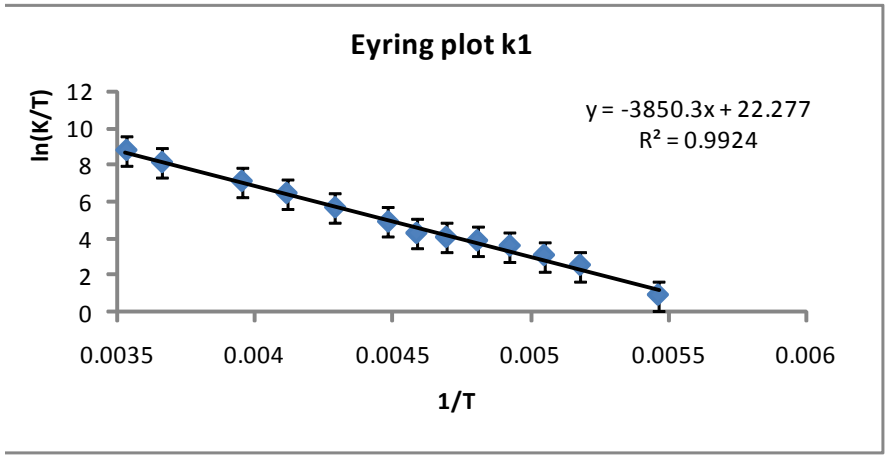

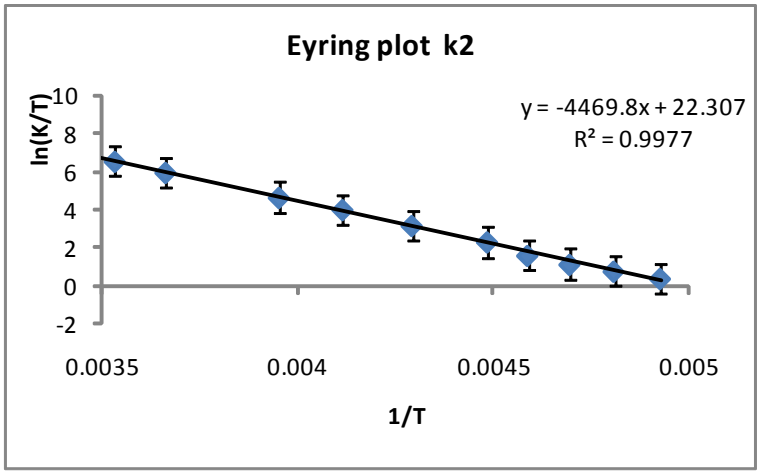

Supplementary Figure 15. Experimental and simulated variable temperature $^{31}P\{^{1}H\}$ NMR spectra of **6** in MeOH:CD_2Cl_2 (2:9) Pd:PPh_2py:CH_3SO_3H = 1:3.1:25. (sample 7).

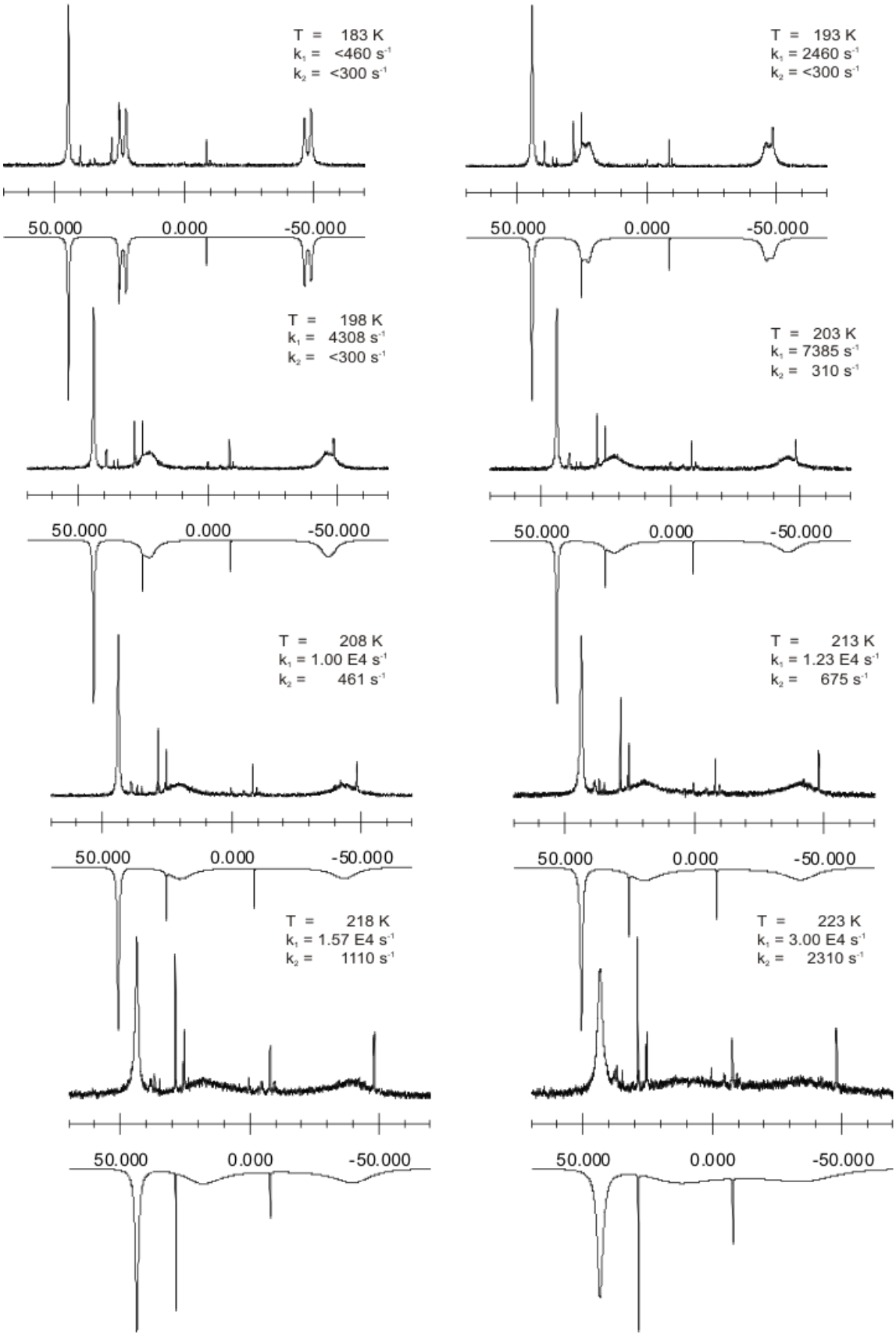

Supplementary Fig 15 continued

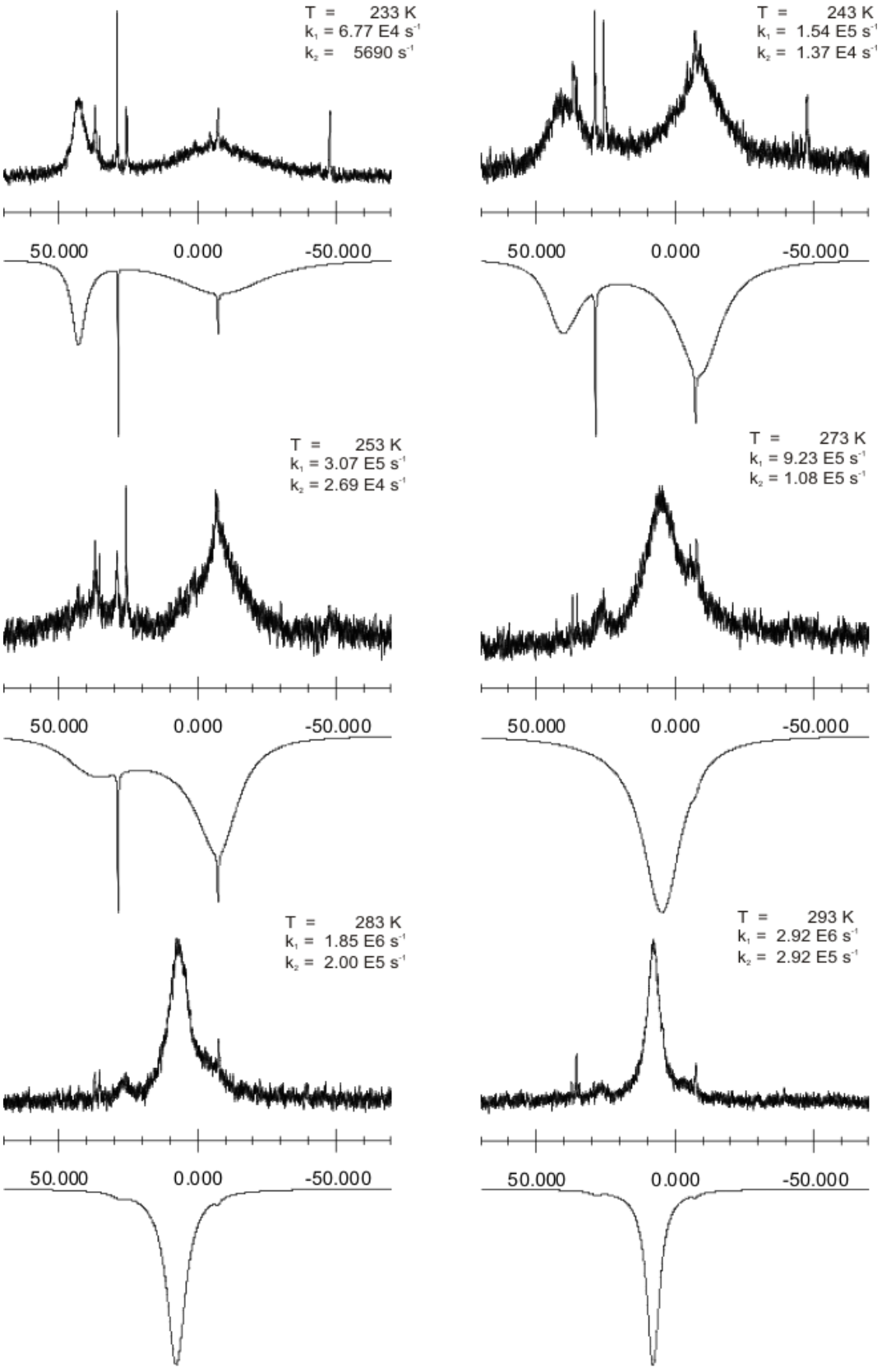

Supplementary Figure 16. Eyring and Arrhenius plots for **6** in MeOH:CD_2Cl_2 (2:9) Pd:PPh_2py:CH_3SO_3H = 1:3.1:25. (sample 7).

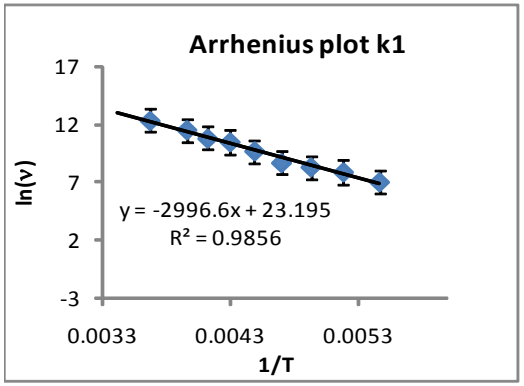

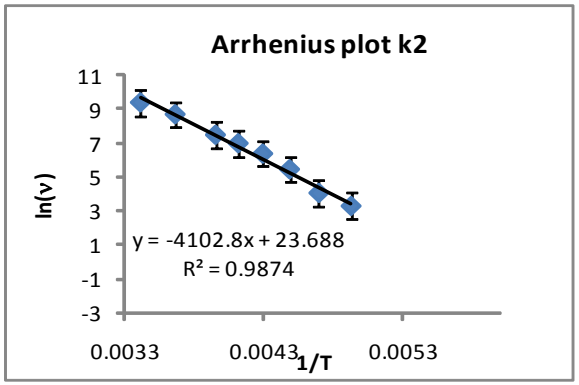

h	6.63E-34		$J\ s^{-1}$
kB	1.38E-23		$J\ K^{-1}$
R	8.314		$J\ mol^{-1}\ K^{-1}$
Eyring	**k1**	**k2**	
intercept	18.78	19.93	
gradEy	-2626	-3861	
ΔH	22	32	$kJ\ mol^{-1}$
ΔS	-41	-32	$J\ K^{-1}\ mol^{-1}$
Arrhenius			
Eact	25	34	$kJ\ mol^{-1}$
gradAhr	-2997	-4103	

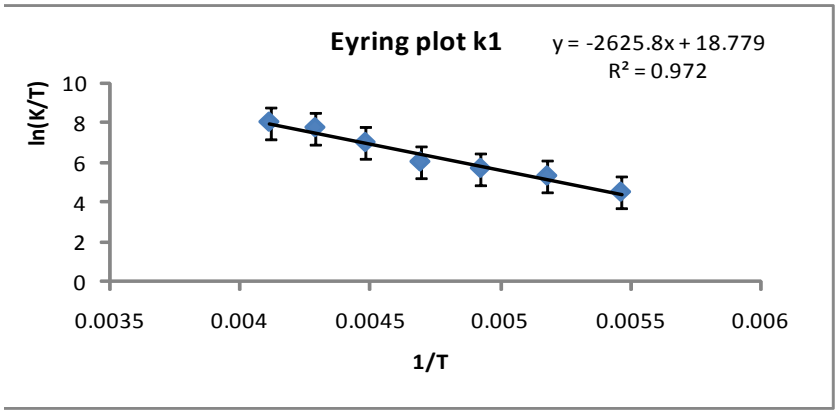

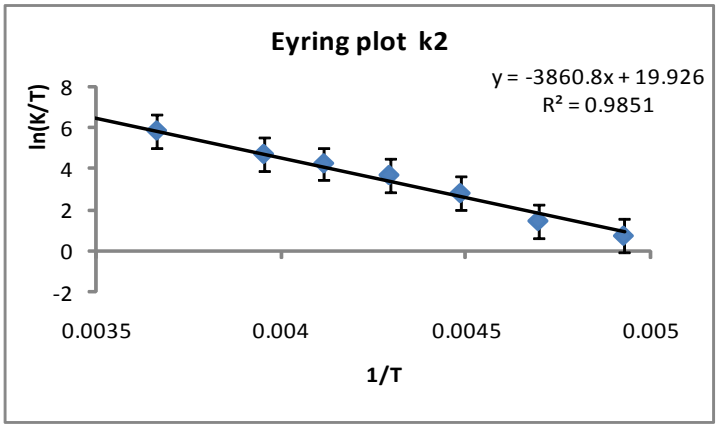

Supplementary Figure 17. Experimental and simulated variable temperature $^{31}P\{^{1}H\}$ NMR spectra of **6** in CD_2Cl_2 Pd:PPh_2py:CH_3SO_3H = 1:2.9:2. (sample 9). Impurities included to aid simulation, but not optimized.

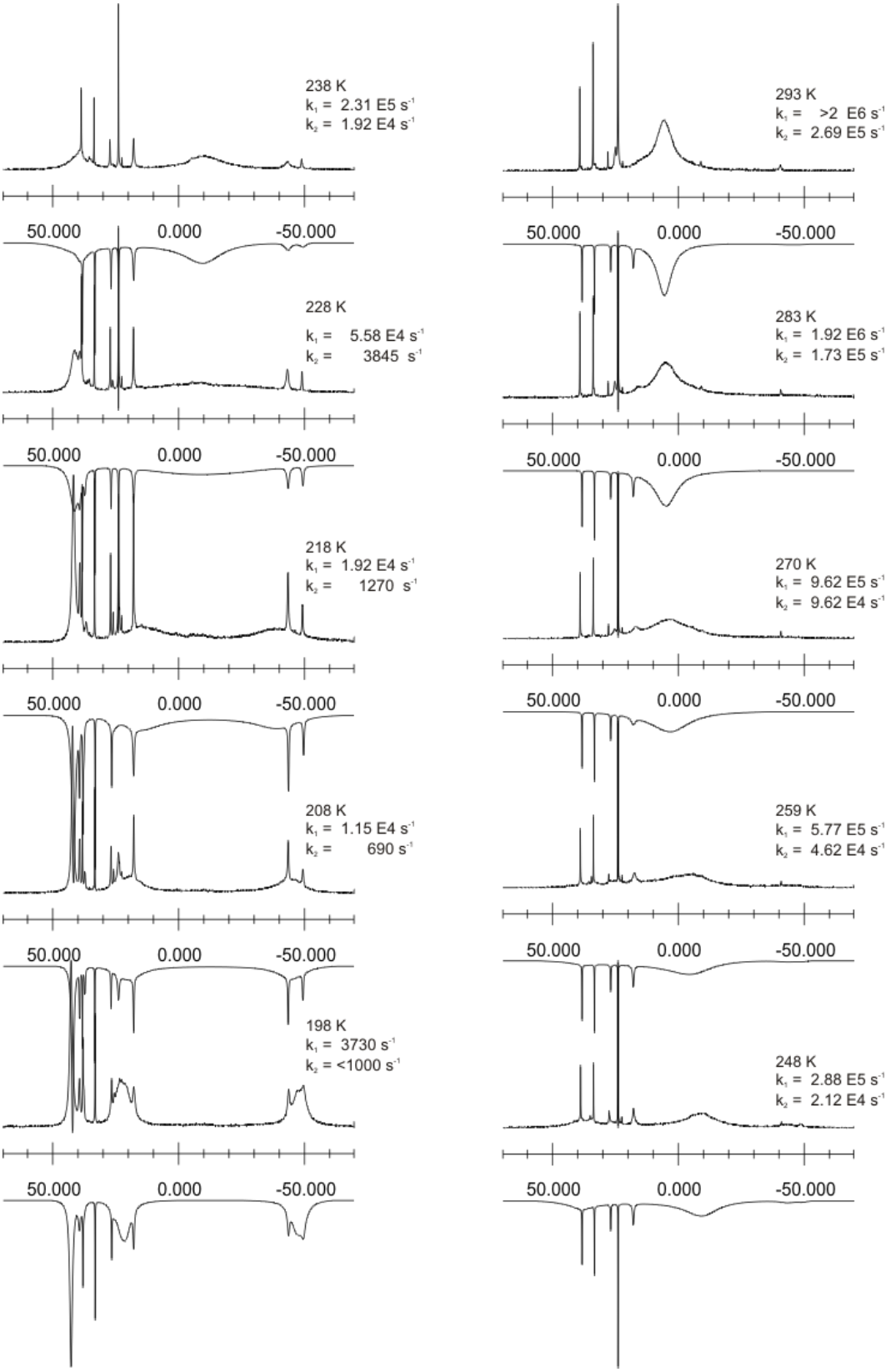

Supplementary Figure 18. Eyring and Arrhenius plots for **6** in CD_2Cl_2 Pd:PPh_2py:CH_3SO_3H = 1:2.9:2. (sample 9).

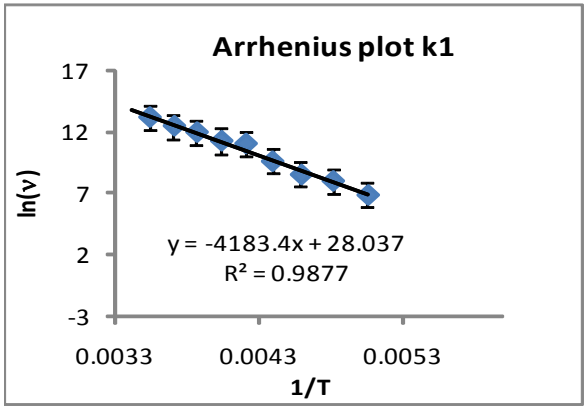

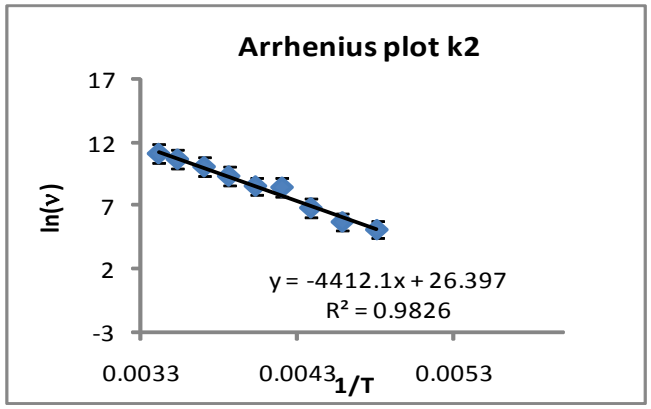

h	6.63E-34	J s^{-1}
kB	1.38E-23	J K^{-1}
R	8.314	J mol^{-1} K^{-1}

Eyring	**k1**	**k2**	
intercept	23.25	21.23	
gradEy	-4022	-4166	
ΔH	33	35	kJ mol^{-1}
ΔS	-4	-21	J K^{-1} mol^{-1}
Arrhenius			
Eact	35	37	kJ mol^{-1}
gradAhr	-4183	-4412	

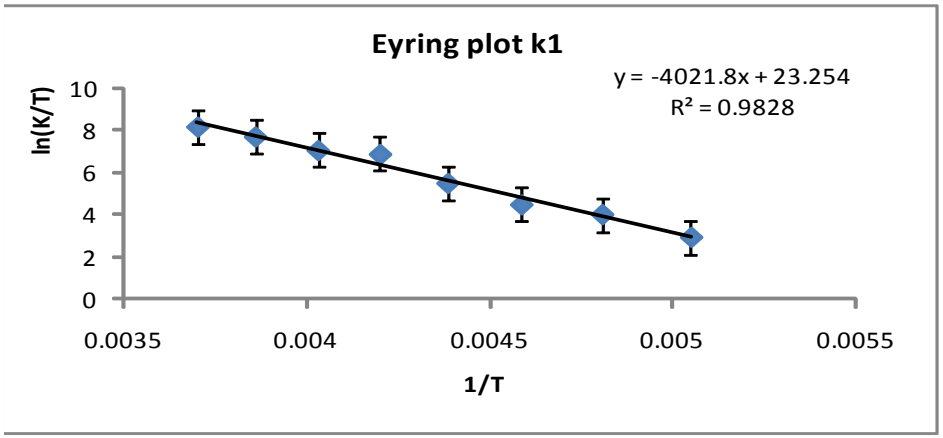

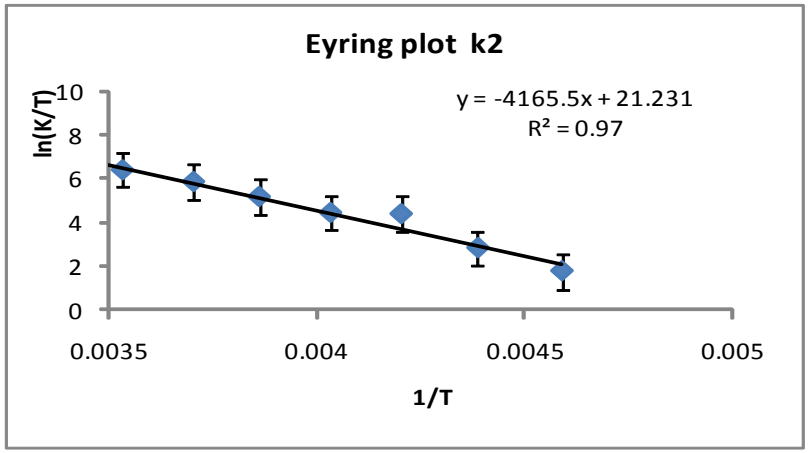

Supplementary Figure 19. Experimental and simulated variable temperature $^{31}P\{^{1}H\}$ NMR spectra of **3**(Cl) in CD_2Cl_2:MeOH (8:1). Note changes in ppm scale at 233, 253, 283 and

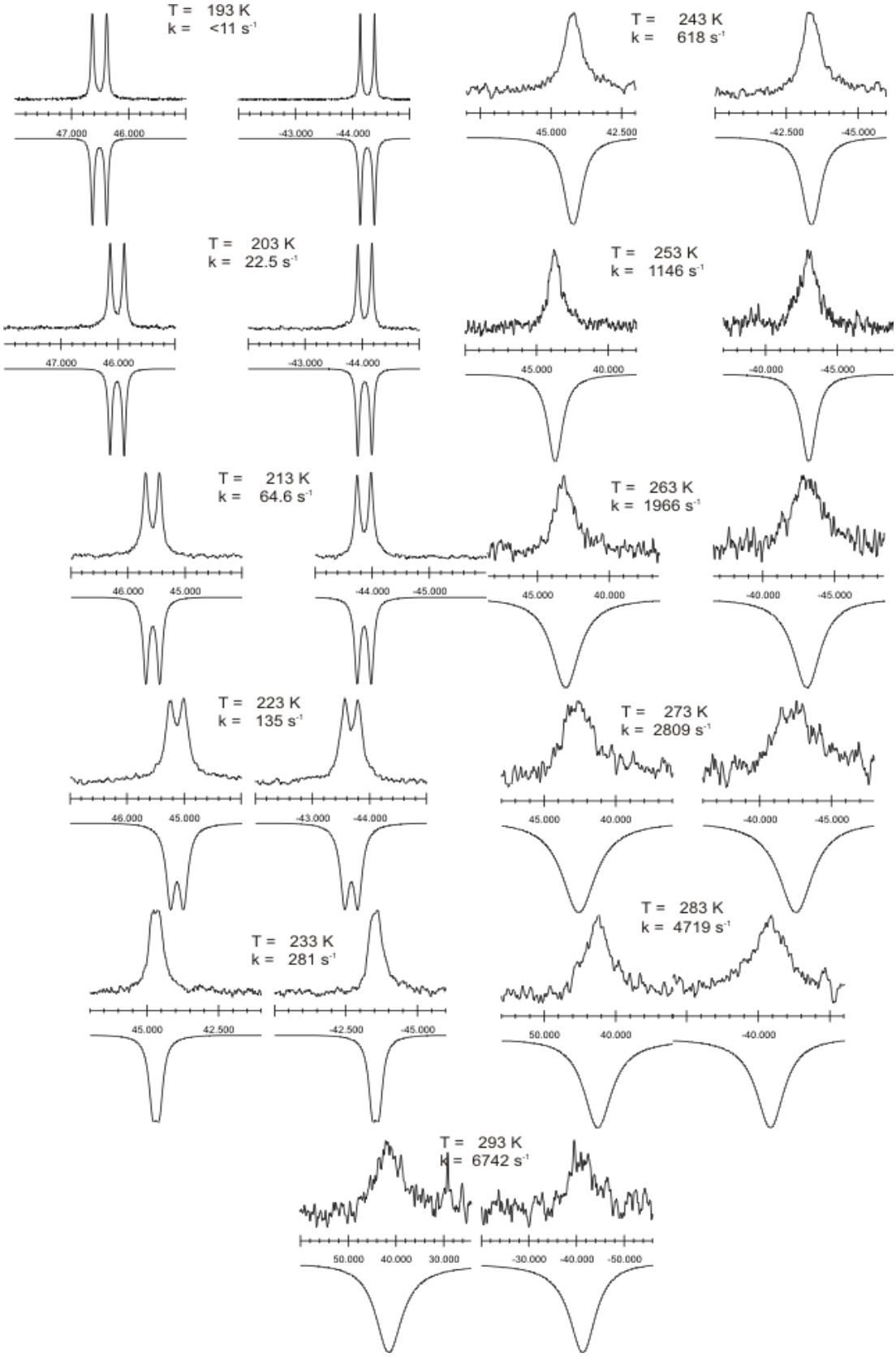

293 K

Supplementary Figure 20. Experimental and simulated variable temperature $^{31}P\{^{1}H\}$ NMR spectra of **3**(OTf) in CD_2Cl_2:MeOH (8:1). Note changes in ppm scale at 223, 263, and 283K.

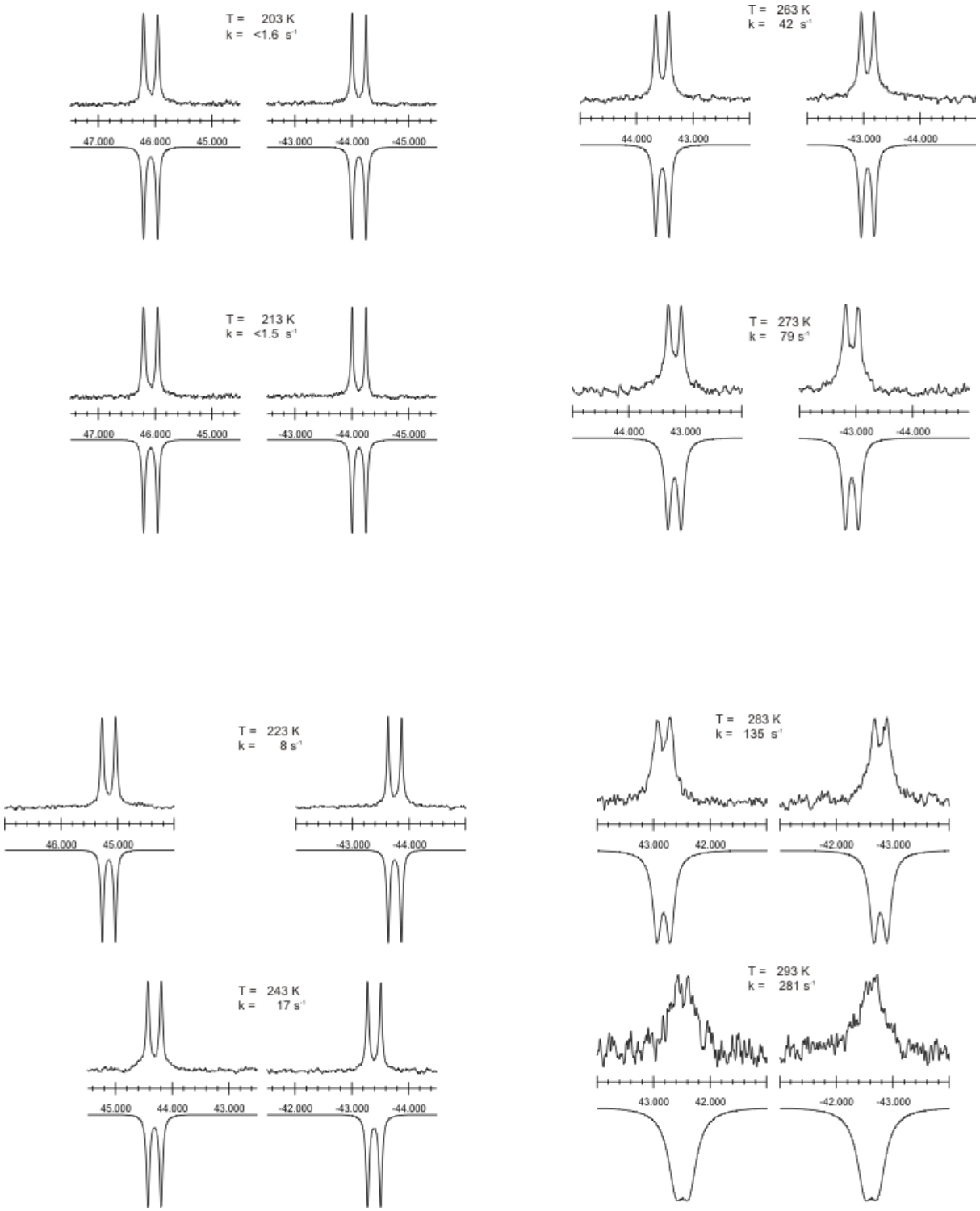

Supplementary Figure 21. Experimental and simulated variable temperature $^{31}P\{^{1}H\}$ NMR spectra of **3**(Cl) in CD_2Cl_2:MeOH (1:1). Note changes in ppm scale at 243, and 273 K

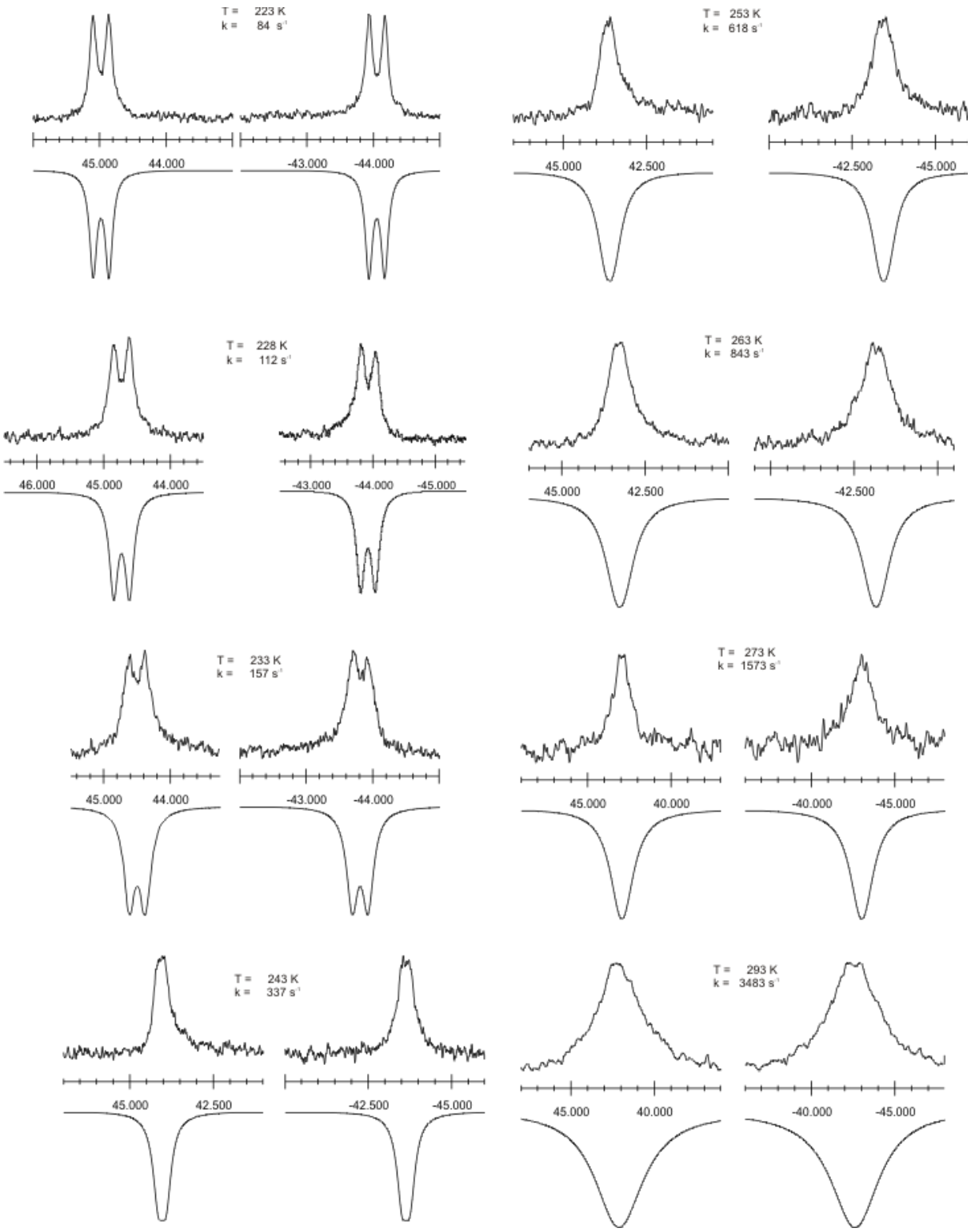

Supplementary Figure 22. Experimental and simulated variable temperature $^{31}P\{^{1}H\}$ NMR spectra of **3**(OTf)in CD_2Cl_2:MeOH (1:

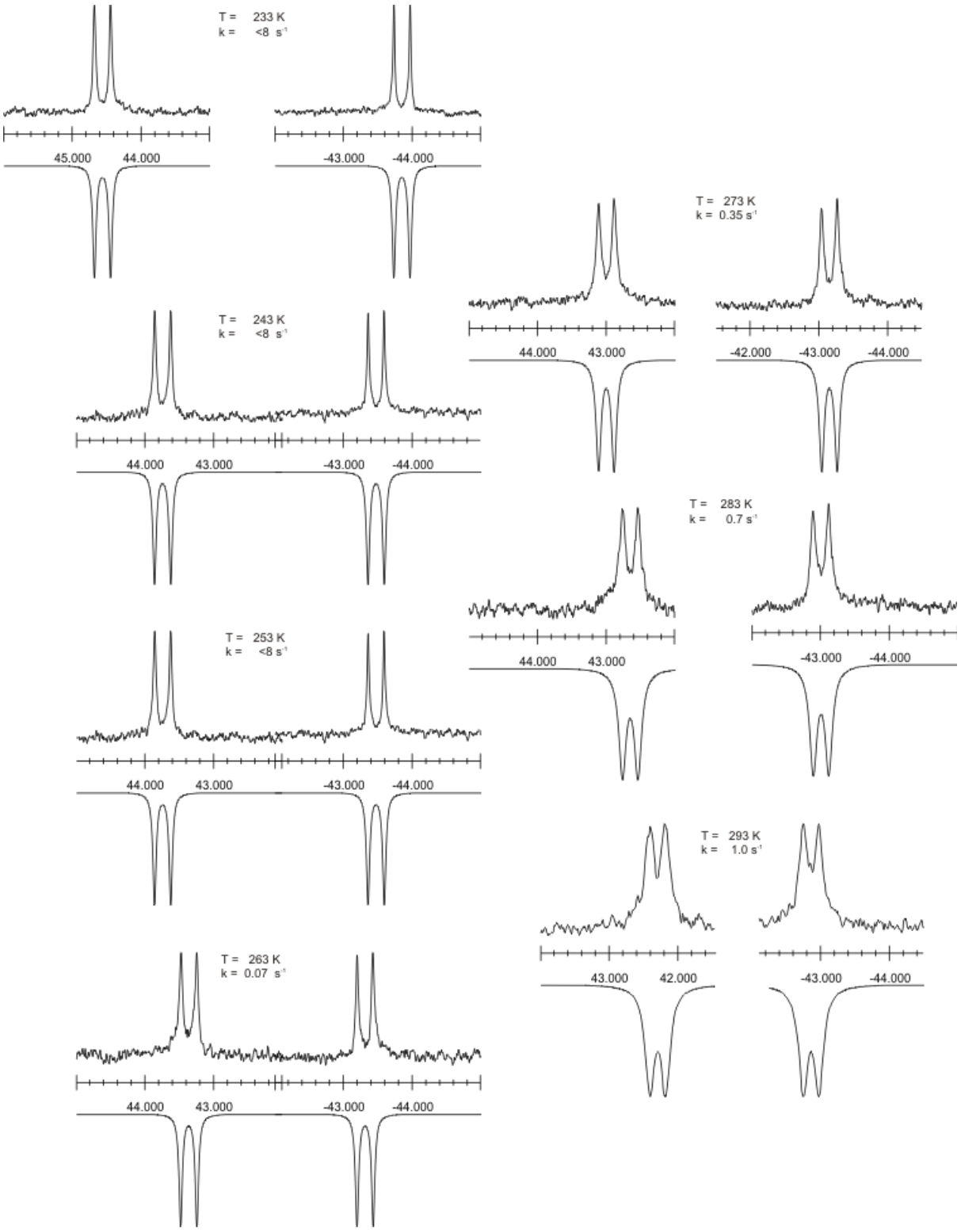

2.11. Reference

1. A. Bader and E. Lindner, *Coordin Chem Rev*, 1991, **108**, 27-110.
2. G. R. Newkome, *Chem Rev*, 1993, **93**, 2067-2089.
3. Z. Z. Zhang and H. Cheng, *Coordin Chem Rev*, 1996, **147**, 1-39.
4. P. Espinet and K. Soulantica, *Coordin Chem Rev*, 1999, **193-5**, 499-556.
5. C. S. Slone, D. A. Weinberger and C. A. Mirkin, *Prog Inorg Chem*, 1999, **48**, 233-350.
6. M. Bassetti, *Eur J Inorg Chem*, 2006, 4473-4482.
7. G. Erdogan and D. B. Grotjahn, *Abstr Pap Am Chem S*, 2010, **239**.
8. J. C. Jeffrey and T. B. Rauchfuss, *Inorg Chem*, 1979, **18**, 2658-2666.
9. R. R. Schrock and J. A. Osborn, *J Am Chem Soc*, 1976, **98**, 4450-4455.
10. P. Braunstein, D. Matt, F. Mathey and D. Thavard, *J Chem Res-S*, 1978, 232-&.
11. P. Braunstein and F. Naud, *Angew Chem Int Edit*, 2001, **40**, 680-699.
12. K. Wajda-Hermanowicz, Z. Ciunik and A. Kochel, *Inorg Chem*, 2006, **45**, 3369-3377.
13. J. Garcia-Anton, J. Pons, X. Solans, M. Font-Bardia and J. Ros, *Eur J Inorg Chem*, 2003, 3952-3957.
14. B. Deklerkengels, J. H. Groen, K. Vrieze, A. Mockel, E. Lindner and K. Goubitz, *Inorg Chim Acta*, 1992, **195**, 237-243.
15. S. J. Chadwell, S. J. Coles, P. G. Edwards and M. B. Hursthouse, *J Chem Soc Dalton*, 1996, 1105-1112.
16. R. R. Schrock and J. A. Osborn, *J Am Chem Soc*, 1976, **98**, 2134-2143.
17. E. Valls, J. Suades and R. Mathieu, *Organometallics*, 1999, **18**, 5475-5483.
18. R. A. Baber, M. F. Haddow, A. J. Middleton, A. G. Orpen, P. G. Pringle, A. Haynes, G. L. Williams and R. Papp, *Organometallics*, 2007, **26**, 713-725.
19. J. H. Xia and K. Matyjaszewski, *Macromolecules*, 1999, **32**, 2434-2437.
20. J. Mathew, T. Thomas and C. H. Suresh, *Inorg Chem*, 2007, **46**, 10800-10809.

21. Strohmei.W and F. J. Muller, *Chem Ber-Recl*, 1967, **100**, 2812-2821.
22. W. D. Horrocks and G. N. Lamar, *J Am Chem Soc*, 1963, **85**, 3512-3513.
23. C. A. Tolman, *Chem Rev*, 1977, **77**, 313-348.
24. E. R. Tucci, *Ind Eng Chem Prod Rd*, 1970, **9**, 516-&.
25. C. Masters, *"Homogeneous Transition-metal Catalysis - a gentle art,"* Chapman and Hall, New York, 1981.
26. E. Drent, P. Arnoldy and P. H. M. Budzelaar, *J Organomet Chem*, 1993, **455**, 247-253.
27. E. Drent, P. Arnoldy and P. H. M. Budzelaar, *J Organomet Chem*, 1994, **475**, 57-63.
28. A. Dervisi, P. G. Edwards, P. D. Newman and R. P. Tooze, *J Chem Soc Dalton*, 2000, 523-528.
29. A. Dervisi, P. G. Edwards, P. D. Newman, R. P. Tooze, S. J. Coles and M. B. Hursthouse, *J Chem Soc Dalton*, 1998, 3771-3776.
30. A. Dervisi, P. G. Edwards, P. D. Newman, R. P. Tooze, S. J. Coles and M. B. Hursthouse, *J Chem Soc Dalton*, 1999, 1113-1120.
31. C. M. Tang, X. L. Li and G. Y. Wang, *Korean J Chem Eng*, 2012, **29**, 1700-1707.
32. J. P. Farr, M. M. Olmstead, F. E. Wood and A. L. Balch, *J Am Chem Soc*, 1983, **105**, 792-798.
33. N. D. Jones, K. S. MacFarlane, M. B. Smith, R. P. Schutte, S. J. Rettig and B. R. James, *Inorg Chem*, 1999, **38**, 3956-3966.
34. K. Nishide, S. Ito and M. Yoshifuji, *J Organomet Chem*, 2003, **682**, 79-84.
35. P. Govindaswamy, Y. A. Mozharivskyj and M. R. Kollipara, *Polyhedron*, 2004, **23**, 3115-3123.
36. V. K. Jain, V. S. Jakkal and R. Bohra, *J Organomet Chem*, 1990, **389**, 417-426.
37. T. Suzuki, M. Kita, K. Kashiwabara and J. Fujita, *B Chem Soc Jpn*, 1990, **63**, 3434-3442.
38. M. M. Olmstead, A. Maisonnat, J. P. Farr and A. L. Balch, *Inorg Chem*, 1981, **20**, 4060-4064.

39. A. Scrivanti, M. Bertoldini, V. Beghetto, U. Matteoli and A. Venzo, *J Organomet Chem*, 2009, **694**, 131-136.
40. D. B. Grotjahn, *Chem Lett*, 2010, **39**, 908-914.
41. C. M. Tang, Y. Zeng, X. G. Yang, Y. C. Lei and G. Y. Wang, *J Mol Catal a-Chem*, 2009, **314**, 15-20.
42. P. Kalck, M. Urrutigoity and O. Dechy-Cabaret, *Top Organometal Chem*, 2006, **18**, 97-123.
43. A. Brennfuhrer, H. Neumann and M. Beller, *Chemcatchem*, 2009, **1**, 28-41.
44. J. K, Sheridan, PhD, University of Liverpool, 2005.
45. P. E. Garrou, *Chem Rev*, 1981, **81**, 229-266.
46. C. G. Arena, E. Rotondo, F. Faraone, M. Lanfranchi and A. Tiripicchio, *Organometallics*, 1991, **10**, 3877-3885.
47. J. P. Farr, F. E. Wood and A. L. Balch, *Inorg Chem*, 1983, **22**, 3387-3393.
48. G. R. Newkome, D. W. Evans and F. R. Fronczek, *Inorg Chem*, 1987, **26**, 3500-3506.
49. Y. Xie, C. L. Lee, Y. P. Yang, S. J. Rettig and B. R. James, *Can J Chem*, 1992, **70**, 751-762.
50. M. M. Olmstead, R. R. Guimerans, J. P. Farr and A. L. Balch, *Inorg Chim a-Article*, 1983, **75**, 199-208.
51. J. A. Casares, P. Espinet and G. Salas, *Chem-Eur J*, 2002, **8**, 4843-4853.
52. J. K. Liu, B. T. Heaton, J. A. Iggo and R. Whyman, *Angew Chem Int Edit*, 2004, **43**, 90-94.
53. J. K. Liu, B. T. Heaton, J. A. Iggo and R. Whyman, *Chem Commun*, 2004, 1326-1327.
54. J. K. Liu, B. T. Heaton, J. A. Iggo, R. Whyman, J. F. Bickley and A. Steiner, *Chem-Eur J*, 2006, **12**, 4417-4430.
55. A. Scrivanti, V. Beghetto, E. Campagna, M. Zanato and U. Matteoli, *Organometallics*, 1998, **17**, 630-635.
56. F. A. Cotton, G. Wilkinson and P. L. Gaus, *"Basic Inorganic Chemistry"*, John Wiley & Sons, New York, Third edn, 1995, p. 209.
57. Z. Y. Lin and M. B. Hall, *Inorg Chem*, 1991, **30**, 646-651.

58. D. T. Richens, *Chem Rev*, 2005, **105**, 1961-2002.
59. Z. Chval, M. Sip and J. V. Burda, *J Comput Chem*, 2008, **29**, 2370-2381.
60. H. Werner, A. Hampp and B. Windmuller, *J Organomet Chem*, 1992, **435**, 169-183.
61. R. G. Wilkins, *Kinetics and Mechanism of reactions of Transation Metal complexes*, Wiley-VCH Verlag GmbH & Co., Weinheim, 2nd edn, 2002, pp. 199-256.
62. J. A. Casares, S. Coco, P. Espinet and Y. S. Lin, *Organometallics*, 1995, **14**, 3058-3067.
63. U. Frey, L. Helm, A. E. Merbach and R. Romeo, *J Am Chem Soc*, 1989, **111**, 8161-8165.
64. R. Romeo, L. M. Scolaro, M. R. Plutino, F. F. de Biani, G. Bottari and A. Romeo, *Inorg Chim Acta*, 2003, **350**, 143-151.
65. A. L. Casado, J. A. Casares and P. Espinet, *Inorg Chem*, 1998, **37**, 4154-4156.
66. S. Q. Niu and M. B. Hall, *Chem Rev*, 2000, **100**, 353-405.
67. K. Tatsumi, R. Hoffmann, A. Yamamoto and J. K. Stille, *B Chem Soc Jpn*, 1981, **54**, 1857-1867.
68. J. P. Stambuli, C. D. Incarvito, M. Buhl and J. F. Hartwig, *J Am Chem Soc*, 2004, **126**, 1184-1194.
69. A. C. Albeniz, A. L. Casado and P. Espinet, *Inorg Chem*, 1999, **38**, 2510-2515.
70. J. J. M. de Pater, C. E. P. Maljaars, E. de Wolf, M. Lutz, A. L. Spek, B. J. Deelman, C. J. Elsevier and G. van Koten, *Organometallics*, 2005, **24**, 5299-5310.
71. M. S. Kharasch, R. C. Seyler and F. R. Mayo, *J Am Chem Soc*, 1938, **60**, 882-884.

Chapter Three

Coordination chemistry of Pd(II) chelate complexes of 1,2-bis (di-tert-butyl-phosphinomethyl)benzene in hydroesterification of alkene

Chapter Three

Coordination chemistry of Pd(II) chelate complexes of 1,2-bis (di-*tert*-butylphosphinomethyl)benzene in hydroesterification of alkene..... 115

Coordination chemistry of Pd(II) chelate complexes of 1,2-bis (di-*tert*-butylphosphinomethyl)benzene in hydroesterification of alkene

3.1. Introduction

Palladium-catalyzed hydroesterification reactions of ethene with carbon monoxide and alcohols are popular for academic investigations because they are considered one of the more useful and economic methods to produce esters with high atom efficiency and purity compared to hydroxycarbonylations.[1-5] This reaction leads to the formation, for example, of industrially important carboxylic acid esters (Scheme 3.1).[6, 7] Similar dihydroesterification reactions can produce diesters.[8, 9]

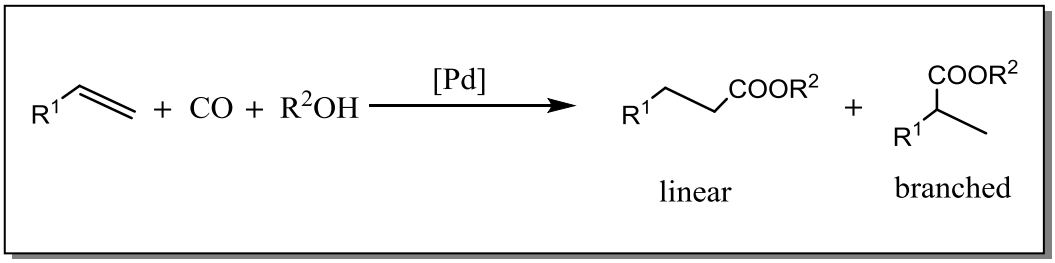

Scheme 3.1. Palladium catalyzed hydroesterification of alkenes.

There have been many experimental[10, 11] and theoretical[12] studies of the mechanisms of these reactions as described previously in chapter one (Scheme 1.12), and both the "hydride" and "carboalkoxy" catalytic cycles have recently been demonstrated at the molecular level for a highly active catalyst.[13] Alcohols are suitable solvents for the reaction; not only do they initiate the reaction, but they also function as chain transfer agents in copolymerization and are required for termination in hydroesterification. The hydride mechanism pathway is more accepted than the carboalkoxy pathway in hydroesterification reactions.[14]

Depending on the catalytic system, the phosphine ligands (nature of the phosphane ligand, bite angle), the presence of acid and the reaction condition used, hydroesterification usually yields a mixture of linear and branched chain esters.

For example, Elsevier and co-workers[15] reported that using [Pd(PPh_3)$_2$- (alkene)] complexes as catalyst precursors for the methoxycarbonylation of styrene at 80 °C, and after 90 min, 80 % conversion and a branched to linear ratio of 41:59 was achieved. But on changing the temperature of the catalytic system to 60 °C, lower conversion but higher selectivity (63 %) towards the branched ester was obtained (Scheme 3.2). Therefore, several studies have been conducted to find efficient catalysts affording good regioselectivity as well as high catalytic activity and stability.[16-20]

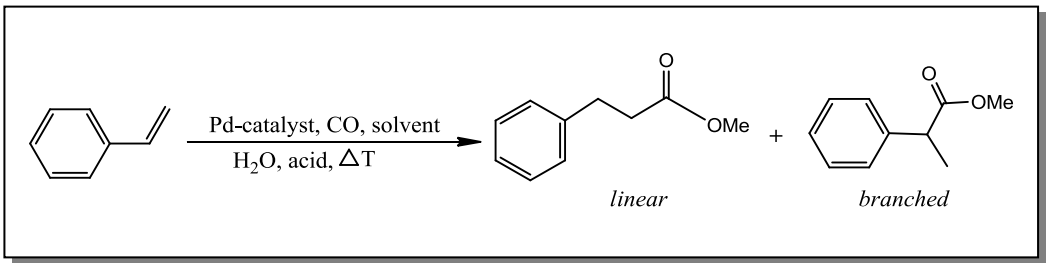

Scheme 3.2. Palladium-catalyzed methoxycarbonylation of styrene.

In general, the use of palladium (0) or palladium (II) precursors in combination with bulky chelating ligands, for example, bis(phosphaadamantyl)alkane,[21] 1,2-bis(di-tert-butylphosphainemethyl)benzene (d^{t}bpx),[22] 1,1-bis (diphenylphospha-nyl)metallocenes,[23] or other bidentate phosphanes,[24, 25] result in a greatly improved regioselectivity towards linear esters. Also, [Pd(d^{t}bpx)(dba)]/ CH_3SO_3H (dba = trans,trans-dibenzylideneacetone) has been used to synthesise important α,ω-dicarboxylic acid esters with selectivities up to 95% by methoxycarbonylation of unsaturated acids or esters (Scheme 3.3).[26]

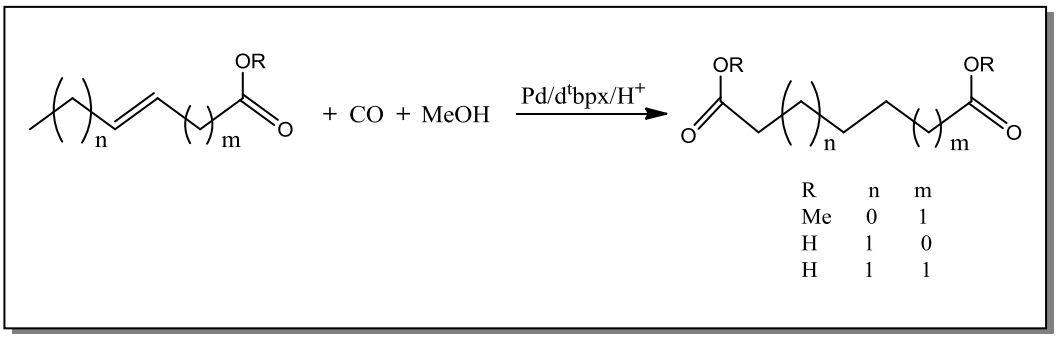

Scheme 3.3. The formation of α,ω -diesters from methoxycarbonylation of esters or carboxylic acids containing double bonds at various positions in the chain.

In 2006, Cole-Hamilton[22] and co-workers applied this catalyst system to convert renewable natural oils into potentially high value terminal esters by a one-pot metathesis-isomerization-methoxycarbonylation-transesterification reaction sequence.[27]

The palladium catalysed carbonylation of ethene in methanol has attracted considerable interest from both industrial and academic labs due to the wide variety of products that can be obtained, e.g. methoxycarbonylation to produce esters, oligomeric keto-esters/di-esters/ diketones, or mono-carbonylated products such as diethyl ketone (Scheme 3.4) (DEK).[3, 6]

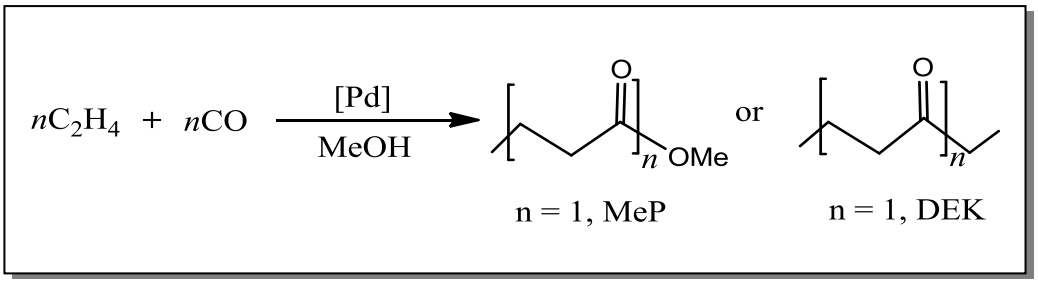

Scheme 3.4. Potential products of the palladium-catalysed carbonylation of ethene with carbon monoxide in methanol.

Methyl propanoate (MeP) is used in the manufacture of methyl methacrylate,[28] whereas polyketones are promising engineering thermoplastics.[2] The reaction shows high selectivity for one class of product depending on the nature of the phosphine ligand, acid and the reaction conditions used.

In the 1990s, Lucite International developed a highly active and selective catalyst for the formation of methyl propanoate with a high production rate and 99.98 % selectivity under mild conditions employing [Pd(d^tbpx)(dba)] /CH_3SO_3H as a catalyst. This process uses the sterically bulky strongly electron donating diphosphine ligand 1,2-bis (di-*tert*-butylphosphinomethyl)benzene (d^tbpx) also known as ALPHA, and strongly favours ester formation over polymerization.[29] The process uses readily available reagents ethene, carbon monoxide and methanol and has been commercialised as the Lucite Alpha process. The catalyst is generated *in situ* from $Pd_2(dba)_3$, ALPHA ligand and methanesulfonic acid.[30]

3.2. The effect of acid

In these hydroesterification reactions, phosphine ligands and the presence of acid (anion) are required to stabilize the palladium intermediates.[31] Choice of the ligand and anions is a crucial factor in determining the reaction outcome due to the influence both can have on the electronic properties of the metal centre.

Increasing ligand basicity and weaker acids should lead to a decreasing electrophilicity of the palladium centre. On the other hand, the anion should be easily displaced from the coordination sites around palladium by reactants and weaker acids generally have increasing coordinating strength of the anion (conjugate base) to the palladium centre; strong coordination of anions like halide may lead to inactive catalysts (poison).[32] As a result, basic ligands and strong acids with non-coordinating anions are favoured in hydroesterification; the palladium (II) centre will be ready to coordinate with electron acceptors such as carbon monoxide or ethene and the anions (like RSO_3), can be displaced readily by the reactants giving active catalysts.[3, 6] Furthermore, the Brønsted protic acid can serve as a hydride source for the formation of catalytic active species via the oxidative addition of acid to a palladium(0) complex,[3, 33] considerably accelerating the reaction.[34-37]

Pd catalysed hydroesterification reactions normally show an acceleration of reaction rate on increasing the amount of strong acid present (has weak conjugate base), which is attributed to the formation of the catalytically active Pd-H species being favoured.[30, 38, 39]

For example, in the hydroesterification of styrene with Pd-$(PPh_3)_2X_2$ catalysts, the activity depends on X as follows (Cl^- << BF_4^- < $CF_3SO_3^-$ < *p*-toluensulfonic acid).[40] Also, Chaudhari and co-workers showed that the activity decreased in the order (*p*-TsOH > CH_3SO_3H > CF_3SO_3H > CF_3COOH).[34] The sequence is in the reverse order of the coordination ability of the anion.[6] Ooka et al,[41] used acidic resin with a SO_3H group as the promoter for the hydroesterification of styrene and vinyl acetate. Recently, several Lewis acids have been synthesised by a reaction of metal oxides with Brønsted acids like methanesulfonic acid (CH_3SO_3H) and *p*-toluensulfonic acid (*p*-TsOH). When employed as promoter for hydroesterification of styrene catalysed by

triphenylphosphine-palladium (PPh_3-Pd) complex, the results indicated that the use of a Lewis acid with an apparent pH similar to *p*-TsOH can bring about marked enhancement in the reaction rate and improve the activity of Pd-catalyst for olefin hydroesterification.[42] Also, Ferreira and co-workers[37] reported that the performance of BSA (borosalicylic acid) in the palladium/triphenylphosphine-catalyzed carbonylation of ethene was comparable with that of MSA (methanesulfonic acid and TFA (trifluoroacetic acid) benchmarks (Table 3.1) (TON = mol methyl propanoate (**1**) formed per mol catalyst).

Table 3.1. Palladium-catalyzed methoxycarbonylation of ethylene with various acid promoters.[a]

Entry	acid	T [ºC]	TOF [h^{-1}][b,c]	STY[d]	PPh3 remaining[%][e]
1	MSA	110	2130	4.50	28
2	BSA	110	1020	2.15	>99[f]
3	BSA[g]	110	886	2.02	>99
4	TFA	110	572	1.14	72
5	MSA	120	3528	10.64	9
6	BSA	120	1249	3.77	77
7	TFA	120	812	2.45	10

[a] p_{final} = 20 bar (CO/C_2H_4 1:1), MeOH (120 mL); entries 1–4: Pd(OAc)2 (2 mm), PPh3 (100 mm), acid (200 mm; $[B(OH)_3]$ = 200 mm for BSA, $[B(OH)_3]$/[salicylic acid] 1:2); entries 5–7: $Pd(OAc)_2$ (3 mm), PPh_3 (150 mm), acid (450 mm; for BSA: $B(OH)_3$ (450 mm), salicylic acid (1350 mm)). [b] Calculated after 10 min. [c] Turnover frequency [mol **1** formed per mol Pd and h] calculated according to the gas-uptake curve. [d] Site–time yield [mol **1** consumed per mol active sites and h at low conversion] calculated according to the gas-uptake curve. [e] Calculated after TON=1000. [f] After 10 h, 94% of PPh_3 remained. [g] Preformed BSA was used.

A common feature of the best promoters is their strong acidity (pK_a < 2) and weak coordinating power. On the other hand, the acid component of the hydroesterification catalyst makes the process corrosive. It would be desirable to develop new hydroesterification catalyst processes that do not use traditional Brønsted acid and do not require an acid stabilizer/ activity booster.[6]

As mentioned above methanesulfonic acid is used in the Lucite Alpha process to generate the hydride species in dry methanol via β-hydride elimination; Heaton and co-workers[43] reported that $[Pd(d^tbpx)(\eta^2\text{-}CH_3SO_3)]^+$ is converted

under catalytic conditions to the hydride complex $[Pd(d^tbpx)H(MeOH)]^+$ at 353 K (Scheme 3.5).

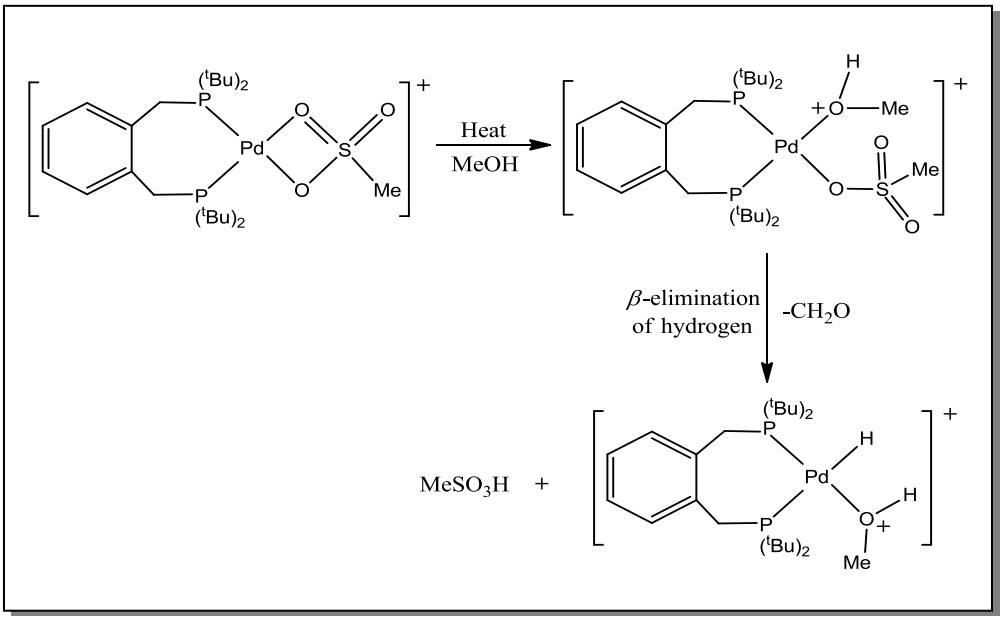

Scheme 3.5. Formation of palladium-hydride.

The last step in the hydride formation is a redox process involving the solvent (Scheme 3.6). This reaction is irreversible and involves β-hydride elimination from a primary or secondary alcohol which is coordinated to the metal; only in such a solvent is the hydride formed.[44]

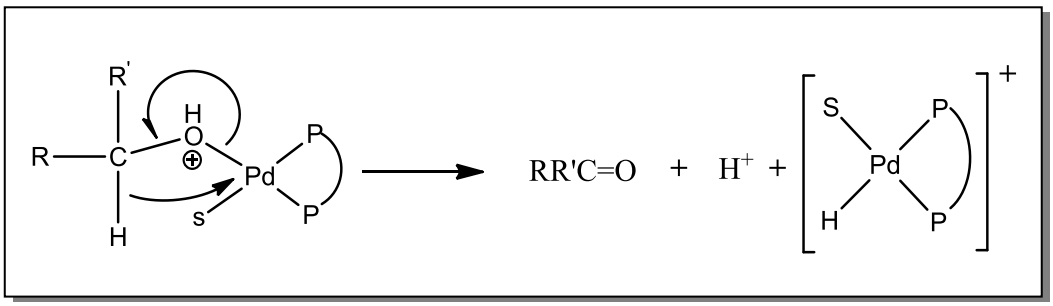

Scheme 3.6. β-hydride elimination.

However, the methanesulfonate anion stays in the reactor during the process, and forms methylsulfonate esters as a result of reaction with MeOH solvent. This cannot easily be removed from the product stream, because, it has a boiling point

very similar to the desired product (methyl propionate) and hence is carried over in small amounts to stage 2 of the process where it poisons the catalyst. We were, therefore, interested in looking at the performance of other alkanesulfonic acids that have a longer chain alkane group which might give higher boiling point esters that are more easily separated.

Long-chain (C_8, C_9, C_{11}, C_{14}, C_{16}, C_{18}) free alkanesulfonic acids are not available commercially,[45] only as the sodium salt. Therefore, we tried to react sodium alkanesulfonate salts with HCl-Et_2O to prepare the free alkanesulfonic acid. However the reaction does not go to completion due to the similar pKas of the acids in organic solvents and the reaction solution contained free chloride anions that are known to be a catalyst poison.[3] So, we decided to follow two strategies to prepare halide free catalysts:

First strategy: use a series of long-chain (C_8, C_9, C_{11}, C_{14}, C_{16}, C_{18}) silver alkanesulfonate salts to prepare $[Pd(d^tbpx)(\eta^2\text{-}RSO_3)]^+$ from $[Pd(d^tbpx)Cl_2]$ by precipitation of AgCl. The study will be of the palladium complexes.

Second strategy: prepare free alkanesulfonic acids by reaction of $HBF_4.O(CH_2CH_3)_2$ with a series of long-chain (C_8, C_9, C_{11}, C_{14}, C_{16}, C_{18}) sodium alkanesulfonate salts because the acid has the weak conjugate base BF_4 ion, that will not poison the palladium catalyst.

3.3. First strategy

3.3.1. Synthesis and characterisation of Silver Alkanesulfonate Salts

There are substantial variations in molecules with complex structures and real experimental data is always the final word, but we can make predictions on the solubility of a compound by counting the ratio of nonpolar CH_2's (hydrophobic tail) to polar functional group (hydrophilic head in the water). If the ratio is less than 4 it will probably be quite soluble in water (and the smaller the ratio, the more soluble it will be). Molecules with 5 or more CH_2 units per polar group will not be very water soluble, and the larger that ratio is, the less soluble the molecule will be.[46-48]

On the other hand, normal alkanes, which are strongly hydrophobic, have been the subject of numerous simulation studies investigating their structure and solubility in aqueous solution.[49-51] In addition, numerous experimental studies have been conducted to determine the solubility of n-alkane in water.[52, 53] As illustrated in (Figure 3.1), the agreement between different sources is poor for chains heavier than *n*-undecane (C_{11}). This is probably due to the difficulty in obtaining pure hydrocarbons with long chain length.

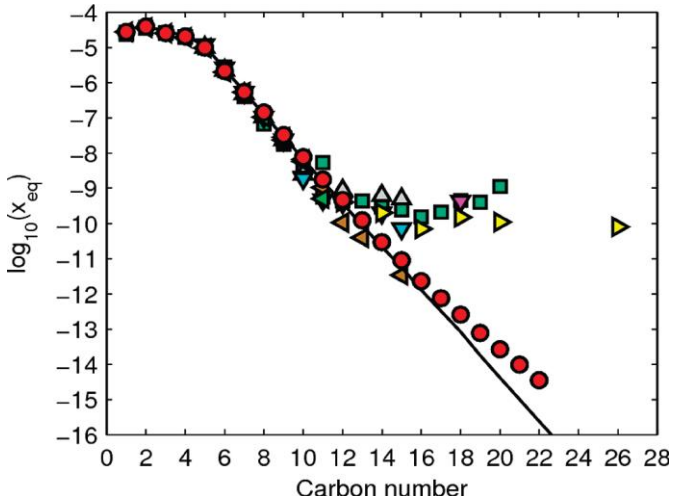

Figure 3.1. Solubilities of *n*-alkanes in water at 298 K and 1 bar. [54] Experimental data: red circles, Ferguson(2009);[54] green squares, Sander (2000);[55] blue squares, Mackay and Shiu (1981);[56] purple up triangle, Tsonopoulos (1999);[57] gray up triangle, Franks (1966);[58] pink down triangle, Baker (1959);[59] blue down triangle, Khadikar et al. (2003); brown left-pointing triangle, Tolls et al. (2002);[52] green left-pointing triangle, McAuliffe (1966, 1969);[60, 61] yellow right-pointing triangle, Sutton and Calder(1974).[62] Group contribution model: solid line, Plyasunov and Shock (2000).[63]

The silver alkanesulfonate salts (RSO_3Ag) required were prepared by two steps: firstly, the sodium alkanesulfonate salts (RSO_3Na) were dissolved in water or hot water/ethanol (18:1) mL ratio) (C_{11}, C_{14}, C_{16}, C_{18}), secondly, reaction with silver nitrate (Scheme 3.7).

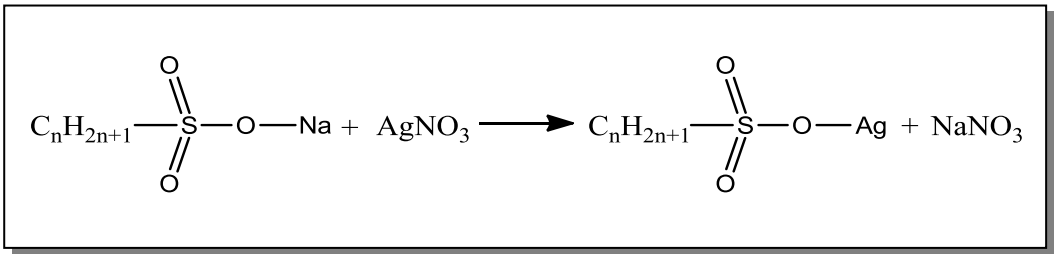

Scheme 3.7. Synthesis of silver alkanesulfonate salt.

Choice of solvent is critical to the metathesis reaction, pure water being the optimal choice for short chain alkanesulfonates Cn, $n \leq 10$, whereas hot water/ethanol 18:1 v/v mixture is required for $n \geq 11$. [45, 64] The chemical structure and purity of the silver salts prepared in this way were checked by proton NMR and elemental analysis (Table 3.2).

Table 3.2. Analytical data and yield of silver alkanesulfonate salts

Silver alkanesulfonate salts (RSO_3Ag)	C Analysis		H Analysis		Yields %
	Theory %	Practical %	Theory %	Practical %	
$C_8H_{17}SO_3Ag$	31.91	31.95	5.69	5.52	60
$C_9H_{19}SO_3Ag$	34.30	35.12	6.08	6.23	71
$C_{11}H_{23}SO_3Ag$	38.49	39.12	6.75	6.98	75
$C_{14}H_{29}SO_3Ag$	43.64	44.52	7.59	7.97	80
$C_{16}H_{33}SO_3Ag$	46.49	48.71	8.05	8.75	55
$C_{18}H_{37}SO_3Ag$	48.98	50.36	8.45	8.85	76

In general, solubility is dependent on the type of salt, temperature and the entropy of solvation. Polarity of the alkane sulfonate (C_{10}-C_{18}) is decreased by increasing of chain length, so we used the temperature and entropy as factors to increase the solubility of salts.

When mixing two solvents like ethanol and water, molecular substances which have O−H bonds, the strength of the attractions between the particles in solution and the structure of the solution are very similar to the attractions and structure found in the separate liquids as (ethanol and water). When these properties are not meaningfully different in the solution than in the separate liquids, we can suppose that the solution has higher entropy than the separate liquids as a result of water-water and ethanol-ethanol attractions being broken and ethanol-water bond are formed. On the other hand, exothermic changes lead to an increase in the energy of the surroundings, which leads to an increase in the number of ways that that energy can be arranged in the surroundings, and therefore, leads to an increase in the entropy of the surroundings.[65]

3.3.2. Synthesis and characterisation of $[Pd(d^tbpx)(\eta^2\text{-}RSO_3)]^+$ from $[Pd(d^tbpx)Cl_2]$

A series of palladium-ALPHA-alkanesulfonate complexes were then prepared by metathesis of $[Pd(d^tbpx)Cl_2]$ with these Ag(alkanesulfonate) salts. The required $[Pd(d^tbpx)Cl_2]$ was prepared from $Pd(dba)_2$ by a modification of the literature procedure.[66] Direct addition of (d^tbpx) ALPHA ligand to $Pd(dba)_2$ in toluene solution, (metal: ligand ratio is 1:1) gave a solution showing 3 peaks in the $^{31}P\{^1H\}$ NMR (Figure 3.2) spectrum at room temperature. The two high frequency resonances, at δ(P) 49.0 and 51.0 ppm, are characteristic of $[Pd(d^tbpx)(dba)]$.[67]

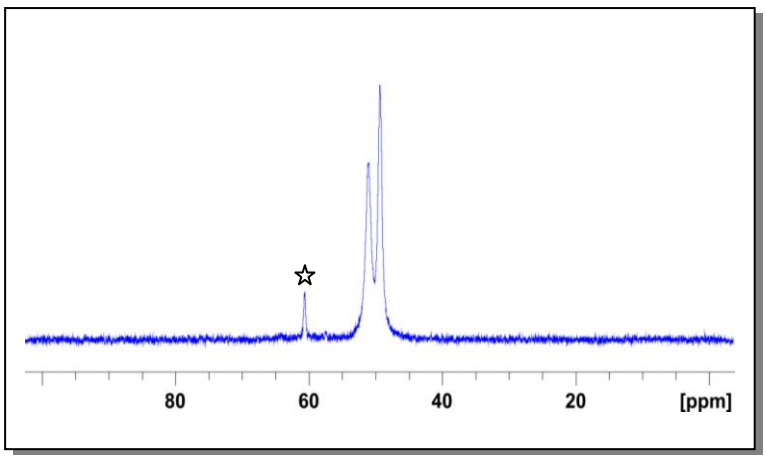

Figure 3.2. $^{31}P\{^1H\}$NMR spectra of $[Pd(d^tbpx)(dba)]$, ☆impurity.

10 equivalents of $HCl.Et_2O$ ($HCl.Et_2O$ is used instead of HCl because it is anhydrous) was then added directly to the toluene solution containing Pd(d^tbpx)(dba), resulting in an immediate change in colour of the solution from orange to yellow and a yellow precipitate formed. The $^{31}P\{^1H\}$ NMR spectrum of the precipitate dissolved in CH_2Cl_2, recorded at 293 K, showed a broad singlet (Figure 3.3), at δ(P) 36.7 ppm, indicative of formation of the desired [Pd(d^tbpx)Cl_2] complex.

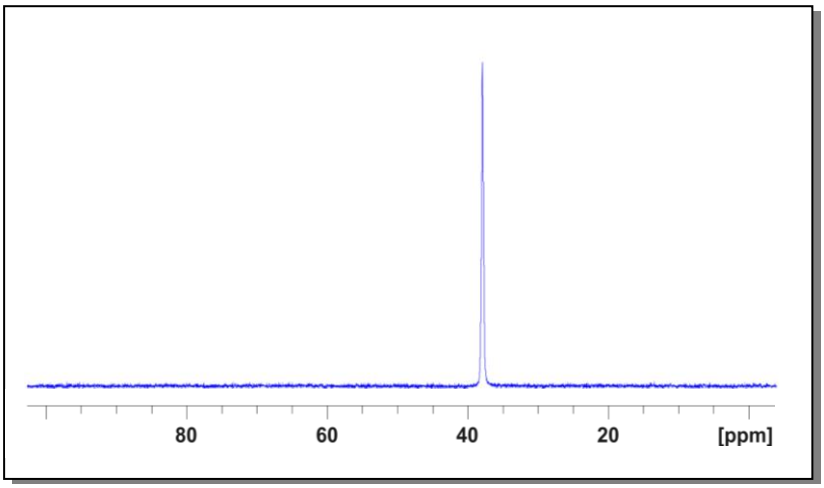

Figure 3.3. $^{31}P\{^1H\}$NMR spectra of [Pd(d^tbpx)Cl_2].

The reaction proceed, by protonation of [Pd(d^tbpx)(dba)] to give [Pd(d^tbpx)(dbaH)]$^+$. The protonation can occur on a C=C bond or the C=O bond. Spencer[68, 69] has reported examples in which protonation of Pd(d^tbpx)(olefin) containing simple olefins (*e.g.* ethene, styrene, nonrborn-2-ene) gives [Pd(d^tbpx)(alkyl)]$^+$ which contains a β-agostic Pd-H interaction as a result of the protonation of the C=C bond. This should be contrasted with protonation of the benzoquinone ligand in Pd(COD)(BQ)[70] which results in protonation of the oxygen atom. Hence, it seems that when the ligand is an α,β-unsaturated ketone, protonation of the oxygen atom is preferred (Scheme 3.8). In agreement with this conclusion, the complex [Pd(dcpx)(dbaH)]$^+$ (dcpx = 1,2-bis (dicyclohexylphosphinomethyl)benzene) has been isolated during the protonation of Pd(dcpx)(dba).[43]

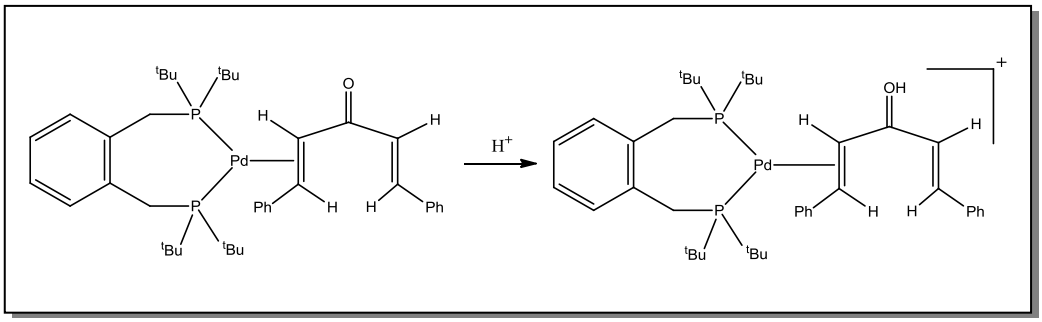

Scheme 3.8. Protonation of [Pd(d^{t}bpx)(dba)].

When an acid containing a strongly coordinating anion like HCl is used, Pd(d^{t}bpx)Cl_2 is formed because the chloride anion can be coordinated to the metal centre and the dba accepts an electron like the oxidizing agent, to transform the starting Pd(0) complex into an appropriate Pd(II) precursor (Scheme 3.9) This contrasts with other acids having weak conjugate anion such as ($MeSO_3H$, TsOH (para-toluenesulfonic acid)) which need an oxidizing agent like O_2 or BQ benzoquinone for oxidation of Pd(0) into Pd(II).[44]

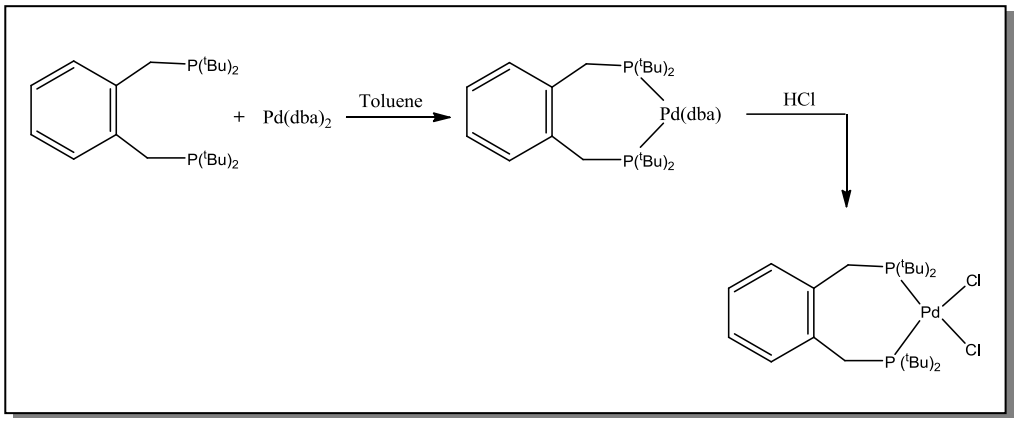

Scheme 3.9. Formation Pd(d^{t}bpx)Cl_2.

Finally, the palladium alkanesulfonate complexes were obtained by addition of 2.25 equivalents of silver alkanesulfonate to [Pd(d^{t}bpx)Cl_2] to give solutions of the [Pd(d^{t}bpx)(η^2-RSO_3)][RSO_3] (R = C_nH_{2n+1}) palladium (II) complexes (Scheme 3.10).

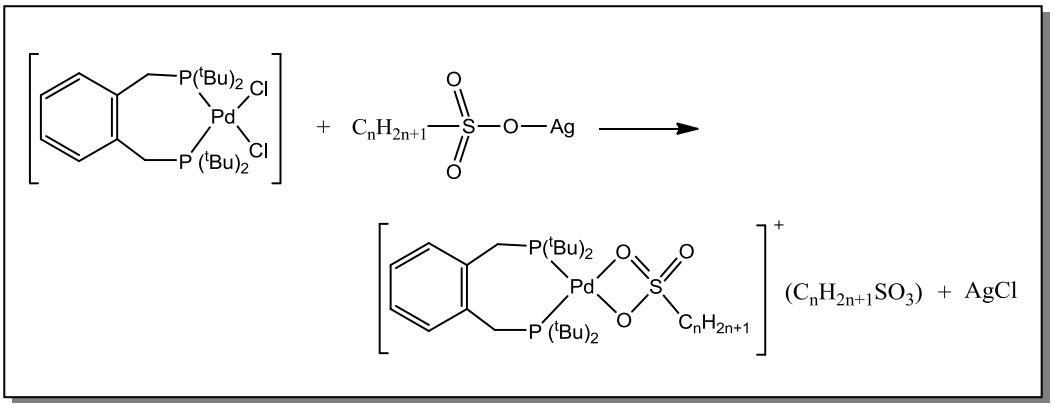

Scheme 3.10. Synthesis of palladium(II) complex.

There have been many studies of RSO_3^- coordinating to metal complexes as a chelating $[Pd(d^tbpx)(\eta^2\text{-}RSO_3)][RSO_3]$[30, 44] or monodentate $[Pd(d^tbpx)(RSO_3)_2]$ ligand.[71] The coordination of (RSO_3) as a monodentate ligand is more common due to the fact that the sulfonate anion is a stronger base when it acts as a monodentate ligand rather than when it co-ordinates as a chelating ligand. The $^{31}P\{^1H\}$ NMR spectra of the new complexes e.g. $[Pd(d^tbpx)(\eta^2\text{-}C_8H_{17}SO_3)][C_8H_{17}SO_3]$ (Figure 3.4) show one peak at room temperature. The high frequency resonance, at δ(P) 68.0 ppm, is characteristic of $[Pd(d^tbpx)(\eta^2\text{-}C_8H_{17}SO_3)]^+$ and indicates that $C_8H_{17}SO_3$ coordinates to the palladium complex as a chelating ligand.[30, 44]

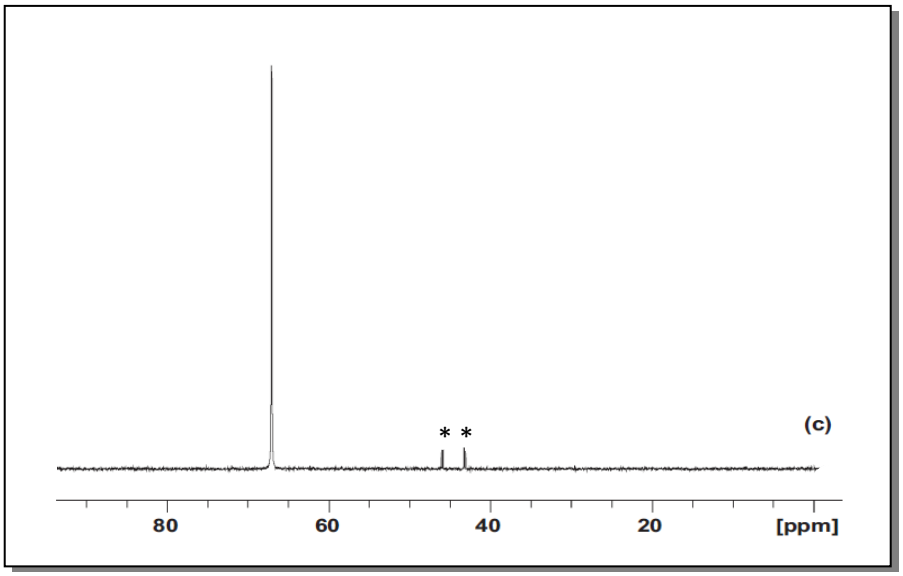

Figure 3.4. $^{31}P\{^1H\}$NMR spectra of $[Pd(d^tbpx)(\eta^2\text{-}C_8H_{17}SO_3)]^+$, * impurity.

On dissolution of $[Pd(d^tbpx)(\eta^2\text{-}C_{18}H_{37}SO_3)]^+$ in MeOH solution the hydride complex $[Pd(d^tbpx)H(MeOH)]^+$ is formed at room temperature, the ^{31}P NMR spectrum showed two broad resonances due to the inequivalent *cis*-P-atoms at [δ = 74.76 and δ = 23.66 ppm; $^2J(P_A\text{-}P_B)$ = 18 Hz]. The resonance at δ = 74.76 is assigned to P_B since it shows additional coupling to the *trans*-hydride [$^2J(P_B\text{-}H)$ = 182 Hz], confirming the assignment of the hydride-solvent complex (Figure 3.5).

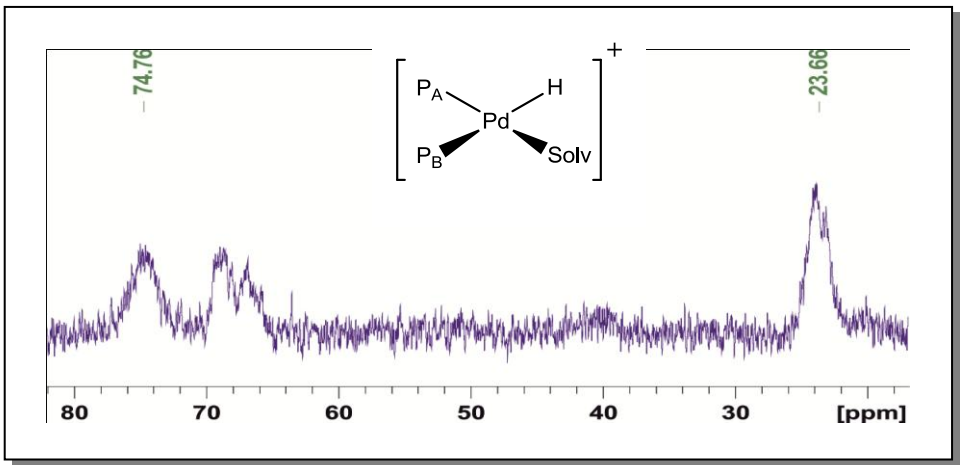

Figure 3.5. $^{31}P\{^1H\}$ spectrum of $[Pd(d^tbpx)H(MeOH)]^+$ in MeOH solution at 295 K.

This ready formation of the hydride complex at 295 K contrasts with the report of Heaton and co-workers,[14] who found that $[Pd(d^tbpx)(\eta^2\text{-}CH_3SO_3)]^+$ is converted under catalytic conditions to the hydride complex only at 353 K.

Thus, the use of alkanesulfonate anion RSO_3 (R = C_8, C_{18}) as conjugate base of the acid rather than $MeSO_3^-$ in the hydroesterification of ethene should be viable and may be advantageous since it can be more easily removed or displaced from the coordination sites around Pd centre to generate the Pd hydride complex and the alkanesulfonate esters may be more easily removed from the exit stream from stage 1 of the ALPHA process.

Although the methoxycarbonylation of ethene reaction is well known. But, the ethyl complex intermediate is unstable except under C_2H_4 atmosphere or during the catalytic cycle. Therefore, the vinyl acetate (VAM) was used as a model substrate instead of ethene to explore the reactivity of the hydrate complex due to

the formation of a more stable "*β*-chelate" intermediate contrary of ethyl complexes.

3.3.3. Reactivity of $[Pd(d^tbpx)(\eta^2\text{-}RSO_3)]^+$ with VAM

This chemistry offers an alternative route to lactate esters, via the hydroesterification of cheap and readily available vinyl acetate. Drent[72] has reported the methoxycarbonylation of vinyl acetate using palladium acetate and (propane-1,3-diyl)bis[di(*tert*-butyl)phosphine] as the catalyst system. Also, Kudo *et al.*[73] reported that methoxycarbonylation of vinyl acetate can be catalysed by $PdCl_2/PPh_3$ in the presence of 2,6-lutidine (= 2,6-dimethylpyridine). A different selectivity issue arises in the palladium/ALPHA/$MeSO_3H$ catalysed hydroesterification of vinyl acetate (VAM) – 1,2- vs 2,1-insertion of VAM into the Pd-H bond of the catalyst leading to linear (*l*) or branched (*b*) ester respectively (Scheme 3.11).[36, 74, 75] In principle this might lead to the resonances of the intermediates to both products being observed, although both Liu and de la Fuente report that only the intermediate leading to the branched product is observed.[30, 76]

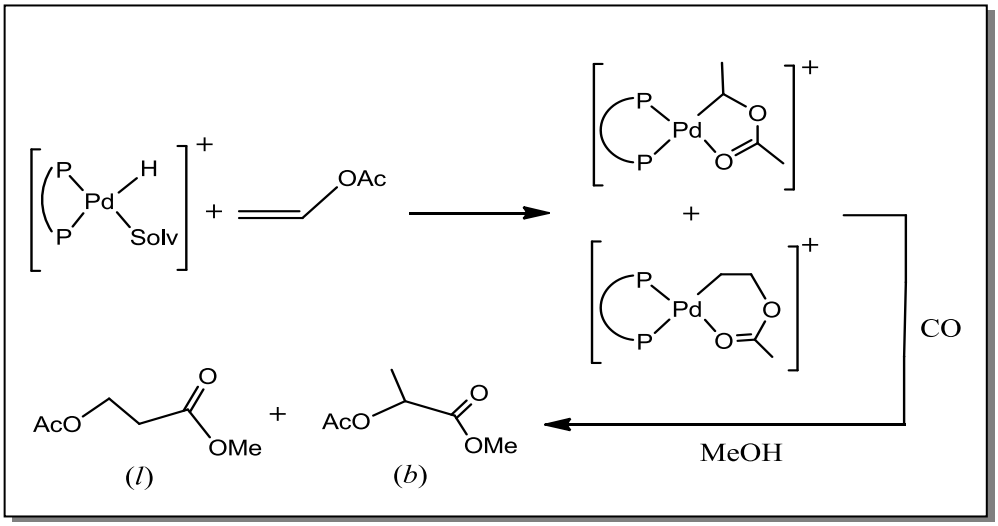

Scheme 3.11. Hydroesterification of vinyl acetate.

The stability of vinyl acetate during the catalyst process is very important. We found that on interaction of solutions of $[Pd(d^tbpx)(\eta^2\text{-}C_8H_{17}SO_3)]^+$ with vinyl acetate/toluene in methanol, the majority of VAM is converted to methyl acetate MeOAc (Scheme 3.12) even at room temperature (Figure 3.5).

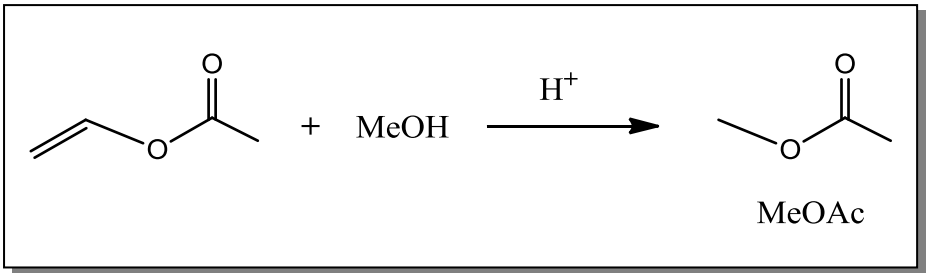

Scheme 3.12. Decomposition of vinyl acetate.

This is evidenced by disappearance of peaks of vinyl at δ = 4.5 and 4.8 ppm, and the change in shift of methyl group at δ = 2.0 ppm in the $\{^1H\}$ NMR spectrum of vinyl acetate, (Figure 3.6). Corresponding changes are seen in the $^{13}C\{^1H\}$ NMR spectrum.

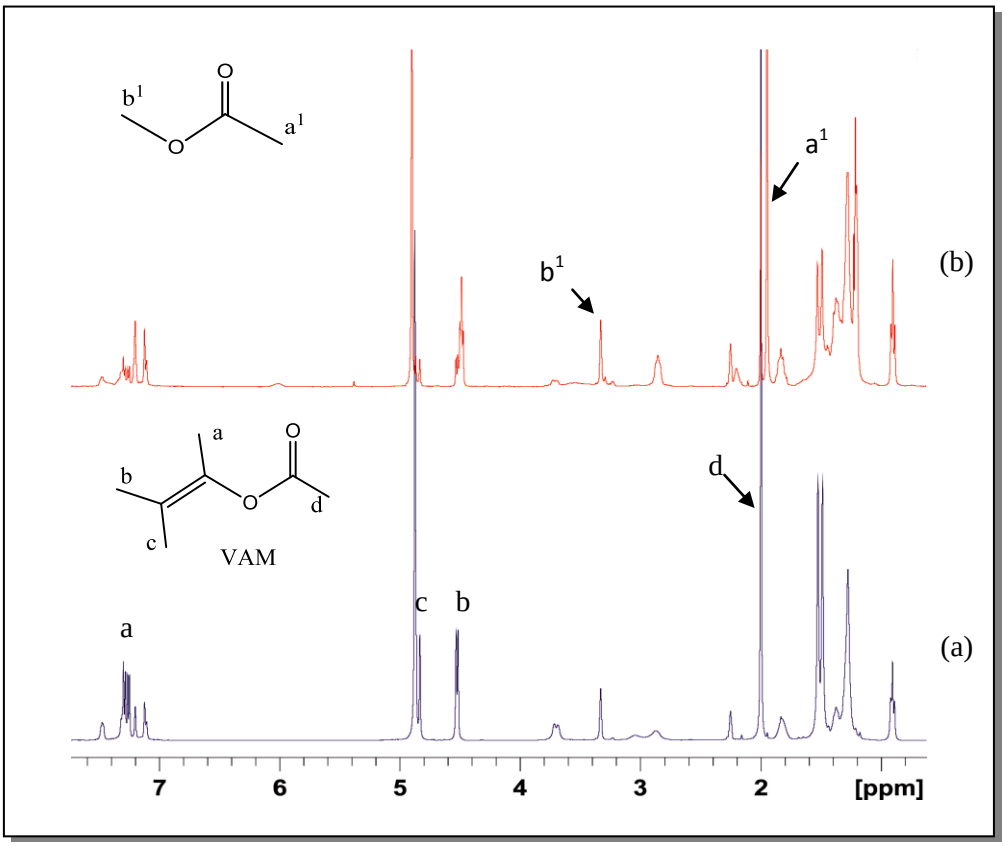

Figure 3.6. $\{^1H\}$NMR spectra of a mixture of complex $[Pd(d^tbpx)(\eta^2\text{-}C_8H_{17}SO_3)]^+$ with VAM at 298 K (a) beginning of the interaction (b) after 8 hours.

The methanolysis of VAM is due to the presence of acid. Acid is produced as a side product in the formation of $[Pd(d^tbpx)H(MeOH)]^+$ from reaction of MeOH with $[Pd(d^tbpx)(\eta^2\text{-}C_8H_{17}SO_3)]^+$ (Scheme 3.5). The transesterification of VAM is

known to be catalysed by acid.[74] This result agrees with the results of previous studies.[41, 74, 75] However, if excess phosphine is present there is minimal degradation of VAM (Table 3.3), the phosphine being protonated instead.

Table 3.3. Stability of vinyl acetate in the presence of MeOH[a]

MSA/ mmol	ALPHA/ mmol	25 °C		80 °C	
		VAM (%)	MeOAc (%)	VAM (%)	MeOAc (%)
0	0	100	0	100	0
1	0	50	50	0	100
0	1	100	0	100	0
1	1	100	0	100	0

[a] Reaction conditions: vinyl acetate (VAM) (2 cm^3), MeOH (2 cm3), toluene (9 cm3), reaction time 3 h. MSA = methanesulfonic acid

Thus, addition of excess ALPHA ligand to the palladium complex solution before the addition of VAM, ensures that no free acid is present in the system and hence that degradation of VAM does not occur, as shown in Figure 3.7.

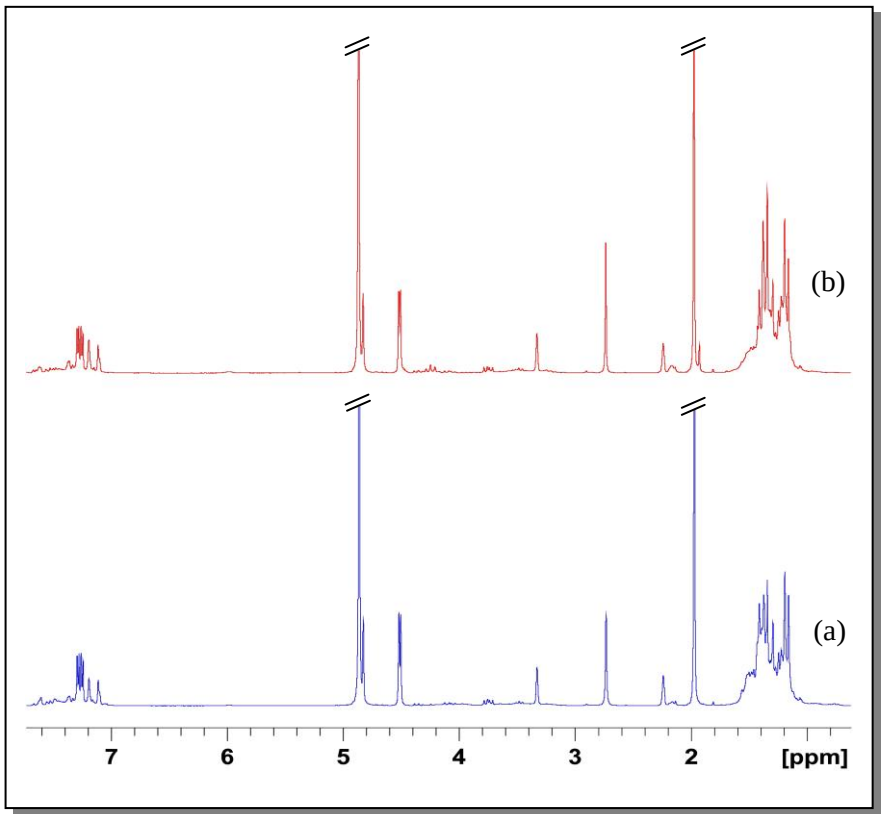

Figure 3.7. {^{1}H}NMR spectra of a mixture of [Pd(d^tbpx)(η^2-$MeSO_3$)]$^+$ with VAM at 298 K (a) beginning of the interaction (b) after 3 days.

The characteristic resonances of the palladium hydride complex at at [δ = 74.76 and δ = 23.66 ppm] disappear from the $^{31}P\{^{1}H\}$ NMR spectrum to be replaced by two pairs of doublets at **a** δ_p = 59.9 ppm, and 24.3 ppm (^{2}J(P-P) = 35 Hz) and **b** δ_p = 57.9 ppm, and 26.3 ppm (^{2}J(P-P) = 37 Hz) (Figure 3.8) which can be assigned (*vide infra*) to the VAM insertion complexes **a/b** [Pd(d^{t}bpx)(k^2-CH(Me) OC(O)CH_3]$^{+}$. Integration of the NMR resonances of **a/b** shows that these compounds are present in the ratio 1:1,4.

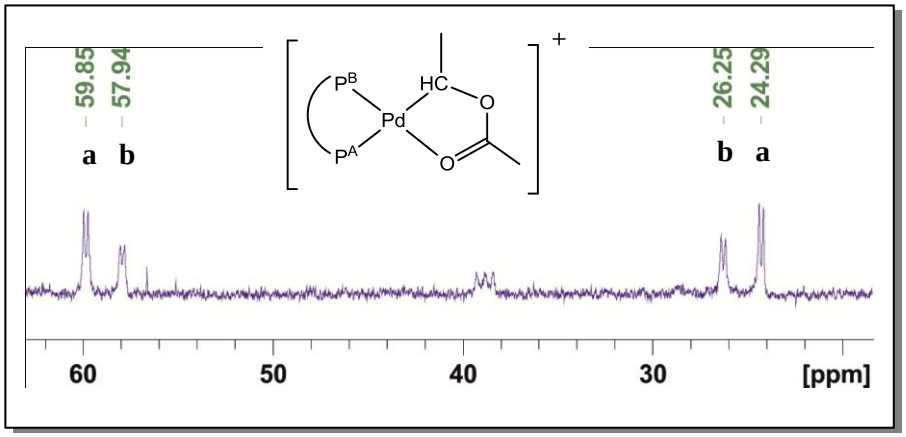

Figure 3.8. $^{31}P\{^{1}H\}$ NMR spectra of [Pd(d^{t}bpx)(k^2-CH(Me)OC(O)CH_3]$^{+}$ in CD_3OD solution at 298 K.

Previous studies by de la Fuente[30] and by Liu have shown from extensive 1D and 2D NMR spectroscopic measurements that these resonances are due to conformers/diastereoisomers of the β-chelate complexes [Pd(d^{t}bpx)(k^2-CH (Me) OC(O)CH_3]$^{+}$ arising from 2, 1 insertion of VAM into the Pd-H bond and not from the products of 2-1 and 1-2 insertion (Scheme 3.11),

Isomers resulting from differences in the conformation adopted by the Pd(d^{t}bpx) ring with respect to the other ligands present in each complex. Extensive 1D and 2D exper

We also studied the direct reaction of the alkanesulfonate complexes [Pd(d^{t}bpx)(η^2-RSO_3)]$^{+}$ (R = C, C_8, C_{18}) with VAM in MeOH solution and successfully generated the [Pd(d^{t}bpx)(k^2-CH(Me)OC(O)CH_3]$^{+}$ complexes required by the hydride pathway.

Finally we can conclude the following from the first approach:

i. Pd(ALPHA) – alkanesulfonates should be viable in the catalysis.
ii. Pd-H is formed more readily.
iii. Alkene insertion is not affected by the change of anion.

As a result, catalysts should be viable, however, the free acid not accessible. Therefore, we moved on to the second strategy.

3.4. Second strategy

3.4.1. Reactivity of [Pd(d^{t}bpx)(dba)] with acid: the HBF_4 system

Zacchini and co-workers[14, 44] have studied the effect on the observable isolable intermediates of different acids HX (X = $MeSO_3^-$, *p*-TsO^-, $CF_3SO_3^-$, BF_4^-) as promoters in the hydroesterification of ethene. The phosphorus spectrum at 193 K of the resulting compounds shows four doublets with nearly the same chemical shift, coupling constant and intensities for all four acids examined. In particular, in the case of HBF_4 no P-F coupling has been observed. This clearly shows that the resulting product does not contain a direct interaction between the metal and the anion.

Thus, we studied the use of the acid HBF_4 for the preparation *in situ* of different alkane sulfonic acid (RSO_3H) (R = C_8, C_9, C_{11}, C_{14}, C_{16}, C_{18}), and studied the reaction of [Pd(d^{t}bpx)(dba)] with these *in situ* prepared alkane sulfonic acids by NMR and *in-situ* HP-NMR spectroscopy methods[77] to investigate if these alkanesulfonates follow the same hydride mechanism established by Heaton *et al* for the methylsulfonate Pd salts/complexes in hydroesterification of ethene. The BF_4^- anion is considerably less coordinating compared with RSO_3^- anion. We can, therefore, hypothesise that the chemistry observed should relate to the interaction of the alkanesulfonate with the Pd centre.

3.4.2. Formation of Alkanesulfonic acid

The alkanesulfonic acids (RSO_3H) (R = C_1, C_8, C_9, C_{11}, C_{14}, C_{16}, C_{18}) were prepared *in situ* by dissolving the sodium alkanesulfonate salt (RSO_3Na) in a 70/30 w/w MeP/MeOH solvent mixture followed by addition of fluoroboric acid ($HBF_4.Et_2O$) (Scheme 3.13).

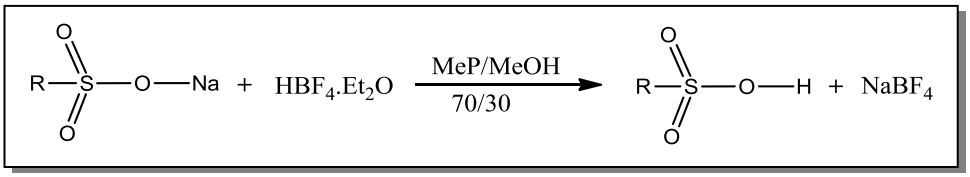

Scheme 3.13. Preparation of Alkanesulfonic acid.

In practice, solubility of the alkanesulfonate salt (RSO_3Na) in a 70/30 w/w MeP/ MeOH mixture solvent is not the same for all salts, since the polarity of the alkane group (C_1- C_{18}) decreases with increasing chain length. Some reactions therefore used slurry of the sodium alkanesulfonate. However, on addition of HBF_4 the alkane sulfonate salt dissolved, indicating formation of the free acid.

3.4.3. Synthesis and characterisation of $[Pd(d^tbpx)(\eta^2\text{-}RSO_3)]^+$ from $[Pd(d^tbpx)(dba)]$

The catalytic systems were prepared *in situ* by addition of a 70/30 w/w MeP/MeOH solvent mixture to a solid mixture of $Pd_2(dba)_3$ and d^tbpx ligand to form $[Pd(d^tbpx)(dba)]$ followed by addition of a solution of alkanesulfonic acid (RSO_3H) prepared *in situ* (reaction of RSO_3Na with HBF_4 in a 70/30 w/w MeP/MeOH) as described above, to give the catalyst precursors $[Pd(d^tbpx)(\eta^2\text{-}RSO_3)][RSO_3]$. The catalytic solutions were then introduced into the sapphire tube under nitrogen. The initial deep-red solution of $[Pd(d^tbpx)(dba)]$, becomes a pale-yellow at the end of reaction, as a result of formation of $[Pd(d^tbpx)(\eta^2\text{-}RSO_3)]^+$.

As previously mentioned, in all solvents, only one singlet at ca. 68 ppm is present in the $^{31}P\{^{1}H\}$ NMR spectra at room temperature of $[Pd(d^{t}bpx)(\eta^{2}\text{-}RSO_3)]^{+}$. Iggo and co-workers[44] have previously found that on cooling the solution of the palladium complex to 193 K, two separate singlets appear at all e.g. (MeOH, MeP) solvents expect CH_2Cl_2. This was attributed to the complex $[Pd(d^{t}bpx)(\eta^{2}\text{-}CH_3SO_3)]^{+}$ existing in solution as two conformers, which differ only in orientation of the benzene ring of the $d^{t}bpx$ ligand with respect to the Me-group of the chelating $MeSO_3^{-}$ anion relative to the plane determined by Pd and the two coordinated oxygen atoms, as shown (Scheme 3.14).

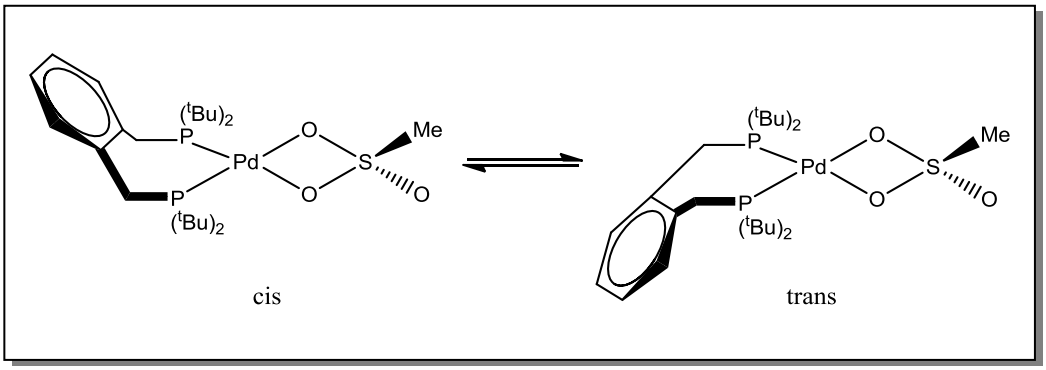

Scheme 3.14. Orthogonal representations of the proposed conformers of $[Pd(d^{t}bpx)(\eta^{2}\text{-}CH_3SO_3)]^{+}$.

3.4.4. Reactivity of $[Pd(d^{t}bpx)H(Solvent)][RSO_3]$ with C_2H_4

Palladium hydrides are usually quite reactive and unstable species, especially in the presence of labile ligands, such as weakly coordinating solvent molecules.[78] Iggo *et al*[13, 14, 44, 79] have elucidated the intermediates of the hydride cycle for Lucite International's ALPHA process. Toniolo *et al*[38] had previously reported that there is circumstantial evidence for the involvement of a Pd-H species in the catalytic hydroesterification of ethene to MeP.

The reaction between metal-hydrides and olefins is one of the classic routes for the synthesis of metal-alkyl complexes.[80] One of the problems associated with the compounds obtained in this way is that they contain a β-hydrogen and,

as a result, the reaction is readily, reversed *via* β-H-elimination. In all cases, β-H-elimination is one of the main reasons for the decomposition of metal-alkyl complexes,[80] and this is widely exemplified in palladium chemistry.[81] Spencer[68, 82, 83] has reported the synthesis of new nickel, palladium and platinum ethyl complexes, stabilised by bulky diphosphine ligands and an agostic interaction between the metal and one of the β-hydrogens of the ethyl ligand. Spencer also showed that these complexes are in equilibrium with the ethene-hydride form, which can lose ethene resulting (in the case of platinum) in a binuclear di-hydride species, (Scheme 3.15). The ground state of the complex (*i.e.* the β-agostic ethyl compound or the ethene-hydride one) and the possibility of the formation of the dimer, is completely controlled by the phosphine used. Bulky and basic diphosphines (*e.g.* d^{t}bpx[31, 84, 85] and d^{t}bpp[3]) favour the β-agostic ethyl compound, whereas, decreasing the size of the ligand, the ethene-hydride forms and, then, the dimer becomes the main species present in solution (in the case of Pt).

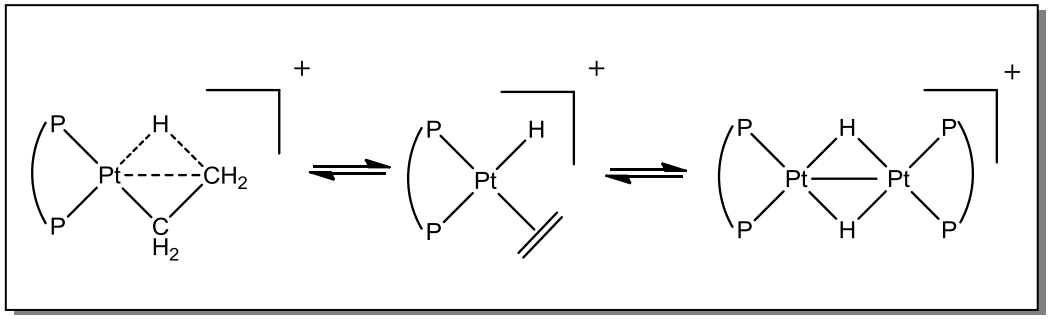

Scheme 3.15. Equilibrium of the ethene-hydride.

Agostic complexes are widely invoked as intermediates in the activation of C-H bonds in organometallic chemistry.[86, 87] The term agostic refers specifically to 3-centre-2-electron interaction involving M-H-C groups. Agostic interactions have considerable precedent in the stabilisation of coordinatively unsaturated metal centres.[88]

Heaton *et al*[14] showed in their work that on heating a methanolic solution of $[Pd(d^tbpx)(\eta^2\text{-}CH_3SO_3)]^+$, traces of the hydride complex $[Pd(d^tbpx)H(MeOH)]^+$ are formed and that in the presence of ethene, these are trapped as the ethyl

complex $[Pd(d^tbpx)(CH_2CH_3)]^+$, the $^{31}P\{^1H\}$ NMR spectrum of which shows at 298 K two peaks at δp_A = 38.7 and δp_B = 70 ppm, (Figure 3.9).

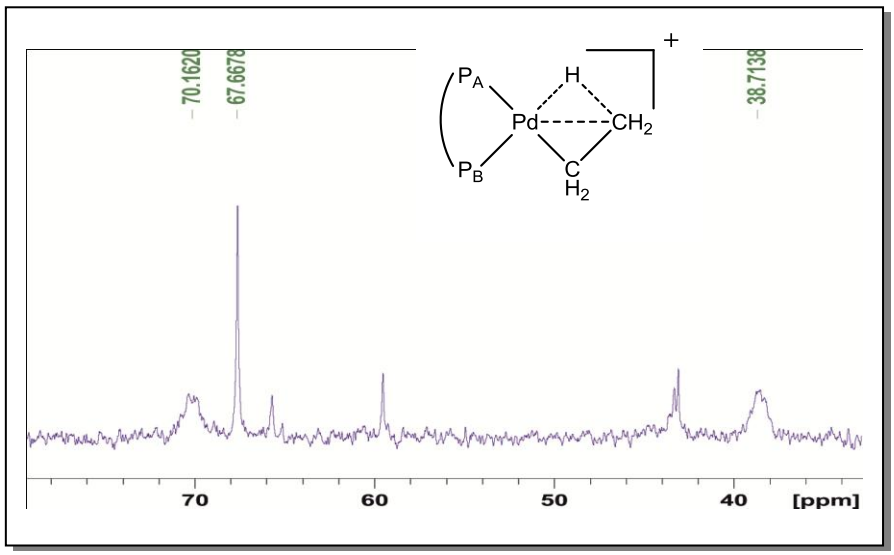

Figure 3.9. $^{31}P\{^1H\}$ NMR spectra of $[Pd(d^tbpx)(CH_2CH_3)]^+$ in MeP/MeOH solvents at 298 K.

However, insertion of ethene is reversible,[30] giving the hydride complex $[Pd(d^tbpx)H(MeOH)]^+$ transiently on removal of ethene from solution. $[Pd(d^tbpx)H(MeOH)]^+$ itself is unstable and returns to the precursor complex $[Pd(d^tbpx)(\eta^2\text{-}CH_3SO_3)]^+$, as shown (Scheme 3.16).

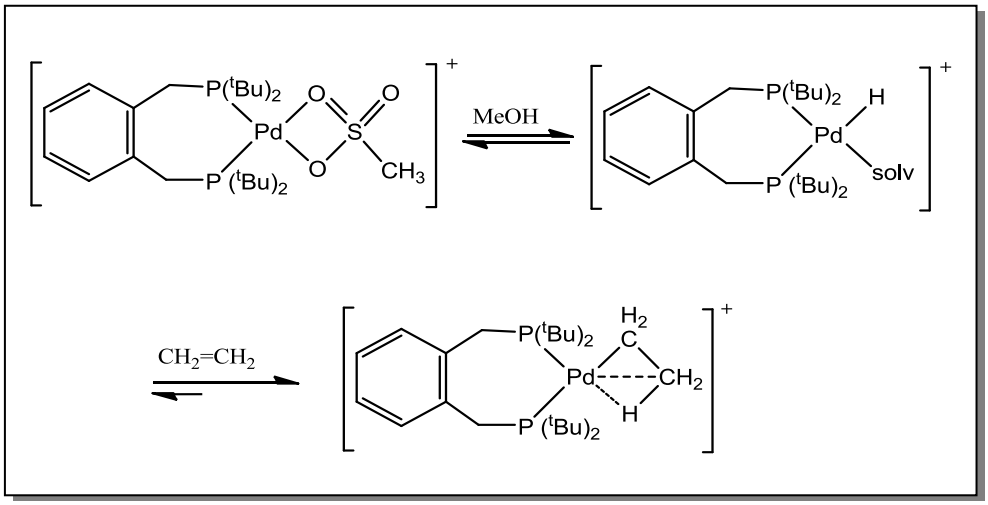

Scheme 3.16. Formation of $[Pd(d^tbpx)(CH_2CH_3)]^+$.

To investigate the effect, if any, of changing the methylsulfonate anion for an alkanesulfonate, the catalytic solutions described earlier were introduced into the sapphire tube under nitrogen, and 1 bar ethene charged after heating the sapphire NMR tube to 343 K in a MeP/MeOH 70/30 solvent. After 30 minutes the tube was cooled to 293 K, to suppress ligand exchanges and the $^{31}P\{^{1}H\}$ NMR spectra (Figure 3.9) showed the presence of two doublets which can be assigned to the Pd-ethyl only for (CH_3SO_3Na), the two doublet peaks of the Pd-ethyl were not seen at room temperature (Figure 3.10) using the other salts acids (RSO_3Na) (R = C_8, C_{11}, C_{18}). This situation is due to the solubility of salts in MeP/MeOH solvents. We found that the solubility of salts is decreased with increased number of carbons of alkanesulfonate in MeP/MeOH solvents.

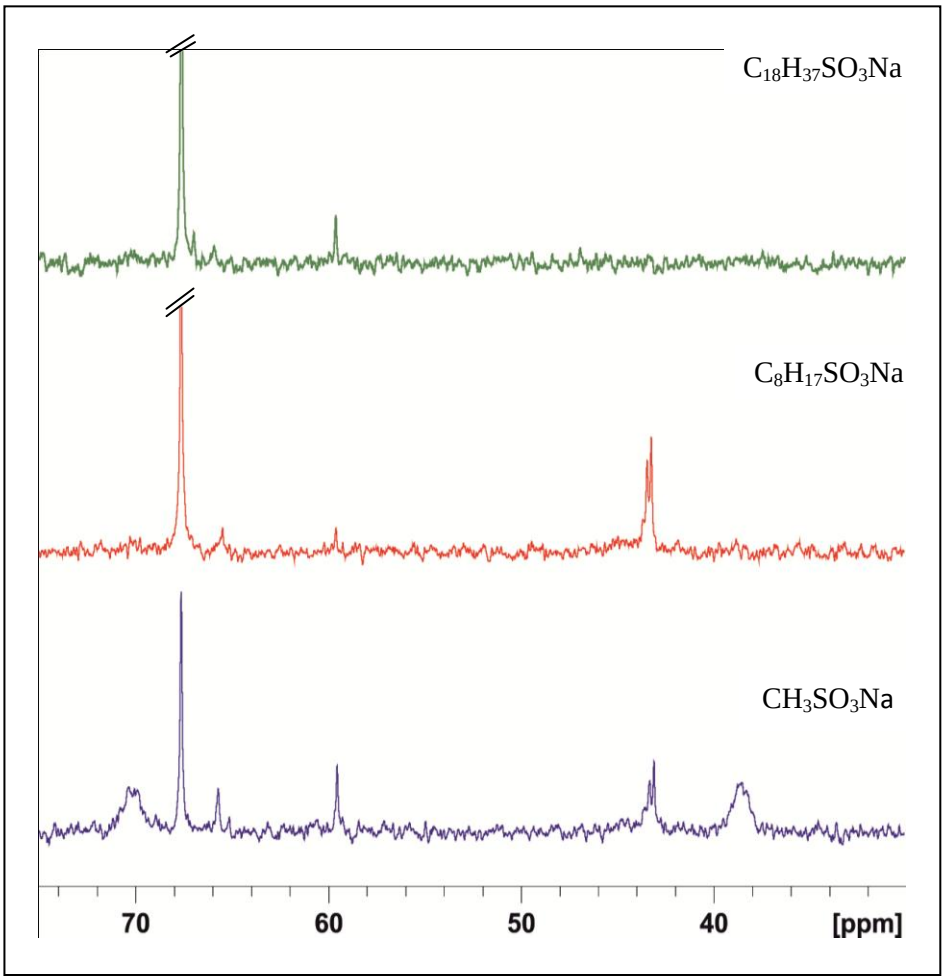

Figure 3.10. $^{31}P\{^{1}H\}$ NMR spectra of $[Pd(d^{t}bpx)(\eta^{2}\text{-}RSO_3)]^{+}$, (R = C_8, C_{11}, C_{18}) with 1 bar ethene gas in MeP /MeOH solvents at 298 K.

Therefore, we carried out the same reaction in CD_2Cl_2/MeOH solvent. The $^{31}P\{^1H\}$ NMR spectra showed the presence of two doublets which can be assigned to the Pd-ethyl with all alkanesulfonate sodium salts (Figure 3.11), traces of $[Pd(d^tbpx)(\eta^2\text{-}RSO_3)]^+$ and phosphonium salt can also be seen in the $^{31}P\{^1H\}$ NMR spectrum. That means, the accessibility of the Pd-ethyl depends on the solvent used. In addition, the further addition of ethene (up to 10 bar) does not result in any change in the product formed.

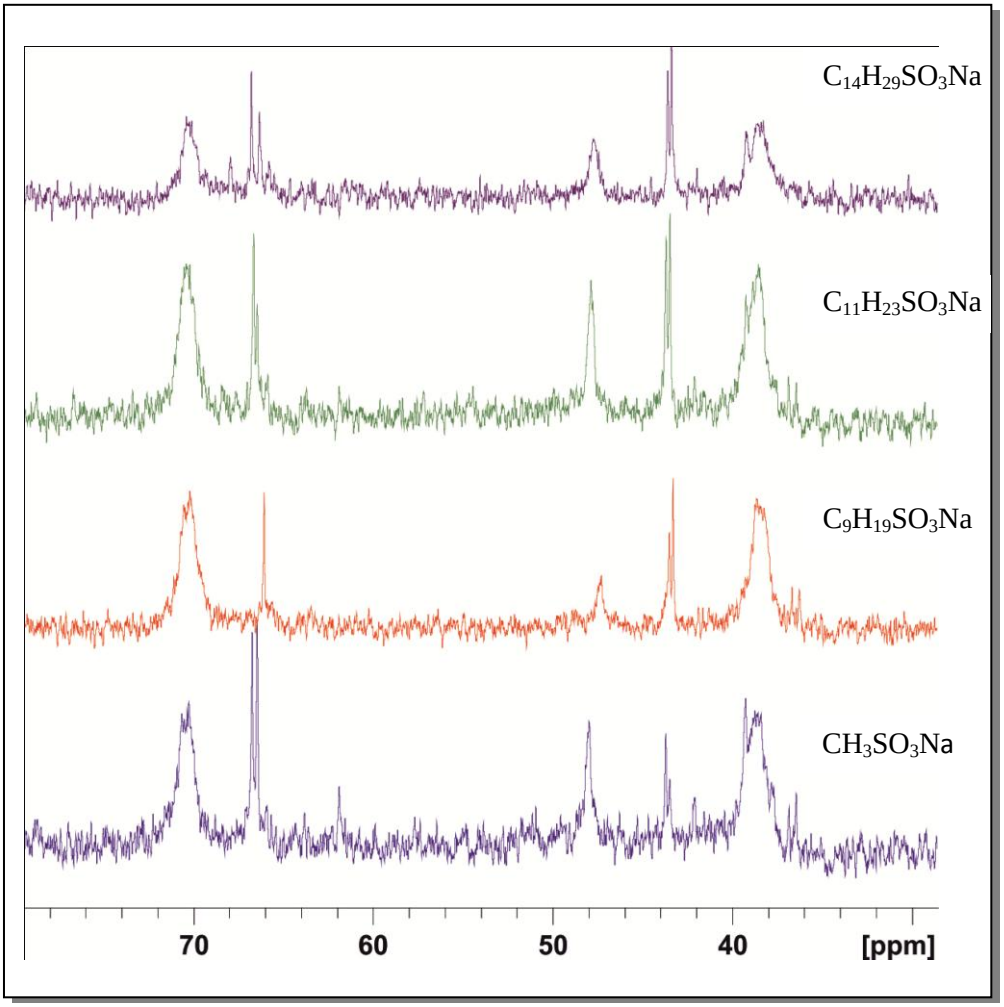

Figure 3.11. $^{31}P\{^1H\}$ NMR spectra of $[Pd(d^tbpx)(CH_2CH_3)]^+$ in (1: 2 ml) CD_2Cl_2 / MeOH solvents and 1bar ethene gas at 298 K.

In CD_2Cl_2/MeOH solvent, the ethyl complex is stable on removal of ethene from the solution, e.g. the resonances of the ethyl complexes are still present in the

$^{31}P\{^{1}H\}$ NMR spectrum of the solution after more than one hour at room temperature using $C_{14}H_{29}SO_3Na/HBF_4$ as acid.

The last step in order to close the catalytic cycle is to add carbon monoxide. CO insertion into a M-alkyl bond is a classic reaction for the synthesis of metal-acyl complexes.[89] Pd-acyl compounds are usually not very stable.[17]

Carbon monoxide coordinates much more strongly to palladium(II) than does ethene, and the hydride–carbonyl complex $[Pd(d^tbpx)H(CO)]^+$is very unstable, its formation leading to, decomposition of the catalyst.[43]

Insertion of CO following alkene insertion to the hydride catalytic cycle is followed by rapid methanolysis to MeP forms. After monitoring formation of the ethyl complex $[Pd(d^tbpx)(CH_2CH_3)]^+$ in dichloromethane by $^{31}P\{^{1}H\}$ NMR spectroscopy for each alkanesulfonate, carbon monoxide was bubbled through the solutions of the corresponding alkyl-palladium precursor at 343 K to form a transient acetyl-palladium complex $[Pd(d^tbpx)(COEt)(MeOH)]^+$ which undergoes rapid methanolysis to give MeP. Thus the resonances of the acetyl complex could not be observed, instead MeP was detected by $^{13}C\{^{1}H\}$ NMR spectroscopy, (Figure 3.12).

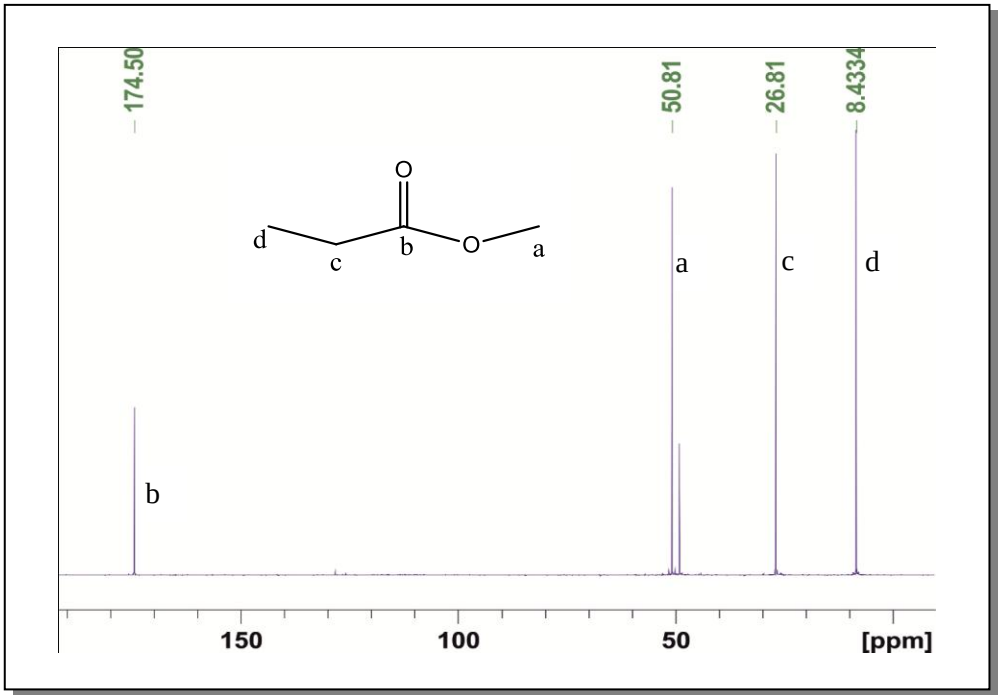

Figure 3.12. $^{31}C\{^{1}H\}$ NMR spectra of methyl propanoate MeP in CD_2Cl_2/MeOH solvents at 298 K.

Having established that the formation of the expected Pd-Et complexes *via* the intermediary of a Pd-H is viable using *in situ* generated alkanesulfonic acid, we preformed catalytic reactions in the sapphire tube and monitored the catalytic reaction by *in situ* $^{31}P\{^{1}H\}$ and $^{13}C\{^{1}H\}$ NMR spectroscopy. Figure 3.13 shows the $^{13}C\{^{1}H\}$ NMR spectrum of the product solution of each reaction.

This shows that, other alkane sulfonic acids such as ($C_9H_{19}SO_3$, $C_{11}H_{23}SO_3$, $C_{14}H_{29}SO_3$) are effective in the Lucite ALPHA process.

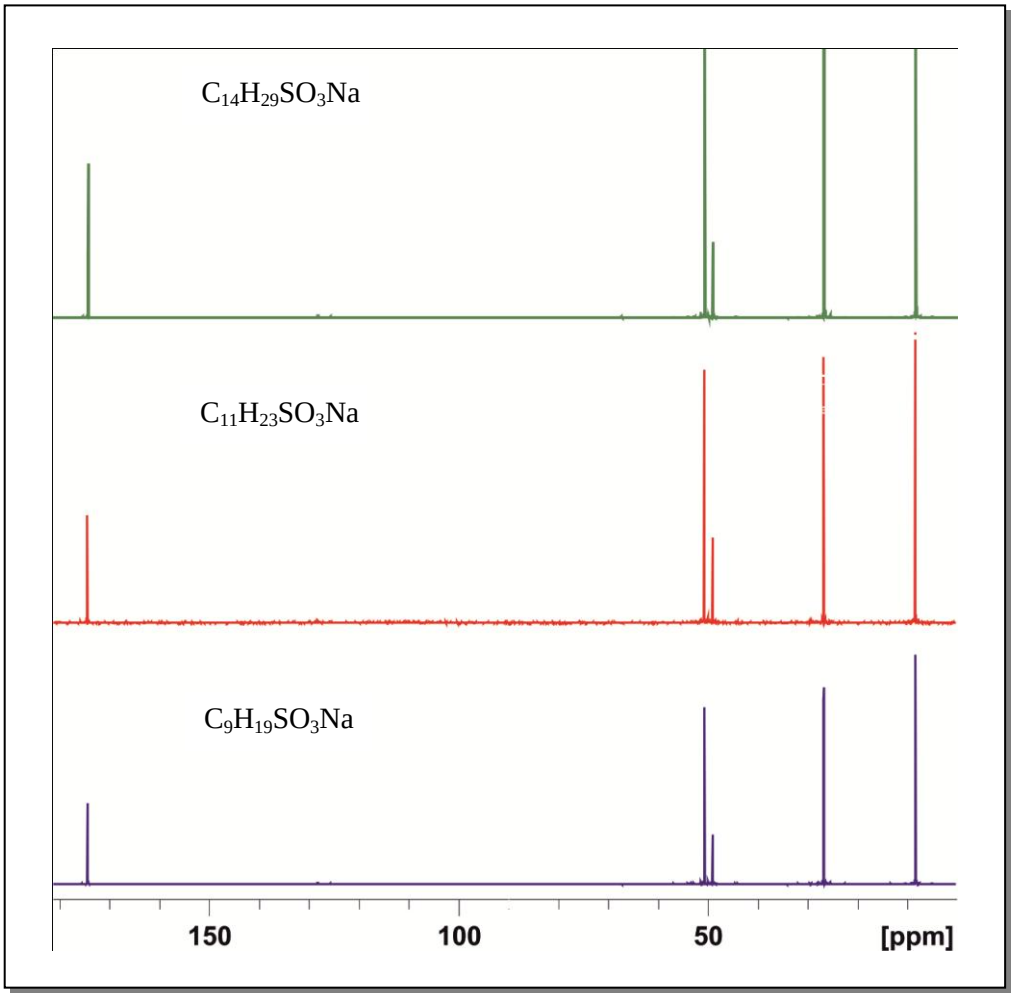

Figure 3.13. $^{31}C\{^{1}H\}$ NMR spectra of MeP obtained by use different alkanesulfonate salt samples in CD_2Cl_2/MeOH solvents at 298 K.

3.5. Conclusion

This work has shown that $MeSO_3H$ can be replaced by other alkanesulfonic acids without detriment to the catalytic performance provided the acid is soluble in the reaction solvent. Since these acids are not commercially available, two strategies were devised to study catalytic and pre-catalytic systems based on alkane sulfonic acids. Firstly, alkanesulfonate sodium salts (C_8, C_9, C_{11}, C_{14}, C_{16}, C_{18}) were transformed to silver salts by metathesis with silver salts and the resulting product reacted with $[Pd(d^tbpx)Cl_2]$ to precipitate AgCl, and affording the complex $[Pd(d^tbpx)(\eta^2\text{-}RSO_3)]^+$ ($R = C_nH_{2n+1}(C_8, C_9, C_{11}, C_{14}, C_{16}, C_{18})$). The reactions of these alkanesulfonate complexes with VAM were studied and the expected palladium complexes $[Pd(d^tbpx)(\kappa^2\text{-}CH(Me)OC(O)CH_3][RSO_3]$ obtained. All steps of these reactions were monitored by $^{31}P\{^1H\}$ NMR spectroscopy. We found that in MeOH the palladium hydride complex $[Pd(d^tbpx)H(MeOH)][RSO_3]$ can be obtained at room temperature instead of high temperature previously reported to be required for the transformation of the analogous Pd-$MeSO_3$ complex into the hydride.

In the second approach, HBF_4 was added to $NaSO_3R$ to prepare the alkanesulfonate acid *in situ*. *In situ* NMR and HPNMR spectroscopy studies confirmed steps in the catalytic cycle and allowed detection and characterization of the ethyl palladium catalytic intermediate complexes.

The alkanesulfonic acids (C_8, C_9, C_{11}, C_{14}, C_{16} and C_{18}) were tested and all proved to be good acids to promote the hydroesterification of ethene, MeP being produced in similar amount when alkanesulfonic acids other than methanesulfonic acid are used.

Choice of solvent the use of long chain acids is very important e.g. methanesulfonate sodium salt dissolve in MeP/MeOH but with increasing alkane group of RSO_3Na the solubility is decreased. Therefore, we carried out the same reaction in CD_2Cl_2/MeOH solvent. Using long chain alkylsulfonates in this solvent system, a Pd-Et species is observed in the presence of ethene gas.

3.6. Experimental

3.6.1. General methods and procedures

All reactions and sample manipulations were carried out using standard Schlenk techniques under nitrogen. Most solvents were dried and distilled under nitrogen following standard literature methods; *i.e.* MeOH over $Mg(OMe)_2$, CH_2Cl_2 over CaH_2, THF over Na/benzophenone, Et_2O over Na/benzophenone, n-hexane over Na and toluene over Na. All the other solvents were degassed under *vacuum* and stored under nitrogen. VAM and CD_2Cl_2 were subjected to three freeze-pump-thaw cycles and stored over 4 Å sieves under nitrogen for at least 24 hours prior to use. All high pressure reactions were carried out in a 5 mm NMR tube and 10 mm sapphire HPNMR tube, unless stated otherwise. Most of the reactive catalytic intermediate compounds have been characterised in solution; thus, no yield or elemental analysis is reported for them. All experiments have been carried out following standard safety procedures.

All ex situ $^{31}P\{^1H\}$, $^{13}C\{^1H\}$, ^1H NMR spectra were recorded using a Bruker Avance-II 400 or DPX400. HPNMR spectra were recorded on a Bruker AMX-II 200 spectrometer. Chemical shifts (δ) are reported in ppm referenced to the tetramethylsilane (TMS) following IUPAC guidelines. Microanalyses were performed at the University of Liverpool using a CE440 CHN analyser.

All the chemicals were purchased from Aldrich Chemical Co., except $Pd(dba)_2$,[66] which was prepared by published methods. Bis(ditertiarybutylphosphino-methyl)benzene (d^tbpx) was donated by Lucite International.

3.6.2. Experiments

A- <u>Synthesis of silver alkanesulfonate.</u>

1. The synthesis of silver alkanesulfonate (C_8, C_9), is a follows. Sodium alkanesulfonate (4.3 mmol) was dissolved at room temperature in water (3 mL) and a silver nitrate aqueous solution (4.3 mmol in 1mL) was then added dropwise. Silver alkanesulfonate precipitated instantly and was collected by filtration and dried *in vacuo*.

For (C_8) yield 0.77 g (60%). Anal. Calc for $C_8H_{17}O_3SAg$ (M = 301.15): C 31.91, H 5.09. Found (%): C 31.95, H 5.52 %. For (C_9) yield 0.97 g (71%). Anal. Calc for $C_9H_{19}O_3SAg$ (M = 315.18): C 34.30, H 6.08. Found (%): C 35.12, H 6.23 %.

2. Synthesis of silver alkanesulfonate (C_{11}, C_{14}, C_{16}, C_{18}), is a follows. Sodium alkanesulfonate (4.3 mmol) was dissolved at room temperature in hot water/ethanol (18 mL/ 1 mL) and a silver nitrate aqueous solution (4.3 mmol in 1mL) was then added dropwise. Silver alkanesulfonate precipitated instantly and was collected by filtration and dried *in vacuo*.
For (C_{11}) yield 1.15 g (78%). Anal. Calc for $C_{11}H_{23}O_3SAg$ (M = 343.23): C 38.49, H 6.75. Found (%): C 39.12, H 6.98 %. For (C_{14}) yield 1.33 g (80%). Anal. Calc for $C_{14}H_{29}O_3SAg$ (M = 385.31): C 43.64, H 7.59. Found (%): C 44.52, H 7.97 %. For (C_{16}) yield 0.97 g (55%). Anal. Calc for $C_{16}H_{33}O_3SAg$ (M = 413.36): C 46.49, H 8.05. Found (%): C 48.71, H 8.75 %. For (C_{18}) yield 1.44 g (76%). Anal. Calc for $C_{18}H_{37}O_3SAg$ (M = 441.42): C 48.98, H 8.45. Found (%): C 5.36, H 8.85 %.

B- Synthesis of Pd(d^{t}bpx)(dba).

In a 100 mL two-necked round-bottomed flask equipped with a magnetic stirring bar and a gas inlet tube (N_2), d^{t}bpx (0.672 g, 1.7 mmol) was added to a solution of $Pd(dba)_2$ (1 g, 1.7 mmol) dissolved in toluene (20 mL) The deep purple colour of the starting solution of $Pd(dba)_2$ changed to bright orange after 1 hour stirring. The reaction solution was stirred for a further 16 hours during which no further colour change occurred. The reaction solution was filtered through celite to remove any palladium metal, and used immediately to prepare Pd(d^{t}bpx)Cl_2.
$^{31}P\{^1H\}$ NMR in toluene at 293 K: δ (ppm) = 49 (br), 51 (br).

C- Synthesis of Pd(d^{t}bpx)Cl_2.

To the solution of Pd(d^{t}bpx)(dba) prepared above, HCl,Et_2O (1.7 mL, 34 mmol) was slowly added *via* a syringe. The solution turned from orange to yellow in colour immediately and a yellow precipitate began to form after 15 minutes. The

reaction mixture was stirred for a further 1.5 hours before the precipitate was collected by filtration and dried *in vacuo*.

Yield 0.72 g (74%). Anal. Calc for $C_{24}H_{44}Cl_2P_2Pd$ (M = 571.88): C 50.41, H 7.76. Found: C 50.83, H 7.74 %. $^{31}P\{^1H\}$ NMR in CH_2Cl_2 at 293 K: δ (ppm) = 37.0 (s).

D- Synthesis of [Pd(d^{t}bpx)(η^2-RSO$_3$)][RSO$_3$]. Method 1, ex situ using Ag(RSO$_3$)

$C_8H_{17}SO_3Ag$ (1.58 g, 5.25 mmol) (taken as an example) was added to a solution of Pd(d^{t}bpx)Cl_2 (1.0 g, 1.75 mmol) in CH_2Cl_2 (60 mL) in a 100 mL two-necked round-bottomed flask equipped with a magnetic stirring bar and a gas inlet tube (N_2). A white precipitate of AgCl was immediately formed. The reaction was stirred for a further 1 hour before the precipitate was removed by filtration. The volume of solution was, then, reduced *in vacuo* to *ca*. 20 mL and the product precipitated by addition of n-hexane (60 mL).

Yield 0.92 g (76 %). Anal. Calc for $C_{40}H_{78}O_6P_2PdS_2$ (M = 694.25): C 54.13, H 8.86. Found: C 53.71, H 8.99 %, and Anal. Yield 1.53 g (75 %) for (C_{18}). Anal. Calc $C_{60}H_{118}O_6P_2PdS_2$ (M = 1168.07),: C 61.69, H 10.18. Found: C 61.16, H 10.10 %. $^{31}P\{^1H\}$ NMR in CH_2Cl_2 at 293 K for both complexes (C_8, C_{18}): δ (ppm) = 68.0 (s).

E- Synthesis of [Pd(d^{t}bpx)(k^2-CH(Me)OC(O)CH$_3$]$^+$.

To a solution of [Pd(d^{t}bpx)(η^2-$C_{18}H_{37}SO_3$)]$^+$ (0.033 g, 0.028 mmol), taken as an example, in CD_3OD (0.8 mL) in a 5 mm NMR tube, 5 equivalent of CH_2=CHOC(O)CH_3 (0.2 mL) was added. A compound of [Pd(d^{t}bpx)(k^2-CH(Me)OC(O)CH_3]$^+$ was formed immediately, as indicated by the $^{31}P\{^1H\}$ NMR spectrum.

$^{31}P\{^1H\}$NMR at 293 K for all alkanesulfonate complexes give same resonance positions: δ (ppm) = 59.9 (d), 24.3 (d) (^2J(P-P) = 35 Hz); δ (ppm) = 57.9 (d), 26.3 (d) (^2J(P-P) = 37 Hz).

HP-NMR measurements

In a typical experiment, the sapphire NMR tube was charged under N_2 with a solution containing the palladium precursor (0.011 mmol), the corresponding ligand (0.022 mmol) in CD_2Cl_2 and the corresponding acid HBF_4,Et_2O with $NaRSO_3$ (0.077 mmol, respectively) in methanol. The tube was then pressurised with ethylene and carbon monoxide to the desired pressure and the reaction monitored by NMR spectroscopy. Most of the compounds reported below have not been isolated due to their instability or the reversible nature of the reaction involved. However, 1D NMR spectroscopic measurements allow all of these compounds to be assigned unambiguously.

A- **Synthesis of [Pd(d^{t}bpx)(η^2-RSO_3)][RSO_3]. Method 2, in situ, using HBF_4/$NaRSO_3$ (general procedure):**

Bidentate phosphine ligand (0.09 g, 0.022 mmol) and $Pd_2(dba)_3$ (0.01 g, 0.011 mmol) were combined in a schlenk flask in CD_2Cl_2 (1 mL). A MeOH (2 mL) solution of ($C_9H_{19}SO_3Na$) (0.02 g, 0.077 mmol), taken as an example, and $HBF_4.Et_2O$ (10.5 µL, 0.077 mmol) was then added and the resultant solution stirred for 15 min at room temperature. The solution was transferred to the sapphire tube NMR under N_2. The $^{31}P\{^1H\}$NMR spectrum indicated that the reaction had gone to completion affording [Pd(d^{t}bpx)(η^2-RSO_3)][RSO_3] $^{31}P\{^1H\}$NMR at 293 K: δ (ppm) = 67.8 (s).

$RSO3^-$	δp (ppm)
$CH_3SO_3^-$	68.0
$C_8H_{17}SO_3^-$	67.7
$C_9H_{19}SO_3^-$	67.8
$C_{11}H_{23}SO_3^-$	67.8
$C_{14}H_{29}SO_3^-$	67.7

B- **Synthesis of $[Pd(d^tbpx)(CH_2CH_3)]^+$ (general procedure):**

The solution of $[Pd(d^tbpx)(\eta^2\text{- } C_9H_{19}SO_3SO_3)]^+$ in CD_2Cl_2/MeOH (1:2 mL) solvents prepared above was heated to 343 K to form the palladium hydride, and ethene was then bubbled through the solution for a 30 min at 343 K, and the progress of the reaction monitored by using $^{31}P\{^1H\}$NMR spectroscopy. The solution was then cooled to room temperature, and bubbling of ethene stopped.
$^{31}P\{^1H\}$NMR at 293 K: δp_A = 38.7 (br), δp_B = 70 (br) (ppm).

$RSO3^-$	δp_A (ppm)	δp_B (ppm)
$CH_3SO_3^-$	39.2	70.3
$C_9H_{19}SO_3^-$	38.6	70.2
$C_{11}H_{23}SO_3^-$	38.5	70.4
$C_{14}H_{29}SO_3^-$	38.3	70.4

C- Synthesis of $CH_3CH_2C(O)OCH_3$.

The solution of $[Pd(d^tbpx)(CH_2CH_3)]^+$ in CD_2Cl_2/MeOH (1:2 mL) from the procedure above was heated again to 343 K ,and ethene and carbon monoxide (1:1) bubbled through the solution for a 30 min at 343 K. The solution was then cooled to room temperature without bubbling of ethene and carbon monoxide. The formation of MeP was indicated by $^{13}C\{^1H\}$NMR spectroscopy and no other organic products being detected.
$^{13}C\{^1H\}$NMR at 293 K: δ (ppm) = 8.45 (s), 26.88 (s), 50.95 (s), 174.61 (s).

3.7. References

1. D. Konya, K. Q. A. Lenero and E. Drent, *Organometallics*, 2006, **25**, 3166-3174.
2. E. Drent and P. H. M. Budzelaar, *Chem Rev*, 1996, **96**, 663-681.
3. R. I. Pugh and E. Drent, *Catalytic Synthesis of Alkene-Carbon Monoxide Copolymers and Cooligomers, Vol. 27 (ed,: A. Sen), Kluwer, Dordrecht*, 2003.
4. A. Brennfuhrer, H. Neumann and M. Beller, *Chemcatchem*, 2009, **1**, 28-41.
5. R. Jennerjahn, I. Piras, R. Jackstell, R. Franke, K. D. Wiese and M. Beller, *Chem-Eur J*, 2009, **15**, 6383-6388.
6. G. Kiss, *Chem Rev*, 2001, **101**, 3435-3456.
7. B. R. Sarkar and R. V. Chaudhari, *Catal Surv Asia*, 2005, **9**, 193-205.
8. C. Bianchini, G. Mantovani, A. Meli, W. Oberhauser, P. Bruggeller and T. Stampfl, *J Chem Soc Dalton*, 2001, 690-698.
9. J. J. Lin and J. F. Knifton, *Catal Lett*, 1996, **37**, 199-205.
10. C. Bianchini, A. Meli, W. Oberhauser, A. M. Segarra, C. Claver and E. J. G. Suarez, *J Mol Catal a-Chem*, 2007, **265**, 292-305.
11. P. C. J. K. M. A Zuideveld, P. W. M. N. van Leeuwen, P. A. A. Klusener, H. A. Stil, C. F. Roobeek, *J. Am. Chem. Soc*, 1998, **120**, 7977-7978.
12. E. Zuidema, P. W. N. M. van Leeuwen and C. Bo, *Organometallics*, 2005, **24**, 3703-3710.
13. J. K. Liu, B. T. Heaton, J. A. Iggo, R. Whyman, J. F. Bickley and A. Steiner, *Chem-Eur J*, 2006, **12**, 4417-4430.
14. G. R. Eastham, B. T. Heaton, J. A. Iggo, R. P. Tooze, R. Whyman and S. Zacchini, *Chem Commun*, 2000, 609-610.
15. J. J. M. de Pater, D. S. Tromp, D. M. Tooke, A. L. Spek, B. J. Deelman, G. van Koten and C. J. Elsevier, *Organometallics*, 2005, **24**, 6411-6419.
16. G. Cavinato, A. Vavasori, L. Toniolo and A. Dolmella, *Inorg Chim Acta*, 2004, **357**, 2737-2747.
17. J. K. Liu, B. T. Heaton, J. A. Iggo and R. Whyman, *Angew Chem Int Edit*, 2004, **43**, 90-94.

18. P. W. N. M. van Leeuwen, M. A. Zuideveld, B. H. G. Swennenhuis, Z. Freixa, P. C. J. Kamer, K. Goubitz, J. Fraanje, M. Lutz and A. L. Spek, *J Am Chem Soc*, 2003, **125**, 5523-5539.
19. O. V. Gusev, A. M. Kalsin, P. V. Petrovskii, K. A. Lyssenko, Y. F. Oprunenko, C. Bianchini, A. Meli and W. Oberhauser, *Organometallics*, 2003, **22**, 913-915.
20. G. Cavinato, A. Vavasori, L. Toniolo and F. Benetollo, *Inorg Chim Acta*, 2003, **343**, 183-188.
21. R. I. Pugh, E. Drent and P. G. Pringle, *Chem Commun*, 2001, 1476-1477.
22. C. J. Rodriguez, D. F. Foster, G. R. Eastham and D. J. Cole-Hamilton, *Chem Commun*, 2004, 1720-1721.
23. C. Bianchini, A. Meli, W. Oberhauser, S. Parisel, O. V. Gusev, A. M. Kal'sin, N. V. Vologdin and F. M. Dolgushin, *J Mol Catal a-Chem*, 2004, **224**, 35-49.
24. Y. Yamamoto, T. Koizumi, K. Katagiri, Y. Furuya, H. Danjo, T. Imamoto and K. Yamaguchi, *Org Lett*, 2006, **8**, 6103-6106.
25. R. I. Pugh and E. Drent, *Adv Synth Catal*, 2002, **344**, 837-840.
26. C. Jimenez-Rodriguez, G. R. Eastham and D. J. Cole-Hamilton, *Inorg Chem Commun*, 2005, **8**, 878-881.
27. Y. L. Zhu, J. Patel, S. Mujcinovic, W. R. Jackson and A. J. Robinson, *Green Chem*, 2006, **8**, 746-749.
28. Nexant's, *PERP Program - Methyl Methacrylate*, Nexant's *ChemSystems* Process Evaluation/Research Planning program, July 2006.
29. E. Zuidema, C. Bo and P. W. N. M. van Leeuwen, *J Am Chem Soc*, 2007, **129**, 3989-4000.
30. V. de la Fuente, M. Waugh, G. R. Eastham, J. A. Iggo, S. Castillon and C. Claver, *Chem-Eur J*, 2010, **16**, 6919-6932.
31. W. Clegg, G. R. Eastham, M. R. J. Elsegood, R. P. Tooze, X. L. Wang and K. Whiston, *Chem Commun*, 1999, 1877-1878.
32. K. R. Reddy, W. W. Tsai, K. Surekha, G. H. Lee, S. M. Peng, J. T. Chen and S. T. Liu, *J Chem Soc Dalton*, 2002, 1776-1782.
33. I. del Rio, C. Claver and P. W. N. M. van Leeuwen, *Eur J Inorg Chem*, 2001, 2719-2738.

34. A. Seayad, A. A. Kelkar, L. Toniolo and R. V. Chaudhari, *J Mol Catal a-Chem*, 2000, **151**, 47-59.
35. G. Cavinato, L. Toniolo and A. Vavasori, *J Mol Catal a-Chem*, 2004, **219**, 233-240.
36. I. A. Shuklov, N. V. Dubrovina, J. Schulze, W. Tietz, K. Kuhlein and A. Borner, *Arkivoc*, 2012, 66-75.
37. A. C. Ferreira, R. Crous, L. Bennie, A. M. M. Meij, K. Blann, B. C. B. Bezuidenhoudt, D. A. Young, M. J. Green and A. Roodt, *Angew Chem Int Edit*, 2007, **46**, 2273-2275.
38. A. Vavasori, G. Cavinato and L. Toniolo, *J Mol Catal a-Chem*, 2001, **176**, 11-18.
39. A. Seayad, S. Jayasree, K. Damodaran, L. Toniolo and R. V. Chaudhari, *J Organomet Chem*, 2000, **601**, 100-107.
40. S. Oi, M. Nomura, T. Aiko and Y. Inoue, *J Mol Catal a-Chem*, 1997, **115**, 289-295.
41. H. Ooka, T. Inoue, S. Itsuno and M. Tanaka, *Chem Commun*, 2005, 1173-1175.
42. J. Yang and Y. Z. Yuan, *Catal Lett*, 2009, **131**, 643-648.
43. S. Zacchini, Ph.D. Thesis, The University of Livewrpool 2000.
44. W. Clegg, G. R. Eastham, M. R. J. Elsegood, B. T. Heaton, J. A. Iggo, R. P. Tooze, R. Whyman and S. Zacchini, *J Chem Soc Dalton*, 2002, 3300-3308.
45. F. Mathevet, P. Masson, J. F. Nicoud and A. Skoulios, *Chem-Eur J*, 2002, **8**, 2248-2254.
46. H. S. Ashbaugh, S. Garde, G. Hummer, E. W. Kaler and M. E. Paulaitis, *Biophys J*, 1999, **77**, 645-654.
47. G. C. Boulougouris, J. R. Errington, I. G. Economou, A. Z. Panagiotopoulos and D. N. Theodorou, *J Phys Chem B*, 2000, **104**, 4958-4963.
48. E. M. Yezdimer, A. A. Chialvo and P. T. Cummings, *Fluid Phase Equilibr*, 2001, **183**, 289-294.
49. P. R. ten Wolde and D. Chandler, *P Natl Acad Sci USA*, 2002, **99**, 6539-6543.

50. M. V. Athawale, G. Goel, T. Ghosh, T. M. Truskett and S. Garde, *P Natl Acad Sci USA*, 2007, **104**, 733-738.
51. R. D. Mountain and D. Thirumalai, *J Am Chem Soc*, 2003, **125**, 1950-1957.
52. J. Tolls, J. van Dijk, E. J. M. Verbruggen, J. L. M. Hermens, B. Loeprecht and G. Schuurmann, *J Phys Chem A*, 2002, **106**, 2760-2765.
53. P. V. Khadikar, D. Mandloi, A. V. Bajaj and S. Joshi, *Bioorg Med Chem Lett*, 2003, **13**, 419-422.
54. A. L. Ferguson, P. G. Debenedetti and A. Z. Panagiotopoulos, *J Phys Chem B*, 2009, **113**, 6405-6414.
55. R. H. s. L. C. Sander, *In NIST chemistry WebBook, NIST standard Reference Database No. 69*, Linstrom, P. J., Mallartd, W. G., Eds.; National Institute of Standards and Technology: Gaithersburg, MD. , 2005; http://webbook.nist.gov.
56. D. Mackay and W. Y. Shiu, *J Phys Chem Ref Data*, 1981, **10**, 1175-1199.
57. C. Tsonopoulos, *Fluid Phase Equilibr*, 1999, **156**, 21-33.
58. F. Franks, *Nature*, 1966, **210**, 87-&.
59. E. G. Baker, *Science*, 1959, **129**, 871-874.
60. Mcauliff.C, *J Phys Chem-Us*, 1966, **70**, 1267-&.
61. Mcauliff.C, *Science*, 1969, **163**, 478-&.
62. C. Sutton and J. A. Calder, *Environ Sci Technol*, 1974, **8**, 654-657.
63. A. V. Plyasunov and E. L. Shock, *Geochim Cosmochim Ac*, 2000, **64**, 439-468.
64. F. Mathevet, P. Masson, J. F. Nicoud and A. Skoulios, *J Am Chem Soc*, 2005, **127**, 9053-9061.
65. R. K. Harris and C. T. G. Knight, *J Chem Soc Farad T 2*, 1983, **79**, 1539-1561.
66. T. Ukai, H. Kawazura, Y. Ishii, J. J. Bonnet and J. A. Ibers, *J Organomet Chem*, 1974, **65**, 253-266.
67. B. T. H. G. R. Eastham, J. A. Iggo, R. P. Tooze, R. Whyman, S. Zacchini, *Chem. Commun*, 2000, 609.
68. F. M. Conroylewis, L. Mole, A. D. Redhouse, S. A. Litster and J. L. Spencer, *J Chem Soc Chem Comm*, 1991, 1601-1603.

69. L. E. Crascall and J. L. Spencer, *J Chem Soc Dalton*, 1992, 3445-3452.
70. H. Grennberg, A. Gogoll and J. E. Backvall, *Organometallics*, 1993, **12**, 1790-1793.
71. H. Werner, M. Bosch, M. E. Schneider, C. Hahn, F. Kukla, M. Manger, B. Windmuller, B. Weberndorfer and M. Laubender, *J Chem Soc Dalton*, 1998, 3549-3558.
72. E. Drent, *Eur. Pat.*,495 548 A2, 1992.
73. K. Kudo, Y. Oida, K. Mitsuhashi, S. Mori, K. Komatsu and N. Sugita, *B Chem Soc Jpn*, 1996, **69**, 1337-1345.
74. A. J. Rucklidge, G. E. Morris and D. J. Cole-Hamilton, *Chem Commun*, 2005, 1176-1178.
75. A. J. Rucklidge, G. E. Morris, A. M. Z. Slawin and D. J. Cole-Hamilton, *Helv Chim Acta*, 2006, **89**, 1783-1800.
76. J. Liu, P. J. Pogorzelec, J. Pelletier, F. Zuidema, C. Bo, D. Cole-Hamilton, I. A. J, R. Whyman, G. R. Eastham and P. Richards, Unpublished.
77. A. Torres, N. M. Perez, G. Overend, N. Hodge, B. T. Heaton, J. A. Iggo, J. Satherley, R. Whyman, G. R. Eastham and D. Gobby, *Acs Catal*, 2012, **2**, 2281-2289.
78. V. V. Grushin, *Chem Rev*, 1996, **96**, 2011-2033.
79. W. Clegg, G. R. Eastham, M. R. J. Elsegood, B. T. Heaton, J. A. Iggo, R. P. Tooze, R. Whyman and S. Zacchini, *Organometallics*, 2002, **21**, 1832-1840.
80. C. Elschenbroich and A. Salzer, *Organometallics: A Concise Introduction*, Wiley-VCH Verlag GmbH, 2003.
81. A. J. canty, *Comprehensive Organometallic Chemistry II*, eds. W. Adel, F. G. A. Stone and G. Wilkinson, Pergamon Pess, New York, 1995, vol. 9, p.225.
82. L. Mole, J. L. Spencer, N. Carr and A. G. Orpen, *Organometallics*, 1991, **10**, 49-52.
83. N. Carr, L. Mole, A. G. Orpen and J. L. Spencer, *J Chem Soc Dalton*, 1992, 2653-2662.
84. T. Fanjul, G. Eastham, N. Fey, A. Hamilton, A. G. Orpen, P. G. Pringle and M. Waugh, *Organometallics*, 2010, **29**, 2292-2305.

85. I. E. Nifant'ev, S. A. Batashev, S. A. Toloraya, A. N. Tavtorkin, N. T. Sevost'yanova, A. A. Vorob'ev, V. V. Bagrov and V. A. Aver'yanov, *Kinet Catal+*, 2012, **53**, 462-469.
86. R. G. Bergman, *Nature*, 2007, **446**, 506-506.
87. T. Kesharwani, A. K. Verma, D. Emrich, J. A. Ward and R. C. Larock, *Org Lett*, 2009, **11**, 2591-2593.
88. M. Brookhart, M. L. H. Green and G. Parkin, *P Natl Acad Sci USA*, 2007, **104**, 6908-6914.
89. B. E. Ali, H. Alper, M. Beller and C. Bolm, *in Transition Metals for Organic Synthesis*, Wiley-VCH, Weinheim, 2008, pp. 49-67.

Chapter Four

Conclusions

Conclusions

4.1. Introduction

The palladium-catalyzed addition of carbon monoxide to alkynes or alkenes in the presence of suitable nucleophile has received considerable attention in recent years and has been used to prepare a range of important industrial products.[1-10] The aim of this study was to investigate the mechanistic origins of ligand and acid effects in the hydroesterification of alkynes and alkenes catalysed by Pd-phosphine complexes. Chapter one outlines the background of the literature surrounding this aim. Chapter two focuses on the role of hemilability of pyridylphosphine ligands in alkyne hydroesterification while Chapter three investigates the role of the counterion in Pd-diphosphine catalysed alkene hydroesterification.

4.2. Conclusions of Chapter Two

Drent[11] proposed that the active species in the Pd-pyridylphosphine catalyzed hydroesterification of alkynes has both chelating and monodentate phosphorus bound Ph_2Ppy ligands coordinated to the Pd(II) metal centre, however, examples of such compounds in the literature are scarce. Sheridan[12] showed that such complexes can be prepared from $[Pd(\kappa^2\text{-}Ph_2Ppy)Cl_2]$ by the use of the mixed solvent system of CH_2Cl_2/MeOH, in which MeOH acts to solvate the chloride ion, thus facilitating the chelation of a nitrogen atom of one of the Ph_2Ppy ligands. Alternatively, the presence of strongly coordinating ligands can be avoided altogether through the reaction of $Pd(OAc)_2$, Ph_2Ppy and CH_3SO_3H, all of which are integral compounds of the catalytic system, indicating the possibility of a Pd(II)-'chelate-monodentate' complex as the catalytically active species.

The presence of severe strain in the Pd(κ^2-Ph_2Ppy) ring in 'chelate-monodentate' complexes suggests that Ph_2Ppy could act as a hemilabile ligand, furnishing a vacant coordination site through the 'lability' of the chelating nitrogen. This has been suggested as a factor in its high selectivity and reactivity in the palladium catalysed carbonylation of alkynes.

Analysis of the variable temperature $^{31}P\{^1H\}$spectra of complex **6** reveals that the pyridyl phosphorus exchange process in **6** is associative rather than dissociative since a negative entropy of activation is observed for both exchange processes, consistent with formation of a five-coordinate intermediate in an associative mechanism and considered the rate determining step of a ligand substitution on Pd(II) metal centre.

The dynamic exchange process observed in **3** is also probably associative but involves recoordination of the counterion displacing the chelating nitrogen. Although there is exchange between the chelate and monodentate pyridyl ligands this exchange does not provide a lightly stabilised coordination site in this system. Thus, ligands such as $CH_3SO_3^-$, $CF_3CO_2^-$, $CF_3SO_3^-$ (OTf), CO and MeOH are unable to displace the chelating pyridyl unit, although, as one would expect, in the presence of ligands that have strong binding properties such as Cl^-, the nitrogen atom is easily displaced. Furthermore, in **6** it is an intramolecular associative process which could explain why this does not provide a lightly stabilised site for substrate coordination.

Thus, although "Pd(κ^2-PPh_2py)" complexes may well be present in catalyst systems using Ph_2Ppy as a ligand, it is not certain that the catalytic reaction will proceed *via* ligand hemilability. Indeed, when weakly coordinating ligands, such as methanesulphonate are present, it is these, and not the nitrogen of the chelating Ph_2Ppy ligand, which are the more labile despite the strain in the chelate ring. We conclude that the role of the pyridyl phosphine ligand is not to provide a lightly stabilised coordination site for substrate.

We cannot rule out the possibility for an uncoordinated nitrogen ligand of a phosphorus coordinated Ph_2Ppy ligand acting as a 'proton relay'. The nitrogen of Ph_2Ppy ligand, whether free in solution or coordinated via phosphorus to Pd is protonated upon addition of the appropriate molar equivalence of acid when in dichloromethane solution. In the presence of methanol, however, the protonation appears to be reversible. This is not surprising since it is well known that methanol is a proton sponge. Nonetheless, we are not able to totally rule out the possibility of a proton relay since, if equilibrium exists between nitrogen protonation and methanol protonation then trace amounts of protonated nitrogen may be present in the system which is enough to facilitate the catalysis.

4.3. Conclusions of Chapter Three

Drent and Pugh have previously noted the complex influence of ligand basicity and acid strength on catalyst selectivity in palladium-diphosphine carbonylation catalysis.[13] Lucite International have developed a highly active and selective catalytic process for the formation of methyl propanoate *via* the hydroesterification of alkene catalysed by a palladium/bidentate phosphine (ALPHA) ligand/ acid (methanesulfonic acid) system.[14, 15] A strong acid such as methanesulfonic acid (MSA) containing a weakly coordinating anion ($MeSO_3^-$) which can be easily displaced by reactants from the coordination sites around metal centre, is required. However, formation of estersulfonate by reaction of methanesulfonic acid with MeOH solvent during catalysis is a potential problem in the Lucite ALPHA process since it is not easily removed from the product stream due to its similar boiling point to methyl propanoate.

We have, therefore, investigated the potential of other alkanesulfonic acids in the Lucite ALPHA process.

Alkanesulfonic acids other than methanesulfonic acid are not commercially available. Therefore, we devised two strategies to replace of $MeSO_3H$ by RSO_3H ($R \neq Me$) without detriment to the catalytic performance.

In the first strategy, sodium alkanesulfonate salts were metathesized with $AgNO_3$ to afford silver alkanesulfonate salts (R = C_8, C_9, C_{11}, C_{14}, C_{16}, C_{18}). The solubility of alkane in water depends on the carbon number, the solubility of *n*-alkane in water decreasing with increased carbon number in the molecule. Alkanesulfonate sodium salts (C_8, C_9) are soluble in water but with C_{11} and more carbon number, a two solvent, hot water/ethanol (18:1) solvent system was required for the metathesis because of the strongly hydrophobic nature of the alkane group. The silver alkanesulfonate salts were reacted with the palladium chloride complex [Pd(d^tbpx)Cl_2] (prepared from $Pd(dba)_2$ with (d^tbpx) ligand and HCl,Et_2O) to precipitate AgCl, and affording the complex [Pd(d^tbpx)(η^2-RSO_3)]$^+$ (R = C_nH_{2n+1}(C_8, C_9, C_{11}, C_{14}, C_{16}, C_{18}) . The $^{31}P\{^1H\}$ NMR spectrum recorded at 293 K, showed a broad singlet, at δ(P) 36.7 ppm, indicative of [Pd(d^tbpx)Cl_2], and a singlet at δ(P) 68.0 ppm, characteristic of [Pd(d^tbpx)(η^2-RSO_3)]$^+$.

On dissolution of the palladium alkanesulfonate complex [Pd(d^tbpx)(η^2-RSO_3)]$^+$ in methanol, it is transformed into the palladium hydride complex [Pd(d^tbpx)H (MeOH)]$^+$ at room temperature. This contrasts with the previously reported high temperature required for transformation of the similar Pd-$MeSO_3$ complex to the palladium hydride. Reaction of the alkanesulfonate complexes with VAM, a model substrate, instead of ethene, afforded the new palladium complexes [Pd(d^tbpx)(k^2-CH(Me)OC(O)CH_3]$^+$. The $^{31}P\{^1H\}$ NMR spectrum of the new complexes showed two pairs of doublets at δ_p = 59.9 ppm, and 24.3 ppm (^2J(P-P) = 35 Hz) and δ_p = 57.9 ppm, and 26.3 ppm (^2J(P-P) = 37 Hz) as a result of conformers diastereoisomers of palladium complexes [Pd(d^tbpx)(k^2-CH(Me)OC (O)CH_3]$^+$.

The results indicate that these palladium alkanesulfonate complexes should be viable in the catalysis and that the catalytic cycle should follow a hydride pathway.

In the second strategy, free alkanesulfonic acid was prepared *in situ*, *via* reaction of $HBF_4.O(CH_2CH_3)_2$ (that has a weaker conjugate base for coordination than

RSO_3^-) with a series of long-chain (C_8, C_9, C_{11}, C_{14}, C_{16}, C_{18}) sodium alkanesulfonate salts and added to a solution of Pd(d^tbpx)(dba) in a sapphire tube for HPNMR spectroscopy and used for studies to confirm steps of the catalytic cycle which succeeded in detection and characterization of the ethyl palladium catalytic intermediates complexes.

Choice of solvent is critical to the accessibility of the ethyl palladium intermediate complex, thus we find that the ethyl complex is not seen in MeP/MeOH solvents when used long chain acid but can be observed in CH_2Cl_2/MeOH by NMR in the absence of CO. The catalytic reaction can be performed in CH_2Cl_2/MeOH solvent using this catalyst system, i.e. alkanesulfonic acids RSO_3^- (R = C_8, C_9, C_{11}, C_{14}, C_{16}, C_{18}) can used as the acid to promote the hydroesterification of ethene and produce methyl propanoate with similar activity as when methanesulfonic acid is used. That means, alkanesulfonate salts (C_8, C_9, C_{11}, C_{14}, C_{16}, C_{18}) can be used in the Lucite Alpha process instead of methanesulfonic acid, avoiding formation of the methyl estersulfonate.

4.4. References

1. I. Omae, *Coordin Chem Rev*, 2011, **255**, 139-160.
2. I. Fleischer, R. Jennerjahn, D. Cozzula, R. Jackstell, R. Franke and M. Beller, *Chemsuschem*, 2013, **6**, 417-420.
3. C. M. Tang, X. L. Li and G. Y. Wang, *Korean J Chem Eng*, 2012, **29**, 1700-1707.
4. A. Brennfuhrer, H. Neumann and M. Beller, *Chemcatchem*, 2009, **1**, 28-41.
5. P. Kalck, M. Urrutigoity and O. Dechy-Cabaret, *Top Organometal Chem*, 2006, **18**, 97-123.
6. G. A. Korneeva, E. M. Karas'kova, M. G. Makarov and E. V. Slivinskii, *Kinet Catal+*, 2005, **46**, 43-46.
7. K. Nagai, *Appl Catal a-Gen*, 2001, **221**, 367-377.
8. G. Kiss, *Chem Rev*, 2001, **101**, 3435-3456.
9. V. de la Fuente, M. Waugh, G. R. Eastham, J. A. Iggo, S. Castillon and C. Claver, *Chem-Eur J*, 2010, **16**, 6919-6932.
10. A. Scrivanti, V. Beghetto and U. Matteoli, *Adv Synth Catal*, 2002, **344**, 543-547.
11. E. Drent, P. Arnoldy and P. H. M. Budzelaar, *J Organomet Chem*, 1993, **455**, 247-253.
12. J. K, Sheridan, PhD, University of Liverpool, 2005.
13. R. I. Pugh and E. Drent, *Adv Synth Catal*, 2002, **344**, 837-840.
14. W. Clegg, G. R. Eastham, M. R. J. Elsegood, R. P. Tooze, X. L. Wang and K. Whiston, *Chem Commun*, 1999, 1877-1878.
15. W. Clegg, G. R. Eastham, M. R. J. Elsegood, B. T. Heaton, J. A. Iggo, R. P. Tooze, R. Whyman and S. Zacchini, *Organometallics*, 2002, **21**, 1832-1840.